Two nanomachines drive evolution in diverse *Vibrio* species

Thèse N° 9718

Présentée le 11 octobre 2019

à la Faculté des sciences de la vie
Unité de la Prof. Blokesch
Programme doctoral en approches moléculaires du vivant

pour l'obtention du grade de Docteur ès Sciences

par

Noémie MATTHEY

Acceptée sur proposition du jury

Prof. E. Oricchio, présidente du jury
Prof. M. Blokesch, directrice de thèse
Prof. F. Le Roux, rapporteuse
Prof. J. R. van der Meer, rapporteur
Prof. B. Lemaitre, rapporteur

2019

ÉCOLE POLYTECHNIQUE
FÉDÉRALE DE LAUSANNE

A ma Mémé et à ma Mimu,

ABSTRACT

Horizontal gene transfer (HGT) has a major impact on bacterial evolution, leading to acquisition or deletion of genes and gene clusters, including those encoding antibiotic resistances and virulence factors. HGT therefore contributes to pathogen emergence, which can have a major impact on human health. As a mode of HGT, natural competence for transformation allows bacteria to directly acquire DNA from the environment and to integrate parts of this genetic material within their genomes. The human pathogen *Vibrio cholerae* is naturally competent when it grows in association with the chitinous exoskeletons of zooplankton. Under this condition, the competence state is initiated by the regulatory protein TfoX, which co-induces a molecular killing device known as the type VI secretion system (T6SS). The co-regulation of the T6SS and competence results in the lysis of non-immune neighboring bacteria and the subsequent acquisition of their DNA, which fosters HGT. In *V. cholerae*, the T6SS is also activated by the TfoX homologue protein, named TfoY.

In this study, we aimed at studying the regulatory pathways and the co-regulation of interbacterial predation and DNA uptake in order to provide new insights into the environmental lifestyle of *V. cholerae* and other vibrios. We first investigated the conserved function of TfoX- and TfoY in *V. fischeri, V. alginolyticus,* and *V. parahaemolyticus* using diverse methods such as qRT-PCR, interbacterial killing assays, and motility assessments. We demonstrated that TfoX-mediated T6SS and competence induction and TfoY-induced motility are conserved phenotypes in the tested *Vibrio* species, whereas the TfoY-mediated T6SS regulation varied. These variations might reflect diverse defense mechanisms, as these different species have adapted to cope with their environmental niches.

Next, we tested the outcome of the TfoX-mediated co-regulation of the T6SS and competence in *V. cholerae*. Under conditions mimicking the bacterium's natural habitat, we showed for the first time the extent of DNA that was integrated on *V. cholerae*'s genome after T6SS-mediated interbacterial predation. Indeed, we demonstrated that T6SS-dependent bacterial predation not only increased the transformation rates but also fostered the exchange of multiple and huge fragments of DNA. We also showed the necessity of an exquisite co-regulation between the T6SS, the competence-related DNA uptake machinery, and the competence-repressed nuclease. Finally, we disclosed that prey-released DNA is not a private good of the attacking bacterium but also accessible to other surrounding cells that have likewise entered the competence state.

Altogether, our findings shed light on the conservation of the TfoX- and TfoY-driven phenotypes in several *Vibrio* species. We also contributed to a better understanding of the interplay between neighbor predation and DNA uptake and the consequences that this interplay has on genome plasticity.

Keywords: Horizontal gene transfer, Natural competence for transformation, *Vibrio cholerae, Vibrio* species, Type VI secretion system, DNA uptake, Bacterial evolution, Regulatory networks.

RÉSUMÉ

Les transferts de gènes horizontaux (TGH) ont un impact majeur sur l'évolution bactérienne, en permettant l'acquisition de nouveaux gènes incluant ceux codants pour la résistance aux antibiotiques ou les facteurs de virulence. Les TGH contribuent donc à l'émergence de pathogènes, qui peuvent avoir un impact majeur sur la santé humaine, La compétence est un mode de TGH qui permet aux bactéries d'acquérir directement de l'ADN de l'environnement et de l'intégrer dans leurs génomes. Le pathogène humain *Vibrio cholerae* est naturellement compétent lorsqu'il se trouve en association avec l'exosquelette de zooplankton, qui est composé de chitine. Sous ces conditions, la compétence est initiée par la protéine régulatrice TfoX, qui co-induit une arme moléculaire appelée le Système de Sécrétion de Type VI (SST6). La co-régulation du SST6 et de la compétence résulte dans la lyse des bactéries non-immunes, suivie de l'acquisition de leur ADN, favorisant les TGH. Chez *V. cholerae*, le SST6 est également activé par l'homologue de TfoX, appelé TfoY.

Dans cette thèse, nous avons voulu étudier la voie de régulation et de co-régulation de la prédation inter-bactérienne et de l'acquisition d'ADN, de manière à fournir de nouvelles idées sur la vie environnementale de *V. cholerae* ainsi que d'autres espèces de *Vibrio*. Nous avons d'abord investigué la nature conservatrice des phénotypes conduits par TfoX et TfoY chez *V. fischeri*, *V. alginolyticus*, et *V. parahaemolyticus* en utilisant diverses méthodes telles que la qRT-PCR, des tests de prédation inter-bactériens, et des tests de motilité. Nous démontrons que l'induction de la compétence et du SST6 médiées par TfoX ainsi que l'induction de la motilité induite par TfoY, sont des phénotypes conservés dans les espèces de *Vibrio* testées, tandis que la régulation du SST6 par TfoY varie. Ces variations peuvent refléter différentes réactions de défense, chaque espèce devant faire face à sa propre niche environnementale.

Ensuite, nous avons testé la conséquence de la co-régulation entre le SST6 et la compétence médiés par TfoX. Dans des conditions mimant l'habitat naturel de la bactérie, nous montrons pour la première fois l'ampleur des tailles d'ADN qui sont integrées dans le génome de *V. cholerae* après induction de son SST6. En effet, nous démontrons que la prédation inter-bactérienne dépendante du SST6, non seulement augmente l'efficacité de transformation, mais permet également de favoriser l'échange multiple de larges fragments d'ADN. Nous montrons également la nécessité d'une co-régulation entre le SST6, la machinerie d'acquisition d'ADN, et de la répression de la nucléase. Finalement, nous

révélons que l'ADN relargué de la bactérie ciblée n'est pas uniquement acquis par la bactérie attaquante, mais est également accessible aux bactéries environnantes qui sont également en état de compétence.

Globalement, nos recherches montrent que les phénotypes médiés par TfoX et TfoY sont conservés chez différentes espèces de *Vibrio*. De plus, nous avons contribué à une meilleure connaissance concernant la coopération entre la prédation inter-bactérienne et l'acquisition d'ADN, ainsi que les conséquences qu'ont cette coopération sur la plasticité génomique.

Mots clefs: Transfert de gène horizontal, Compétence naturelle pour la transformation, *Vibrio cholerae*, Espèces de *Vibrio*, Système de sécrétion de type VI, Acquisition d'ADN, Évolution bactérienne, Réseau de régulation

TABLE OF CONTENTS

LIST OF FIGURES

LIST OF TABLES

ABBREVIATIONS

AI-2	autoinducer 2
bp	base pair
CRP	cAMP receptor protein
CCR	carbon catabolite repression
CAI-1	cholera autoinducer 1
CTX	cholera toxin
chr	chromosome
CFU	colony forming units
cAMP	cyclic adenosine monophosphate
c-di-GMP	cyclic diguanlyate monophosphate
DUS	DNA uptake sequence
dsDNA	double stranded DNA
E-I_{A2}	E-I pair of the auxiliary cluster 2
E-I_{LC}	E-I pair of the large cluster
E-I	Effector immunity pair
FRT	Flippase recognition target
gDNA	genomic DNA
GEI	genomic island
HCD	High cell density
HGT	horizontal gene transfer
kbp	kilo base pair
MSHA	mannose-sensitive hemagglutinin pilus
MGE	Mobile genetic element
GlcNAc	N-Acetylglucosamine
PAI	pathogenicity island
PCR	polymerase chain reaction
QstR	QS- and TfoX-dependent regulator
QS	quorum sensing
ssDNA	single stranded DNA
SNP	single-nucleotide polymorphism
SD	standard deviation
TCP	toxin-coregulated pilus
tDNA	transforming DNA
Tn	transposon
T4P	Type IV pili
T6SS	Type VI secretion system
VPI	*Vibrio* pathogenicity islands
VSP	vibrio seventh pandemic islands
WGS	whole genome sequencing
WT	wildtype
WHO	World Health Organization

1. GENERAL INTRODUCTION

1.1 BACTERIAL EVOLUTION VIA HORIZONTAL GENE TRANSFER

Since the first two complete bacterial genomes sequenced in mid '90s, sequencing technologies have rapidly improved. High-throughput techniques allowed the sequencing of thousands of complete bacterial genomes and, through comparative genomics and phylogenetic studies, the complex evolution of bacteria has been revealed. Bacteria can evolve through genome variations such as for example single nucleotide mutations and gene duplications. However, these chromosomal mutations do not explain the entire extent of genetic diversity. In fact, bacterial evolution can, in addition, be explained by horizontal gene transfer (HGT), which refers to the transfer of genetic material from one organism to another. Indeed, in the latter case, genetic information is not transmitted vertically from parent to progeny but laterally between unrelated species or between members of the same species. Horizontal transfers were even observed between species from different kingdom. Similarly to the acquisition of mutations, horizontally acquired genes can be beneficial, neutral or deleterious and will be subjected to natural selection. HGT therefore constitutes an important driving force for rapid bacterial evolution. Thereby, the process of HGT allows bacteria to rapidly adapt to novel environmental niches ([1,2]).

There is evidence that HGT can lead to the acquisition of novel metabolic functions, such as the utilization capacity for new food sources. However, HGT is also extensively associated with acquisition of virulence factors and resistances to antibiotics ([3]). The latters acquisitions constitute a major threat to public health ([4]).

In some pathogenic bacteria, genes encoding virulence factors are located on a class of genomic island (GEI) specifically called Pathogenicity islands (PAIs). Notably, non-pathogenic bacteria of an identical or a closely related species usually do not harbor these PAIs. The term PAI originated from the late 1980s to describe the genetic regions encoding virulence in uropathogenic isolates of *Escherichia coli* (UPEC; [5]). GEIs, including PAIs, are large (often between 10 and 200 kbp in size) chromosomal regions of foreign origin that were acquired by HGT. These GEIs are often identifiable in the bacterial genome as they usually harbor a distinct GC content compared to the rest of the genome and have often additional characteristics such as: i) genes encoding integrases, transposases or recombinases; ii) an insertion site at tRNA genes; or iii) the presence of direct repeats in their flanking regions ([3]). The virulence factors encoded on PAIs mediate diverse functions involved in pathogenicity such as adherence to or invasion into host cells, and secretion of toxins that can kill the host

or modulate its function ([3,6]). Therefore, bacterial evolution has a direct consequence onto human society and public health, as bacteria, including commensals, can become virulent pathogens through horizontal acquisition of PAIs ([7]).

As mentioned above, genes conferring resistance to antibiotics can likewise be horizontally acquired. Such antibiotic resistance genes are spreading rapidly within or between bacterial genomes through means of HGT, leading to the emergence of multidrug resistant (MDR) bacteria ([8]). The emergence of these MDR bacteria and their spread is currently a major concern. Indeed, in 2019 the World Health Organization (WHO) classified antimicrobial resistance as one of the world's top ten threat to global human health ([9]). It is estimated that, by 2050, antimicrobial-resistant infections will kill 10'000'000 people per year, which will exceed the number of death caused by cancer ([10]). It is therefore important to better understand how the multiple mechanisms of HGT contribute to the emergence of new pathogenic and antibiotic resistant bacteria.

Two years ago, the WHO published a list of 12 species marked as priority pathogens due to their resistances to antibiotics ([11]). Remarkably, the majority of these species are capable of acquiring new genes through one mechanism of HGT, namely natural competence for transformation ([12]). Natural competence for transformation is, together with conjugation and transduction, one out of three major mechanisms of HGT ([1,2]). Conjugation and transduction mediate exchange of DNA fragment by diverse mobile genetic elements such as plasmid and bacteriophages, respectively, with the former relying on direct cell-to-cell contact and the latter being mostly driven by the infecting phage. Natural transformation, on the other hand, does not necessarily rely on cell-to-cell contact and is solely driven by the recipient bacterium, which can acquire exogenous DNA from the environment (Fig. 1.1).

1.1.1 CONJUGATION AND TRANSDUCTION

The conjugation process is mediated by mobile genetic elements (MGEs) such as conjugative plasmids or integrative and conjugative elements (ICE). These MGEs can harbor diverse genes encoding proteins involved in for example virulence, symbiosis or metabolism, as well as proteins implicated in their mobility. Conjugative plasmids have an autonomous replication, whereas ICEs are integrated into the chromosome. ICEs have the ability to excise from the chromosome in a plasmid-like form before being transferred to a recipient

bacterium. The conjugation process occurs when a conjugative pilus belonging to the family of type IV secretion systems (T4SS) creates a link from a donor to a recipient cell, which ultimately allows the transfer of DNA. The conjugative pilus is a dynamic extracellular filament that binds to a recipient cells and, by retraction, will mediate a close cell-to-cell contact between the donor and recipient cells. In the donor cell, the conjugative plasmid is nicked at a specific site by a relaxase in order to transfer one DNA strand into the recipient cell through the formation of a mating bridge between the donor and recipient cells. In the recipient bacterium the single-stranded DNA is circularized and further replicated (Fig. 1.1). Additionally, in the case of ICE, the double stranded plasmid-like molecule is then integrated into the recipient chromosome through the aid of an integrase ([13,14]). After termination of the conjugation process, the recipient cell that acquired a MGE becomes a donor cell and, accordingly, can transfer the MGE to other recipient cells.

Transduction is a process by which DNA is injected into bacterial cell by bacteriophages. Depending on their lifestyles, bacteriophages can be classified as temperate or lytic phages. Temperate phages are integrated into the bacterial host chromosome, whereas lytic phages use the host bacteria as a reservoir for their own replication. The latter replication of lytic phages is followed by their active release into the environment through bacterial lysis. Under stressful conditions, temperate phages can exit their quiescent state and induce the lytic cycle. Notably, when excision of the phage genome is imprecise the phage machinery incorporates part of the flanking host DNA regions, a process that is called specialized transduction. Also, during the lytic cycle, parts of the host genome can be accidentally packaged into the infective virion, which is a process known as generalized transduction. The bacterial DNA packaged into the virions, through both mechanisms (specialized and generalized transduction), can later be injected and integrated into a new bacterium (Fig. 1.1; [15,16]).

The mechanism of natural competence for transformation refers to the uptake of exogenous DNA present in the environment, which can be subsequently integrated into the chromosome in case of sufficient sequence homology (Fig. 1.1; [17]). The natural transformation process will be further developed in the next paragraph.

Remarkably, other mechanisms to transfer DNA have been described recently such as: nanotubes forming intercellular connections between bacteria, membrane vesicles carrying DNA to new hosts, gene transferring agents (GTAs) resembling phage that carried genetic material ([2]), or a transfer of chromosomal DNA called distributive conjugal transfer, which

occurs in *Mycobacteria.* The latter process involves again donor and recipient cells and results in transconjugants with blended genomes compared to the parental strains ([18]).

1.1.2 NATURAL COMPETENCE FOR TRANSFORMATION

In 1928, Frederick Griffith performed the first description of HGT by natural transformation, which he called the transforming principle. Griffith observed that a commensal *Streptococcus pneumoniae* could become a pathogen through the acquisition of virulence factor. At that time, it was not yet identified that DNA encoded proteins and was therefore responsible for the transfer of virulence traits. In his experiment, mice were infected with a mixture of non-viable heat-inactivated virulent *S. pneumoniae* bacteria concomitantly with viable non-virulent *S. pneumoniae*. The outcome of his study was that the viable, originally non-virulent, *S. pneumoniae* became virulent and ended up being lethal for the mice. Hence, he was able to extract the viable virulent strain of *S. pneumoniae* from a blood sample of the dead mouse. In 1944, Avery, MacLeod, and McCarty identified that DNA was the transforming principle. It became evident that the non-virulent *S. pneumoniae* acquired and integrated DNA derived from the dead virulent strain that encoded the capsule acting as virulence factor ([19,20]). The process by which bacteria acquire DNA from the environment and recombine it into their genome was latter coined as natural transformation (Fig. 1.1). The physiological state in which bacteria are able to acquire DNA on the other hand is called natural competence for transformation ([17,20]).

Natural competence is present in many prokaryotes, Gram-positive, Gram-negative bacteria, as well as Archaea. It was reported few years ago that more than 80 bacterial species are naturally competent ([20]). Among them are pathogenic bacteria such as *Acinetobacter baumannii, Streptococcus pneumoniae, Neisseria gonorrhoeae, Campylobacter jejuni, Helicobacter pylori, Haemophilus influenzae, Legionella pneumophila* and *Vibrio cholerae*. In most bacteria, natural competence is a highly regulated process that is often transient and dependent on environmental signals such as high cell density, nutrient depletion, DNA damage, or pheromone signaling ([17,21,22]).

During competence the so-called competence genes are expressed leading to the production and assembly of the DNA-uptake machinery. As its name implies, this machinery is involved in the acquisition of exogenous DNA by competent bacteria. As the cell walls of

the Gram-positive and Gram-negative bacteria are different, the uptake process in naturally competent bacteria of each type differs slightly. Indeed, DNA needs to pass through the dense peptidoglycan layer of Gram-positive bacteria while it has to cross an additional membrane and the somewhat thinner peptidoglycan layer in the case of Gram-negative bacteria. The main components of the DNA-uptake machinery are, however, often conserved among Gram-positive and Gram-negative bacteria, with the central part resembling type IV pilus fibers (recently reviewed in [23–25]). The conservation of these proteins let suggest that the uptake process could be universal. In addition to the central competence pilus, other proteins contribute to the efficient acquisition and integration of DNA into the genome. There is a unique exception, the bacterium *Helicobacter pylori,* in which, the DNA uptake is mediated by a type IV secretion system instead of a type IV pilus ([26]). This unique case will not be further discussed in this introduction.

1.1.2.1 TYPE IV PILI

Type IV pili (T4P) are widely represented in Gram-negative as well as Gram-positive bacteria and are evolutionary related to type II secretion system (T2SS), which translocate proteins across the outer membrane (Fig. 1.2). T4P are thin appendages that arise from the cell envelope and that are composed primarily of major pilin subunits ([27,28]). These surface-exposed appendages are flexible and can measure several micrometers in length. T4P serve different functions such as: twitching motility, surface-sensing, adhesion to surfaces and biofilm development, microcolony formation, host cell adhesion and colonization, phage attachment, and natural transformation ([28]).

Despite the differences in membrane structure of the Gram-negative and Gram-positive bacteria, the respective T4P remain similar (Fig. 1.2). T4P have been primarily studied in Gram-negative bacteria, and their core T4P machinery is composed of: a prepilin peptidase, a cytoplasmic elongation ATPase, an inner membrane platform, an outer membrane secretin pore and the pilus filament ([23,29]). The major pilins are synthesized in a precursor form, the prepilin, with a hydrophilic signal peptide, which needs to be cleaved by the prepilin peptidase (PilD) to allow pilus assembly. After this processing step, the pilins are assembled into helical filaments at the inner membrane complex (PilC). The polymerization of the pilins is catalyzed by the elongation ATPase (PilB), which is located in the cytoplasm. In Gram-negative bacteria, the pilus filament passes through the outer membrane secretin PilQ, which

forms an oligomeric gated channel. Some bacteria also produce one or several retraction ATPase (PilT/PilU) involved in the disassembly and therefore retraction of the T4P (Fig. 1.2; [29,30]). Through retraction, these ATPases can generate considerable mechanical force, which is of particular importance for all T4P-mediated processes such as twitching motility, host cell adhesion or natural transformation ([23,28,31,32]).

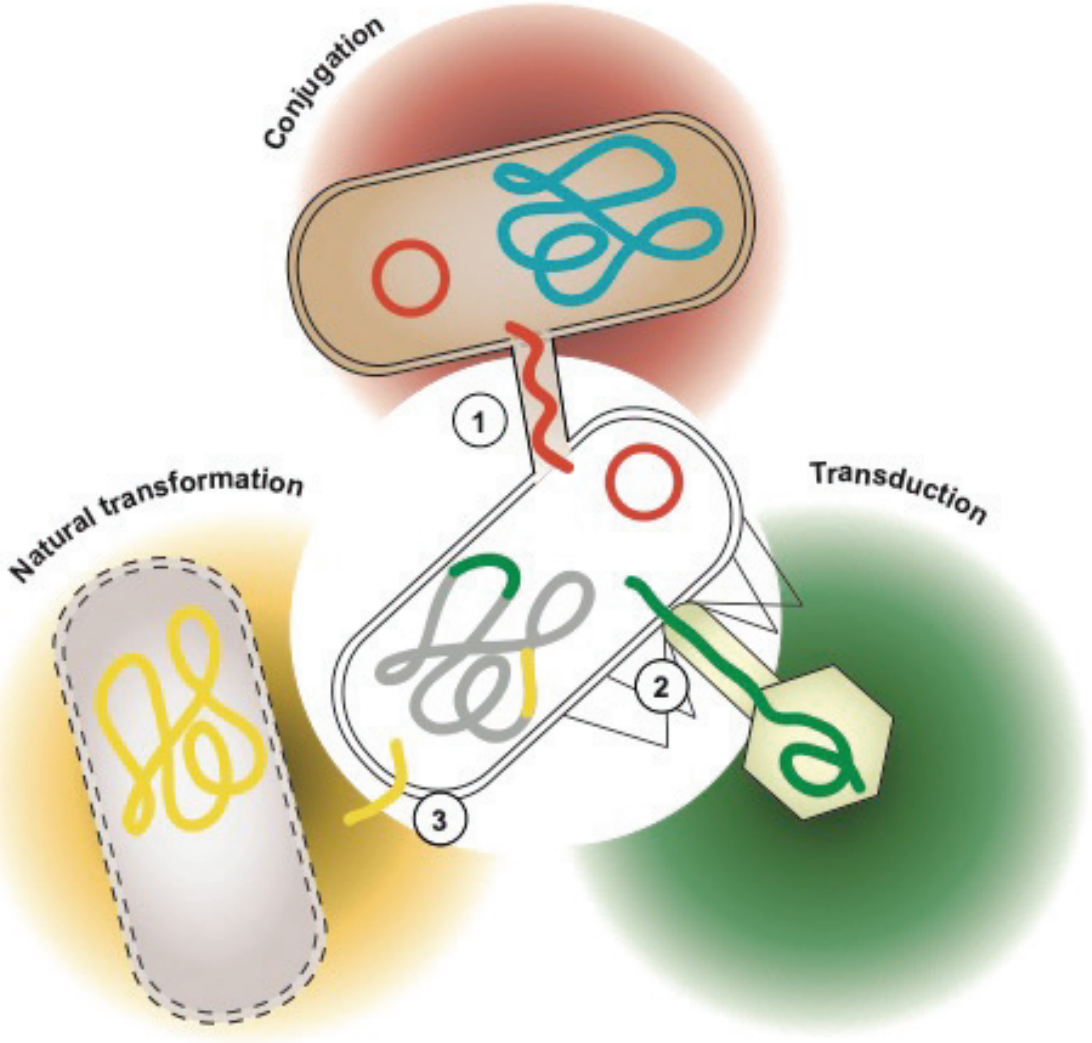

Figure 1.1: Major modes of horizontal gene transfer. This representative scheme shows the three major modes of HGT, which are numbered (① to ③). ① Conjugation leads to the transfer of DNA from a donor (beige bacterium) to a recipient (white bacterium) cell. Conjugative plasmids (as represented, here in red) or integrative and conjugative elements (ICEs) can be acquired through conjugation. Acquired plasmids replicate autonomously, whereas ICEs are integrated into the recipients' chromosome. ② Transduction represents the process by which bacteriophages are injecting DNA (in green) into the cytoplasm of a recipient cell. The DNA transferred by this mean is either of phage origin or derived from a previously infected bacterium in which case host DNA was accidentally packaged into the phage capsid during the lytic cycle. ③ Natural transformation is the process by which free DNA from the environment (e.g., released by bacterial lysis, as represented by the gray bacterium) is taken up by the competent cell. The recipient bacterium needs to enter the competence state to perform this process.

1.1.2.2 TRANSPORT OF DNA FROM THE EXTRACELLULAR MILIEU TO THE BACTERIAL CYTOPLASM

During the process of natural transformation, the T4P and additional competence proteins are required to proceed to the efficient acquisition and integration of DNA into the bacterial chromosome. In the following paragraphs, the transport of DNA will be described starting with the acquisition of exogenous DNA from the environment until its recombination into the genome (Fig. 1.2).

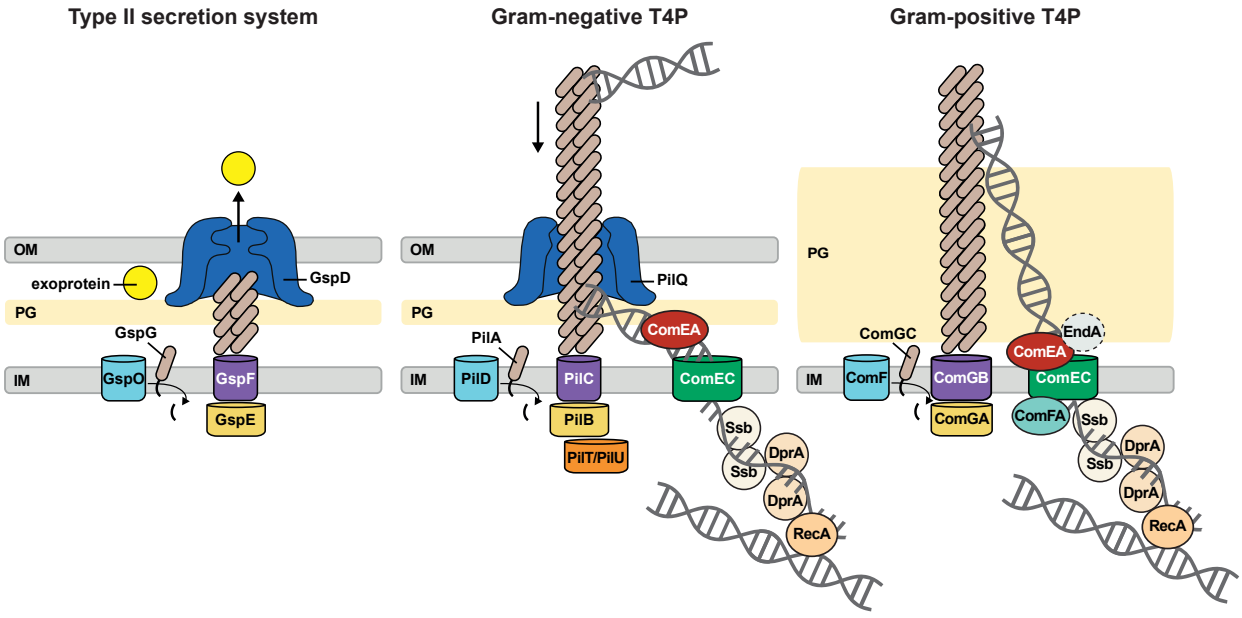

Figure 1.2: Comparison of the type II secretion system with the T4P of the DNA-uptake machinery in Gram-negative and Gram-positive bacteria. Scheme representing secretion by the type II secretion system and DNA acquisition by the DNA-uptake machinery in Gram-negative or Gram-positive bacteria. For simplicity, not all components are shown. Conserved components are depicted with the same color code. The prepilin peptidase (light blue) cleaves the signal peptide of the major pilins (brown), which are assembled into a pilus at the inner membrane complex (purple). ATPases mediate the pilus elongation and retraction (yellow and orange, respectively). In Gram-negative bacteria, the pilus crosses the outer membrane through a secretin channel (dark blue). For the acquisition of DNA, the DNA-binding protein (red) pulls the DNA, which is then further translocated into the cytoplasm through an inner membrane channel (green). In the cytoplasm, the absorbed and by now single stranded DNA is protected by single-strand DNA-binding proteins such as Ssb and DprA (in shades of light orange) and further recombined into the bacterial genome by RecA. The protein EndA is represented as a dashed circle as it is not present in all Gram-positive bacteria. Abbreviations: OM, outer membrane; PG, peptidoglycan; IM, inner membrane; T4P, type IV pilus. Figure based on ([29,30])

The mechanism of initial DNA binding remains unknown in several competent bacteria and might vary among species. The first step of the DNA uptake is dependent on the T4P, and it is currently thought that the DNA is acquired through direct interaction with the pilus

and subsequent retraction. The DNA-uptake machinery has been extensively studied in the Gram-positive bacterium *Bacillus subtilis*, in which it was first characterized in details. In *B. subtilis*, the DNA-uptake machinery is composed of a competence pseudopilus formed of a major pilin (ComGC; Fig. 1.2). However, DNA does not bind to the ComGC proteins of the pilus ([33]). In a recent study, Mirouze and colleagues showed that, during competence, the glycopolymers named teichoic acids, which are attached to the peptidoglycan layer of the cell wall, are modified to mediate the initial DNA-binding at the surface of *B. subtilis* cell ([34]). In *Streptococcus pneumoniae*, it was recently determined that the T4P structure directly binds exogenous DNA ([35]). Indeed, the competence pilus of *S. pneumoniae*, which is composed of the major pilin ComGC, was shown to function as the primary receptor for DNA binding although the exact binding mechanism remains unclear as the major pilin did not bind directly to DNA *in vitro* ([36]).

Interestingly, the Gram-negative *Neisseria* species and *Haemophilus influenzae* acquire only DNA from their own specie due to the presence of specific sequence motifs in their genomic DNA. These specific sequence motifs are called DNA uptake sequence (DUS) and uptake signal sequence (USS) for *Neisseria* species and *H. influenzae*, respectively ([37–39]). In *Neisseria*, the DNA receptor protein mediating binding to DUS was identified as being the minor pilin subunit ComP, which is exposed at the surface of the T4P ([40,41]). However, no homologue of ComP was identified in *H. influenzae,* leaving the specific DNA-binding receptor unknown in this bacterium. A similar DNA-binding mechanism was recently identified in *V. cholerae*. Two minor pilins subunits (VC0858 & VC0859) play a role in the pilus-DNA binding process. These minor pilins might localize at the tip of the T4P and could potentially be initial receptors for DNA binding ([42]). However, in contrast to the species-specific DNA binding observed in *Neisseria* and *H. influenzae*, the DNA-uptake in *V. cholerae* displays no differentiation between species-specific and species-unspecific DNA ([43]).

It is thought that the retraction of the pilus allows the first step of DNA translocation. However, the potential pilus-DNA interaction is not sufficient to drag DNA across the cell wall in case of Gram-positive bacteria or across the outer membrane secretin pore (PilQ) in case of Gram-negative bacteria. Instead, a DNA-binding protein, ComEA (Fig. 1.2) is also required to mediate efficient natural transformation as shown in e.g. *B. subtilis, S. pneumoniae,* and *V. cholerae* ([29,44,45]). This DNA-binding protein is highly conserved and binds to DNA in a non-sequence-specific manner due to its two helix-hairpin-helix domains

([46]). In Gram-positive bacteria, ComEA is anchored to the membrane, whereas it is localized to the periplasm in Gram-negative bacteria ([33,45,47]). Based on data in the latter organisms, it was suggested that the incoming dsDNA is pulled inside the periplasm by a Brownian ratchet mechanism exerted by ComEA. Indeed, the binding of ComEA to DNA prevents the retrograde movement of DNA and therefore fosters uptake ([45,48]). A similar mechanism was proposed for the uptake of the DNA across the peptidoglycan layer of Gram-positive bacteria.

After ComEA triggers absorption, the incoming DNA is further translocated into the cytoplasm via the inner membrane channel ComEC ([45]). ComEC is highly conserved in both Gram-positive and Gram-negative bacteria (Fig. 1.2). Previous studies support the idea that only a single strand of the incoming DNA passes through ComEC. However, it is currently unclear for most competent bacteria how the ComEA-bound dsDNA is converted into single-stranded DNA (ssDNA). Indeed, the degradation of one strand was only conclusively shown for the EndA nuclease of *S. pneumoniae* (Fig. 1.2; [29]). However, *in silico* analysis performed in *B. subtilis* showed that the C-terminal domain of ComEC might function as a nuclease. It was therefore proposed that ComEC might not solely act as a translocase in this organism but also as a nuclease that could degrade one strand of DNA concomitantly to the translocation process ([49]). In Gram-positive bacteria such as *B. subtilis* and *S. pneumoniae,* an additional ATPase (ComFA; Fig. 1.2) is thought to be involved in the translocation of the ssDNA across the cytoplasmic membrane ([24,29]).

Finally, after translocation of the incoming genetic material, the ssDNA-binding proteins Ssb and DprA (DNA processing A) will be loaded onto the DNA (Fig. 1.2) and protect it from nuclease-mediated degradation ([50]). DprA further promotes the loading of the recombinase RecA onto the ssDNA, which ultimately catalyzes the homologous recombination ([51]). Indeed, the nucleoprotein filament formed by RecA-ssDNA catalyzes a strand exchange in a region of sufficient homology between the incoming ssDNA and the recipient's genome. This leads to the formation of a heteroduplex between the incoming/transforming DNA and recipient's DNA, which will be converted to homogeneous dsDNA through DNA replication and cell division ([17,52]). Therefore, DprA and RecA are essential proteins for natural transformation, as demonstrated for example in *V. cholerae* and *S. pneumoniae* ([43,44,50,52]).

1.1.2.3 BENEFITS OF NATURAL TRANSFORMATION

The evolutionary advantages of DNA uptake by competent bacteria remain unclear. To date, three main hypotheses have been discussed, which suggest that DNA is either used as a source of nutrient, for repair purposes, or for evolution. Indeed, bacteria could use DNA as a food source, as the sugars, phosphates, and nitrogenous bases of DNA are important nutrients and *de novo* nucleotide synthesis is a costly process ([53]). A previous study by McDonough and colleagues demonstrated that *V. cholerae* could use nucleotides as a phosphate source to sustain growth using extracellular nucleases and phosphatases. Based on their results, the authors proposed a model in which the nucleotides released by nucleases can cross the outer membrane through porins and then are cleaved by phosphatases (PhoX, CpdB, AshA). The released phosphates are further transported into the cytoplasm by the phosphate specific transport system ([54]). Currently, limited support has been provided to support the theory that competence has primarily evolved to acquire DNA as food or building blocks. One major reason that somewhat contradicts this hypothesis is that DNA entering the cytoplasm of the cell via natural competence is specifically protected against degradation as explained above (by Ssb and DprA; Fig. 1.2; [50,51,53]). This protection would not be required if the purpose of the incoming DNA would be to provide premade nucleotides. Instead, the fact that the competent bacterium aims at keeping the incoming DNA intact suggests its ultimate integration into the genome.

B. subtilis was used as a model to investigate whether natural competence could be a benefit for the repair of DNA damage. In condition of high cell density and nutritional limitation, the competence is induced in *B. subtilis.* Moreover*,* in the population of *B. subtilis*, only a minority of cells enter competence ([55]). In their study, Michod and colleagues used increasing dosage of UV light to cause DNA damage in *B. subtilis*. Next, transforming DNA was added before or after UV irradiation and the proportion of transformed "sexual" cells was calculated in comparison to the number of "asexual" cells. Interestingly, when DNA was added after UV irradiation, the proportion of transformed cells increased. In contrast, the frequency of transformed cells decreased when DNA was added before UV treatment. The authors concluded that the enhanced survival of transformed cells is either explained by an enhanced transformation rate due to DNA damages, or, by an increase survival of damaged cells, which had repaired the deleterious damages caused by the UV treatment. These two hypotheses support the usage of transformation as a DNA repair mechanism ([56]). However it is still unclear whether *B. subtilis* can indeed increase its competence under DNA-damaging

conditions according to a study from Redfield in 1992 ([57]). Moreover, it was further shown that DNA damaging agents induce competence in few transformable bacteria (e.g. *H. pylori* ([58]), *Legionella pneumophila* ([59]), and *S. pneumoniae* ([60])). However, there are also contradictory results as bacterial strains lacking essential proteins for DNA uptake did not show an increased sensitivity to genotoxic agents ([58,59]).

Another relevant information to support the hypothesis that natural transformation is used for DNA repair is that several competent bacteria, such as *H. influenzae* and *Neisseria* species, preferentially acquire DNA from the same or a closely related species as they contain specific sequence motifs (DUS) ([37–39,61]). Interestingly, Davidsen and colleagues shown that the highest frequencies of DUSs are present in genes involved in DNA repair and recombination ([62]). The authors proposed that the integrity of the repair machinery is maintained through a potential preference in the acquisition of genes implicated in genome maintenance. Indeed, such important genes when damaged by genotoxic agents should have first priority when it comes to DNA repair.

In addition, fratricide (killing of siblings) represents another strategy for the acquisition of species-specific DNA. The competent *S. pneumonia* cells acquire DNA from their siblings by secreting toxic cell-wall targeting enzymes that lyse non-competent siblings ([63]). The killing of these kin bacteria leads to the release of highly homologous DNA that can serve for repair purposes in the competent attacking cell.

The last hypothesis that aims to explain the evolutionary advantage of maintaining natural competence suggest that transformation increases genetic diversity by the acquisition of new genes. However, one might wonder whether bacteria would often have the possibility to acquire intact DNA of sufficient coding capacity in their natural environment. Indeed, even if free DNA is abundant in the environment, the majority of this pool of DNA is highly fragmented ([64,65]). Such damaged DNA fragments will not permit the transfer of intact genes or even larger gene clusters. Similarly, it was also argued that exogenous DNA would hardly be beneficial for evolution or repair as it was released from dead bacterial cell ([66,67]). The underlying rationale is that these bacteria were less adapted and died because of this fitness disadvantage. However, the acquisition of large DNA fragments, including GEIs, was reported to occur by natural transformation, as for example mentioned above for pathogenic *S. pneumoniae*. Indeed, the genes that encode the polysaccharide capsule, which were transferred by natural transformation in Griffith's experiment, are carried on a GEI ([70]). Thus, DNA acquired by natural competence can foster evolution and the emergence of pathogenic

bacteria. Similarly, exchange of the O-antigen region was observed in *V. cholerae*. The O-antigen, which is a component of the outer membrane lipopolysaccharides, is exposed at the surface of the cell and represents a target for host antibodies and a receptor for environmental phages ([71]). The O-antigen is variable between bacterial species and between strains of same species. In *V. cholerae,* the O-antigen cluster can be acquired from different serogroup strains via natural transformation, a process known as serogroup conversion ([72]). In addition to O-antigen diversity, comparative genomics also shed light on the high genetic diversity of *V. cholerae* ([73,74]). For example, Chun *et al.* compared 23 different strains of *V. cholerae* and identified in total 73 different GEIs, including several PAIs. The authors concluded that "*V. cholerae* undergoes extensive genetic recombination via lateral gene transfer" ([73]). To study how competence for transformation can shape bacterial genomes might therefore help us to better understand the evolution of *V. cholerae* and, potentially also, explain how pathogenic variants of it arose.

1.2. *VIBRIO CHOLERAE*

The Gram-negative bacterium *V. cholerae* belongs to the family of *Vibrionaceae*. It is a comma-shaped bacterium of roughly 1-2 μm, which is motile by its single polar flagellum (Fig. 1.3; [75,76]). *V. cholerae* is the causative agent of the diarrheal disease cholera. The first link between the disease and the pathogen was made in 1854 by Dr. Filippo Pacini, who observed *V. cholerae* in intestines of corpses of the cholera epidemic in Italy ([77–79]). Pacini described the bacterial disease as a massive loss of fluid and electrolytes (sodium, chloride and potassium). In addition, Pacini recommended intravenous injection of saline solution in case of extreme dehydration ([78,80]). Unfortunately, at that time, the scientific community ignored the data of Pacini ([77]). Thirty years after Pacini's discovery, Robert Koch isolated *V. cholerae* during a cholera epidemic in India ([75]). Since then, many studies have focused on the physiology and the epidemiology of this organism.

A first complete genome of *V. cholerae* was published in 2000 by Heidelberg *et al*., which is composed of two chromosomes: a large chromosome (chr 1) of 2.96 Mbp and a small chromosome (chr 2) of 1.07 Mbp ([81]). The large chromosome encodes essential cell functions as well as the primary PAIs, whereas the small chromosome contains several hypothetical genes and is thought to have originated from a megaplasmid. The small chromosome also contains a large gene capturing system called the integron island ([82]).

Comparative genomics are of major importance to understand how environmental bacteria evolve towards pathogens. Since the first whole genome sequence in 2000, over 1'000 clinical and environmental *V. cholerae* isolates were sequenced. Several comparative genomics and phylogenetic analyses studies have shed light onto the global spread of cholera and onto the evolution of this pathogen ([83–86]).

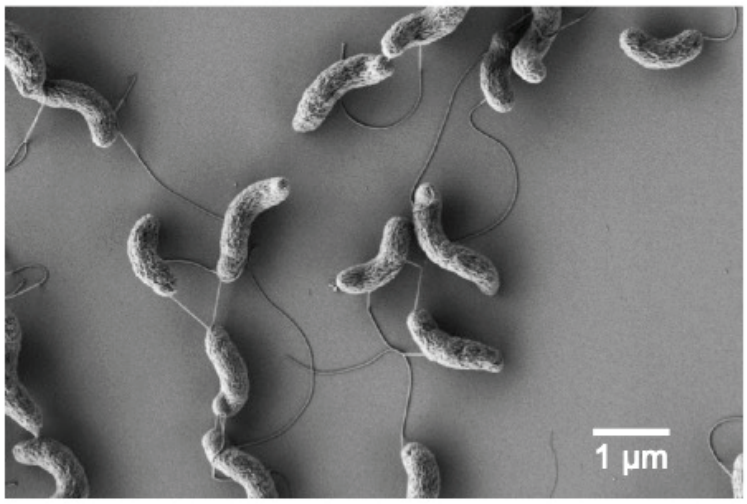

Figure 1.3: Scanning electron micrograph of the Gram-negative bacterium *V. cholerae*. The picture shows the curvature (comma-shape) of *V. cholerae* as well as its single polar flagellum. Scale bar: 1 µm as indicated. Sample preparation and image credits: Melanie Blokesch and Graham Knott (EPFL BioEM facility).

1.2.1 CHOLERA DISEASE

V. cholerae is the causative agent of the diarrheal disease cholera. The disease is considered to have originated from the Indian subcontinent and has spread rapidly in all major continents ([79,80,87,88]). Cholera is still a major health problem and is endemic in more than 47 countries. Cholera is characterized by acute diarrhea with fluid losses up to 1 liter per hour for severe cases and this fluid loss can even be enhanced due to concomitant vomiting of the patients. If left untreated, severe cases can rapidly dehydrate and die within few hours ([79,89,90]). In contrast to developed countries where cholera is extremely rare and mostly caused by imported cases, there are still an estimated 1-3 million annual cholera cases (1'227'391 estimated cases reported in 2017; [91]) in developing countries with thousands of people dying of the disease every year. Indeed, cholera mostly occurs in areas with lack of potable water, inadequate hygiene and sanitation. However, cholera reporting is not mandatory, which leads to epidemiological data that most likely underestimate the actual numbers of cases. Cholera affects people from all ages, although high morbidity and mortality numbers are especially recorded in children ([92]). It was also observed that the genetics of the host influenced the

severity of the illness, as individuals of blood type O are more susceptible to severe cholera infection ([93]). On the other hand, some infected patients do not develop the symptoms. And while the process of asymptomatic carriage is still not well understood, such individuals might contribute also to the rapid propagation of the disease by disseminating the bacteria back into the environment ([89]).

Drinking clean water, eating cooked food and a good hygienic behavior, such as handwashing with soap after defecation and prior contact with food, are recommendations that can efficiently prevent cholera infection. However, poverty and poor hygiene are of major concern in developing countries and cause great difficulties with respect to the prevention of the disease. In addition, natural disasters such as earthquakes, floods or droughts affect water resources and, therefore, intensify the risk of cholera outbreaks by increasing the risk of exposure to the pathogen ([80,88,90]).

Individuals get infected through the ingestion of contaminated food or water. Based on volunteer studies, it was shown that more than 10^8 bacterial cells are needed to induce symptoms that are associated with cholera infections. After the ingestion of such high number of pathogenic *V. cholerae*, some bacteria survive the passage through the acid barrier of the stomach. These cells colonize the epithelium of the small intestine, which is facilitated by a T4P called the toxin-coregulated pilus (TCP). TCP together with cholera toxin (CTX) are the two major virulence factors of this pathogen and the latter is primarily responsible of the diarrheal disease symptoms. Indeed, after colonization in the small intestine, *V. cholerae* produces CTX, which itself is secreted by the T2SS into the extracellular environment. The CTX, which is composed of an active (A) subunit and five smaller binding (B) subunits, is translocated into intestinal epithelial cells wherein it indirectly activates the adenylate cyclase leading to increased cyclic AMP (cAMP) levels. This increased cAMP level causes the opening of the main chloride channel and, therefore, deregulates the efflux of water and electrolytes. The loss of water and electrolytes ultimately leads to severe diarrhea ([89,94–97]). Notably, the typical rice-water stool shed by cholera patients can contain up to 10^9 virulent *V. cholerae* colony forming units (CFU) per milliliter, which contributes to the rapid propagation of the disease ([98]). TCP and CTX are encoded in two distinctive genomic regions, which were horizontally acquired by *V. cholerae*. Indeed, the genes encoding the TCP pilus are part of a large cluster known as the *Vibrio* pathogenicity island 1 (VPI-1). The cholera toxin is encoded by the filamentous phage CTXϕ, which is integrated into the chromosome of *V. cholerae* as a prophage. Interestingly, the receptor used by CTXϕ to enter

the bacterial cell is TCP, which suggests that TCP was acquired prior to the integration of the prophage CTXϕ ([99]).

Fortunately, cholera can be treated and the rate of mortality (case-fatality rate; CFR) is low in case of appropriate treatment. The treatment consists of an oral rehydration therapy, which was developed in the 20th century and consists of oral infusion of water and electrolytes. This therapy is successful in 80% of the cases and lead to a CFR below 1% (0.5% in 2017, [91]). For extreme cholera cases antibiotics are added to the oral rehydration solutions to accelerate the recovery and shorten the duration of the disease. Vaccines also exist against *V. cholerae*, even though the first vaccine attempts failed in containing the disease. Nowadays an oral vaccine produced with dead cells is available and can play an important role in preventing cholera outbreaks. However the vaccine confers short-term protection and is, therefore, not an optimal solution to completely eradicate the disease ([79,80,96]).

1.2.2 CHOLERA PANDEMICS AND GENETIC DIVERSITY OF *V. CHOLERAE*

While hundreds of *V. cholerae* strains have been isolated so far, only a fraction of these strains is able to cause disease. More than 200 serogroups of *V. cholerae* have been classified based on the sugar composition of their surface O-antigen, which is a component of the outer membrane lipopolysaccharides. However, only the O1 and O139 serogroups have been associated with pandemic and epidemic cholera. Other *V. cholerae* strains, which occasionally cause diarrhea, are therefore classified as non-O1 non-O139 serogroups (Fig. 1.4). The O1 serogroup is further divided into two biotypes, classical and El Tor and in two serotypes, Ogawa and Inaba ([74,80,100,101]).

Even if cholera outbreaks have been reported in the 16th century and before, the first officially recorded cholera pandemic occurred in the 19th century. Six pandemics were recorded ever since (e.g., between 1817 and 1961) and all of these pandemics were thought to have been caused by the O1 classical biotype of *V. cholerae*. The currently ongoing seventh pandemic is the longest pandemic ever recorded. It began in 1961 in Indonesia and the causative agent responsible for this pandemic was categorized as O1 El Tor biotype ([79,88]). In comparison to the classical biotype, the O1 El Tor biotype carries two newly acquired gene clusters called *Vibrio* seventh pandemic islands I and II (VSP-I & VSP-II). VSP-I encodes a nucleotide cyclase gene (*dncV*) that plays a role in pathogenicity by promoting efficient

intestinal colonization ([102]), whereas the potential epidemiological function of VSP-II is not yet fully established ([103,104]). The El Tor biotype is considered to be more environmentally fit than the classical biotype, due to its capacity to take over the classical biotype during the last pandemic. By contrast the classical biotype is more virulent as it produces a larger amount of variant of the cholera toxin ([105,106]). Importantly, variations of the clinical El Tor isolates of *V. cholerae* occurred since 1995. These so-called hybrid strains produce classical-type cholera toxin while maintaining an El Tor-like genomic backbone ([107,108]). These strains are therefore thought to benefit from higher virulence and environmental persistence, which contribute to their dispersion around the globe ([80]).

As stated above, both O1 and O139 serogroups are causing the diarrheal disease. The O139 serogroup was first identified as the causative agent in 1992 in Bangladesh and India. At that time, the O139 serogroup spread rapidly across South-East Asian countries raising the fear of the beginning of a 8th cholera pandemic ([109]). Ten years later another cholera outbreak caused by O139 serogroup strains led to the same concern ([110]). However in both situations, the O139-associated cholera cases declined and the overall disease burden was therefore not considered as a separate pandemic compared to the ongoing O1 El Tor-caused 7th pandemic.

Remarkably, the emergence of the O139 serogroup was most likely the result of a HGT between a (donor) non-O1 and an acceptor O1 El Tor strain, as, apart from the O antigen encoding region that for O139 also carries the information for a polysaccharide capsule, both strains are genetically very similar to each other ([111–113]). In addition, Blokesch and Schoolnik provided experimental evidence that such O1-to-O139 serogroup conversion can easily occur in the natural environment of *V. cholerae*. More particularly, they showed that the entire O-antigen region (42 kbp) from the O139 serogroup could be acquired by the O1 serogroup strain by mean of natural transformation, demonstrating the evolutionary impact of HGT in pathogen emergence ([72]).

1.2.3 NATURAL HABITAT OF *V. CHOLERAE*

Until the early 1980s, the normal habitat of *V. cholerae* was thought to be the human gut. This idea originated as *V. cholerae* could not be isolated from the aquatic environment except in cases of epidemic. Colwell and colleagues were the first to show that *V. cholerae* was an aquatic bacterium ([114,115]). More advanced techniques led to the frequent isolation of both O1

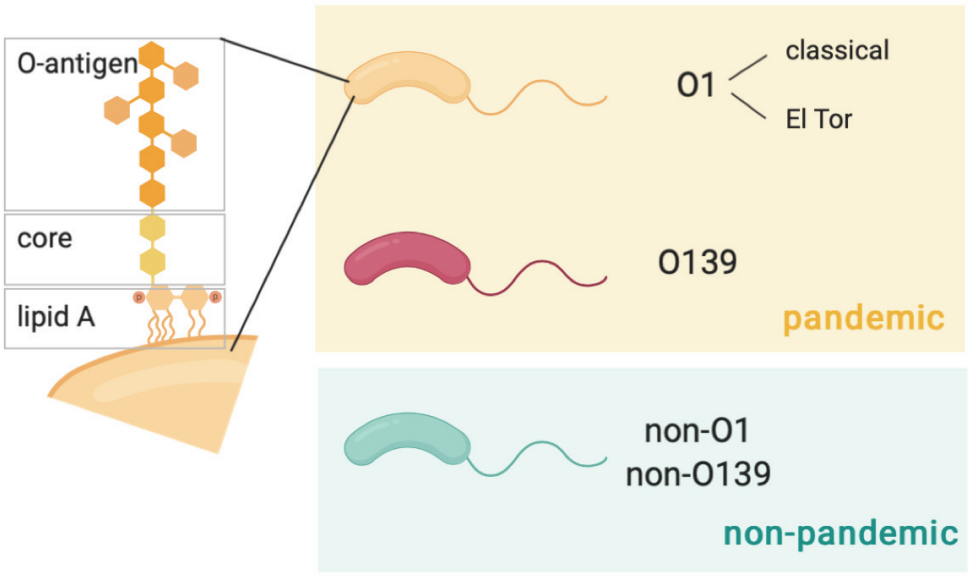

Figure 1.4: Schematic representation of the serogroups of *V. cholerae*. Strains of *V. cholerae* have been classified based on the composition of the O-antigen of their outer membrane lipopolysaccharides (LPS). A general scheme of the LPS is represented. From the more than 200 existing serogroups, only serogroup O1 and O139 are responsible of cholera pandemics. The O1 serogroup is divided into two biotypes, classical and El Tor. Other non-pandemic serogroups are usually classified as non-O1 non-O139. Figure created with BioRender.com

and non-O1 strains of *V. cholerae* in the aquatic environment and it is now clear that *V. cholerae* is a common inhabitant of aquatic ecosystems, like other members of the *Vibrionaceae* ([116,117]). *V. cholerae* is found in estuaries, costal water and rivers, where it lives as a free-living organism or associated with abiotic and biotic surfaces such as phytoplankton and zooplankton. The exoskeletons of marine organisms provide a source of nutrients to the bacteria and, in addition, the bacterial growth on such biotic surfaces leads to increased stress resistance, which altogether confers an ecological advantage. Importantly, the capability to survive and replicate to high number has also an epidemiological impact ([118–120]). Indeed, as high numbers of cells are necessary to cause cholera infection, it was suggested that the natural mode of transmission could be via ingestion of infective *V. cholerae* biofilms. As the exoskeletons of zooplankton such as copepods were found with up to 10^4 bacteria attached to them, the association and growth of *V. cholerae* on such biotic surfaces was considered as a considerable risk for ingestion of the infectious dose required to cause disease symptoms ([97,118,121]). Interestingly, it was shown that the removal of large particles (> 20 µm) through filtration of collected water using a sieve of folded sari cloth led to a 48% reduction in cholera burden in rural Bangladesh ([122]). As free-living *V. cholerae* cells of around 1 micron in size would not be retained during this filtration procedure, it was concluded that *V.*

cholerae cells attached to plankton or other (biotic) surfaces might be responsible for cholera outbreaks in the control villages in which filtration was not practiced.

Environmental and climatic factors are also thought to impact cholera outbreaks in endemic areas. For example, the seasonal variations in Bangladesh, due to monsoon, affect the sea surface water temperature and are associated with planktonic blooms and cholera outbreaks ([123,124]). In this endemic region, two peaks of cholera outbreaks occur seasonally and correlate with increased water temperature. Environmental factors such as rainfall, variation of water salinity, pH, or temperature, and plankton population have an impact on the ecological fitness of *V. cholerae* and, therefore, influence the appearance of outbreaks ([119,125–128]). Few studies have reported associations of *V. cholerae* with larger marine animals such as turtles or fish but the relevance of these associations for cholera transmission is still unknown ([129–131]).

As mentioned above, the association of *V. cholerae* to phyto- and zooplankton, which represent a source of nutrient, is thought to bring an ecological advantage to the bacterium. Furthermore, this relationship has an influence on the evolution of *V. cholerae*. The major component of the exoskeleton of zooplankton is chitin. Chitin is a polymer of N-Acetylglucosamine (GlcNAc) and it is the most abundant carbon source in the aquatic environment ([97,132,133]). Besides being a source of carbon and nitrogen, chitin induces natural competence in *V. cholerae* ([134]).

1.2.4 REGULATION OF NATURAL COMPETENCE IN *V. CHOLERAE*

The cascade inducing natural competence in *V. cholerae* is tightly regulated and depends on the following environmental factors: chitin sensing, carbon catabolite repression (CCR) and quorum sensing (QS) ([43,134–137]). The next paragraphs will focus on the regulatory circuit of natural competence leading to the production of the DNA-uptake machinery in *V. cholerae*.

1.2.4.1 CHITIN SENSING

V. cholerae and other marine bacteria colonize chitin and degrade it to obtain the nutrients. Different factors are implicated in the adhesion of *V. cholerae* to chitinous surfaces (e.g. zooplankton) such as the GlcNAc-binding protein GbpA and the mannose-sensitive hemagglutinin pilus (MSHA). MSHA is a T4P that promotes adherence to biotic surfaces and

that participates in biofilm formation ([133,138–142]). After attachment, extracellular chitinases secreted by *V. cholerae* degrade chitin into short oligomers with dimers of N-Acetylglucosamine [$(GlcNAc)_2$ or chitobiose] being primarily released. These dimers are further transported through outer membrane porins into the periplasm, which initiate the chitin-signaling cascade through the activation of the sensor kinase ChiS ([143]). The exact regulatory cascade is still unknown, however ChiS activation results in the expression of the master regulator of transformation, *tfoX*. Moreover, it was shown that chitin sensing not only results in transcriptional activation but also in translational activation of *tfoX* ([144]). The latter translational activation is signaled through another chitin sensor, the transmembrane regulatory protein TfoS. TfoS promotes the transcription of the small regulatory RNA *tfoR*. In the presence of the RNA chaperone Hfq, this sRNA interacts with the *tfoX* mRNA thereby releasing the Shine-Dalgarno sequence for translation initiation (Fig. 1.5A; [137,143,145–147]). Yamamoto and colleagues also suggested that ChiS might enhance TfoS activity; however, the mechanism remains unknown. Interestingly, it was shown that these regulators are highly conserved in diverse *Vibrio* species, suggesting that natural competence for transformation might be a conserved mechanism ([143,145,146]). Once TfoX is produced in *V. cholerae*, this regulator induces directly and indirectly expression of the competence genes, which code for the DNA-uptake machinery that is required for natural transformation (Fig. 1.5A; Fig. 1.6B). The competence genes that are thought to be directly regulated by TfoX encode components of the DNA-uptake pilus (*pilABCD, pilMNOPQ* ; [43,133–136]).

1.2.4.2 CARBON CATABOLITE REPRESSION

Even though TfoX is essential to induce competence, it was demonstrated that it is not sufficient ([134,149,150]). Carbon catabolite repression (CCR), a phenomenon that allows bacteria to respond and adapt to the availability of sugars, induces competence in condition with limiting preferred carbon source ([149]). Several preferred sugars such as glucose are transported into the cell by the phosphoenolpyruvate-carbohydrate phosphotransferase system (PTS). When the environment lacks such preferred carbon sources, the PTS system and its associated signaling cascade activates the enzyme adenylate cyclase to produce cyclic adenosine monophosphate (cAMP). The rise of cAMP in the cell leads to the formation of an active complex between the cAMP receptor protein (CRP) and cAMP (Fig. 1.5B), which allows the bacteria to metabolically adapt to alternative sugars ([151,152]). In addition, the active

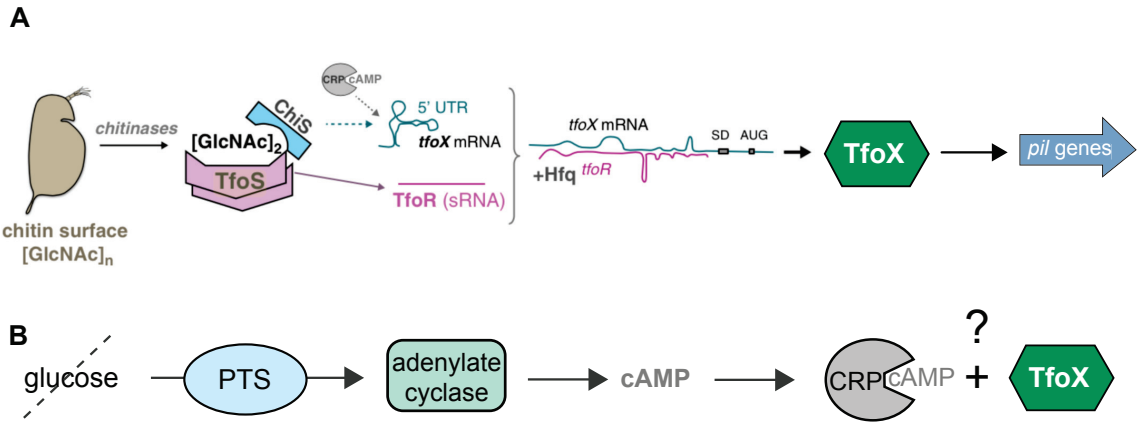

Figure 1.5: Chitin sensing and carbon catabolite repression activate competence. (A) Production of the master regulator of transformation TfoX upon chitin sensing. Figure adapted from ([148]). *V. cholerae* cells grow on chitin surfaces (e.g., exoskeleton of zooplankton) and degrade chitin using extracellular chitinases. These enzymes release chitin oligosaccharides such as $(GlcNAc)_2$, which are detected by two chitin sensors (TfoS, ChiS). ChiS, as well as the complex of CRP-cAMP, positively regulate *tfoX* transcription. TfoS promotes the transcription of the sRNA TfoR, which allows the translation of the *tfoX* mRNA by exposing the Shine-Dalgarno (SD) sequence. The base pairing of TfoR to *tfoX* mRNA requires the RNA chaperone Hfq. The master regulator of transformation TfoX regulates the genes encoding the central pilus structure of the DNA-uptake machinery (*pil* genes). (B) Activation of competence by carbon catabolite repression. In absence of a preferred carbon source such as glucose, the unsaturated PTS indirectly activates the adenylate cyclase, which leads to increased levels of the secondary messenger cAMP. High levels of cAMP result in the formation of an active complex between CRP and cAMP. Supposedly, this complex, in combination with TfoX, leads to the activation of competence genes. Abbreviations: PTS, phosphoenolpyruvate-carbohydrate phosphotransferase system; cAMP, cyclic adenosine monophosphate; CRP, cAMP receptor protein.

cAMP-CRP complex leads to the induction of natural competence genes. Consistently, in presence of PTS sugar like glucose the competence of *V. cholerae* is significantly reduced ([134,149]). Although the exact mode of action activating competence genes through CCR remains unclear, it was recently shown that the complex of cAMP-CRP binds to the promoter region of *tfoX* and initiates its transcription (Fig. 1.5A; [153]). However, the importance of CCR in competence induction cannot be limited to the activation of *tfoX*. Indeed, a previous study showed that the artificial expression of TfoX could not restore the transformability in knockouts strains deficient in the adenylate cyclase (producing cAMP) and CRP, demonstrating their requirement in competence regulation downstream of TfoX ([149]). Based on observations on the TfoX homolog in *H. influenzae* it was thought that the active cAMP-CRP complex, in concert with TfoX, binds specific DNA sequence motifs to promote competence genes transcription (Fig. 1.5B; [149,154]). However, work from our lab does not support this assumption.

1.2.4.3 QUORUM SENSING

The third environmental factor required for competence induction is high cell density, which is detected by quorum sensing (QS) ([43,134,150]). QS is a process of bacterial communication based on the production and sensing of small molecules. These molecules, named autoinducers, are produced and secreted into the environment, where they are sensed by neighboring bacteria and report back on cell density. The concentration of autoinducers increases as the bacterial population grows, which enables the bacteria to modulate and switch gene expression between low and high cell density ([155,156]). *V. cholerae* produced two major autoinducers: Cholera Autoinducer 1 (CAI-1) and Autoinducer 2 (AI-2), which serve for intra- and interspecies communication, respectively ([157–159]). The autoinducers are detected by several QS receptors ([160]), which are mostly two-component sensor histidine kinase containing both kinase and phosphatase activities. At low cell density, when the concentration of autoinducers is low, the QS receptors act as kinase and ultimately leads to the phosphorylation of the transcription factor LuxO. The latter induces the expression of a set of four small regulatory RNAs (Qrr1 to 4), which then post-transcriptionally repress the master regulator of QS, *hapR* ([161,162]). At high cell density, the autoinducers bind to the QS receptors, which switch to phosphatase activity accordingly. This leads to the dephosphorylation of LuxO, which abolishes production of the Qrrs and therefore fosters production of HapR (Fig. 1.6A; [156,163]).

For natural competence, the intraspecies autoinducer CAI-1 plays the primary role ([43,135]). As alluded to above, HapR is produced at high CAI-1 concentrations and subsequently represses genes for virulence and biofilm formation while it indirectly activates a subset of the competence genes (see below; [135,164–167]). In addition, HapR plays a major role in natural transformation by repressing the nuclease *dns*. Two extracellular nucleases Dns and Xds are produced in *V. cholerae*; however, only Dns was shown to affect natural transformation. Moreover, previous studies showed that Dns is not only secreted into the extracellular milieu but also localized in the periplasm, where it can directly degrade transforming DNA ([45,150,168,169]). Thus, when HapR is not produced because of a low cell density state, exogenous DNA is degraded by Dns and cannot serve as transforming material. Indeed, it was shown that *V. cholerae* isolates that are deficient in QS (and therefore Dns overproducing) are not transformable, while *dns*-minus strains are hypertransformable. Consequently, the repression of *dns* through HapR binding in the gene's upstream region is crucial for natural transformation to occur (Fig. 1.6B; [135,150]).

In addition to the downregulation of *dns*, HapR positively regulates a subset of competence genes through an intermediate transcriptional regulator. This regulator is co-regulated by HapR and TfoX and was therefore named QS-dependent and TfoX-dependent regulator, QstR (Fig. 1.6B ; [167]). Previous studies showed that QstR further represses *dns* and that it also induces competence genes whose gene products are involved in the translocation of exogenous DNA over the outer and inner membrane (ComEA, ComEC; [45,135,167,170]). Interestingly, Jaskólska and colleagues also observed that the transcriptional activation of *comEA* was not directly mediated by QstR binding but rather involved another unknown intermediate regulator. In their study, the authors also identified that the competence genes *comM* and *comF* were positively regulated in a QstR-dependent manner (Fig. 1.6B ; [170]). ComF is thought to be involved in translocation across the inner membrane, whereas *comM* was shown to encode a helicase that promotes integration of heterologous DNA, as previously demonstrated for the homolog (RadA) in *Streptococcus pneumoniae* ([44,171–173]).

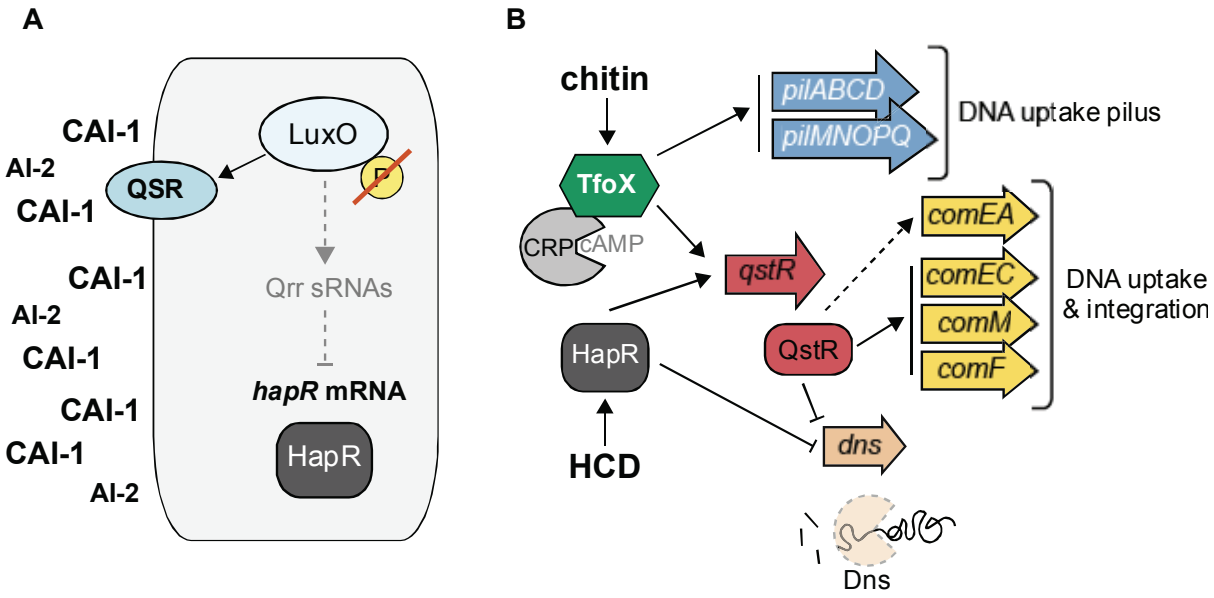

Figure 1.6: Competence regulation in *V. cholerae*. (A) Production of the master regulator of quorum sensing, HapR. The quorum sensing receptors (QSR) act as kinase or phosphatase according to the concentration of autoinducers detected in the environment. The scheme represents condition at high cell density when the autoinducers CAI-1 and AI-2 are abundant. The autoinducers bind to the quorum sensing receptors, which act as phosphatase. The signaling cascade is reverted and the transcription factor LuxO is dephosphorylated. This inactivates the production of the small regulatory RNAs (Qrr sRNAs), which would otherwise block the translation of *hapR*. (B) Model of competence regulation. Chitin sensing, limitation of preferred carbon sources and high cell density lead to the induction of competence by the production of TfoX and HapR. TfoX, which potentially works in concert with CRP-cAMP, induces genes encoding the DNA-uptake pilus. The remaining set of competence genes, required for successful DNA uptake, inner membrane translocation, and integration, are co-regulated by TfoX and HapR through the intermediate regulator QstR. In addition, HapR and QstR repress the transcription of the nuclease gene *dns*. The dashed line highlights that QstR does not bind the upstream region of *comEA* suggesting that another intermediate regulator might be required for *comEA* transcription. (A-B) Abbreviations: QSR, quorum sensing receptors; HCD, high cell density.

1.2.5 THE DNA-UPTAKE MACHINERY OF *V. CHOLERAE*

Upon growth to high cell density on chitinous surfaces, the regulators TfoX, HapR and QstR activate competence including those genes that encode the DNA-uptake machinery. The latter is required for the successful translocation of DNA across the bacterial cell envelope. Even though many questions remain open, studies in the last decade have shed light on the understanding of the DNA-uptake machinery of *V. cholerae* ([44,45,168,174]), as described in the following paragraphs.

At first, parts of the genes encoding the DNA-uptake machinery were discovered due to their transcription on chitin surfaces as assessed by microarray expression profiling ([133]). Meibom and colleagues named this set of genes predicted to encode a T4P, the chitin-regulated pilus (ChiRP). It is now clear that ChiRP proteins are part of the DNA-uptake complex produced during competence. Furthermore, based on expression profiling upon competence induction, homology to other naturally transformable bacteria and conservation in other *Vibrio* species, Seitz and Blokesch identified the minimum set of DNA-uptake machinery components in *V. cholerae.* The majority of these genes were predicted to encode proteins involved in the biogenesis and the structural components of a T4P ([44]). In accordance with a previous study that showed that *V. cholerae* takes up DNA in a species-unspecific manner ([43]), the DNA-uptake machinery did not contain any homolog of species-specific minor pilin ComP of *N. meinigitidis.* However, as the regulation of competence in *V. cholerae* involves species-specific autoinducers (CAI-1) a bias towards the uptake of DNA from closely related species might still occur in this organism ([43]).

1.2.5.1 THE TYPE IV PILUS AND ITS DYNAMIC

The T4P constitutes the central part of the DNA-uptake machinery and is encoded by the *pil* genes (*pilABCD*, *pilMNOPQ*, *pilF* and *pilT;* Fig. 1.7A). Among them, *pilA* is coding for the major pilin subunit of the T4P while *pilB* and *pilT* code for two ATPases that are involved in pilus elongation and retraction, respectively. The T4P was first visualized by Seitz and Blokesch using immunofluorescence microscopy in which a functional tagged version of PilA was detected. Using this technique in combination with fluorescently labeled fusion proteins, the DNA-uptake pilus was shown to be a *bona fide* T4P and to extends beyond the outer membrane pore complex formed by the secretin PilQ (Fig. 1.7A). The majority of the piliated cells displayed only a single pilus and its localization was not restricted to the cell

poles, as previously reported for *B. subtilis* ([44,175,176]). Moreover, based on microscopy imaging of diverse fluorescently labeled components of the DNA-uptake machinery, it was hypothesized that several preassembled membrane-bound scaffold components of the T4P are located around the cell periphery. However, pilus polymerization only occurs at one site at a time and seemed to be driven by the temporal interaction of the PilB ATPase with the scaffold structure ([44,175]).

In addition, two recent studies used a cysteine labeling approach to visualize the dynamics of the DNA-uptake T4P ([42,174]). In these studies, cells likewise displayed one or two pili with a length of around 1-2 μm even though pili up to 10 μm were also observed. The assembly and the retraction of the pilus appeared as highly dynamic with cells producing 1-2 pili per minute. Moreover, these two key studies showed that the entry of DNA into the periplasm followed pilus retraction events, which confirmed the previously proposed model of DNA uptake ([42,44,174]). In addition, Ellison and colleagues showed that the tip of the cysteine-labeled pilus could interact with large clusters of covalently labeled dsDNA and that a minor pilin was most likely involved in this binding. Among components of the DNA-uptake machinery, five minor pilins (VC0857-VC0861) have been previously identified, which could potentially be involved in pilus biogenesis ([44,177]) or, could be incorporated into the T4P and be implicated in DNA-binding, as shown for the minor pilin ComP of *N. meningitidis* ([40]). In their study, Ellison and colleagues hypothesized that non-specific DNA binding could be promoted by ionic interactions with these pilins. To test this idea, the authors generated site-directed mutants in which positively charged residue(s) were replaced by uncharged residue(s), and they identified reduced pilus-DNA binding with the two modified minor pilins VC0858 and VC0859. Consequently, mutants strains producing these modified minor pilins showed reduce natural transformability and reduce DNA internalizing while the pilus dynamics was maintained. The authors proposed that these minor pilins promote DNA binding at the tip of the pilus ([42]). Notably, none of these experiments were performed on natural chitinous surface colonization conditions, under which competence is induced in *V. cholerae*. Indeed, under such conditions, the DNA-uptake pilus is known to form dense networks structures ([174]), which leaves the question open whether the binding of DNA at the tip of the pilus is of biological relevance in nature. Apart from the initial DNA binding question, work from our group showed that the pilus alone is not sufficient to drive DNA uptake into the periplasm but that the periplasmic DNA-binding protein ComEA was also required ([42,45]).

1.2.5.2 TRANSLOCATION OF DNA ACROSS THE CELL ENVELOPE

Seitz and Blokesch demonstrated that the competence-induced DNA-uptake machinery of *V. cholerae* relies on two spatially coupled but temporally independent steps ([44,168]). The first step of DNA uptake is T4P-dependent and concerns the translocation of dsDNA through the outer membrane by pilus retraction, as described above. However, another competence protein, ComEA, is also required to absorb dsDNA into the periplasm ([45]; Fig. 1.7A).

ComEA is a competence protein essential for transformation ([134]). Due to its two helix-hairpin-helix (HhH) motives, ComEA was assumed to be a DNA binding protein, which was later experimentally demonstrated ([45,178]). Moreover, using a translation fusion of ComEA and mCherry, it was observed that the protein displayed a uniform localization within the periplasm. However, upon addition of external transforming DNA (tDNA), ComEA-mCherry was shown to relocalize and form distinctive foci due to its binding to the incoming DNA (Fig. 1.7B; [45]). Based on Atomic Force Microscopy of ComEA and 3D modeling, specific interactions between ComEA and tDNA were predicted and these predictions were supported by subsequent genetic analyses. The resulting model for ComEA-mediated DNA uptake suggested that ComEA functions as a Brownian ratchet to absorb DNA into the periplasm. Indeed, the binding of ComEA prevents retrograde movement of the incoming DNA and therefore guides the tDNA into the periplasm ([45]).

After uptake across the outer membrane, the incoming tDNA is further translocated from the periplasm into the cytoplasm. This translocation occurs through the inner membrane channel ComEC ([44,171,179]). Due to comparable phenotypes of a *comEC* and *comF* mutant strains, namely the accumulation of tDNA within the periplasmic space, it was hypothesized that ComF might work in conjunction with ComEC in this translocation step ([44]; Fig. 1.7A). Moreover, based on knowledge acquired from research on competent Gram-positive bacteria, it is assumed that only one strand reaches the cytoplasm in *V. cholerae.* This incoming ssDNA is protected against degradation through binding of single-stranded binding (Ssb) proteins and DprA. Finally DprA promotes the loading of the recombination protein RecA, which is required for further integration into the bacterial chromosome through homologous recombination ([43,50,51]; Fig. 1.7A).

As mentioned above, translational fusions of ComEA can be used to visualize the uptake of DNA across the outer membrane ([45]; Fig. 1.7B). The translocation of DNA into the cytoplasm was indirectly visualized using a translational fusion between GFP and RecA.

Indeed, using time-lapse microscopy imaging Seitz and Blokesch reported the spatial localization of the DNA-binding ComEA protein in close proximity to RecA foci. However, a delay between the appearance of ComEA-mCherry and RecA-GFP foci were observed, indicating a spatially but not temporally coupling of the two DNA-binding processes. It was therefore concluded that the DNA uptake process across the outer and inner membrane are temporally uncoupled, supporting the hypothesis that DNA can be stored within the periplasm in-between both events ([168]).

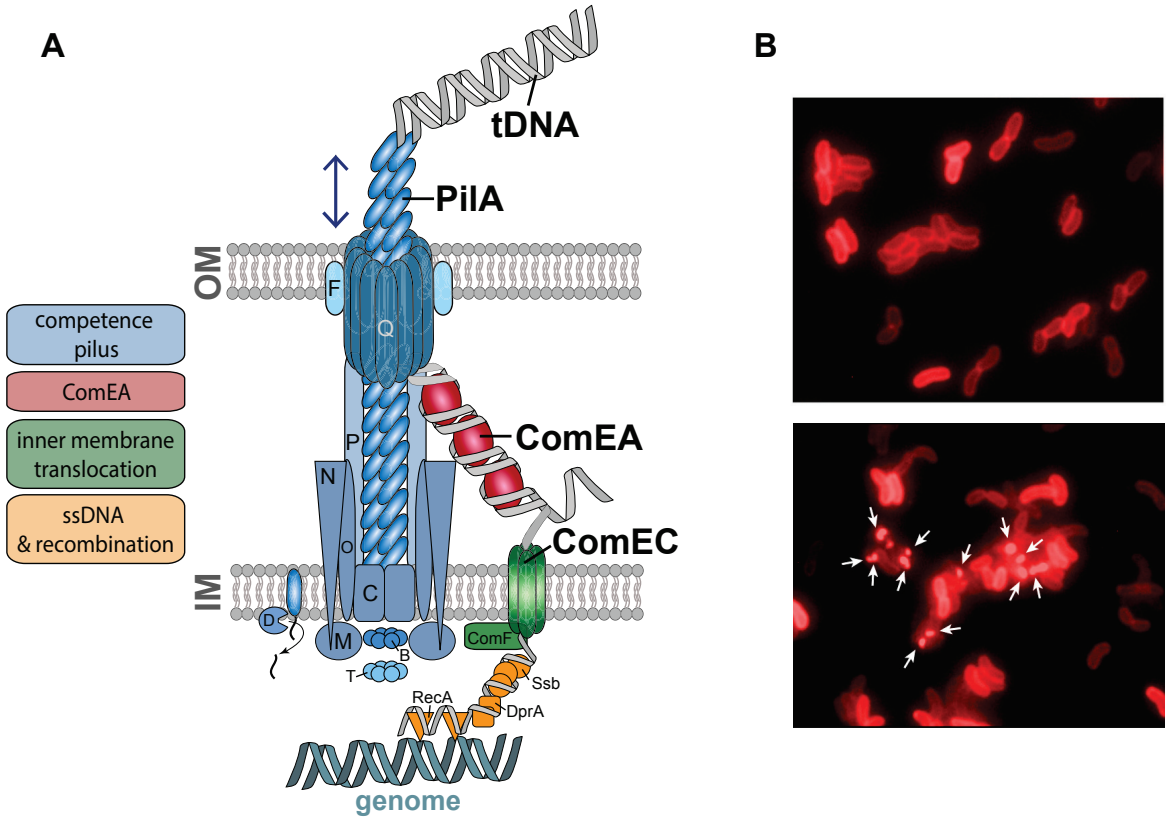

Figure 1.7: The DNA-uptake machinery of *V. cholerae*. Figure adapted from ([171]). (A) Model of the DNA-uptake machinery. This nanomachine is composed of a T4P (in blue; the single letters represent protein names preceded by "Pil"). The prepilin peptidase (PilD) cleaves the signal peptide of the major pilin subunits (PilA), which are assembled into a pilus filament at the inner membrane complex (PilC). Two ATPases, PilB and PilT, drive the pilus elongation and retraction, respectively. The retraction of the pilus is thought to initiate the translocation of the external tDNA across the outer membrane. Next, the DNA-binding protein ComEA (in red) pulls the tDNA into the periplasm through a Brownian ratchet mechanism. The tDNA crosses the inner membrane through the ComEC channel protein, which might act in concert with ComF (in green). In the cytoplasm, the single-strand DNA binding proteins (Ssb and DprA) bind the tDNA and protect it from degradation. Finally, DprA recruits RecA (in orange), which recombines the tDNA into the bacterial genome in case of sufficient homology. The minor pilins (VC0857-VC0861) are not represented for simplicity. Abbreviations: tDNA, transforming DNA; OM, outer membrane; IM, inner membrane. (B) Fluorescent microscopy pictures of ComEA before and after binding to tDNA. A translational fusion of ComEA-mCherry was visualized (red signal). The upper panel shows the distribution of ComEA within the periplasm of competent *V. cholerae*. The lower panel shows the accumulation of ComEA in distinctive foci (highlighted by white arrows), due to the binding of protein to the incoming tDNA inside the bacterial periplasm. Representative pictures adapted from ([171]) are depicted.

1.2.6 BACTERIAL PREDATION FOSTERS THE ACQUISITION OF DNA

As mentioned above, *V. cholerae* is a naturally competent bacterium that acquires DNA upon growth on chitin surfaces. Interestingly, a recent RNA sequencing approach by our group revealed that the TfoX-induced competence regulon extended beyond those genes that encode the DNA-uptake machinery and included genes for the organism's type VI secretion system (T6SS; [180]). The T6SS is a molecular killing device used to target eukaryotic and bacterial cells through the delivery of toxic proteins ([181]). It was therefore concluded that upon competence induction successful T6SS attacks towards neighboring non-sister cells would provoke the release of their DNA, which subsequently served as tDNA for the competent attacker cell. A new role of the T6SS was therefore proposed, namely that of an active DNA acquisition system that enhances HGT in *V. cholerae* and other competent bacteria ([180,182]). The next section will give an overview of the T6SS discovery and its function and will highlight the regulation of the T6SS in *V. cholerae*.

1.3 THE TYPE VI SECRETION SYSTEM (T6SS)

The T6SS belongs to the sophisticated nanomachines used by bacteria to secrete macromolecules across the cell envelope. Pathogenic bacteria possess diverse specialized secretion systems to deliver virulence factors into the environment or directly into eukaryotic or prokaryotic cells. Secretion systems have been primarily studied in Gram-negative bacteria (with the exception of T7SS) and to date nine secretion systems have been identified, which are designated type 1 to type 9 secretion systems (T1SS-T9SS). These machineries are mostly encoded by one or several operons and are often carried within genomic islands or on plasmids. Secretion systems are frequently characterized based on whether secretion occurs across the complete cell envelope in a single step or as a two-step mechanism (which is, for example, the case for protein export via the T2SS). The T6SS spans both the inner membrane and the outer membrane and, therefore, transport the toxic macromolecules from the cytoplasm into target cells through a one-step mechanism. Even though secretion systems are often associated with pathogenic species, the T6SS is also prevalent in non-pathogenic bacteria. It is estimated that approximately 25% of sequenced Gram-negative bacteria harbor one or several T6SS(s) ([181,183–186]).

1.3.1 DISCOVERY OF THE T6SS

The T6SS was identified and characterized in 2006 ([187]). However, the first data suggesting the existence of the T6SS was obtained 10 years earlier. Indeed, in 1996, the first component of T6SSs was identified, namely the haemolysin coregulated protein (Hcp), while virulence factor secreted by *V. cholerae* were studied. In this study, it was observed that Hcp was secreted without cleavage of a signal peptide suggesting a novel transport mechanism ([188]). However, in the latter study, the mode of secretion of Hcp was not elucidated. Some years later an *in silico* comparative genomics analysis identified the loci of the T6SS by investigating homologue of a protein associated with the T4SS, called IcmF, in *V. cholerae* and other proteobacteria. These homologous proteins of IcmF were often part of a cluster encoding approximately 15 genes, which had no homology to other T4SS proteins or components of other known secretion systems. These conserved clusters were named IcmF-associated homologous protein (IHAP) and it was suggested that they encode a secretion apparatus ([189]). In 2006, the link between Hcp secretion and the IHAP cluster was made and, therefore, these loci were renamed as novel and at that time sixth identified secretion system (T6SS) ([187,190]).

Pukatzki and colleagues revealed in their study that a non-O1 non-O139 *V. cholerae* strain (strain V52) used this novel secretion pathway to secrete virulence factor directly into eukaryotic cells. They used the bacteria-grazing amoeba *Dictyostelium discoideum* as a model host to identify novel virulence mechanism that might help bacteria to resist predation. Notably, the tested *V. cholerae* strain killed this amoeba efficiently in a cell-cell contact dependent manner. Based on transposon mutagenesis, the authors identified the genes responsible of the killing of *Dictyostelium* amoeba by *V. cholerae* and they named these genes VAS for virulence-associated secretion. In addition, the authors showed that four proteins, including Hcp, were secreted and they therefore suggested that these secreted proteins might be involved in the cytotoxicity observed against amoeba and mammalian macrophages ([187]).

The same year, another study by the Mekalanos lab demonstrated that the virulence locus that correlated with chronic infections by *Pseudomonas aeruginosa* also encoded a T6SS ([190]). Using specific antibodies, Hcp proteins were identified in the sputum of cystic fibrosis patients. In addition, an antibody response against Hcp was measured in blood sera of cystic fibrosis patients supporting the implication of this virulence locus in infection. Furthermore,

Mougous and colleagues determined the crystal structure of Hcp hexameric rings. Due to the large diameter of the ring structures, the authors suggested that these rings might form a channel through which substrates could be secreted ([190]). Nowadays, the detection of secreted extracellular Hcp proteins provides a first hint on the existence of a functional T6SS in diverse bacteria and is often used as a tool to check for T6SS functionality.
Since these initial reports on the T6SS, multiple studies have shed light onto the structure and the mode-of-action of the T6SS.

1.3.2 THE T6S MACHINERY AND ITS ASSEMBLY

The T6SS genes are generally organized in a large cluster of at least 13 core genes and can comprise additional clusters located elsewhere on the genome, which are named auxiliary clusters ([181,191,192]). The large cluster of the *V. cholerae* T6SS encodes several component that share structural and functional homology with contractile bacteriophage tails ([193–195]). The auxiliary clusters are smaller and encode genes involved in the secreted inner Hcp tube and the VgrG tip protein as well as pairs of effector and immunity proteins. Indeed, as the T6SS secretes effectors proteins into neighboring cells, kin cells need to be protected from such attacks through the production of matching immunity proteins (e.g., prevention of self-intoxication; [181,196–198]). It is also important to note that T6SSs can be present as single or multiple copies in diverse species. *Pseudomonas aeruginosa,* for example, contains three T6SS in its genome, *V. parahaemolyticus* and *V. alginolyticus* carry two distinctive T6SS clusters, while pandemic *V. cholerae* encode solely a single T6SS ([187,199–201]). It is currently thought that bacteria encoding several T6SS use distinct regulatory circuits in order to activate one or the other T6SS and that these different T6SS most likely serve different purposes. It should be noted though that the environmental cues that trigger T6SS production are often unknown, as was the case for pandemic *V. cholerae* before our lab identified chitin as a trigger of the system ([180]).

The T6SS is often described as an inverted contractile phage tail that is anchored to the cell envelope and that expels toxic effector proteins into neighboring cells. In fact, several studies have led to the identification of these important homologies between the T6SS and the bacteriophage tail. First, based on bioinformatics analysis, Pukatzki and colleagues suggested that the T6SS tip protein VgrG (for valine-glycine repeat protein G) is a homologue of the needle or spike of the bacteriophage T4, which the phage uses as a cell-

puncturing device ([193]). In addition, two other major components of the T6SS, namely the sheath proteins VipA and VipB, were shown to assemble in tubules that resembled T4 contracted tail sheath ([195]). Remarkably, Leiman and colleagues were the first to propose that the T6SS structure resembles both structurally and functionally a bacteriophage tail. They suggested that the phage tail tube like structure, composed of Hcp, might power the translocation of the needle (VgrG) carrying the toxic effectors by a similar mechanism as contractile phage tails ([194]). Several years later, Basler, Pilhofer and colleagues observed the dynamics of the T6SS in *V. cholerae* using fluorescent microscopy and electron cryotomography. This study thereby confirmed that the T6SS is, indeed, functionally and structurally similar to contractile phage tail ([202]).

Concerning the overall structure, the T6SS consists basically of two main complexes, a membrane-associated complex and an assembly complex, containing components similar to the tail sheath and tail tube proteins of the bacteriophage. A model of the T6SS assembly was proposed which suggests that the complexes are recruited from the outer membrane to the cytoplasm while building up the secretion apparatus (Fig. 1.8). The membrane-associated complex that spans the cell envelope is assembled first followed by the recruitment of the baseplate complex ([203–205]). The needle homolog in T6SSs is composed of VgrG trimers and PAAR (proline alanine alanine arginine) proteins and is assembled at the center of the baseplate complex. PAAR binds the distal end of the trimeric VgrG to sharpen the spike of the machinery and the effectors are loaded onto or fused to the needle complex. The baseplate complex also controls the assembly of the cytoplasmic contractile sheath tail composed of VipA/VipB heterodimers that surrounds a tube of hexameric Hcp proteins (Fig. 1.8). The T6SS in an extended conformation is ready to launch the secretion of the effectors and contracts upon a conformational change within the baseplate complex. This conformational change triggers sheath structure contraction leading to the translocation of the inner Hcp tube and sharp needle-like tip through the cell envelope. This outward propulsion of the VgrG-PAAR/Hcp complex leads to the puncture of neighboring cells and the release of the associated toxic effectors (Fig. 1.8). Finally, the ClpV ATPase disassembles the contracted sheath (Fig. 1.8) and recycles its components for the construction of a novel extended sheath apparatus at the maintained membrane complex ([195,202,206,207]). The T6SS is a powerful killing device, which assembles in 20 to 30 seconds per micrometer and contracts within 5 milliseconds ([186,192,202,208]). Overall, the T6SS constitutes an important weapon

involved in the intoxication of eukaryotic host cell as well as in bacterial warfare, as discussed in the following paragraph.

1.3.3 EFFECTORS PROTEINS

Diverse effectors with different toxic activities are secreted by the T6SS. It was initially thought that the aim of the T6SS was to target eukaryotic cell ([187]). However, further studies showed that the T6SS is primarily implicated in inter-bacterial competition. The first key studies that showed that the T6SS could be used against bacteria are based on the T6SS of *P. aeruginosa* called H1-T6SS ([197,209]). The H1-T6SS secretes three effectors proteins, which Hood and colleagues identified as Tse1, Tse2 and Tse3 for type VI secretion exported 1-3. The authors showed that Tse2 has a toxic activity towards bacteria, as it was impossible to obtain a mutant of its associated immunity gene *tsi2*. This finding further suggested that the immunity protein Tsi2 was produced to prevent self-intoxication. Indeed, the toxic activity was shown by expressing Tse2 in the cytoplasm of eukaryotic and prokaryotic species, which resulted in their lysis. However, the contact between eukaryotic cells and *P. aeruginosa* did not lead to the translocation of Tse2 and no cytotoxicity was therefore observed towards eukaryotic cells. Strikingly, Hood and colleagues investigated whether Tse2 could be used to target another prokaryotic cell by mixing *P. aeruginosa* strains with and without Tsi2 immunity (WT and Δ*tse2*Δ*tsi2*, respectively) either in liquid medium or on a solid surface. Comparing these two conditions resulted in different outcomes: whereas no killing was detected under liquid conditions, the secreted Tse2 protein killed non-immune bacteria (lacking Tsi2) on solid surfaces. Thus, in addition to showing that the T6SS could serve as an antimicrobial weapon, these experiments also demonstrated that T6SS-mediated bacterial intoxicating was based on a cell-cell contact dependent mechanism ([209]). Interestingly, in the same year another study suggested that the T6SS was not active against Gram-positive bacteria but solely against Gram-negative bacteria, even though further studies should confirm these observations with a larger and more diverse set of bacteria ([210]).

As mentioned above, the effectors secreted via the contraction of the T6SS can target eukaryotic or/and bacterial cells. Remarkably and as briefly mentioned above, to prevent self- of sibling-intoxication, each effector has a cognate immunity protein that neutralizes its toxic effect. The immunity gene is usually encoded adjacent to the effector gene (e.g., effector immunity pair or E-I for short).

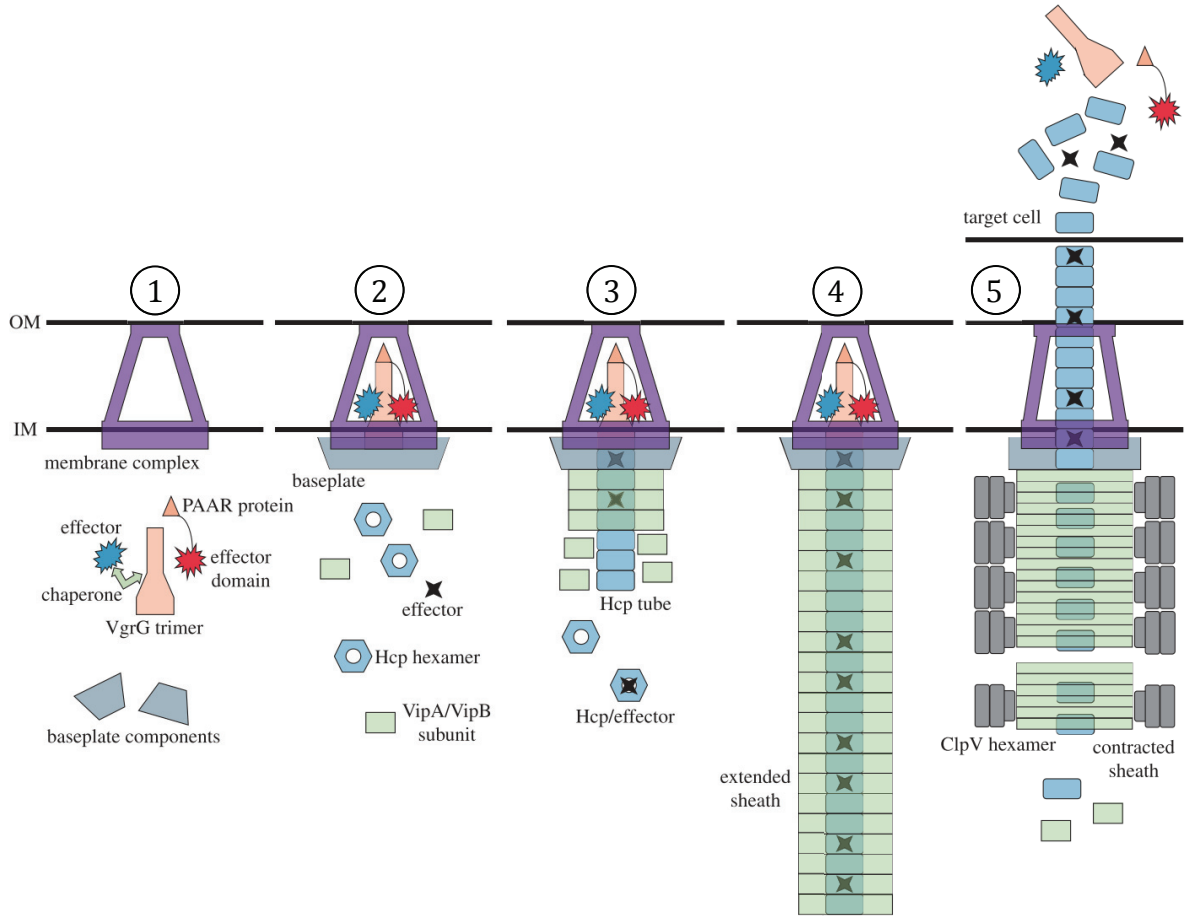

Figure 1.8: Model of the type VI secretion system. Figure adapted from ([207]). Scheme representing the mode of action of the T6SS, from the assembly to the contraction. (1) The assembly starts with the recruitment of the membrane complex, which spans the cell envelope. The effectors secreted by the T6SS are either fused or loaded to the needle composed of trimeric VgrG and PAAR. The effectors loaded are directly or indirectly (through aid of a chaperone) attached to VgrG/PAAR. (2) The VgrG/PAAR/effector complex and the baseplate complex assemble at the center of the membrane complex. (3) The formation of the baseplate complex initiates the assembly of the tube (Hcp) and surrounding sheath (VipA/VipB). (4) The T6SS is in its extended and therefore "ready to fire" conformation. (5) A conformation switch in the baseplate/membrane complex triggers the contraction of the sheath. The contracted sheath expels the Hcp tube, the tip and its associated effectors from the cell envelope and into a potential target cell. Inside the attacker cell, the ATPase ClpV recognizes the contracted sheath and disassembles it for recycling purposes. Abbreviations: OM, outer membrane; IM, inner membrane.

On the basis of their transport mechanism, effectors can be divided into two categories: "specialized" and "cargo" effectors. Specialized effectors are extension domains fused to structural components such as Hcp, VgrG or PAAR ([193,211,212]). Cargo effectors interact directly with Hcp or the VgrG spike or are loaded with the help of accessory chaperone proteins (Fig. 1.8; [213–215]). According to their molecular target, antimicrobial effectors have been classified into three main categories: cell wall-targeting, membrane-targeting and nucleic acids-targeting ([216,217]).

The cell wall-specific effectors usually target the peptidoglycan, which is the major structural component of the bacterial cell wall. This molecule confers a mechanical rigidity to the cell and helps in maintaining the cellular shape. The peptidoglycan is a polymer composed of long chains of alternating polysaccharides (N-Acetylglucosamine and N-Acetylmuramic acid), which are crosslinked by peptide bridges ([218]). Due to the conservation of peptidoglycan, it is not too surprising that T6SS effector target this structure. Peptidoglycan degrading T6SS effectors have been classified into two groups, amidase and glycoside hydrolase. Type VI amidase effectors (Tae) catalyze the hydrolysis of the peptide crosslinks, whereas type VI glycoside hydrolase effectors (Tge) target the glycan backbone of peptidoglycan ([216,219]). By targeting the peptidoglycan, these enzymes digest the cell wall of Gram-negative bacteria. The second category of effectors targets the membrane, which is likewise a conserved and essential component of the bacterial cell. Two groups are yet again represented among the effectors targeting the cell membrane: phospholipases and the membrane pore-forming effectors. Phospholipases effectors (also known as type VI lipase effectors) hydrolyze the phospholipids of the bacterial membrane ([220]). The cellular membrane can also be disrupted by the insertion of pore-forming proteins, which dissipate essential chemiosmotic gradients ([213,221]). The last primary category of effectors targets nucleic acids, which means that these effectors reach the cytoplasm. These nuclease activity-harboring effectors are usually called type VI DNase effectors (Tde) ([222]). Overall, T6SS effectors target highly conserved and essential molecules, which allow them to successfully intoxicate a broad array of competitors.

1.3.4 REGULATION

The T6SS is supposedly energetically costly for bacteria due to its cycle of assembly, contraction and disassembly. Therefore, it is not surprising that the expression of the T6SS is often a tightly regulated process so its production only occurs in response to diverse environmental signals. These environmental cues can be e.g. QS-mediating autoinducers, iron depletion, thermoregulation or salinity ([223–226]).

For example, the *sci1* T6SS gene cluster of enteroaggregative *E. coli* (EAEC) varies from an OFF to an ON (and ON to OFF) state in response to iron availability ([225]). In presence of iron, the Ferric uptake regulator binds to the consensus Fur binding sequences (Fur boxes) in the promoter region of the *sci1* T6SS, which further block access to the RNA polymerase,

therefore repressing *sci1* T6SS expression. In contrary, in iron depletion condition, Fur is relieved from the promoter of the *sci1* T6SS, RNA polymerase can then access the DNA and leads to the expression of the T6SS cluster ([225]).

Another example would be the marine bacterium *Vibrio parahaemolyticus* in which the two T6SSs are regulated differentially. Salomon and colleagues showed that the T6SS1 was active at low cell density under conditions of high salinity, whereas the T6SS2 was expressed at high cell densities under low salt conditions ([223]). Thus, different T6SSs within a single bacterium can be expressed under different environmental conditions and therefore serve different purposes in the lifestyle of the bacterium.

1.3.5 THE T6SS OF *V. CHOLERAE*

V. cholerae harbors a single T6SS that is organized in one large cluster of 20 genes (VCA0105-VCA0124) and three auxiliary clusters (auxiliary cluster 1 to 3: VC1415-VC1421, VCA0017-VCA0021 and VCA0284-VCA0286; [187,227–229]). The large cluster and the auxiliary clusters 2 and 3 are located on the small chromosome (chr 2), whereas the auxiliary cluster 1 is located on the large chromosome (chr 1). Most of the core components of the secretion machinery are encoded in the large cluster including genes whose gene products form the membrane and the baseplate complexes as well as one of the three VgrG proteins. The auxiliary clusters 1 and 2 each carry an *hcp* gene (*hcp1* and *hcp2*), a *vgrG* gene (*vgrG-1* and *vgrG-2*) and a unique pair of E-I genes (*tseL*/*tsiV1* and *vasX*/*tsiV2*). The auxiliary cluster 3 and the large cluster also contain an E-I pair (*tseH*/*tsiH* and *vgrG-3/tsiV3*). The VgrG proteins form a trimeric cap at the tip of the Hcp tube, which itself is sheathed by VipA and VipB proteins. The rapid contraction of the sheath expels the inner Hcp tube and its effectors from the cell and into adjacent cells ([202,212,230–232]). In *V. cholerae*, the T6SS fires repeatedly and in random directions leading to the shooting of kin (sister) and non-kin bacteria. However, as noted above, kin cells are immune against intoxication and those cells can even recycle the translocated components for the assembly of their own T6SS structure. This mechanism increases the chances to successfully kill competitors while not titrating T6SS components out from the clonal population by T6SS-mediated firing at kin cells ([233]).

1.3.5.1 ACTIVITY OF THE EFFECTORS

All *V. cholerae* strains sequenced so far encode a single T6SS. Even though the T6SS clusters are conserved, the E-I proteins are very diverse among *V. cholerae* isolates ([227]). Consequently, strains with identical sets of E-I proteins are immune against each other, while strains with different sets can efficiently kill each other. This diversity is thought to contribute to bacterial competition and to impact colonization of environmental niches.

Each effector has a specific activity, which can intoxicate eukaryotic or prokaryotic cells as described previously. In pandemic *V. cholerae* isolates, five effectors have been characterized. VgrG-1 is a specialized effector, which contains a C-terminal effector extension. This C-terminal extension consists of an actin-crosslinking domain that causes cytotoxicity against eukaryotic predator ([193]). VasX and TseL disrupt the cell membranes of both eukaryotes and prokaryotes through pore forming and lipase activity, respectively ([198]). The last two effectors likewise have cytotoxic activities towards prokaryotic cells. Both the C-terminal effector domain of VgrG-3 and the amidase TseH target peptidoglycan ([229,234]). Interestingly, no effector with nuclease activity was identified in pandemic O1 *V. cholerae*. As a matter of fact, nuclease effector proteins are rarely identified in *V. cholerae* genome sequences ([227]), which favors the idea of preserving the DNA released by prey lysis for further efficient acquisition via the DNA-uptake machinery.

1.3.5.2 REGULATION OF THE T6SS UPON COMPETENCE INDUCTION

Most studies on the T6SS of *V. cholerae* have focused on non-pandemic strains, which exhibit constitutive T6SS activity. Pandemic strains on the other hand are known to be T6SS-silent under laboratory conditions. It was first discovered that a putative activator of RpoN (Sigma 54), named VasH and encoded by the large cluster of the T6SS, was essential for T6SS function ([187,225]). VasH in conjunction with RpoN control the transcription of the two auxiliary clusters 1 and 2 while the large cluster encoding the structural component of the machinery as well as VasH itself is not regulated by these two proteins. The environmental cues leading to the activation of the major cluster in pandemic strains were therefore unknown until our laboratory showed that the T6SS of 7th pandemic *V. cholerae* strains was activated during competence ([180]). In this study, Borgeaud and colleagues showed that the T6SS is activated by the growth to high cell density on chitinous surfaces concomitantly with the DNA-uptake machinery. Using multiple techniques, including RNA-seq, qRT-PCR,

interbacterial killing assays, and visualization of the T6SS structures by fluorescence microscopy, the authors showed that the T6SS is activated in a TfoX-, HapR- and QstR-dependent manner (Fig. 1.9; [180]). As a reminder: TfoX is the master regulator of transformation activated upon chitin sensing; HapR is the master regulator of QS, which is activated at high cell density; and both TfoX and HapR coregulate QstR (see section 1.2.4. above). Moreover, it was shown that QstR activates the large T6SS cluster and that expression of the large cluster then proceeds via production of VasH towards the transcription of the auxiliary clusters 1 and 2 ([170,228]).
Moreover, it was shown that TfoX through QstR activates the first genes of the large cluster of the T6SS, encoding the component of the secretory apparatus. The successful activation and production of the T6SS requires additionally the previously identified activator VasH (Fig. 1.9). Indeed, through the activation of the large cluster the activator σ^{54} vasH is produced, which subsequently activates the transcription of the two *hcp* auxiliary clusters required for secretion ([170, 228]).

The simultaneous activation of the T6SS and the DNA-uptake machinery results in the attack and lysis of non-immune neighboring cells followed by the uptake of the prey-released DNA. Indeed, using a selective marker located on the chromosome of the non-immune bacteria, the authors showed that competent predatory *V. cholerae* killed their neighbors and further integrated the selective marker into their own chromosome ([180]). The induction of the T6SS upon competence induction in *V. cholerae* therefore constituted a novel and exciting model for bacterial evolution.

1.3.5.3 A SECOND MAJOR REGULATOR OF THE T6SS

A number of minor and major regulators of the T6SS have been identified in *V. cholerae,* as reviewed by Joshi and colleagues ([232]). Some of the environmental cues identified include quorum sensing and catabolite repression, which are integrated into the regulation of the T6SS upon competence induction. For simplicity, this introduction solely focuses on the major regulators of the T6SS that were identified in *V. cholerae*. Remarkably, the homolog of TfoX, named TfoY, is also a major regulator of the T6SS, as demonstrated by our group ([228]). TfoY was initially annotated as a competence regulator, even though it is not implicated in natural competence in *V. cholerae* ([228]). The regulation of the T6SS by TfoY is different from TfoX induction, as it does not require chitin or quorum sensing-mediating autoinducers as environmental stimuli. Indeed, T6SS induction by TfoY occurs independently of TfoX,

HapR, or QstR (Fig. 1.9). Additionally, Jaskólska and colleagues observed that QstR represses *tfoY,* which reinforces the idea of an independent regulation of the T6SS by TfoX or TfoY ([170]).

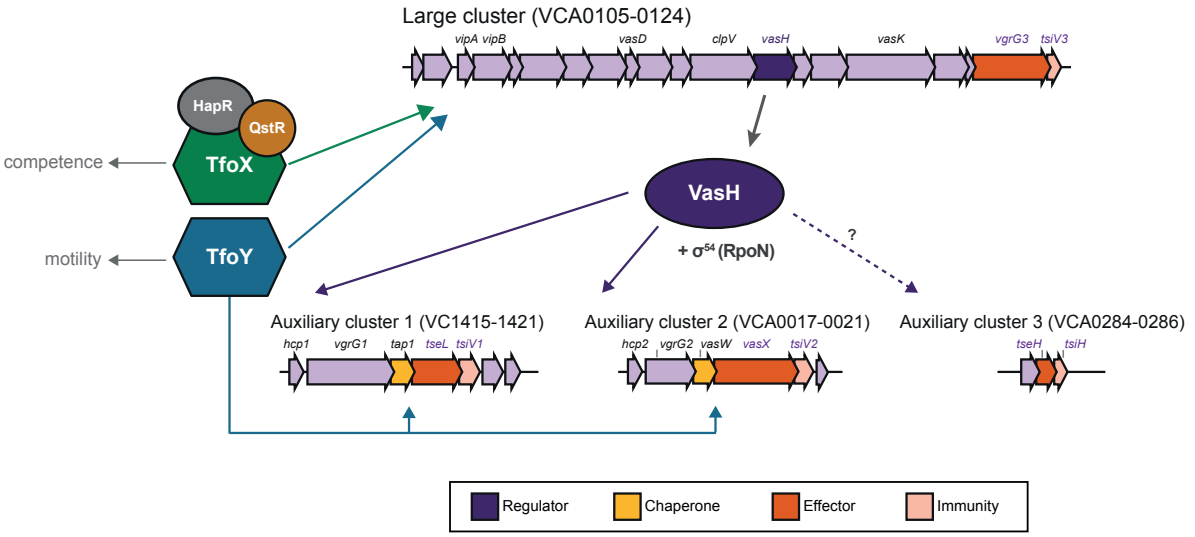

Figure 1.9: Regulation of the type VI secretion system in *V. cholerae*. Adapted from ([235]). In *V. cholerae*, the T6SS genes are organized in a large and three auxiliary clusters, as indicated. The two major regulators of the T6SS are TfoX and TfoY. TfoX induces the T6SS in a HapR- and QstR-dependent manner, whereas TfoY activates the T6SS independently of HapR and QstR. Both, TfoX and TfoY regulate the auxiliary clusters of the T6SS in a VasH-dependent manner. However, TfoY additionally drives the expression of the effector and immunity proteins of the auxiliary cluster 1 and 2. In this scheme, the regulatory gene *vasH*, the genes pair encoding the effector and immunity proteins, as well as the chaperone (required for the attachment of some effectors to the VgrG tip proteins) are color-coded. Moreover, the competence and motility phenotypes that are associated with the production of TfoX and TfoY, respectively, are represented.

Although both TfoX and TfoY activate the T6SS core structure in a VasH-dependent manner, TfoY additionally drives the expression of the E-I pairs of the auxiliary clusters 1 and 2 in a VasH-independent manner. By contrast, expression of *tseL/tsiV1* and *vasX/tsiV2* are dependent on VasH for TfoX-mediated T6SS induction (Fig. 1.9). The latter effectors, in contrast to the third effector encoded in the large T6SS cluster, have been implicated in cytotoxicity against both prokaryotic and eukaryotic cells and it was therefore hypothesized that eukaryotic predators might be preferentially targeted through TfoY-dependent T6SS activation. The environmental cues that might potentially enhance *tfoY* expression remain unknown. However, it was shown that TfoY production depends on low intracellular c-di-GMP levels ([228]), most likely due to a translation inhibiting c-di-GMP riboswitch, which is located in the 5' UTR of the *tfoY* mRNA ([228,236]). Thus, at low c-di-GMP level (e.g. in planktonic cell) TfoY is produced, whereas *tfoY* translation is inhibited at high c-di-GMP concentrations (e.g. within biofilms; [237,238]). TfoY induction also leads to an enhanced

motility phenotype and to the production of two extracellular enzymes, hemolysin and lecithinase, which are likewise thought to target eukaryotic cells ([239–241]). Based on these observations, Metzger and colleagues suggested that TfoY induces the T6SS as part of a defensive reaction against eukaryotic predators, while the T6SS activation mediated by TfoX leads to bacterial killing with the purpose of acquiring prey-released genomic DNA ([180]). Hence, the dual expression pattern of a single T6SS in *V. cholerae* could serve different needs.

1.4 RATIONALE AND THESIS OUTLINE

Since the discovery that *V. cholerae* is naturally competent for transformation upon growth on chitinous surfaces in 2005, considerable research effort has focused on the identification of both the regulatory pathways and the mechanistic aspects of the DNA uptake process. Furthermore, our laboratory recently showed the implication of the T6SS as a bacterial weapon during competence in pandemic *V. cholerae* strains ([180]). Whereas the T6SS of most environmental isolates and toxigenic strains of *V. cholerae* is constitutively active, the T6SS of pandemic *V. cholerae* is silent under standard laboratory conditions ([187,239,242]). TfoX was identified as the first major regulator of the T6SS in a *V. cholerae* strain responsible of the seventh pandemic ([180]). In addition, its homolog TfoY was also shown to activate the T6SS most likely in response to a so far unrecognized environment signal ([228]). Importantly, studying the T6SS regulatory pathways in pandemic *V. cholerae* strains can provide important new insight into the system's biological function(s). Moreover, the gained knowledge on the regulatory process in one model *V. cholerae* strain might be more broadly applicable to other cholera and non-cholera *Vibrio* species. The main objective of this thesis was therefore to get insights into the conservation of the two regulatory pathways implicated in T6SS activation and to further investigate the biological function linked to the co-regulation of the T6SS with the DNA-uptake machinery.

In the first part of this work, we aimed to identify the conservation of the T6SS regulation by TfoX and TfoY in other pandemic strains of *V. cholerae* as well as other *Vibrio* species. As *tfoX* and *tfoY* are present in all sequenced *Vibrionaceae* ([243]), we focused on three different *Vibrio* species (*Vibrio fischeri, Vibrio alginolyticus* and *Vibrio parahaemolyticus*), in which the genetic organization of the T6SS was already known ([223,244–246]). We determined the conservation of TfoX and TfoY among these *Vibrio* species by studying their associated

phenotypes, which included: T6SS induction by TfoX and TfoY ([180,228]), competence induction by TfoX ([134,135]) and the enhancement of bacterial motility by TfoY ([228]). Upon the individual induction of each regulator in the different *Vibrio* species we shed light onto the potential conservation and importance of their mediated biological functions (Chapter 2).

In the second part of this thesis, we aimed to better characterize the outcome of the co-regulation of the T6SS and the DNA-uptake machinery with respect to the evolution potential of *V. cholerae*. Borgeaud and colleagues showed that the simultaneous production of these two nanomachines fostered HGT in this organism ([180]). In the latter study, the horizontal transfer of a single gene was investigated, whereas the T6SS activation may generate a pool of DNA derived from diverse *V. cholerae* and other bacterial species, which could result in the acquisition of novel genes and functions. Importantly, the co-production of these two nanomachines might contribute to the emergence of new pathogenic strains. It seemed therefore of prime importance to us to gain deeper insight into the co-regulation of the T6SS-killing machine and DNA-uptake complex. Moreover, using a whole genome sequencing approach, we determined the full extent of the HGT events that occurred in naturally transformed cells. In addition, we compared the pattern of transferred DNA under varying conditions in which the transforming material was either acquired in a T6SS-dependent or a T6SS-independent manner (Chapter 3).

Lastly, as we had determined that the simultaneous production of the T6SS and the DNA-uptake machinery can foster the transfer of large clusters of genes, we wondered whether contact maintenance was required to ensure that the attacking bacterium could fully benefit from the prey-released genetic material. Thus, based on the knowledge that T4P serve different biological functions including adhesion, we aimed to investigate if the T4P of the DNA-uptake machinery could serve as a fishing rod and could concomitantly ensure a close contact between cells during T6SS attacks. We also tested whether solely the attacker cell itself acquired the prey-released DNA or whether any close-by cells could likewise benefit from the killing event (Chapter 4).

In summary, the results presented in this work enabled us to gain insights into the conservation of the distinct biological functions mediated by TfoX and TfoY in diverse *Vibrio,* which might even be conserved in other species of the genus *Vibrio*. Moreover, we contributed significantly to the understanding of the evolution potential that the simultaneous induction of the T6SS and the DNA-uptake machinery might provide to *V. cholerae*.

1.5 REFERENCES

1. Ochman H, Lawrence JG, and Groisman EA. Lateral gene transfer and the nature of bacterial innovation. *Nature*. **405**:299-304 (2000).
2. Hall JPJ, Brockhurst MA, Harrison E. Sampling the mobile gene pool: Innovation via horizontal gene transfer in bacteria. *Philos Trans R Soc B Biol Sci*. **372**:20160424 (2017).
3. Juhas M, Van Der Meer JR, Gaillard M, Harding RM, Hood DW, and Crook DW. Genomic islands: Tools of bacterial horizontal gene transfer and evolution. *FEMS Microbiol Rev*. **33**:376-393. (2009).
4. UN Interagency Coordination Group on Antimicrobial Resistance (IACG). No Time To Wait: Securing the Future From Drug-Resistant Infections. *Rep April 2019* (2019).
5. Hacker J, Bender L, Ott M, *et al.* Deletions of chromosomal regions coding for fimbriae and hemolysins occur *in vitro* and *in vivo* in various extra intestinal *Escherichia coli* isolates. *Microb Pathog* **8**:213-225 (1990).
6. Dobrindt U, Hochhut B, Hentschel U, and Hacker J. Genomic islands in pathogenic and environmental microorganisms. *Nat Rev Microbiol*. **2**(5):414-424 (2004)
7. Coburn PS, Baghdayan AS, Dolan GT and Shankar N. Horizontal transfer of virulence genes encoded on the *Enterococcus faecalis* pathogenicity island. *Mol Microbiol*. **63**(2):530-544. (2007).
8. von Wintersdorff CJH, Penders J, van Niekerk JM, *et al.* Dissemination of Antimicrobial Resistance in Microbial Ecosystems through Horizontal Gene Transfer. *Front Microbiol*. **7**:173. doi:10.3389/fmicb.2016.00173 (2016)
9. WHO. https://www.who.int/emergencies/ten-threats-to-global-health-in-2019. (2019)
10. Walsh F. Superbugs to kill "more than cancer" by 2050. BBC. (2014)
11. WHO. Global priority list of antibiotic-resistant bacteria to guide research, discovery, and development of new antibiotics. (2017)
12. Blokesch M. In and out—contribution of natural transformation to the shuffling of large genomic regions. *Curr Opin Microbiol*. **38**:22-29. (2017).
13. Frost LS, Leplae R, Summers AO, Toussaint A. Mobile genetic elements: The agents of open source evolution. *Nat Rev Microbiol*. **3**(9):722-732. (2005)
14. Waksman G. From conjugation to T4S systems in Gram‐negative bacteria: a mechanistic biology perspective. *EMBO Rep*. **20**(2):e47012. (2019)
15. Penadés JR, Chen J, Quiles-Puchalt N, Carpena N, and Novick RP. Bacteriophage-mediated spread of bacterial virulence genes. *Curr Opin Microbiol*. **23**:171-178. (2015)
16. Jamet A, Touchon M, Ribeiro-Gonçalves B, *et al.* A widespread family of polymorphic toxins encoded by temperate phages. *BMC Biol*. **15**(1):75. (2017)
17. Johnston C, Martin B, Fichant G, Polard P, Claverys JP. Bacterial transformation: Distribution, shared mechanisms and divergent control. *Nat Rev Microbiol*. **12**(3):181-196. (2014)
18. Gray TA and Derbyshire KM. Blending genomes: distributive conjugal transfer in mycobacteria, a sexier form of HGT. *Mol Microbiol*. **108**(6):601-613 (2018)
19. Petsko GA. Transformation. *Genome Biol*. **7**:117. (2006)
20. Blokesch M. Natural competence for transformation. *Curr Biol*. **26**(21):R1126-R1130 (2016)
21. Seitz P. and Blokesch M. Cues and regulatory pathways involved in natural competence and transformation in pathogenic and environmental Gram-negative bacteria. *FEMS Microbiol Rev*.**37**(3):336-363. (2013)
22. Bernstein H, Bernstein C and Michod RE. Sex in microbial pathogens. *Infect Genet Evol*.

57:8-25. (2018)
23. Mccallum M, Burrows LL, Howell PL. The Dynamic Structures of the Type IV Pilus. *Microbiol Spectrum* 7(2):PSIB-0006-2018 (2019)
24. Muschiol S, Aschtgen M-S, Nannapaneni P, Henriques-Normark B. Gram-Positive Type IV Pili and Competence. *Microbiol Spectr*. **7**(1):PSIB-0011-2018 (2019)
25. Krüger NJ, Stingl K. Two steps away from novelty - principles of bacterial DNA uptake. *Mol Microbiol*. **80**(4):860-867. (2011)
26. Hofreuter D, Odenbreit S, Haas R. Natural transformation competence in *Helicobacter pylori* is mediated by the basic components of a type IV secretion system. *Mol Microbiol*. **41**(2):379-391 (2001).
27. Berry JL, Pelicic V. Exceptionally widespread nanomachines composed of type IV pilins: The prokaryotic Swiss Army knives. *FEMS Microbiol Rev*. **39**(1):134-154. (2015)
28. Giltner CL, Nguyen Y, Burrows LL. Type IV Pilin Proteins: Versatile Molecular Modules. *Microbiol Mol Biol Rev*. **76**(4):740-772. (2012)
29. Chen I, Dubnau D. DNA uptake during bacterial transformation. *Nat Rev Microbiol*. **2**(3):241-249 (2004).
30. Melville S, Craig L. Type IV Pili in Gram-Positive Bacteria. *Microbiol Mol Biol Rev*. **77**(3):323-341 (2013).
31. Maier B, Potter L, So M, Long CD, Seifert HS, Sheetz M. Single pilus motor forces exceed 100 pN *Proc Natl Acad Sci USA* **99**(25):16012-16017 (2002).
32. Biais N, Ladoux B, Higashi D, So M, Sheetz M. Cooperative retraction of bundled type IV pili enables nanonewton force generation. *PLoS Biol*. **6**(4):907-913 (2008).
33. Provvedi R, Dubnau D. ComEA is a DNA receptor for transformation of competent *Bacillus subtilis*. *Mol Microbiol*. **31**(1):271-280. (1999)
34. Mirouze N, Ferret C, Cornilleau C, Carballido-López R. Antibiotic sensitivity reveals that wall teichoic acids mediate DNA binding during competence in *Bacillus subtilis*. *Nat Commun*. **9**:5072 (2018).
35. Laurenceau R, Péhau-Arnaudet G, Baconnais S, *et al.* A Type IV Pilus Mediates DNA Binding during Natural Transformation in *Streptococcus pneumoniae*. *PLoS Pathog*. **9**(6):e1003473. (2013)
36. Balaban M, Battig P, Muschiol S, *et al.* Secretion of a pneumococcal type II secretion system pilus correlates with DNA uptake during transformation. *Proc Natl Acad Sci USA*. **111**(7):E758-E765 (2014)
37. Elkins C, Thomas CE, Seifert HS, Sparling PF. Species-specific uptake of DNA by gonococci is mediated by a 10-base-pair sequence. *J Bacteriol*. **173**(12):3911-3913 (1991).
38. Sisco KL, Smith HO. Sequence-specific DNA uptake in *Haemophilus* transformation. *Proc Natl Acad Sci USA*. **76**(2):972-976 (1979).
39. Danner DB, Deich RA, Sisco KL, Smith HO. An eleven-base-pair sequence determines the specificity of DNA uptake in *Haemophilus* transformation. *Gene*. **11**:311-318 (1980).
40. Cehovin A, Simpson PJ, McDowell MA, *et al.* Specific DNA recognition mediated by a type IV pilin. *Proc Natl Acad Sci USA*. **110**(8):3065-3070 (2013).
41. Berry JL, Xu Y, Ward PN, Lea SM, Matthews SJ, Pelicic V. A Comparative Structure/Function Analysis of Two Type IV Pilin DNA Receptors Defines a Novel Mode of DNA Binding. *Structure*. **24**(6):926-934. (2016)
42. Ellison CK, Dalia TN, Vidal Ceballos A, *et al.* Retraction of DNA-bound type IV competence pili initiates DNA uptake during natural transformation in *Vibrio cholerae*. *Nat Microbiol*. **3**(7):773-780 (2018).
43. Suckow G, Seitz P, Blokesch M. Quorum sensing contributes to natural transformation of

Vibrio cholerae in a species-specific manner. *J Bacteriol*. **193**(18):4914-4924 (2011).
44. Seitz P and Blokesch M. DNA-uptake machinery of naturally competent *Vibrio cholerae*. *Proc Natl Acad Sci USA*. **110**(44):17987-17992 (2013).
45. Seitz P, Pezeshgi Modarres H, Borgeaud S, *et al.* ComEA Is Essential for the Transfer of External DNA into the Periplasm in Naturally Transformable *Vibrio cholerae* Cells. *PLoS Genet*. **10**(1):e1004066 (2014)
46. Doherty AJ, Serpell LC, Ponting CP. The helix-hairpin-helix DNA-binding motif: A structural basis for non-sequence-specific recognition of DNA. *Nucleic Acids Res* **24**(13):2488-2497 (1996).
47. Inamine GS, Dubnau D. ComEA, a *Bacillus subtilis* integral membrane protein required for genetic transformation, is needed for both DNA binding and transport. *J Bacteriol*. **177**(11):3045-3051 (1995).
48. Hepp C, Maier B. Kinetics of DNA uptake during transformation provide evidence for a translocation ratchet mechanism. *Proc Natl Acad Sci USA*. **113**(44):12467-12472 (2016).
49. Baker JA, Simkovic F, Taylor HMC, Rigden DJ. Potential DNA binding and nuclease functions of ComEC domains characterized *in silico*. *Proteins Struct Funct Bioinforma*. **84**(10):1431-1442 (2016).
50. Bergé M, Mortier-Barrière I, Martin B, Claverys JP. Transformation of *Streptococcus pneumoniae* relies on DprA- and RecA-dependent protection of incoming DNA single strands. *Mol Microbiol*. **50**(2):527-536 (2003)
51. Mortier-Barrière I, Velten M, Dupaigne P, *et al.* A Key Presynaptic Role in Transformation for a Widespread Bacterial Protein: DprA Conveys Incoming ssDNA to RecA. *Cell*. **130**(5):824-836 (2007).
52. Claverys JP, Martin B, Polard P. The genetic transformation machinery: Composition, localization, and mechanism. *FEMS Microbiol Rev*. **33**(3):643-656 (2009).
53. Ambur OH, Engelstädter J, Johnsen PJ, Miller EL, Rozen DE. Steady at the wheel: Conservative sex and the benefits of bacterial transformation. *Philos Trans R Soc B Biol Sci*. **371**:20150528 (2016).
54. Mcdonough E, Kamp H, Camilli A. *Vibrio cholerae* phosphatases required for the utilization of nucleotides and extracellular DNA as phosphate sources. *Mol Microbiol*. **99**(3):453-469 (2016).
55. Dubnau D. Genetic competence in *Bacillus subtilis*. *Microbiol Rev* **55**(3):395-424 (1991).
56. Michod RE, Wojciechowski MF, Hoezler MA. DNA repair and the evolution of transformation in the bacterium *Bacillus subtilis*. *Genetics*. **118**(1):31-39 (1988).
57. Redfield RJ. Evolution of natural transformation: Testing the DNA repair hypothesis in *Bacillus subtilis* and *Haemophilus influenzae*. *Genetics*. **133**(4):755-761 (1993).
58. Dorer MS, Fero J, Salama NR. DNA damage triggers genetic exchange in *Helicobacter pylori*. *PLoS Pathog*. **6**(7):e1001026 (2010).
59. Charpentier X, Kay E, Schneider D, Shuman HA. Antibiotics and UV radiation induce competence for natural transformation in *Legionella pneumophila*. *J Bacteriol*. **193**(5):1114-1121 (2011).
60. Prudhomme M, Attaiech L, Sanchez G, Martin B, Claverys JP. Antibiotic stress induces genetic transformability in the human pathogen *Streptococcus pneumoniae*. *Science* **313**:89-91 (2006).
61. Frye SA, Nilsen M, Tønjum T, Ambur OH. Dialects of the DNA Uptake Sequence in *Neisseriaceae*. *PLoS Genet*. **9**(4):e1003458 (2013).
62. Davidsen T, Rødland EA, Lagesen K, Seeberg E, Rognes T, Tønjum T. Biased distribution of DNA uptake sequences towards genome maintenance genes. *Nucleic Acids Res* **32**(3):1050-

1058 (2004).
63. Claverys JP, Håvarstein LS. Cannibalism and fratricide: Mechanisms and raisons d'être. *Nat Rev Microbiol*. **5**(3):219-229 (2007).
64. Overballe-Petersen S, Harms K, Orlando LAA, *et al.* Bacterial natural transformation by highly fragmented and damaged DNA. *Proc Natl Acad Sci USA*. **110**(49):19860-19865 (2013).
65. Nielsen KM, Johnsen PJ, Bensasson D, Daffonchio D. Release and persistence of extracellular DNA in the environment. *Environ Biosafety Res*. **6**:37-53 (2007).
66. Redfield RJ. Do bacteria have sex? *Nat Rev Genet*. **2**:634-639 (2001).
67. Rocha EPC. Using Sex to Cure the Genome. *PLoS Biol*. **14**(3):e1002417 (2016)
68. Draghi JA, Turner PE. DNA secretion and gene-level selection in bacteria. *Microbiology*. **152**(9):2683-2688 (2006).
69. Ibáñez de Aldecoa AL, Zafra O, González-Pastor JE. Mechanisms and regulation of extracellular DNA release and its biological roles in microbial communities. *Front Microbiol*. **8**:1390 (2017).
70. Johnston C, Martin B, Granadel C, Polard P, Claverys JP. Programmed Protection of Foreign DNA from Restriction Allows Pathogenicity Island Exchange during Pneumococcal Transformation. *PLoS Pathog*. **9**(2):e1003178 (2013)
71. Lerouge I, vanderleyden jos. O‐antigen structural variation: mechanisms and possible roles in animal/plant–microbe interactions. *FEMS Microbiol Rev*. **26**(1):17-47 (2001).
72. Blokesch M, Schoolnik GK. Serogroup conversion of *Vibrio cholerae* in aquatic reservoirs. *PLoS Pathog*. **3**(6):0733-0742 (2007).
73. Chun J, Grim CJ, Hasan NA, *et al.* Comparative genomics reveals mechanism for short-term and long-term clonal transitions in pandemic *Vibrio cholerae*. *Proc Natl Acad Sci USA*. **106**(36):15442-15447 (2009).
74. Banerjee R, Das B, Balakrish Nair G, Basak S. Dynamics in genome evolution of *Vibrio cholerae*. *Infect Genet Evol*. **23**:32-41 (2014).
75. Koch R. An address on cholera and its bacillus. *Br Med J*. **403-407** (1884).
76. McCarter LLMC. Polar Flagellar Motility of the *Vibrionaceae*. *Microbiol Mol Biol Rev*. **65**(3):445-462 (2001).
77. Bentivoglio M, Pacini P. Filippo Pacini: A determined observer. *Brain Res Bull*. **38**(2):161-165 (1995).
78. Lippi D, Gotuzzo E. The greatest steps towards the discovery of *Vibrio cholerae*. *Clin Microbiol Infect*. **20**(3):191-195 (2014).
79. Harris JB, LaRocque RC, Qadri F, Ryan ET, Calderwood SB. Cholera. *Lancet*. **379**(9835):2466-2476 (2012).
80. Lekshmi N, Joseph I, Ramamurthy T, Thomas S. Changing facaded of *Vibrio cholerae*: an enigma in the epidemiology of cholera. *Indian J Med Res*. **147**:133-141 (2018).
81. Heidelberg JF, Eisen JA, Nelson WC, *et al*. DNA sequence of both chromosomes of the cholera pathogen *Vibrio cholerae*. *Nature*. **406**(6795):477-483 (2000).
82. Mazel D, Dychinco B, Webb VA, Davies J. A Distinctive Class of Integron in the *Vibrio cholerae* Genome. *Science* **280**:605-609 (1998).
83. Mutreja A, Kim DW, Thomson NR, *et al*. Evidence for several waves of global transmission in the seventh cholera pandemic. *Nature*. **477**(7365):462-465 (2011).
84. Domman D, Quilici M, Dorman MJ, *et al.* Integrated view of *Vibrio cholerae* in the Americas. *Science* **358**:789-793 (2017).
85. Weill F, Domman D, Njamkepo E, *et al.* Genomic history of the seventh pandemic of cholera in Africa. *Science* **358**:785-789 (2017).

86. Weill F, Domman D, Njamkepo E, *et al.* Genomic insights into the 2016-2017 cholera epidemic in Yemen. *Nature*. **565**:230-234 (2019).
87. Reidl J, Klose KE. *Vibrio cholerae* and cholera: Out of the water and into the host. *FEMS Microbiol Rev*. **26**(2):125-139 (2002).
88. Awofeso N, Aldabk K. Cholera, Migration, and Global Health – A Critical Review. *Int J Travel Med Glob Heal*. **6**(3):92-99 (2018).
89. Nelson EJ, Harris JB, Morris JG, Calderwood SB, Camilli A. Cholera transmission: The host, pathogen and bacteriophage dynamic. *Nat Rev Microbiol*. **7**(10):693-702 (2009).
90. WHO. Cholera: the forgotten pandemic. https://www.who.int/cholera/the-forgotten-pandemic/en/.
91. WHO. Weekly Epidemiological Record, 21 September 2018. *Wkly Epidemiol Rec*. **93**(38):489–500 (2018).
92. Deen JL, von Seidlein L, Sur D, *et al.* The high burden of cholera in children: Comparison of incidence from endemic areas in Asia and Africa. *PLoS Negl Trop Dis*. **2**(2):e173 (2008).
93. Harris JB, Khan AI, LaRocque RC, *et al.* Blood group, immunity, and risk of infection with *Vibrio cholerae* in an area of endemicity. *Infect Immun*. **73**(11):7422-7427 (2005).
94. Finkelstein RA. Cholera, *Vibrio cholerae* O1 and O139, and Other Pathogenic Vibrios. *Med Microbiol*. chapter 24 (1996).
95. Sánchez J, Holmgren J. Cholera toxin structure, gene regulation and pathophysiological and immunological aspects. *Cell Mol Life Sci*. **65**(9):1347-1360 (2008).
96. Clemens J, Shin S, Sur D, Nair GB, Holmgren J. New-generation vaccines against cholera. *Nat Rev Gastroenterol Hepatol*. **8**(12):701-710 (2011).
97. Conner JG, Teschler JK, Jones CJ, Yildiz FH. Staying Alive: *Vibrio cholerae's* Cycle of Environmental Survival, Transmission, and Dissemination. *Virulence Mech Bact Pathog Fifth Ed*. Chapter **21**:593-633 (2016).
98. LaRocque RC, Harris JB, Dziejman M, *et al.* Transcriptional profiling of *Vibrio cholerae* recovered directly from patient specimens during early and late stages of human infection. *Infect Immun*. **73**(8):4488-4493 (2005).
99. Faruque SM, Mekalanos JJ. Phage-bacterial interactions in the evolution of toxigenic *Vibrio cholerae*. *Virulence*. **3**:7:556-565 (2012).
100. Zuckerman JN, Rombo L, Fisch A. The true burden and risk of cholera: implications for prevention and control. *Lancet Infect Dis*. **7**(8):521-530 (2007).
101. Chatterjee SN, Chaudhuri K. Lipopolysaccharides of *Vibrio cholerae*: I. Physical and chemical characterization. *Biochim Biophys Acta - Mol Basis Dis*. **1639**(2):65-79 (2003).
102. Davies BW, Bogard RW, Young TS, Mekalanos JJ. Coordinated Regulation of Accessory Genetic Elements Produces Cyclic Di-Nucleotides for *V . cholerae* Virulence. *Cell*. **149**(2):358-370 (2012).
103. Dziejman M, Balon E, Boyd D, Fraser CM, Heidelberg JF, Mekalanos JJ. Comparative genomic analysis of *Vibrio cholerae*: Genes that correlate with cholera endemic and pandemic disease. *Proc Natl Acad Sci USA*. **99**(3):1556-1561 (2002).
104. Nguyen TH, Pham TD, Higa N, *et al.* Analysis of *Vibrio* seventh pandemic island II and novel genomic islands in relation to attachment sequences among a wide variety of *Vibrio cholerae* strains. *Microbiol Immunol*. **62**(3):150-157 (2018).
105. Ghosh-Banerjee J, Senoh M, Takahashi T, *et al.* Cholera toxin production by the El Tor variant of *Vibrio cholerae* O1 compared to prototype El Tor and classical biotypes. *J Clin Microbiol*. **48**(11):4283-4286 (2010).
106. Olsvik O, Wahlberg J, Petterson B, *et al.* Use of automated sequencing of polymerase chain reaction-generated amplicons to identify three types of cholera toxin subunit B in *Vibrio*

cholerae O1 strains. *J Clin Microbiol*. **31**(1):22-25 (1993).
107. Raychoudhuri A, Mukhopadhyay AK, Ramamurthy T, Nandy RK, Takeda Y, Nair GB. Biotyping of *Vibrio cholerae* O1: Time to redefine the scheme. *Indian J Med Res*. **128**(6):695-698 (2008).
108. Raychoudhuri A, Patra T, Ghosh K, *et al.* Classical ctxB in *Vibrio cholerae* O1, Kolkata, India. *Emerg Infect Dis*. **15**:131-132 (2009).
109. Swerdlow DL, Ries AA. *Vibrio cholerae* non-O1-the eighth pandemic? *Lancet*. **342**:382-383 (1993).
110. Faruque SM, Chowdhury N, Kamruzzaman M, *et al.* Reemergence of Epidemic *Vibrio cholerae* O139, Bangladesh. *Emerg Infect Dis*. **9**(9):1116-1122 (2003).
111. Faruque SM, Sack DA, Sack RB, Colwell RR, Takeda Y, Nair GB. Emergence and evolution of *Vibrio cholerae* O139. *Proc Natl Acad Sci USA*. **100**(3):1304-1309 (2003).
112. Bik EM, Bunschoten AE, Gouw RD, Mooi FR. Genesis of the novel epidemic *Vibrio cholerae* O139 strain: evidence for horizontal transfer of genes involved in polysaccharide synthesis. *EMBO J*. **14**(2):209-216 (1995).
113. Mooi FR, Bik EM. The evolution of epidemic *Vibrio cholerae* strains. *Trends Microbiol*. **5**(4):161-165 (1997).
114. Colwell RR, Seidler RJ, Kaper J, *et al.* Occurrence of *Vibrio cholerae* serotype O1 in Maryland and Louisiana estuaries. *Appl Environ Microbiol*. **41**(2):555-558 (1981).
115. Colwell RR, Kaper J, Joseph S. *Vibrio cholerae*, *Vibrio parahaemolyticus*, and other Vibrios: occurrence and distribution in Chesapeake bay. *Science*. **198**:394-396 (1977).
116. Lutz C, Erken M, Noorian P, Sun S, McDougald D. Environmental reservoirs and mechanisms of persistence of *Vibrio cholerae*. *Front Microbiol*. **4**:375 (2013).
117. Sack DA, Sack RB, Nair GB, Siddique A. Cholera. *Lancet*. **363**(9404):223-233 (2004).
118. Huq A, Small EB, West PA, Huq MI, Rahman R, Colwell RR. Ecological relationships between *Vibrio cholerae* and planktonic crustacean copepods. *Appl Environ Microbiol*. **45**(1):275-283 (1983).
119. Lipp EK, Huq A, Colwell RR. Effects of Global Climate on Infectious Disease : the Cholera Model. *Clin Microbiol Rev*. **15**(4):757-770 (2002).
120. Pruzzo C, Vezzulli L, Colwell RR. Global impact of *Vibrio cholerae* interactions with chitin. *Environ Microbiol*. **10**(6):1400-1410 (2008).
121. Heidelberg JF, Heidelberg KB, Colwell RR. Bacteria of the γ-subclass Proteobacteria associated with zooplankton in Chesapeake Bay. *Appl Environ Microbiol*. **68**(11):5498-5507 (2002).
122. Colwell RR, Huq A, Islam MS, *et al.* Reduction of cholera in Bangladeshi villages by simple filtration. *Proc Natl Acad Sci USA*. **100**(3):1051-1055 (2003).
123. Thomas K, Nielsen TG. Regulation of zooplankton biomass and production in a temperate, coastal ecosystem. 1. Copepods. *Limnol Oceanogr*. **39**(3):493-507 (1994).
124. Alam M, Kasan NA, Sadique A, *et al.* Seasonal cholera caused by *Vibrio cholerae* serogroups O1 and O139 in the coastal aquatic environment of Bangladesh. *Appl Environ Microbiol*. **72**(6):4096-4104 (2006).
125. Colwell RR. Global Climate and Infectious Disease: The Cholera Paradigm. *Science* **274**(5295):2025-2031 (1996).
126. Huq A, West PA, Small EB, Huq MI, Colwell RR. Influence of water temperature, salinity, and pH on survival and growth of toxigenic *Vibrio cholerae* serovar O1 associated with live copepods in laboratory microcosms. *Appl Environ Microbiol*. **48**(2):420-424 (1984).
127. Vezzulli L, Colwell RR, Pruzzo C. Ocean Warming and Spread of Pathogenic Vibrios in the Aquatic Environment. *Microb Ecol*. **65**(4):817-825 (2013).

128. Sakib SN, Reddi G, Almagro-Moreno S. Environmental Role of Pathogenic Traits in *Vibrio cholerae* . *J Bacteriol*. **200**:e00795-17 (2018).
129. Vezzulli L, Pruzzo C, Huq A, Colwell RR. Environmental reservoirs of *Vibrio cholerae* and their role in cholera. *Environ Microbiol Rep*. **2**(1):27-33 (2010).
130. Almagro-moreno S, Taylor RK. Cholera : Environmental Reservoirs and Impact on Disease Transmission. *Microbiol Spectr*. **1**(2):OH-0003-2012. (2013).
131. Wang J, Yan M, Gao H, Lu xin, Kan B. *Vibrio cholerae* colonization of soft-shelled turtles. *Appl Environ Microbiol*. **83**(14):e00713-17 (2017).
132. Keyhani NO, Roseman S. Physiological aspects of chitin catabolism in marine bacteria. *Biochim Biophys Acta - Gen Subj*. **1473**(1):108-122 (1999).
133. Meibom KL, Li XB, Nielsen AT, Wu C-Y, Roseman S, Schoolnik GK. The *Vibrio cholerae* chitin utilization program. *Proc Natl Acad Sci USA*. **101**(8):2524-2529 (2004).
134. Meibom KL, Blokesch M, Dolganov NA, Wu C-Y, Schoolnik GK. Chitin induces natural competence in *Vibrio cholerae Science* **310**(5755):1824-1827 (2005).
135. Lo Scrudato M, Blokesch M. The regulatory network of natural competence and transformation of *Vibrio cholerae*. *PLoS Genet*. **8**(6):e1002778 (2012).
136. Lo Scrudato M, Borgeaud S, Blokesch M. Regulatory elements involved in the expression of competence genes in naturally transformable *Vibrio cholerae*. *BMC Microbiol* **14**:327 (2014).
137. Metzger LC, Blokesch M. Regulation of competence-mediated horizontal gene transfer in the natural habitat of *Vibrio cholerae*. *Curr Opin Microbiol*. **30**:1-7. (2016).
138. Kirn TJ, Jude BA, Taylor RK. A colonization factor links *Vibrio cholerae* environmental survival and human infection. *Nature*. **438**(7069):863-866 (2005).
139. Wong E, Vaaje-Kolstad G, Ghosh A, *et al.* The *Vibrio cholerae* colonization factor GbpA possesses a modular structure that governs binding to different host surfaces. *PLoS Pathog*. **8**(1):e1002373 (2012).
140. Chiavelli DA, Marsh JW, Taylor RK. The Mannose-Sensitive Hemagglutinin of *Vibrio cholerae* Promotes Adherence to Zooplankton. *Appl Environ Microbiol*. **67**(7):3220-3225 (2001).
141. Watnick PI, Fullner KJ, Kolter R. A role for the mannose-sensitive hemagglutinin in biofilm formation by *Vibrio cholerae* El Tor. *J Bacteriol*. **181**(11):3606-3609 (1999).
142. Watnick PI, Kolter R. Steps in the development of a *Vibrio cholerae* El Tor biofilm. *Mol Microbiol*. **34**(3):586-595 (19999
143. Li X, Roseman S. The chitinolytic cascade in Vibrios is regulated by chitin oligosaccharides and a two-component chitin catabolic sensor/kinase. *Proc Natl Acad Sci USA*. **101**(2):627-631. (2004).
144. Yamamoto S, Morita M, Izumiya H, Watanabe H. Chitin disaccharide $(GlcNAc)_2$ induces natural competence in *Vibrio cholerae* through transcriptional and translational activation of a positive regulatory gene $tfoX^{VC}$. *Gene*. **457**(1-2):42-49 (2010).
145. Yamamoto S, Izumiya H, Mitobe J, *et al.* Identification of a chitin-induced small RNA that regulates translation of the *tfoX* gene, encoding a positive regulator of natural competence in *Vibrio cholerae*. *J Bacteriol*. **193**(8):1953-1965 (2011).
146. Yamamoto S, Mitobe J, Ishikawa T, *et al.* Regulation of natural competence by the orphan two-component system sensor kinase ChiS involves a non-canonical transmembrane regulator in *Vibrio cholerae*. *Mol Microbiol*. **91**(2):326-347 (2014).
147. Dalia AB, Lazinski DW, Camilli A. Identification of a Membrane-Bound Transcriptional Regulator That Links Chitin and Natural Competence in *Vibrio cholerae*. *mBio*. **5**(1):e01028-13 (2014).
148. Metzger LC, Blokesch M. Regulation of competence-mediated horizontal gene transfer in the

natural habitat of *Vibrio cholerae*. *Curr Opin Microbiol*. **30**:1-7. (2016).
149. Blokesch M. Chitin colonization, chitin degradation and chitin-induced natural competence of *Vibrio cholerae* are subject to catabolite repression. *Environ Microbiol*. **14**(8):1898-1912 (2012).
150. Blokesch M, Schoolnik GK. The extracellular nuclease Dns and its role in natural transformation of *Vibrio cholerae*. *J Bacteriol*. **190**(21):7232-7240 (2008).
151. Görke B, Stülke J. Carbon catabolite repression in bacteria: Many ways to make the most out of nutrients. *Nat Rev Microbiol*. **6**(8):613-624 (2008).
152. Deutscher J. The mechanisms of carbon catabolite repression in bacteria. *Curr Opin Microbiol*. **11**(2):87-93 (2008).
153. Wu R, Zhao M, Li J, Gao H, Kan B, Liang W. Direct regulation of the natural competence regulator gene *tfoX* by cyclic AMP (cAMP) and cAMP receptor protein (CRP) in *Vibrios*. *Sci Rep*. 5:14921 (2015).
154. Redfield RJ, Cameron ADS, Qian Q, *et al*. A novel CRP-dependent regulon controls expression of competence genes in *Haemophilus influenzae*. *J Mol Biol*. **347**(4):735-747 (2005).
155. Waters CM, Bassler BL. Quorum Sensing: Cell-to-Cell Communication in Bacteria. *Annu Rev Cell Dev Biol*. **21**(1):319-346 (2005).
156. Papenfort K, Bassler BL. Quorum sensing signal – response systems in Gram-negative bacteria. *Nat Rev Microbiol*. **14**(9):576-588 (2016).
157. Bassler BL, Greenberg EP, Stevens AM. Cross-species induction of luminescence in the quorum-sensing bacterium *Vibrio harveyi*. *J Bacteriol*. **179**(12):4043-4045 (1997).
158. Miller MB, Skorupski K, Lenz DH, Taylor RK, Bassler BL. Parallel quorum sensing systems converge to regulate virulence in *Vibrio cholerae*. *Cell*. **110**(3):303-314 (2002).
159. Xavier KB, Bassler BL. LuxS quorum sensing: More than just a numbers game. *Curr Opin Microbiol*. **6**(2):191-197 (2003).
160. Jung SA, Chapman CA, Ng WL. Quadruple Quorum-Sensing Inputs Control *Vibrio cholerae* Virulence and Maintain System Robustness. *PLoS Pathog*. **11**(4):1-19 (2015).
161. Lenz DH, Mok KC, Lilley BN, Kulkarni R V., Wingreen NS, Bassler BL. The small RNA chaperone Hfq and multiple small RNAs control quorum sensing in *Vibrio harveyi* and *Vibrio cholerae*. *Cell*. **118**(1):69-82 (2004).
162. Bardill JP, Zhao X, Hammer BK. The *Vibrio cholerae* quorum sensing response is mediated by Hfq-dependent sRNA/mRNA base pairing interactions. *Mol Microbiol*. **80**(5):1381-1394 (2011).
163. Ng W, Bassler B. Bacterial Quorum-Sensing Network Architectures. *Annu Rev Genet*. **43**:197-222 (2009).
164. Zhu J, Miller MB, Vance RE, Dziejman M, Bassler BL, Mekalanos JJ. Quorum-sensing regulators control virulence gene expression in *Vibrio cholerae*. *Proc Natl Acad Sci USA*. **99**(5):3129-3134 (2002).
165. Zhu J, Mekalanos JJ. Quorum sensing-dependent biofilms enhance colonization in *Vibrio cholerae*. *Dev Cell*. **5**(4):647-656 (2003).
166. Hammer BK, Bassler BL. Quorum sensing controls biofilm formation in *Vibrio cholerae*. *Mol Microbiol*. **50**(1):101-114 (2003).
167. Lo Scrudato M, Blokesch M. A transcriptional regulator linking quorum sensing and chitin induction to render *Vibrio cholerae* naturally transformable. *Nucleic Acids Res*. **41**(6):3644-3658 (2013).
168. Seitz P, Blokesch M. DNA Transport across the Outer and Inner Membranes of Naturally Transformable *Vibrio cholerae* Is Spatially but Not Temporally Coupled. *mBio*. 5(4):e01409-

14. (2014).
169. Focareta T, Manning PA. Genetic analysis of the export of an extracellular DNase of *Vibrio cholerae* using DNase-β-lactamase fusions. *Gene*. **108**(1):31-37 (1991).
170. Jaskólska M, Stutzmann S, Stoudmann C, Blokesch M. QstR-dependent regulation of natural competence and type VI secretion in *Vibrio cholerae*. *Nucleic Acids Res*. **46**(20):10619-10634 (2018).
171. Matthey N, Blokesch M. The DNA-Uptake Process of Naturally Competent *Vibrio cholerae*. *Trends Microbiol*. **24**(2):98-110 (2016).
172. Nero TM, Dalia TN, Wang JCY, Kysela DT, Bochman ML, Dalia AB. ComM is a hexameric helicase that promotes branch migration during natural transformation in diverse Gram-negative species. *Nucleic Acids Res*. **46**(12):6099-6111 (2018).
173. Marie L, Rapisarda C, Morales V, *et al*. Bacterial RadA is a DnaB-type helicase interacting with RecA to promote bidirectional D-loop extension. *Nat Commun*. **8**:15638 (2017).
174. Adams DW, Stutzmann S, Stoudmann C, Blokesch M. DNA-uptake pili of *Vibrio cholerae* are required for chitin colonization and capable of kin recognition via sequence-specific self-interaction. *Nat Microbiol*. doi:10.1038/s41564-019-0479-5 (2019).
175. Metzger LC, Blokesch M. Composition of the DNA-uptake complex of *Vibrio cholerae* . *Mob Genet Elements* **4**(1):e28142 (2014).
176. Hahn J, Maier B, Haijema BJ, Sheetz M, Dubnau D. Transformation proteins and DNA uptake localize to the cell poles in *Bacillus subtilis*. *Cell*. **122**(1):59-71 (2005).
177. Ng D, Harn T, Altindal T, *et al*. The *Vibrio Cholerae* Minor Pilin TcpB Initiates Assembly and Retraction of the Toxin-Coregulated Pilus. *PLoS Pathog.* **12**(12):e1006109 (2016).
178. Steinbock LJ, Krishnan S, Bulushev RD, *et al.* Probing the size of proteins with glass nanopores. *Nanoscale*. **6**(23):14380-14387 (2014).
179. Draskovic I, Dubnau D. Biogenesis of a putative channel protein, ComEC, required for DNA uptake: membrane topology, oligomerization and formation of disulphide bonds. *Mol Microbiol*. **55**:881-896 (2005).
180. Borgeaud S, Metzger LC, Scrignari T, Blokesch M. The type VI secretion system of *Vibrio cholerae* fosters horizontal gene transfer. *Science* **347**:63-67 (2015).
181. Cianfanelli FR, Monlezun L, Coulthurst SJ. Aim, Load, Fire: The Type VI Secretion System, a Bacterial Nanoweapon. *Trends Microbiol*. **24**:51-62. (2016).
182. Veening JW, Blokesch M. Interbacterial predation as a strategy for DNA acquisition in naturally competent bacteria. *Nat Rev Microbiol*. **15**(10):621-629 (2017).
183. Mecsas J, Green ER. Bacterial Secretion Systems – An overview. *Microbiol Spectr*. **4**:10.1128 (2016).
184. Rapisarda C, Tassinari M, Gubellini F, Fronzes R. Using Cryo-EM to Investigate Bacterial Secretion Systems. *Annu Rev Microbiol*. **72**(1):231-254 (2018).
185. Salomon D, Orth K. Type VI secretion system. *Curr Biol*. **25**(7):R265-R266 (2015).
186. Ho BT, Dong TG, Mekalanos JJ. A view to a kill: The bacterial type VI secretion system. *Cell Host Microbe*. **15**(1):9-21 (2014).
187. Pukatzki S, Ma AT, Sturtevant D, *et al.* Identification of a conserved bacterial protein secretion system in *Vibrio cholerae* using the *Dictyostelium* host model system. *PNAS* **103**(5):1528-1533 (2006).
188. Williams SG, Varcoe LT, Attridge SR, Manning PA. *Vibrio cholerae* Hcp, a secreted protein coregulated with HlyA. *Infect Immun* **64**(1):283-289 (1996).
189. Das S, Chaudhuri K. Identification of a unique IAHP (IcmF associated homologous proteins) cluster in *Vibrio cholerae* and other proteobacteria through *in silico* analysis. *In Silico Biol*. **3**(3):287-300 (2003).

190. Mougous JD, Cuff ME, Raunser S, *et al*. A virulence locus of *Pseudomonas aeruginosa* encodes a protein secretion apparatus. *Science* **312**(5779):1526-1530 (2006).
191. Boyer F, Fichant G, Berthod J, Vandenbrouck Y, Attree I. Dissecting the bacterial type VI secretion system by a genome wide *in silico* analysis: What can be learned from available microbial genomic resources? *BMC Genomics*. **10**:104 (2009).
192. Zoued A, Brunet YR, Durand E, *et al.* Architecture and assembly of the Type VI secretion system. *Biochim Biophys Acta - Mol Cell Res*. **1843**(8):1664-1673 (2014).
193. Pukatzki S, Ma AT, Revel AT, Sturtevant D, Mekalanos JJ. Type VI secretion system translocates a phage tail spike-like protein into target cells where it cross-links actin. *Proc Natl Acad Sci USA* **104**(39):15508-15513 (2007).
194. Leiman PG, Basler M, Ramagopal UA, *et al.* Type VI secretion apparatus and phage tail-associated protein complexes share a common evolutionary origin. *Proc Natl Acad Sci USA*. **106**(11):4154-4159 (2009).
195. Bönemann G, Pietrosiuk A, Diemand A, Zentgraf H, Mogk A. Remodelling of VipA/VipB tubules by ClpV-mediated threading is crucial for type VI protein secretion. *EMBO J*. **28**(4):315-325 (2009).
196. Barret M, Egan F, Fargier E, Morrissey JP, O'Gara F. Genomic analysis of the type VI secretion systems in *Pseudomonas* spp.: Novel clusters and putative effectors uncovered. *Microbiology*.**157**(6):1726-1739 (2011).
197. Russell AB, Hood RD, Bui NK, Leroux M, Vollmer W, Mougous JD. Type VI secretion delivers bacteriolytic effectors to target cells. *Nature*. **475**(7356):343-349 (2011).
198. Dong TG, Ho BT, Yoder-Himes DR, Mekalanos JJ. Identification of T6SS-dependent effector and immunity proteins by Tn-seq in *Vibrio cholerae*. *Proc Natl Acad Sci USA*. **110**(7):2623-2628 (2013).
199. Chen L, Zou Y, She P, Wu Y. Composition, function, and regulation of T6SS in *Pseudomonas aeruginosa*. *Microbiol Res*. **172**:19-25 (2015).
200. Boyd EF, Cohen AL V., Naughton LM, *et al.* Molecular analysis of the emergence of pandemic Vibrio *parahaemolyticus*. *BMC Microbiol*. **8**:110 (2008).
201. Sheng L, Gu D, Wang Q, Liu Q, Zhang Y. Quorum sensing and alternative sigma factor RpoN regulate type VI secretion system I (T6SSVA1) in fish pathogen *Vibrio alginolyticus*. *Arch Microbiol*. **194**(5):379-390 (2012).
202. Basler M, Pilhofer M, Henderson GP, Jensen GJ, Mekalanos JJ. Type VI secretion requires a dynamic contractile phage tail-like structure. *Nature*. **483**(7388):182-186 (2012).
203. Durand E, Nguyen VS, Zoued A, *et al.* Biogenesis and structure of a type VI secretion membrane core complex. *Nature*. **523**:555-560 (2015).
204. Brunet YR, Zoued A, Boyer F, Douzi B. The Type VI Secretion TssEFGK-VgrG Phage- Like Baseplate Is Recruited to the TssJLM Membrane Complex via Multiple Contacts and Serves As Assembly Platform for Tail Tube/Sheath Polymerization. *PLoS Genet*. **11**:e1005545 (2015).
205. Zoued A, Durand E, Brunet YR, *et al.* Priming and polymerization of a bacterial contractile tail structure. *Nature* **531**:59-63 (2016).
206. Basler M, J. MJ. Type 6 secretion dynamics within and between bacterial cells. *Science* **337**:815 (2012).
207. Basler M. Type VI secretion system: Secretion by a contractile nanomachine. *Philos Trans R Soc B Biol Sci*. **370**:20150021 (2015).
208. Wang J, Brodmann M, Basler M. Assembly and Subcellular Localization of Bacterial Type VI Secretion Systems. *Annu Rev Microbiol* **73**:28 (2019).
209. Hood RD, Singh P, Hsu FS, *et al.* A Type VI Secretion System of *Pseudomonas aeruginosa*

Targets a Toxin to Bacteria. *Cell Host Microbe*. **7**(1):25-37 (2010).
210. Schwarz S, West TE, Boyer F, *et al*. Burkholderia type VI secretion systems have distinct roles in eukaryotic and bacterial cell interactions. *PLoS Pathog*. **6**(8):77-78 (2010).
211. Ma J, Pan Z, Huang J, Sun M, Lu C, Yao H. The Hcp proteins fused with diverse extended-toxin domains represent a novel pattern of antibacterial effectors in type VI secretion systems. *Virulence*. **8**(7):1189-1202 (2017).
212. Shneider MM, Buth SA, Ho BT, Basler M, Mekalanos JJ, Leiman PG. PAAR-repeat proteins sharpen and diversify the type VI secretion system spike. *Nature*. **500**:350-353 (2013).
213. Hachani A, Allsopp LP, Oduko Y, Filloux A. The VgrG proteins are "à la carte" delivery systems for bacterial type VI effectors. *J Biol Chem*. **289**(25):17872-17884 (2014).
214. Bondage DD, Lin J-S, Ma L-S, Kuo C-H, Lai E-M. VgrG C terminus confers the type VI effector transport specificity and is required for binding with PAAR and adaptor–effector complex. *Proc Natl Acad Sci USA*. **113**(27):E3931-E3940 (2016).
215. Silverman JM, Agnello DM, Zheng H, *et al.* Haemolysin Coregulated Protein Is an Exported Receptor and Chaperone of Type VI Secretion Substrates. *Mol Cell*. **51**(5):584-593 (2013).
216. Alcoforado Diniz J, Liu YC, Coulthurst SJ. Molecular weaponry: Diverse effectors delivered by the Type VI secretion system. *Cell Microbiol*. **17**(12):1742-1751 (2015).
217. Russell AB, Peterson SB, Mougous JD. Type VI secretion system effectors: Poisons with a purpose. *Nat Rev Microbiol*. **12**(2):137-148 (2014).
218. Vollmer W, Blanot D, De Pedro MA. Peptidoglycan structure and architecture. *FEMS Microbiol Rev*. **32**(2):149-167 (2008).
219. Russell AB, Singh P, Brittnacher M, *et al.* A Widespread Bacterial Type VI Secretion Effector Superfamily Identified Using a Heuristic Approach. *Cell Host Microbe*. **11**(5):538-549 (2012).
220. Russell AB, Leroux M, Hathazi K, *et al.* Diverse type VI secretion phospholipases are functionally plastic antibacterial effectors. *Nature*. **496**(7446):508-512 (2013).
221. Miyata ST, Unterweger D, Rudko SP, Pukatzki S. Dual Expression Profile of Type VI Secretion System Immunity Genes Protects Pandemic *Vibrio cholerae*. *PLoS Pathog*. **9**(12):e1003752 (2013).
222. Ma LS, Hachani A, Lin JS, Filloux A, Lai EM. *Agrobacterium tumefaciens* deploys a superfamily of type VI secretion DNase effectors as weapons for interbacterial competition in planta. *Cell Host Microbe*. **16**(1):94-104 (2014).
223. Salomon D, Gonzalez H, Updegraff BL, Orth K. *Vibrio parahaemolyticus* Type VI Secretion System 1 Is Activated in Marine Conditions to Target Bacteria, and Is Differentially Regulated from System 2. *PLoS One*. **8**(4):e61086 (2013).
224. Moscoso JA, Mikkelsen H, Heeb S, Williams P, Filloux A. The *Pseudomonas aeruginosa* sensor RetS switches Type III and Type VI secretion via c-di-GMP signalling. *Environ Microbiol*. **13**(12):3128-3138 (2011).
225. Brunet YR, Bernard CS, Gavioli M, Lloubès R, Cascales E. An epigenetic switch involving overlapping fur and DNA methylation optimizes expression of a type VI secretion gene cluster. *PLoS Genet*. **7**:e1002205 (2011).
226. Silverman JM, Brunet YR, Cascales E, Mougous JD. Structure and Regulation of the Type VI Secretion System. *Annu Rev Microbiol*. **66**(1):453-472 (2012).
227. Unterweger D, Miyata ST, Bachmann V, *et al*. The *Vibrio cholerae* type VI secretion system employs diverse effector modules for intraspecific competition. *Nat Commun*. **5**:3549 (2014).
228. Metzger LC, Stutzmann S, Scrignari T, Van der Henst C, Matthey N, Blokesch M. Independent Regulation of Type VI Secretion in *Vibrio cholerae* by TfoX and TfoY. *Cell Rep*. **15**(5):951-958 (2016).
229. Altindis E, Dong T, Catalano C. Secretome Analysis of *Vibrio cholerae* Type VI Secretion

System Reveals a New Effector-Immunity Pair. *mBio* **6**(2):e00075-15 (2015).
230. Kudryashev M, Wang RYR, Brackmann M, *et al.* Structure of the Type VI secretion system contractile sheath. *Cell*. **160**(5):952-962 (2015).
231. Vettiger A, Winter J, Lin L, Basler M. The type VI secretion system sheath assembles at the end distal from the membrane anchor. *Nat Commun*. **8**:16088 (2017).
232. Joshi A, Kostiuk B, Rogers A, Teschler J, Pukatzki S, Yildiz FH. Rules of Engagement: The Type VI Secretion System in *Vibrio cholerae*. *Trends Microbiol*. **25**(4):267-279 (2017).
233. Vettiger A, Basler M. Type VI Secretion System Substrates Are Transferred and Reused among Sister Cells. *Cell*. **167**:99-110 (2016).
234. Brooks TM, Unterweger D, Bachmann V, Kostiuk B, Pukatzki S. Lytic activity of the *Vibrio cholerae* type VI secretion toxin VgrG-3 is inhibited by the antitoxin TsaB. *J Biol Chem*. **288**(11):7618-7625 (2013).
235. Metzger LC, Stutzmann S, Scrignari T, Van der Henst C, Matthey N, Blokesch M. Independent Regulation of Type VI Secretion in *Vibrio cholerae* by TfoX and TfoY. *Cell Rep*. **15**(5):951-958 (2016).
236. Link KH, Weinberg Z, Sudarsan N, *et al*. Riboswitches in Eubacteria Sense the Second Messenger Cyclic Di-GMP. *Science* **321**:411-413 (2008).
237. Romling U, Galperin MY, Gomelsky M. Cyclic di-GMP: the First 25 Years of a Universal Bacterial Second Messenger. *Microbiol Mol Biol Rev*. **77**(1):1-52 (2013).
238. Inuzuka S, Matsumura S, Ikawa Y. Optimization of RNA-based c-di-GMP fluorescent sensors through tuning their structural modules. *J Biosci Bioeng*. **122**(2):183-187 (2016).
239. Van der Henst C, Vanhove AS, Drebes Dörr NC, *et al*. Molecular insights into *Vibrio cholerae's* intra-amoebal host-pathogen interactions. *Nat Commun*. **9**:3460 (2018).
240. Fiore AE, Michalski JM, Russell RG, Sears CL, Kaper JB. Cloning, characterization, and chromosomal mapping of a phospholipase (lecithinase) produced by *Vibrio cholerae*. *Infect Immun*. **65**(8):3112-3117 (1997).
241. Alm RA, Stroeher UH, Manning PA. Extracellular proteins of *Vibrio cholerae*: nucleotide sequence of the structural gene (*hlyA*) for the haemolysin of the haemolytic El Tor strain O17 and characterization of the *hlyA* mutation in the non-haemolytic classical strain 569B. *Mol Microbiol*. **2**:481-488 (1988).
242. Bernardy EE, Turnsek MA, Wilson SK, Tarr CL, Hammer BK. Diversity of Clinical and Environmental Isolates of *Vibrio cholerae* in Natural Transformation and Contact-Dependent Bacterial Killing Indicative of Type VI Secretion System Activity. *Appl Environ Microbiol*. **82**(9):2833-2842 (2016).
243. Pollack-Berti A, Wollenberg MS, Ruby EG. Natural transformation of *Vibrio fischeri* requires *tfoX* and *tfoY*. *Environ Microbiol*. **12**(8):2302-2311 (2010).
244. Salomon D, Kinch LN, Trudgian DC, *et al.* Marker for type VI secretion system effectors. *Proc Natl Acad Sci USA*. **111**(25):9271-9276 (2014).
245. Salomon D, Klimko JA, Trudgian DC, *et al.* Type VI Secretion System Toxins Horizontally Shared between Marine Bacteria. *PLoS Pathog*. **10**:1371 (2015).
246. Speare L, Cecere AG, Guckes KR, *et al.* Bacterial symbionts use a type VI secretion system to eliminate competitors in their natural host. *Proc Natl Acad Sci USA* **115**(36):E8528-E8537 (2018).

2. ECOLOGICAL IMPLICATIONS OF GENE REGULATION BY TFOX AND TFOY AMONG DIVERSE *VIBRIO* SPECIES.

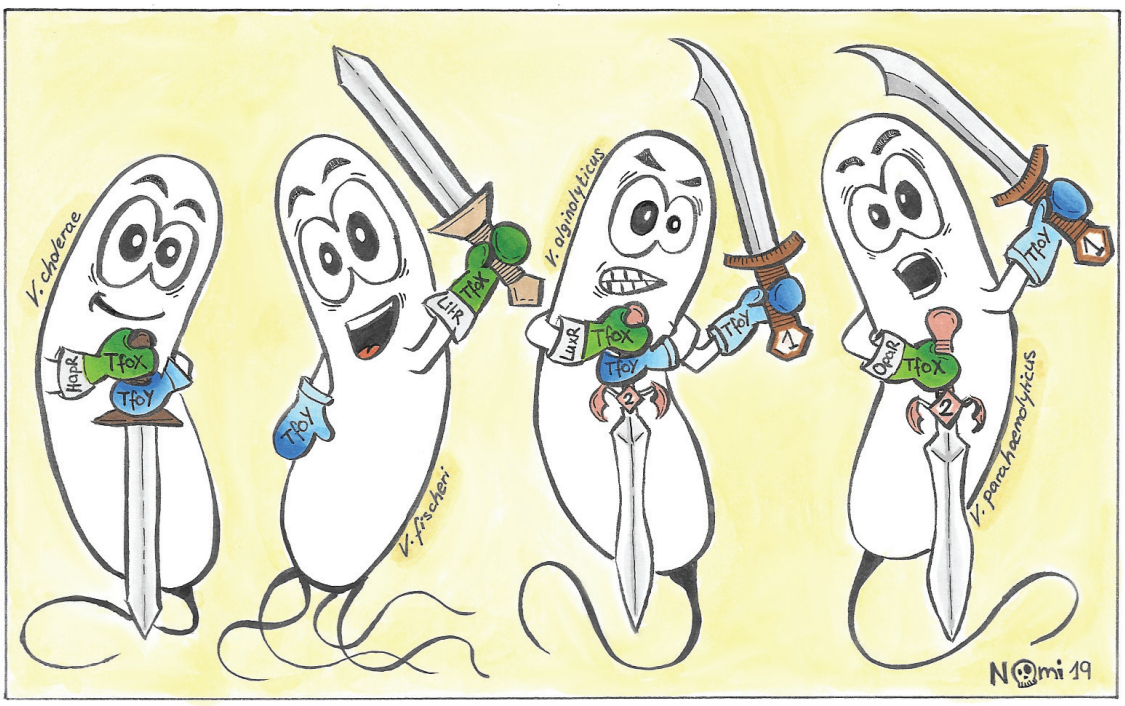

2.1 BACKGROUND INFORMATION

In this chapter, we provide novel insights onto the conservation and role of TfoX and TfoY among diverse *Vibrio* species. While TfoX and TfoY are present in all sequenced *Vibrionaceae*, key knowledge about their biological functions has been gained by studying *V. cholerae* as a model organism ([1–3]). As we investigated the role of TfoX and TfoY in three different *Vibrio* species, the next paragraphs will give a brief overview of these organisms and will highlight some important characteristics linked to natural competence and to their T6SS.

Vibrionaceae represent a family of aquatic gamma proteobacteria, which have been classified in seven genera including the genera Vibrio. As for *V. cholerae*, comparative genomic studies showed high genomic diversity among these species, which occurred, at least in part, through HGT events ([4,5]). Some of these vibrios are pathogens to humans or marine animals, whereas others are nonpathogenic. In the present work, we focused on the following species: *V. parahaemolyticus*, *V. alginolyticus,* and *V. fischeri*. The latter is a symbiotic bioluminescent bacterium commonly found in association with fish or squid, such as the Hawaiian bobtail squid *Euprymna scolopes*, whereas *V. parahaemolyticus* and *V. alginolyticus* engage in a pathogenic lifestyle. Similar to *V. cholerae*, *V. parahaemolyticus* is a foodborne pathogen, which is prevalent worldwide and causes gastroenteritis mostly after the consumption of contaminated seafood. In addition, this emerging pathogen can cause wound infections and, in rare cases, septicemia ([6]). *V. alginolyticus* is a common pathogen of marine animals, but also an opportunistic human pathogen, which causes gastroenteritis or extra-intestinal disease again linked to the consumption of raw or undercooked seafood ([7]).

The master regulator of transformation TfoX, which is required for competence induction in *V. cholerae*, is present in all sequenced *Vibrionaceae*, including *V. parahaemolyticus*, *V. alginolyticus and V. fischeri* ([8]). Moreover, the chitin utilization and chitin sensing pathways, which lead to the production of TfoX in *V. cholerae*, are highly conserved in *Vibrionaceae*. This suggests that chitin-induced natural transformation might occur among other vibrios ([9–12]). However, the regulation of the competence regulon in *V. cholerae* also requires the master regulator of quorum sensing, HapR, which, together with TfoX, co-regulate QstR (see Fig. 1.6B). Interestingly, homologous proteins of the competence regulon, HapR and QstR are found in *V. parahaemolyticus, V. alginolyticus* and *V. fischeri*, with the exception of a QstR-homolog missing in the latter ([13,14]). Even though competence genes are present in

these species, previous studies have only described competence for natural transformation in *V. parahaemolyticus* and *V. fischeri* without in-depth insight into the exact pathways ([8,15]).

It was already suggested in 1990 that *V. parahaemolyticus* is naturally transformable as it was able to pick up exogenous plasmid DNA ([16]). However, a later study showed that the tested strain was in fact a Pseudomonad ([103]). Twenty years later and after natural competence for transformation was formally discovered for *Vibrio* species (e.g., *V. cholerae*; ([1])), Chen and colleagues confirmed the chitin-dependent induction of natural competence in *V. parahaemolyticus*. However, the authors of a more recent study were unable to recover transformants after chitin surface induction, although they could generate transformants through the artificial expression of the *V. cholerae's tfoX* homolog in *V. parahaemolyticus* ([17]). These divergent studies might indicate that not all *V. parahaemolyticus* strains are naturally competent on chitinous surfaces.

The capability of *V. fischeri* to be naturally transformable was discovered by Pollack-Berti and colleagues, who showed that chitin oligosaccharides induce competence in a TfoX-dependent manner. In addition, the authors showed that the TfoX-homolog, TfoY, was required for transformation and concluded that both regulators had a redundant function. However, TfoX, but not TfoY could complement for the loss of the other, and the authors concluded that the effect of these regulators on competence is distinct ([8]). By contrast, TfoY does not induce competence in *V. cholerae*, even though it was originally annotated as a competence regulator ([3]). Instead, TfoY, like TfoX, regulates the T6SS of *V. cholerae* ([3]). In this chapter, we aimed to determine whether TfoX and TfoY, which are present in all sequenced *Vibrionaceae*, influence the activation of the T6SS cluster(s) present in the diverse vibrios as well as their competence program.

As for *V. cholerae*, *V. fischeri* harbors a single T6SS, while *V. parahaemolyticus* and *V. alginolyticus* encode two T6SSs (T6SS1 and T6SS2). One important reason that led us choose these *Vibrio* species, to study the phenotypes associated to TfoX and TfoY production, relies on the fact that the genetic organization of their T6SS cluster(s) is well characterized ([18–22]). By contrast, the regulatory network that initiates T6SS expression in these species remains unclear, although some environmental cues have been identified in *V. parahaemolyticus* and *V. alginolyticus*. For example, in *V. parahaemolyticus*, salinity, QS, surface sensing and temperature were known to influence the production of the T6SSs. Salomon and colleagues determined the effect of these environmental cues on the induction of the T6SS based on the production and secretion of the Hcp proteins, which form the inner

secreted tube of the T6SS. The authors showed that, in *V. parahaemolyticus*, the first T6SS (T6SS1) is active under high salt condition (e.g., marine-like conditions) and at low cell density, whereas the T6SS2 is active under low salt condition (e.g., standard LB medium) and at high cell density (Fig. 2.1). Indeed, the master regulator of quorum sensing, OpaR (HapR-homolog) negatively affects the T6SS1 while it positively regulates the T6SS2. Based on a previous study identifying that surface sensing enhances the expression of some virulence factors ([23]), the authors also investigated and showed that surface sensing up-regulates specifically the T6SS1, which can serve as an antimicrobial weapon ([18,20]). Finally, Salomon and colleagues determined that both T6SS are active at 30°C but inactive at 37°C, indicating they might not participate in cytotoxicity during human infections. Along those lines, Yu and colleagues previously showed that the two T6SSs do not induce cell cytotoxicity. However, the authors suggested that both T6SS are implicated in host cell adhesion ([24]). In a follow up study, the authors showed that the T6SS2 induces autophagy in macrophages, without being accompanied by cytotoxicity. However, further investigations are required to reveal the regulatory network responsible for this phenotype ([25]). Altogether, the two T6SSs of *V. parahaemolyticus* most likely serve different needs due to the opposite environmental cues affecting their expression. Interestingly, all *V. parahaemolyticus* encode the T6SS2, whereas the T6SS1 is mostly found in clinical isolates. The fact that the T6SS1 is active under marine-like conditions and was shown to efficiently kill other bacteria encountered in the natural habitat of *V. parahaemolyticus*, including environmental isolates of *V. parahaemolyticus,* suggests that the T6SS1 enhances the environmental fitness of the pathogen ([24,26]).

The two T6SSs of *V. parahaemolyticus* and *V. alginolyticus* share some homology, with respect to their genetic content and organization. In *V. alginolyticus*, the environmental cues affecting the T6SS activity are salinity, QS, and temperature. It was shown that the master regulator of QS in this organism, LuxR (HapR-homolog), represses the T6SS1 ([27]). Salomon and colleagues further determined that the T6SS1 is active under low salt conditions, whereas the T6SS2 is active in high salt marine-like conditions (Fig. 2.1). Moreover, the two T6SS were shown to be active at 30°C, whereas solely the T6SS2 is also functional at human body temperature (37°C; [21]). It was therefore concluded, that the two T6SSs of *V. alginolyticus* act primarily as antimicrobial weapon and that they are differentially regulated to serve different purposes ([21]).

The environmental clues influencing the T6SS of *V. fischeri* are currently unknown (Fig. 2.1). However, it appears that some isolates of *V. fischeri* harbor a second T6SS (T6SS2). Remarkably, the toxic activity of the T6SS2 against bacterial competitor fosters niche domination within the light organ of the squid ([22]).

Based on the studies highlighted above, it became evident that the different activities of the T6SS(s) in these diverse *Vibrio* species can shape their ecological fitness in the natural environment. By understanding the regulatory pathways that activate these T6SS, we will gain more insight onto their biological functions and their potential implications in niche adaptation.

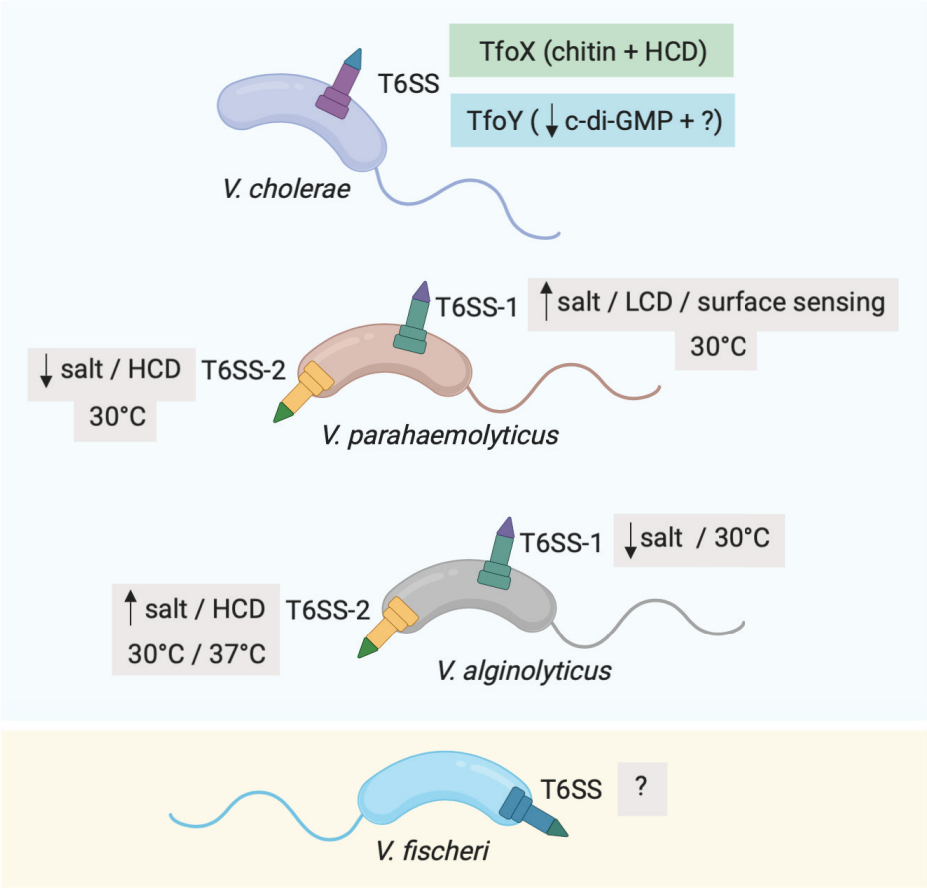

Figure 2.1: Environmental cues enhancing T6SS activity in diverse *Vibrio* species. Pathogenic (*V. cholerae*, *V. parahaemolyticus* and *V. alginolyticus*) and non-pathogenic (*V. fischeri*) vibrios are represented. In *V. cholerae* the major regulators of the T6SS are TfoX and TfoY, which are produced upon chitin sensing plus high cell density (TfoX) and low level of c-di-GMP (TfoY), respectively. In the three non-cholera *Vibrio* species, the regulators activating the T6SS are currently unknown. However, some environmental cues have been identified. In *V. parahaemolyticus,* the T6SS1 is induced in marine-like condition (high salt), at low cell density, and by surface sensing, whereas the T6SS2 is active under low salt condition at high cell density. Moreover both T6SS are induced at 30°C. In *V. alginolyticus,* the T6SS1 is induced by low salt condition at 30°C, while the T6SS2 is active in marine-like condition plus high cell density at either 30° or 37°C. The environmental factors inducing the T6SS in *V. fischeri* were unknown before we performed this study. Abbreviations and symbols: HCD, high cell density; LCD, low cell density; ?, unknown; ↑, increase; ↓, decrease. Figure created with BioRender.com

2.2 OVERVIEW: AIM AND SIGNIFICANCE

In the study presented below, we provide novel insights into the regulatory pathways of TfoX and TfoY. In particular we investigated the conservation of the functions mediated by these two regulators in other pandemic *V. cholerae* strains and in three distinct non-cholera vibrios.

Our first aim was to test whether the T6SS induction by TfoX or TfoY was restricted to one particular pandemic strain of *V. cholerae* or conserved among diverse pandemic strains. Indeed, previous studies from the lab had revealed the dependency of these regulators for T6SS activation but especially the study on TfoY has mostly with a focus on a single pandemic strain that was isolated from South America ([2,3,28,29]). To investigate the potential activation of the T6SS upon TfoX or TfoY production in other pandemic strains, we artificially expressed each of these regulators in the different pandemic *V. cholerae* strains using a previously optimized method ([3,30]). Briefly, a copy of *tfoX* or *tfoY* gene was cloned under the control of an arabinose inducible promoter (P_{BAD}) and inserted into a transposon, which integrates site-specifically into the large chromosome of vibrios. The transposon also contained the gene encoding the regulatory protein AraC, which plays dual role and acts as a repressor or activator in response to the absence and presence of arabinose, respectively. Based on this method, we tested the T6SS-dependent killing activity upon TfoX or TfoY production in five different pandemic strains isolated from Western and Southern Asia, or South America. As TfoX and TfoY induced the T6SS in all tested pandemic strains, we proposed that the T6SS regulation is conserved among pandemic *V. cholerae*.

The next aim was to investigate the potential conservation of TfoX- and TfoY-driven phenotypes in non-cholera *Vibrio* species that are differently adapted to their environmental niches ([4,31]). For this purpose, we first compared the conservation of TfoX and TfoY protein sequences among *V. cholerae* and the three other *Vibrio* species (*Vibrio fischeri, Vibrio alginolyticus,* and *Vibrio parahaemolyticus*). Moreover, we investigated whether the homologous TfoX and TfoY proteins of these non-cholera vibrios were functional when produced in *V. cholerae*. The readout of these experiments was T6SS-killing activity (TfoX and TfoY-dependent), natural transformation (TfoX-driven phenotype), and bacterial motility (TfoY-driven phenotype). We demonstrated that TfoY proteins are highly conserved and, consequently, that the non-cholera TfoY-homologs are fully functional in *V. cholerae*. The homologous TfoX proteins from *V. alginolyticus* and *V. parahaemolyticus* are closely related to *V. cholerae* and appeared as fully functional when expressed in *V. cholerae.* The TfoX

homolog of *V. fischeri,* however, appeared less conserved, which ultimately resulted in intermediate functionality when expressed in this heterologous host (e.g., reduced T6SS-mediated killing and transformability).

At this point, it was still unclear whether the biological functions of TfoX and TfoY were also conserved within the diverse *Vibrio* species. Thus, we investigated the phenotypes driven by the native TfoX and TfoY in each individual non-cholera *Vibrio* strain. We determined that the regulation of competence genes by TfoX and the enhancement of bacterial motility by TfoY were conserved in the four species of interest. We also tested the effect of TfoX and TfoY on each T6SS, as *V. alginolyticus* and *V. parahaemolyticus* harbor two distinct killing machineries. Our results demonstrated that TfoX induces one T6SS in all tested *Vibrio* species. As the TfoX-mediated T6SS killing is dependent on the master regulator of QS (HapR) in *V. cholerae* ([2]), we further studied the role of the HapR-homologues on the T6SS production and activity upon TfoX production. For *V. alginolyticus* and *V. parahaemolyticus,* we showed that TfoX induced killing occurred in a QS-dependent manner. These results strengthened the idea that the biological function of TfoX, namely to foster T6SS-dependent interbacterial predation followed by competence-mediated DNA uptake, is conserved among diverse *Vibrio* species. This mechanism could drive evolution and might explain, at least partially, the high genomic diversity found among these species ([4,5]).

We also demonstrated that the TfoY-dependent regulation of the T6SS(s) diverged among the four tested *Vibrio* species. In *V. fischeri,* TfoY does not regulate its T6SS, while TfoY regulates the single T6SS of *V. cholerae* and one out of the two T6SS of *V. parahaemolyticus* (T6SS1). By contrast to *V. parahaemolyticus*, TfoY activates both T6SS in *V. alginolyticus*. Finally, based on previous studies that linked T6SS1 activation to surface sensing in *V. parahaemolyticus* ([18]) as well as surface sensing to reduced intracellular c-di-GMP levels ([23]), we investigated whether low c-di-GMP also induces TfoY in this species. To do so, we genetically engineered a transcriptional and translational reporter strain that allowed us to measure *tfoY* induction and TfoY production in response to high and low c-di-GMP conditions. Our results showed that low c-di-GMP level induced *tfoY* at the post-transcriptional level in both *V. cholerae* and *V. parahaemolyticus*. We proposed that low c-di-GMP activates TfoY, which in turn induces the T6SS and increases motility in vibrios.

Overall, this study showed the importance of the two regulators, TfoX and TfoY among diverse *Vibrio* species and the conservation of their associated phenotypes. Moreover, the conserved TfoX-dependent induction of the T6SS, used as an antibacterial weapon, concomitantly with competence induction suggests that this regulatory cascade is maintained and potentially drives bacterial evolution in vibrios. Interestingly, while TfoX always induced a single T6SS, the TfoY-dependent activation of the T6SS varied among the different *Vibrio* species. We therefore suggest that the induction of a single or two T6SS simultaneously might trigger different defense reactions that are adapted to the environmental niche of each species.

ECOLOGICAL IMPLICATIONS OF GENE REGULATION BY TFOX AND TFOY AMONG DIVERSE *VIBRIO* SPECIES.

This chapter is a post-print version of an article published in 2019 in Environmental Microbiology in issue 21, volume 7 at pp. 2231-2247 as :

L. C. Metzger*, N. Matthey*, C. Stoudmann, E. J. Collas, and M. Blokesch#. Ecological implications of gene regulation by TfoX and TfoY among diverse *Vibrio* species. *Environ Microbiology* (2019) **21**(7), 2231-2247

Laboratory of Molecular Microbiology, Global Health Institute, School of Life Sciences, Ecole Polytechnique Fédérale de Lausanne (EPFL), Lausanne, Switzerland.

* These authors contributed equally to the work.
# Correspondence: Melanie Blokesch, Station 19, EPFL-SV-UPBLO, Ecole Polytechnique Fédérale de Lausanne (EPFL), CH-1015 Lausanne, Switzerland; Phone: +41 21 693 0653; Email: melanie.blokesch@epfl.ch

Running title: TfoX- and TfoY-dependent phenotypes in vibrios
Keywords: type VI secretion, regulatory networks, *Vibrio* species, natural competence for transformation, motility, c-di-GMP

Contributions: Design of the experiment, data generation (including part of: strain constructions, natural transformation assays, qRT-PCR, motility assays, and killing assays), data analysis, and figure preparation.

2.3 ORIGINALITY-SIGNIFICANCE STATEMENT

This work provides new insight into the regulatory circuits of TfoX and TfoY. Specifically, this study compares the effects of these two regulatory proteins on natural competence, motility, and the primary or secondary type VI secretion systems in diverse *Vibrio* species. This work also shows that decreased c-di-GMP levels in *V. parahaemolyticus* lead to TfoY production without changing *tfoY* transcript levels, thereby indirectly linking TfoY production to surface sensing.

2.4 SUMMARY

Bacteria of the genus Vibrio are common members of aquatic environments where they compete with other prokaryotes and defend themselves against grazing predators. A macromolecular protein complex called the type VI secretion system (T6SS) is used for both purposes. Previous research showed that the sole T6SS of the human pathogen *V. cholerae* is induced by extracellular (chitin) or intracellular (low c-di-GMP levels) cues and that these cues lead to distinctive signalling pathways for which the proteins TfoX and TfoY serve as master regulators. In this study, we tested whether the TfoX- and TfoY-mediated regulation of T6SS, concomitantly with natural competence or motility, was conserved in non-cholera Vibrio species, and if so, how these regulators affected the production of individual T6SSs in double-armed vibrios. We show that, alongside representative competence genes, TfoX regulates at least one T6SS in all tested Vibrio species. TfoY, on the other hand, fostered motility in all vibrios but had a more versatile T6SS response in that it did not foster T6SS-mediated killing in all tested vibrios. Collectively, our data provide evidence that the TfoX- and TfoY-mediated signalling pathways are mostly conserved in diverse Vibrio species and important for signal-specific T6SS induction.

2.5 INTRODUCTION

Secretion systems that enable the export of macromolecules across membranes are often associated with pathogenesis in Gram-negative bacteria. However, these machineries and their substrates also play important roles in the interactions between bacteria and other microorganisms in their natural environment ([32,33]). An important secretion system, the type VI secretion system (T6SS), was first described in *Vibrio cholerae* and is a syringe-like killing device involved in virulence and inter-bacterial warfare ([34–36]). T6SSs are present in ~25% of sequenced Gram-negative bacteria, including pathogenic and non-pathogenic species, and are defined by a set of 13 core components ([37–39]). These components build a macromolecular complex that shares both structural and functional homology with contractile bacteriophage tails, such as in the phage T4 ([40–42]). Briefly, a tail-like structure, which is composed of hemolysin coregulated protein (Hcp) hexamers and sharpened by spike-like tip proteins (VgrG and PAAR), is surrounded by a contractile sheath structure and polymerizes onto a membrane-spanning multi-protein complex. When the sheath contracts, the effector-decorated tip complex is propelled outwards together with the inner tube to puncture the membrane of a neighboring target cell and inject toxic effector proteins (reviewed by ([43,44])). Each T6SS encodes its own sets of variable effector proteins that determine the specificity and the biological function of the system, as they can impact both eukaryotic host cells and bacterial competitors. To prevent self-intoxication and to kin-discriminate siblings, bacteria produce effector-specific neutralizing immunity proteins, which are frequently encoded adjacent to the effector gene in a bicistronic unit ([45,46]). The structural components of the T6SS are mostly encoded within larger gene clusters, which are variable with respect to genetic content and organization. The genes coding for the secreted core components (Hcp, VgrG, PAAR) are often found in smaller auxiliary clusters together with the genes that encode the effectors-immunity pairs ([39]). Many bacterial genomes encode more than one T6SS, which likely serve different needs ([39]). Accordingly, bacteria employ a wide variety of regulatory mechanisms, from common cues to specific regulatory cascades, to ensure appropriate expression of T6SS genes ([47]), which likely vary within species when multiple T6SS systems are present. Studying the various T6SS systems and their regulation is therefore important, as such knowledge sheds light onto the evolution of bacterial species in response to new niches and their interaction with environmental hosts.

V. cholerae O1 El Tor strains, which are responsible for the current 7th pandemic of cholera (further referred to as pandemic strains), harbor a single T6SS. In contrast, many non-cholera Vibrio species encode several T6SSs, such as clinical isolates of *V. parahaemolyticus* and environmental isolates of *V. vulnificus*, both of which carry two T6SSs ([24,48]). The genome of the squid symbiont *V. fischeri*, on the other hand, codes for one T6SS even though a recent study by Speare *et al.* identified a secondary T6SS in several *V. fischeri* isolates that fostered niche domination within the squid's light organ ([22]).

The T6SS of pandemic *V. cholerae* is silent under standard laboratory conditions ([34]). In contrast to pandemic strains, the O37 serogroup strains V52 and ATCC25872 are toxigenic but non-pandemic and their T6SS is constitutively activated, as is the case for most environmental isolates ([34,49–51]). To explain the differences in T6SS activity and to provide insight into the T6SS's biological functions, it is therefore important to understand the underlying regulatory pathways in pandemic *V. cholerae* strains. Accordingly, several minor and major T6SS regulators have been identified in *V. cholerae* ([52]) by changing their abundance through deletion or forced expression of the respective genes, which resulted in changes in T6SS gene expression or T6SS activity. Two of these major regulators, TfoX and TfoY ([2,3]), contain TfoX-like N- and C-terminal domains, and proteins containing such domains are usually annotated as regulators of natural competence for transformation due to the presence of these domains in the competence regulator Sxy of *Haemophilus influenzae* ([53]) and TfoX in *V. cholerae* ([1]). We recently showed that TfoX induces the T6SS in parallel with the competence machinery at a high bacterial cell density (measured by quorum sensing [QS] and signaled through its master regulator, HapR) on chitinous surfaces, leading to T6SS-mediated killing followed by the absorption of prey-released DNA ([2]). Coupling kin-discriminating neighbor killing and competence fosters horizontal gene transfer and, ultimately, evolution ([54]).

Interestingly, *V. cholerae* and most other members of the genus Vibrio (vibrios) contain a TfoX homolog named TfoY ([3,8]). However, despite the homology to TfoX and its common annotation as a competence regulator, TfoY is neither essential nor sufficient for competence induction in *V. cholerae* ([3]). TfoY also induces the T6SS of *V. cholerae*, though the TfoX and TfoY regulons are non-overlapping, with TfoX co-inducing competence and TfoY orchestrating a defensive reaction. This defensive reaction includes enhanced motility and the co-production of the T6SS with additional extracellular enzymes, some of which are known to intoxicate amoebal predators ([3,51]). Moreover, TfoX is naturally produced upon growth on

chitinous surfaces ([1]), while TfoY production is inhibited by c-di-GMP, an secondary messenger in bacteria, such that it is only present at low intracellular c-di-GMP levels ([3,55]).

Given the presence of TfoX and TfoY in many vibrios, we aimed to understand their role in non-cholera species. We show that the T6SS activation is highly conserved across vibrios, with the majority of tested species concomitantly inducing natural competence and motility when TfoX and TfoY, respectively, are produced. Interestingly, we observed different scenarios when comparing those *Vibrio* species that encode more than one T6SS, with TfoX and TfoY not fulfilling the same inducing role for all T6SSs. We therefore conclude that some vibrios specifically induce one or the other T6SS under different environmental conditions driven by either TfoX or TfoY, while other species combine forces to simultaneously induce both T6SSs.

2.6 RESULTS AND DISCUSSION

Conservation of T6SS production by TfoX and TfoY in pandemic isolates of V. cholerae

Since its discovery in a non-pandemic strain of *V. cholerae*, it has been reported that the T6SS of pandemic strains is silent under standard laboratory conditions ([34]). We recently showed that the two regulatory proteins TfoX and TfoY foster T6SS production and, accordingly, inter-bacterial competition in pandemic *V. cholerae* ([2,3]). The previous study that addressed TfoY, however, was based on a single strain of *V. cholerae*, namely strain A1552 ([56]). This human isolate originated from food-borne transmission on an airplane returning to the US from Peru/South America ([29]) and belongs to the West-African South American (WASA) lineage of the currently ongoing seventh cholera pandemic ([28,57]). As strain-specific differences are frequently reported, this study was designed to first confirm the generality of TfoX- and TfoY-dependent T6SS activation in pandemic strains of *V. cholerae*. To do this, we tested five isolates from three different countries (Bangladesh, Peru, and Bahrain) for T6SS-dependent killing of *Escherichia coli*. Notably, we used a derivative of the first sequenced isolates of *V. cholerae*, pandemic strain N16961 ([58]), in which the frameshift mutation in the quorum-sensing regulator gene *hapR* was repaired ([59]). As demonstrated in Figure S2.1, all strains behaved similarly to A1552 upon TfoX or TfoY production. We therefore suggest that the dual control over T6SS by these two regulators is conserved among pandemic *V. cholerae*.

Functionality of TfoX and TfoY homologs from other Vibrio species in V. cholerae

Pollack-Berti and colleagues showed that TfoX and TfoY existed in all fully sequenced *Vibrionaceae* ([8]), so we wondered whether these homologs would act in a comparable manner in non-cholera vibrios despite the fact that these *Vibrio* species are often adapted to different environmental niches ([4]) and their homologous proteins might therefore serve different, adaptation-specific functions. We therefore compared the protein sequences of TfoX and TfoY from four different *Vibrio* species, *V. cholerae, V. parahaemolyticus, V. alginolyticus,* and *V. fischeri,* with the additional species chosen because previous studies had already described the genetic organization of their T6SS ([18,19,21,22]). Moreover, these additional species have isolates that contain two T6SSs. We therefore considered the possibility that TfoX and TfoY, which are produced under vastly different conditions in *V. cholerae* ([60]), might be specialized for the induction of a single T6SS in those organisms that harbor several systems. By aligning the protein sequences, we observed a high level of protein conservation for TfoX and TfoY, with a sequence identity of 68%/66%, 67%/66%, and 59%/67% when the homologous proteins of *V. parahaemolyticus* ($TfoX_{Vp}$/$TfoY_{Vp}$), *V. alginolyticus* ($TfoX_{Va}$/$TfoY_{Va}$), and *V. fischeri* ($TfoX_{Vf}$/$TfoY_{Vf}$) were compared to the respective homologs of *V. cholerae* (Fig. 2.2A). Given these identity values, we concluded that the TfoX of *V. parahaemolyticus* and *V. alginolyticus* were more closely related to the homologous protein of *V. cholerae*, whereas TfoX from *V. fischeri* diverged the most, which is in accordance with the phylogenetic distances between the species (Fig. 2.2A). Notably, TfoY remained equally conserved despite the phylogenetic divergence among the species.

Given the high level of protein conservation, we next tested whether the protein homologs from the non-cholera vibrios could function in *V. cholerae*. For this purpose, we cloned the respective genes preceded by an arabinose-inducible promoter (P_{BAD}) onto a site-specific transposon (mini-Tn7) together with the gene that encodes the arabinose-responsive regulatory protein AraC (Table S2.1). Next, we grew the genetically engineered strains and the parental WT strain in the presence of arabinose (as inducer), isolated their RNA, and then quantified the transcript levels of representative T6SS-encoding genes. As shown in Fig. 2.2B, heterologous production of the diverse TfoX proteins resulted in increased T6SS transcript levels compared to the uninduced conditions, though the level of induction was slightly lower than the production of *V. cholerae*'s own TfoX, especially for the most diverging protein variant from *V. fischeri* ($TfoX_{Vf}$). We confirmed these data at the protein level through the detection of the inner tube protein of the T6SS, Hcp (Fig. 2.2C). Consistent

with the production of Hcp and the increase of the T6SS transcript level, these strains were able to kill *E. coli* in an interbacterial competition assay, with the least predatory behavior observed for the most divergent TfoX$_{Vf}$-carrying variant (Fig. 2.2D).

TfoX of *V. cholerae* was first identified as the master regulator of natural competence for transformation ([1,60]). The TfoX-induced competence regulon includes those genes that encode the structural components of the DNA-uptake machinery, which primarily consists of a central pilus structure (encoded by *pil* genes; ([61]) and the DNA binding protein ComEA that is essential for reeling DNA across the outer membrane and into the periplasmic space ([62–64]). We therefore tested whether the TfoX variants from the other *Vibrio* species would likewise foster competence-gene expression, which was indeed the case (Fig. 2.2E). Compared to the other variants, the more diverse TfoX$_{Vf}$ did not induce the same high transcript levels of *comEA*, which, accordingly, also led to lower transformation frequencies (Fig. 2.2F). Notably, *comEA* expression in *V. cholerae* is regulated by an intermediate transcription factor, QstR, which is dependent on the production of both TfoX and HapR ([65,66]). HapR is the master regulator of the QS system, meaning that *comEA* expression is dependent on a functional QS system and on high cell density. As *V. fischeri* - but not the other tested *Vibrio* species - lacks a QstR homolog, we suggest that TfoX$_{Vf}$ induces *comEA* at lower levels, as it is adapted to the more diverse QS circuit of *V. fischeri* and the absence of QstR ([67,68]).

To assess the functionality of the TfoY homologs in *V. cholerae* we first tested the ability of the TfoY variants to foster natural transformation, given that these proteins are frequently annotated as “DNA transformation protein TfoX” or “TfoX-family DNA transformation protein” due to their similarity to TfoX. However, no transformants were detected upon the production of any of these proteins, indicating their inability to induce natural competence in *V. cholerae* (Fig. 2.2F). Conversely and consistent with the high sequence similarity of the proteins from the four organisms, all TfoY variants functioned at the same level as the *V. cholerae* TfoY to increase T6SS transcript levels (Fig. 2.2G), to induce Hcp protein production (Fig. 2.2H), and, consequently, to foster interbacterial killing of *E. coli* (Fig. 2.2I). In addition, the four TfoY variants were able to induce motility as a T6SS-independent phenotype, as visualized on swarming agar plates and quantified in Fig. 2.2J. Taken together, these data indicate that TfoX and TfoY are conserved proteins among these four *Vibrio* species and that the TfoY variants can fully replace the *V. cholerae* innate protein, while the TfoX variants are functionally replaceable at high levels for TfoX$_{Vp}$/TfoX$_{Va}$ and intermediate levels for TfoX$_{Vf}$.

TfoX but not TfoY induces V. fischeri's primary T6SS

While the complementation assay in *V. cholerae* described above provided a first insight into the conservation of TfoX and TfoY from diverse vibrios by indicating their similarity to those of *V. cholerae*, the experiments did not tell us whether these proteins would be involved in similar phenotypes as in *V. cholerae* in their native hosts. We therefore genetically engineered the different *Vibrio* species to place inducible copies of their own *tfoX* and *tfoY* genes onto a mini-Tn7 transposon that was then integrated into their own genomes (Table S2.1). Next, we analyzed the different phenotypes under uninduced and induced conditions. For *V. fischeri* strain ES114 (Table S2.1), we showed that TfoX production led to a high induction of T6SS transcripts, while TfoY only partially induced a subset of T6SS genes (Fig. 2.3A). Consistent with these expression data, we witnessed the T6SS-mediated killing of *E. coli* only upon TfoX induction, while TfoY induction did not change the number of surviving co-cultured prey bacteria (Fig. 2.3B).

Pollak-Berti *et al*. showed that TfoX was required for natural competence for transformation in *V. fischeri* ([8]), as is the case for *V. cholerae* ([1]). We therefore measured relative transcript levels of representative competence genes in this organism and confirmed their induction upon TfoX production (Fig. 2.3C). Surprisingly, while we only observed a mild induction of *comEA* relative to the levels of induction seen in *V. cholerae* (Fig. 2.2), we witnessed an almost 10-fold upregulation of *litR,* which encodes the main QS regulator LitR (homolog of *V. cholerae*'s HapR). This phenotype differs from what is known about competence regulation in *V. cholerae* in which case *hapR* transcript levels are left unchanged upon TfoX induction ([1,60]). We therefore speculate that an increase in LitR levels can compensate for the lack of the intermediate regulator QstR in *V. fischeri*. Indeed, the QstR of *V. cholerae* is required for competence-mediated DNA uptake in two ways: i) through direct and in-direct induction of certain competence genes, such as *comEA*, as described above; and ii) due to its ability to downregulate the *dns* gene ([65,66]) encoding for the extracellular nuclease Dns, which degrades transforming material outside the cell and within the periplasmic space ([62,69]). Notably, the HapR protein of *V. cholerae* also silences *dns* expression, but only partially in the absence of QstR ([65]). It is therefore likely that the increased production of LitR upon TfoX production in *V. fischeri* compensates for the absence of QstR to ensure sufficient repression of *dns,* which, ultimately, would allow DNA uptake to occur. It is not clear, however, why the *comEA* transcripts were not induced to higher levels, though we recently demonstrated for *V. cholerae* that the *comEA* gene requires

an additional but so far unidentified regulatory input apart from TfoX and QstR ([66]). Indeed, artificial QstR production was sufficient to induce the T6SS genes in this organism at comparable levels as the upstream regulatory protein TfoX, even in the absence of HapR, while the *comEA* transcript levels were only partially increased compared to a non-induced WT strain. We therefore hypothesize that this input signal might be conserved in *V. fischeri*, though missing under the tested conditions. This would lead to a high overall competence-gene induction upon TfoX production but lower *comEA* transcripts as compared to *V. cholerae* (Fig. 2.2E).

Lastly, we determined that the motility of *V. fischeri* changed upon TfoY production (Fig. 2.3D), even though the difference between the TfoY-induced and TfoY-uninduced state was not as pronounced as for *V. cholerae* (Fig. 2.2J). We argue that this might be caused by a basal production level of TfoY in this organism that does not rely on the artificial induction. A higher basal TfoY level would result in a higher basal motility, which would therefore appear as a less pronounced induction upon additional TfoY production. There was also a decrease in motility observable upon TfoX production (Fig. 2.2D), which is consistent with the idea of a basal TfoY level, as the expression data showed that TfoX significantly lowered the *tfoY* transcript levels (Fig. 2.3A). To see whether this is a conserved regulatory phenomenon, we tested whether TfoX production also lowered *tfoY* levels in *V. cholerae*, which was indeed the case with an average repression of 4.85 (± 0.5)-fold (based on three independent biological experiments; p=0.0001). For *V. fischeri* TfoY production lowered *tfoX* transcript levels (Fig. 2.3A), which was likewise the case for *V. cholerae* though to a lower extend (1.45± 0.1-fold; p=0.025), suggesting that both proteins work independently of each other and are mutually exclusive. This finding contradicts a previous study on *V. fischeri* in which the authors concluded that TfoY was required for efficient TfoX-mediated transformation ([8]). Notably, both studies used different conditions (e.g., inducible TfoX/TfoY expression in this study versus a transposon-inserted mutant of *tfoY* ([8])) and further studies are therefore required to conclusively show if TfoY is indeed involved in natural transformation in *V. fischeri* or not, as we suggest based on the herein-described data.

TfoX and TfoY have a different impact on T6SS induction in V. alginolyticus

While *V. cholerae* strains and the examined *V. fischeri* strain ES114 contain only a single T6SS, several other *Vibrio* species contain more than one. Hence, we asked whether, and if so how, TfoX and TfoY affect the production of different T6SSs within the same organism.

To address this question, we first tested the contribution of these regulators to the two T6SSs (T6SS1 and T6SS2) of *V. alginolyticus* in an *E. coli*-killing assay using wildtype (WT) *V. alginolyticus* or its *hcp1* (referred to as ΔT6SS1 throughout the text), *hcp2* (referred to as ΔT6SS2 throughout the text), or double mutant as a predator. Consistent with a previous report by Salomon *et al*. ([21]), WT *V. alginolyticus* did not show interbacterial predation at 37°C on standard LB medium (e.g., without additional salt; Fig. 2.4A). Upon production of TfoX or TfoY, however, predation by the WT was significantly increased. This effect was less pronounced but reproducible in the strain that only carried the complete T6SS2 gene set (ΔT6SS1), while a strain that only carried a complete T6SS1 gene set (ΔT6SS2) was not able to kill the *E. coli* cells, indicating that T6SS1 is non-functional at this temperature. In contrast, both systems were inducible at 30°C, with T6SS1 being specifically induced by TfoY and not TfoX, while T6SS2 was responsive to both regulatory proteins (Fig. 2.4B). Basic killing activity was also observed in the WT and the mutant lacking T6SS1 but not in a mutant lacking T6SS2, suggesting that T6SS2 is induced under the tested conditions (in a TfoX- and TfoY-independent manner; Fig. 2.4C), but can be further boosted upon TfoX and TfoY production (Fig. 2.4B). While this finding seems at first glance to contradict a previous study that reported basal activity for T6SS1 ([21]), it should be noted that the experimental setup differed in that we used an assay in which the *Vibrio* are tested at high cell density, as was previously developed for *V. cholerae* ([2]), while Salomon *et al.* first diluted the cells to low densities. The rationale behind our experimental setup was the knowledge that the TfoX-mediated pathway requires co-induction by HapR in *V. cholerae* (homologs are LuxR in *V. alginolyticus* and OpaR in *V. parahaemolyticus*) ([30,60,66]), which we assumed to be a conserved feature in other *Vibrio* species (see data below).

In addition to T6SS activation, we also tested the level of competence genes transcripts and bacterial motility upon TfoX and TfoY induction. As shown in Fig. 2.4D, a significant TfoX-mediated induction of representative competence genes occurred, indicating the protein's conserved action. Notably, the *comEA* transcript induction levels again turned out to be unexpectedly low compared to the induction levels in *V. cholerae* (Fig. 2.2E). ComEA plays a primary role in ratcheting the DNA into the periplasmic space in competent bacteria ([63]), and we therefore expect that these low transcript levels would lead to insufficient amounts of the ComEA proteins and defective DNA uptake. As *comEA* is co-regulated by the TfoX- and QS pathways in *V. cholerae* ([30,70]), comparable to the T6SS genes ([2,3]), we wondered whether QS was impaired in the tested *V. alginolyticus* strain. As demonstrated in

Figs. 2.4E and F, TfoX-mediated T6SS induction worked efficiently in the WT but was impaired in a *luxR*-minus strain (the *hapR* homolog in this organism; Table S2.1). These data indicate that QS is functional in the WT strain and support the notion that TfoX and LuxR co-regulate the T6SS2, consistent with earlier data that showed a requirement of LuxR for basal T6SS2 activity in *V. alginolyticus* ([71]). TfoY-mediated T6SS activation, however, occurred independently of LuxR (Figs. 2.4E and F) consistent with what is known for *V. cholerae* ([3]). Based on these data, we conclude that the additional but so far unknown regulatory input required for *comEA* expression mentioned above ([66]) might also be a prerequisite in *V. alginolyticus* and that this pathway and not the QS network overall might be non-functional in either the strain used in this study or under the tested conditions or both. The motility-inducing phenotype of TfoY, on the hand, was very pronounced in *V. alginolyticus* (Fig. 2.4G), strengthening the idea that TfoY protein levels and a high motility are linked throughout the genus *Vibrio,* even in organisms that contain lateral flagella in addition to the polar flagellum ([72]).

TfoX and TfoY are both dedicated to one specific T6SS in V. parahaemolyticus

Lastly, we tested the contribution of TfoX and TfoY to T6SS regulation in *V. parahaemolyticus*. As with *V. alginolyticus*, this bacterium also contains two T6SSs, T6SS1 and T6SS2, which were previously shown to be differentially regulated from each other with respect to temperature, salinity, QS inputs and surface sensing ([18]). Indeed, T6SS1 of *V. parahaemolyticus* was found to be most active under marine-like conditions and at low cell densities while system 2 was more adapted to lower salt conditions (e.g., LB medium) and higher cell densities ([18]). Notably, these data on T6SS2 regulation and a previous study that suggested T6SS2 was involved in adhesion to host cells were solely based on the Hcp2 protein levels (inside and outside the cells), while interbacterial killing activity was not directly observed for T6SS2 ([18,24]). This QS-dependent T6SS2 regulation of Hcp production confirmed previous results in *V. cholerae* ([73]) in which the authors demonstrated that HapR was required for *hcp* expression. However, despite the fact that pandemic *V. cholerae* produce detectable levels of Hcp at high cell densities *in vitro*, the bacteria are unable to kill prey under such conditions ([34]), which can be overcome by TfoX or TfoY production ([3]). Indeed, we previously demonstrated that upon induction of these two regulators, the Hcp levels increased further, and T6SS-mediated prey killing was observed. Notably, TfoY-mediated T6SS activity in *V. cholerae* occurred independently of HapR, indicating that TfoY

acts independently from the QS pathway, in contrast with TfoX-mediated T6SS activation ([2,3]).

In *V. parahaemolyticus*, both TfoX and TfoY production led to significant *E. coli* killing (Fig. 2.5A). When testing *V. parahaemolyticus* strains that contained only a complete T6SS2 gene set (ΔT6SS1) or only all T6SS1 genes (ΔT6SS2), it was clear that TfoX specifically induced T6SS2, while TfoY solely led to T6SS1-mediated prey killing (Fig. 2.5A). These data also suggested that the T6SS2 was slightly active in both the WT and the strain lacking T6SS1, even without artificial TfoX/TfoY production, and that neither TfoX nor TfoY caused this basal T6SS2 activity (Fig. 2.5B). Interestingly, a recent study showed T6SS2-dependent killing of a *V. parahaemolyticus* strain that lacked a newly identified effector immunity pair (RhsP and RhsPi) by its parental WT strain, even in the absence of TfoX or TfoY induction ([74]). These data therefore suggest that the basal killing activity that we observed against *E. coli* as a prey might be more enhanced against non-immune siblings or, alternatively, that the experimental conditions were different to the current work and that under such conditions the T6SS2 is highly active. Lastly, we cannot exclude the possibility that strain differences or the domestication of certain strains has caused the difference in basal T6SS activity. Notably, the focus of the current study was on the contribution of TfoX or TfoY to T6SS activity, which we unambiguously demonstrate to enhance T6SS activity in *V. parahaemolyticus*.

Examining other TfoX- and TfoY-mediated phenotypes confirmed the increase of competence gene transcripts and enhanced motility, respectively (Fig. 2.5C and D). However, *comEA* transcript levels were again unexpectedly low even though the induction levels of *qstR* were comparable with what we observed for *V. cholerae* (Fig 2.2E). While these data were similar to the above-described observations for *V. alginolyticus* (Fig. 2.4D), which suggested a *comEA*-specific expression defect, we nonetheless tested whether the *V. parahaemolyticus* strain used in this study was QS proficient or QS deficient. Indeed, previous studies in different *Vibrio* species described gain-of-function mutations in *luxO*, encoding a repressor of HapR/LitR/OpaR synthesis ([23,75,76]) and clinical *V. parahaemolyticus* isolates with such *luxO* mutations were previously described to be locked in a pathogenic state ([77]). To exclude that this has happened in the strain we were working with, we first sequenced *luxO* and *opaR* and confirmed that both genes were mutation free. Additionally, we deleted *opaR* from the WT strain and compared this strain to its TfoX- or TfoY-inducible derivatives (Table S2.1) in an *E. coli*-killing assay. As shown in Fig. 2.5E, the TfoY-induced

prey killing was maintained upon deletion of *opaR*, while the TfoX-mediated T6SS activity was abrogated. Since OpaR is produced at high cell density, its deletion blocks QS-dependent signalling. We therefore conclude that the WT strain has a functional OpaR and that TfoX-mediated T6SS induction in *V. parahaemolyticus* requires co-regulation by OpaR, similar to what we have shown for *V. cholerae* ([2,3]) and for *V. alginolyticus* (Figs. 2.4E and F). These data also support the idea that the low expression levels seem specific for *comEA* and not based on a general mutation within the QS cascade. The low level of the *comEA* transcripts also explains why we were unable to naturally transform *V. parahaemolyticus* even after TfoX induction. Interestingly, Chimalapti *et al.* recently reported rare transformants for competence-induced *V. parahaemolyticus* with frequencies between $1x10^{-8}$ and $2.7x10^{-6}$ ([17]), which corresponds to 0.01% to 1% of what is commonly observed for *V. cholerae* (see Fig. 2.2 and ([30]) despite the ~1000-fold molar excess of the selective resistance marker that was used as transforming DNA in this study. It should be noted that these experiments were based on the heterologous expression of the *V. cholerae tfoX* homolog from a multicopy plasmid, which makes a direct comparison with the current study on the bacterium's indigenous TfoX protein impossible.

Our data suggest that TfoX induces the T6SS2 in *V. parahaemolyticus*. As previous studies showed that the chitin sensors ChiS, TfoS, and the downstream-regulated small RNA TfoR, which is required for *tfoX* mRNA translation, are highly conserved in diverse *Vibrio* species ([10–12]), we suggest that TfoX is exclusively produced upon growth on chitinous surfaces, as first demonstrated for *V. cholerae* ([1,78]). The production of TfoY is less understood. In a previous study on *V. cholerae*, we showed that lowered c-di-GMP levels led to the production of TfoY under standard laboratory conditions (e.g., in LB medium) and we and others suggested that this c-di-GMP-dependent control occurred at the translational level ([3,55]). Interestingly, Gode-Potratz *et al*. demonstrated that growth on surfaces lowered the levels of the secondary messenger c-di-GMP in *V. parahaemolyticus* ([23]). Consistently, Salomon *et al.* established that surface sensing correlated with Hcp1 production in this organism ([18]). Based on these data, we speculated that surface sensing, TfoY production, and T6SS1 induction might be linked. To address this hypothesis and especially the link between low c-d-GMP levels and TfoY production, we genetically engineered *V. parahaemolyticus* to carry a translational fusion between its indigenous *tfoY* gene and the gene that encodes super-folder GFP (sfGFP). In addition, we included a transcriptional mCherry-encoding reporter gene behind this construct, which, ultimately, allowed us to monitor the transcriptional and

translational control of *tfoY*. Next, we incorporated either an empty mini-Tn7 transposon (Tn) or transposons that carried arabinose-inducible genes coding for a c-di-GMP-producing diguanylate cyclase (Tn-*vdcA*) or for a phosphodiesterase (Tn-*cdpA*) into this strain (Table S2.1). These strains as well as the transposon-deficient parental strain and the WT without any fluorescent protein-encoding genes were then grown in the presence of the inducer arabinose followed by a western blot analysis to visualize the TfoY-sfGFP fusion protein or the transcriptional reporter protein mCherry. Using this approach, we observed that TfoY was produced solely at low c-di-GMP levels (Fig. 2.5F). Importantly, based on the comparable levels of mCherry in all reporter strains, we concluded that the *tfoY* transcript levels did not significantly change in response to increased or decreased c-di-GMP levels (Fig. 2.5F). This finding contradicts a recent study in *V. cholerae* that concluded that TfoY was induced at both low and high intracellular concentrations of c-di-GMP and that this regulation occurred at the translational and transcriptional levels, the latter due to activation by the c-di-GMP-dependent transcription factor VpsR ([79]). We therefore constructed a similar dual translational-transcriptional reporter strain in *V. cholerae* (Table S2.1) and tested this strain under normal, increased, or decreased c-di-GMP levels. Using this approach, we were able to detect an increase in the TfoY protein under low c-di-GMP levels compared to normal conditions, while an increase in intracellular c-di-GMP did not result in higher TfoY protein levels (Fig. S2.2), consistent with our previous findings ([3]). Importantly, we also did not observe a change in the transcriptional reporter under high c-di-GMP conditions (Fig. S2.2), despite normal VpsR function in the pandemic *V. cholerae* strain (A1552) used in this study ([80]), which confirmed the data presented above for *V. parahaemolyticus*. An explanation for this discrepancy might be that we engineered the construct at the native locus of *tfoY* within the *V. parahaemolyticus* or *V. cholerae* genomes, while Pursley *et al.* were unsuccessful in detecting tagged TfoY variants using a similar approach. They therefore decided to construct a TfoY-GFP translational-fusion-encoding reporter gene on a plasmid, which could change the expression pattern compared to the gene's native locus. In addition, these authors performed their experiments in a *Vibrio* polysaccharide mutant as parental strain (ΔvpsL), which is deficient in biofilm formation ([79]), while our strain maintained a normal ability for this process.

Collectively, we conclude that the lowered c-di-GMP levels observed in surface-sensing *V. parahaemolyticus* ([23]) might trigger TfoY induction, which induces the T6SS1 and subsequently initiates motility, though the exact mechanism for the latter remains to be

discovered. The data provided here for *V. parahaemolyticus* therefore support our previous suggestion that TfoY triggers a defensive escape reaction that might allow *Vibrio* species to defend themselves against bacterial competitors and eukaryotic predators. Interestingly, a recent study that profiled the gene expression of *V. parahaemolyticus* reported increased *tfoY* expression (VP1028; falsely annotated as *tfoX* and therefore discussed as competence regulator in this study) within infected infant rabbits when compared to *in vitro* conditions ([81]), suggesting that TfoY might also play a role *in vivo* and therefore in pathogenesis.

2.7 CONCLUSION

In this study, we investigated the ecological implications upon TfoX and TfoY production in diverse *Vibrio* species. We showed a conserved pattern of competence and motility induction by TfoX and TfoY, respectively, and demonstrated that the link between the TfoX and TfoY regulatory proteins and T6SSs is highly conserved among cholera and non-cholera *Vibrio* strains (Fig. 2.6), highlighting the general importance of these regulators. Notably, TfoX induced at least one T6SS in every tested species concomitantly with an interbacterial killing phenotype. Hence, we suggest that chitin-mediated TfoX production ([1,60]) and the resulting coupling between T6SS-facilitated neighbor killing and competence-mediated DNA uptake ([2]) might be an ancient phenotype maintained in most *Vibrio* species. Our study also suggests that TfoX and TfoY are mutually exclusive (Fig. 2.3A and data presented above). Indeed, TfoX-mediated *tfoY* repression seems like a prerequisite for proper colonization of chitinous surfaces, as TfoY-induced motility would otherwise counteract this process. Thus, even upon contact with the surface and the reported decrease in c-di-GMP levels ([23]), *tfoY* translation would not occur on chitin due to the absence/low levels of the template mRNA. In contrast, when vibrios sense non-chitinous surfaces, resulting in the absence of the chemoattracting chitin-degradation product chitobiose ([82]), TfoY would be produced. Interestingly, the effects of TfoY turned out to be more versatile compared to TfoX (Fig. 2.6). While the c-di-GMP-dependent inhibition of TfoY translation seemed conserved, at least in the two tested *Vibrio* species (Fig. 2.5E and Fig. S2.2), the regulons seems to have diverged in the different organisms. Indeed, TfoY induces both T6SSs in *V. alginolyticus* and one T6SS in *V. cholerae* and *V. parahaemolyticus* (out of two T6SSs present in the latter bacterium) but this regulator does not impact the activity of the T6SS of *V. fischeri* under the tested conditions. However, several isolates of *V. fischeri,* other than the squid isolate ES114*,* contain a secondary T6SS.

This T6SS2 is located on a strain-specific genomic island on the small chromosome and was recently shown to contribute to competitor elimination within the host's light organ ([22]). While we were unable to genetically engineer the T6SS2-containing fish symbiont MJ11 strain for technical reasons, it is tempting to speculate that this secondary T6SS of *V. fischeri* might be controlled by the TfoY protein. In line with this idea is the fact that *V. fischeri*'s secondary T6SS is broadly conserved among vibrios and is similar to the TfoY-inducible T6SS1 of *V. alginolyticus* and *V. parahaemolyticus* ([22]), which we confirmed by BLAST analyses of *V. fischeri*'s T6SS2 genes VFMJ11_A0804 to VFMJ11_A0809. Notably, Speare *et al*. proposed the possibility that this secondary T6SS2 was present in the common ancestor of *V. fischeri* and related *Vibrio* species but was eventually lost in niche-adapted strains for which interbacterial killing was no longer advantageous. We extend this hypothesis and speculate that niche-adapted vibrios might no longer require a TfoY-mediated defensive response against either competing bacteria or grazing predators. Future studies are required to address these interesting evolutionary hypotheses.

2.8 EXPERIMENTAL PROCEDURES

Bacterial strains, plasmids, and growth conditions

The *V. cholerae, V. alginolyticus, V. parahaemolyticus,* and *V. fischeri* strains and plasmids used in this study are listed in Table S2.1. *Escherichia coli* strains DH5α ([83]), TOP10 (Invitrogen), SM10λpir ([84]), S17-1λpir ([84]) and MFDpir ([85]) were used for cloning purposes and/or served as donor in bacterial mating experiments.

Unless otherwise stated, the *V. cholerae, V. alginolyticus, V. parahaemolyticus,* and *E. coli* strains were grown aerobically in Lysogeny broth (LB; 10 g/L of tryptone, 5 g/L of yeast extract, 10 g/L of sodium chloride; Carl Roth) or on LB agar plates at 30°C or 37°C. *V. fischeri* strains were cultured aerobically in LB salt (LBS) medium (10 g/L of tryptone, 5 g/L of yeast extract, 20 g/L of sodium chloride, 20 mM Tris-HCl [pH 7.5], 0.2% glycerol, adapted from ([86,102])) or LBS agar plates at 28°C. LB/LBS motility plates had less agar (0.3%) than standard LB/LBS agar plates (1.5%). The following were added if required at the given concentrations: arabinose (0.02% or 0.2%), diaminopimelic acid (DAP; 0.3 mM), or the antibiotics kanamycin (75 μg/ml), gentamicin (50 μg/ml), ampicillin (100 μg/ml), and chloramphenicol (2.5 μg/ml or 5 μg/ml). L-arabinose-supplemented medium was used for the expression of *tfoX* or *tfoY* under the control of the P_{BAD} promoter. DAP was added as an essential growth supplement for *E. coli* strain MFDpir ([85]). Medium without DAP was used to counter-select MFDpir strains after tri-parental mating with *V. fischeri*. For the *E. coli* counter-selection after tri-parental mating with *V. cholerae, V. alginolyticus,* and *V. parahaemolyticus,* Thiosulfate Citrate Bile Salts Sucrose (TCBS) agar plates were used and prepared following the manufacturer's instructions (Sigma-Aldrich/Fluka, Buchs, Switzerland). Marine broth 2216 (BD Difco™ 2216) was used to isolate single colonies of *V. alginolyticus* and *V. parahaemolyticus* after *E. coli* counter-selection.

Genetic engineering of strains and plasmids

DNA manipulations were performed according to standard molecular biology-based protocols ([87]). Enzymes were purchased from the listed companies and were used as recommended by the manufacturer: Pwo polymerase (Roche), Taq polymerase (Promega), restriction enzymes (New England Biolabs). Following initial screening by PCR (using bacterial cells as templates), genetically engineered strains and plasmids were verified by Sanger sequencing (Microsynth, Switzerland).

V. cholerae strains were genetically modified using both a gene-disruption method based on the counter-selectable plasmid pGP704-Sac28 ([78]) or the TransFLP gene disruption method previously described by our group ([88–90]). This transformation-based genetic engineering technique was used to replace the *tfoY* gene by a translational and transcriptional *tfoY-mCherry::gfp* fusion at the natural locus on the *V. cholerae* A1552 chromosome. Plasmid pGP704-Sac-Kan (see below), derived from pGP704-Sac28, was used for genetic modifications of *V. parahaemolyticus* and *V. alginolyticus*.

To construct the counter-selectable plasmid pGP704-Sac-Kan, the *aph* gene was amplified from a kanamycin-resistance gene (*aph*)-carrying transposon using primers with overhanging *Ssp*I and *Bsa*I restriction sites. A restriction digestion was performed on both the PCR product and the vector pGP704-Sac28, which were subsequently ligated, to replace the *bla* gene of pGP704-Sac28 with the *aph* gene, resulting in plasmid pGP704-Sac-Kan (Table S2.1).

All pBAD-derived plasmids harboring *tfoX-strep* or *tfoY-strep* genes from different *Vibrio* species were constructed in the following way: The genes were amplified with *Strep-tagII*-encoding primers using gDNA of the respective parental *Vibrio* strain as a template. The restriction-enzyme-digested PCR product was subsequently cloned into plasmid pBAD/MycHisA (Table S2.1). The resulting plasmids served as templates for fragments containing *araC*, the arabinose-inducible promoter P_{BAD}, and the respective *tfoX* or *tfoY* genes, which were subcloned into the mini-Tn7-containing delivery plasmids (Table S2.1). The plasmid pGP704-Tn-Cm^R is a derivative of pGP704-mTn*7*-minus-SacI ([91]), where the *aacC1* gene within the mini-Tn7 was replaced by the *cat* gene. To this end, the PCR-amplified *cat* gene (including its promoter) of pBR-FRT-Cat-FRT2 ([3]) was cloned into pGP704-mTn*7*-minus-SacI, which was digested using restriction enzymes *Sbf*I and *Eco*RV. For the insertion of this mini-Tn7 transposon into the *Vibrio spp.* chromosomes, a tri-parental mating strategy was employed ([92]). The donor plasmids are indicated in Table S2.1.

Natural transformation assay

Natural transformation assays in liquid were performed with minor modifications to the previous protocol ([30]). This assay is chitin-independent and uses strains carrying an arabinose-inducible copy of *tfoX-strep* or *tfoY-strep* (both from *V. cholerae, V. alginolyticus, V. parahaemolyticus*, or *V. fischeri*) on the chromosome. *V. cholerae* strains were pre-grown overnight in LB medium and further grown in the presence of the arabinose inducer up to an

optical density at 600 nm (OD_{600}) of 1.0. At this point, 0.5 ml of the cultures were supplemented with 1 µg of genomic DNA. For all natural transformation assays, the genomic DNA of A1552-lacZ-Kan ([93]) served as transforming material. Cells were further incubated under shaking conditions at 30°C for 4 hours. Serial dilutions were spotted on LB to count the total number of cells and on kanamycin-containing LB agar plates to select the transformants. Transformation frequencies were calculated as the number of colony-forming units (CFUs) of the transformants divided by the total number of CFUs. Averages of at least three biologically independent experiments are provided. For statistical analyses, the data were log-transformed ([94]) and significant differences were determined by the two-tailed Student's t-test. When no transformants were recovered, the value was set to the detection limit to allow for statistical analysis.

Gene expression analysis by quantitative reverse transcription PCR (qRT-PCR)

Quantitative reverse transcription PCR (qRT-PCR)-based transcript scoring in *V. cholerae, V. alginolyticus, V. parahaemolyticus*, and *V. fischeri* was performed following a previously established protocol ([30]). Strains with and without an arabinose-inducible copy of specified genes (*tfoX-strep* or *tfoY-strep*) were grown for 6 hours in 2.5 ml LB or LBS supplemented with 0.2% arabinose. Cultures (2 ml) were processed for RNA isolation and subsequent cDNA synthesis. Relative gene expression values were normalized against the *gyrA* transcript levels. Fold changes were determined using the relative expression values of the induced strains divided by the values of the parental WT strain (as specified for each inducible construct in the figures). Averages of at least three biologically independent experiments (± standard deviation) are provided with statistical analyses (two-tailed Student's t-test) being done on the log-transformed data ([94]).

Interbacterial killing assay using E. coli as prey

The *E. coli* killing assay was performed following a previously established protocol with minor adaptions ([2]). The *E. coli* prey cells and the given predator cells were mixed at a ratio of 10:1 and spotted onto membrane filters on pre-warmed LB and/or LBS agar plates (± 0.2% ara). After 4 h of incubation at 28°C (predator: *V. fischeri*) or 30°C and 37°C (as indicated for the predators *V. cholerae, V. alginolyticus*, *and V. parahaemolyticus*), bacteria were resuspended and serial dilutions were spotted onto antibiotic-containing LB agar plates to enumerate the CFUs (shown as CFU/ml). Arabinose-uptake-deficient *E. coli* TOP10 and its

derivative TOP10-TnKan served as prey. Significant differences were determined by a two-tailed Student's t-test on log-transformed data of at least three biological replicates. If no prey cells were recovered, the value was set to the detection limit to allow calculation of the average of the three independent biological experiments and statistical analysis.

Motility assay

The motility of the *Vibrio* species was assessed by spotting 2 µl of the respective overnight culture onto freshly prepared LB and/or LBS motility agar plates (containing 0.3% agar) with or without 0.2% arabinose. Following the incubation at 30°C for 6h for *V. cholerae, V. parahaemolyticus*, and *V. alginolyticus*, or at room temperature for 7h for *V. fischeri*, the diameters of the bacterial swarming were determined. The motility induction was calculated by dividing the swarming diameter of induced versus uninduced strains. The averages of at least three independent experiments (± standard deviation) are provided. For statistical analyses, a two-tailed Student's t-test was performed.

SDS-PAGE and western blotting

Cell lysates were prepared as described previously ([3]). In brief, after cultivation with or without arabinose for 3 or 6 hours, bacterial cell pellets were resuspended in Laemmli buffer, adjusting for the total number of bacteria according to the OD_{600} values. Proteins were separated by sodium dodecyl sulfate (SDS)-polyacrylamide gel electrophoresis and western blotted as described ([30]). Primary antibodies against Hcp (Eurogentec; ([3])), GFP (Roche, Switzerland), and mCherry (BioVision, USA distributed via LubioScience, Switzerland) were used at 1:5,000 dilutions, and *E. coli* Sigma70 (BioLegend, USA distributed via Brunschwig, Switzerland) was used at a 1:10,000 dilution. Goat anti-rabbit horseradish peroxidase (HRP) and goat anti-mouse HRP (both diluted 1:20,000; Sigma-Aldrich, Switzerland) served as secondary antibodies. Lumi-Light^{PLUS} western blotting substrate (Roche, Switzerland) was used as an HRP substrate and the signals were detected using a ChemiDoc XRS+ station (BioRad).

ACKNOWLEDGMENTS

We thank members of the Blokesch lab and Frédérique Le Roux for fruitful discussions, Nina Vesel for constructing plasmid pGP704-Sac-Kan, and Sandrine Stutzmann, Julien Chambaud, and Tiziana Scrignari for technical assistance. We acknowledge Dor Salomon for providing the *V. parahaemolyticus* and *V. alginolyticus* strains, for discussing unpublished data, and for arranging co-submission. This work was supported by the Swiss National Science Foundation (31003A 162551) and a Consolidator Grant from the European Research Council (ERC; 724630-CholeraIndex). M.B. is a Howard Hughes Medical Institute (HHMI) International Research Scholar (grant 55008726).

AUTHOR CONTRIBUTIONS

Conception, design and analysis: L.C.M, N.M., and M.B.; performed research: L.C.M, N.M., C.S., E.J.C., and M.B; wrote the manuscript: L.C.M. and M.B. with input from N.M..

2.9 FIGURES

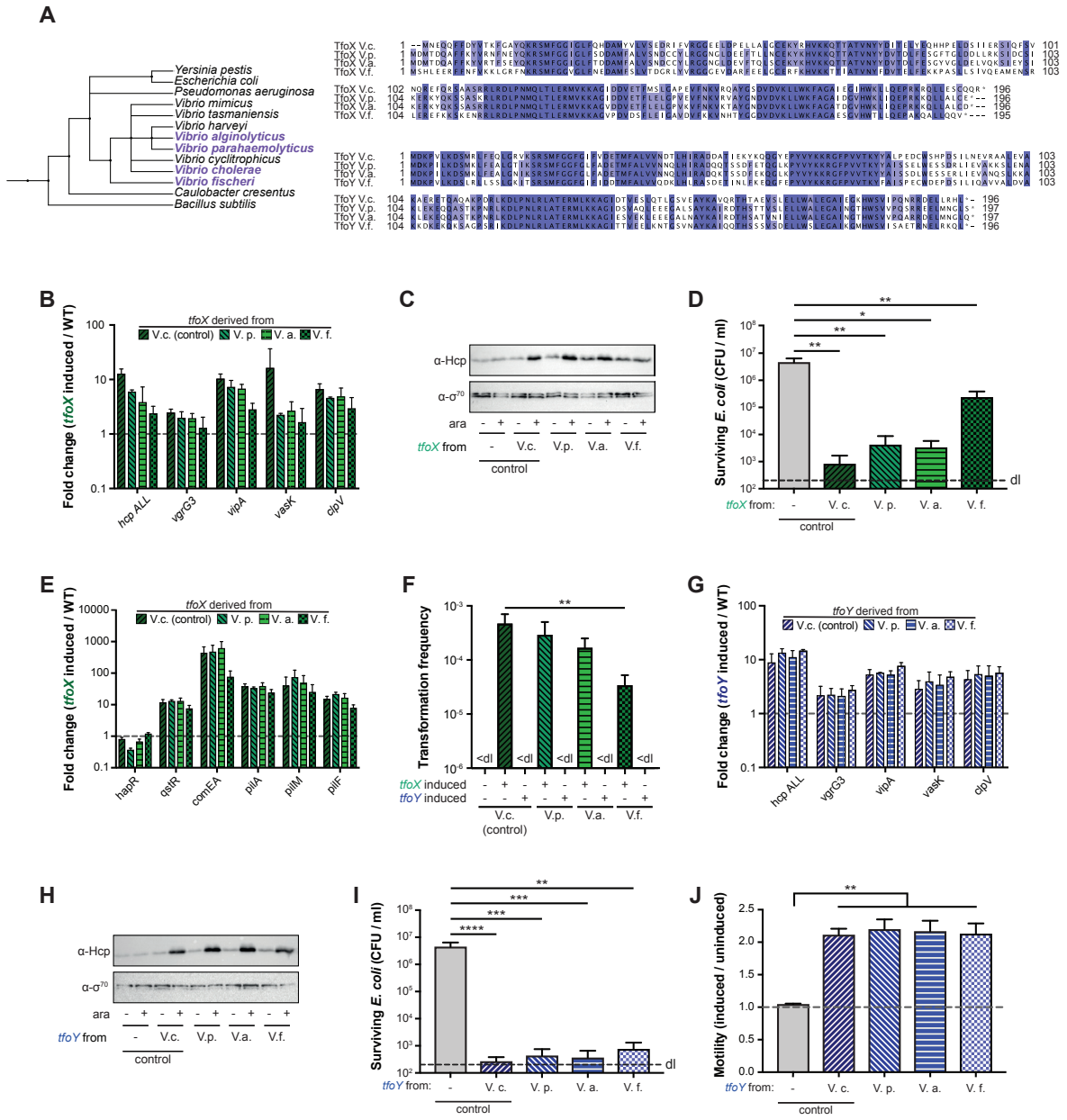

Figure 2.2: TfoX and TfoY proteins from diverse *Vibrio* species are functional in *V. cholerae*. (A) Phylogenetic tree and protein sequence conservation of TfoX and TfoY across *Vibrio* species. The phylogenetic tree was generated on phlyot.biobyte.de, a phylogenetic tree generator, based on NCBI taxonomy. The protein sequences of TfoX and TfoY were aligned using ClustalOmega, and subsequently modified with Jalview. Identical residues are highlighted in shades of blue (above threshold of 65%). (B-J) Chromosomally-located *tfoX* and *tfoY* from cholera (*V. cholerae*) and non-cholera *Vibrio* species (*V. parahaemolyticus*, *V. alginolyticus,* and *V. fischeri*) were expressed under the control of the arabinose-inducible P_{BAD} promoter in *V. cholerae*. The color code (TfoX-induced, green; TfoY-induced, blue) is used throughout the graphs. The WT strain lacking an inducible copy of *tfoX* or *tfoY* served as the negative control. The fold change (*tfoX*- or *tfoY*-induced over parental WT strain) of relative gene expression of (B, G) T6SS genes or (E) representative competence genes. (C, H) Detection of Hcp protein produced by TfoX- and TfoY-expressing cells. Cells were grown in the absence or the presence of the inducer (arabinose) as indicated below the image. Detection of σ^{70} served as a loading control. (D, I) Interspecies killing assay with *E. coli* as prey. *V. cholerae* harboring different inducible versions of (D) *tfoX* or (I) *tfoY* were co-cultured with the prey on LB agar plates supplemented with arabinose. The

survival of the prey was determined on selective LB agar plates and is depicted as CFU per ml. (F) Natural transformation using genomic DNA is maintained in a *V. cholerae* strain expressing *tfoX* from non-cholera vibrios but that is non-functional upon *tfoY* expression. The indicated strains were grown under inducible conditions, and the genomic DNA of A1552-lacZ-Kan served as the transforming material. Transformation frequencies reflect the number of transformants divided by the total number of CFUs. < dl, below detection limit. (J) Motility was scored on soft agar with and without arabinose as an inducer. The motility phenotype was quantified as the ratio between the induced and uninduced conditions, as shown on the Y-axis. Abbreviations: V.c., *Vibrio cholerae* A1552, V.p., *Vibrio parahaemolyticus* RIMD2210633; V.a., *Vibrio alginolyticus* 12G01; V.f., *Vibrio fischeri* ES114. Bar plots represent the average of at least three independent biological replicates (± SD). Statistical significance is indicated (*$p < 0.05$; **$p < 0.01$; ***$p < 0.001$; ****$p < 0.0001$).

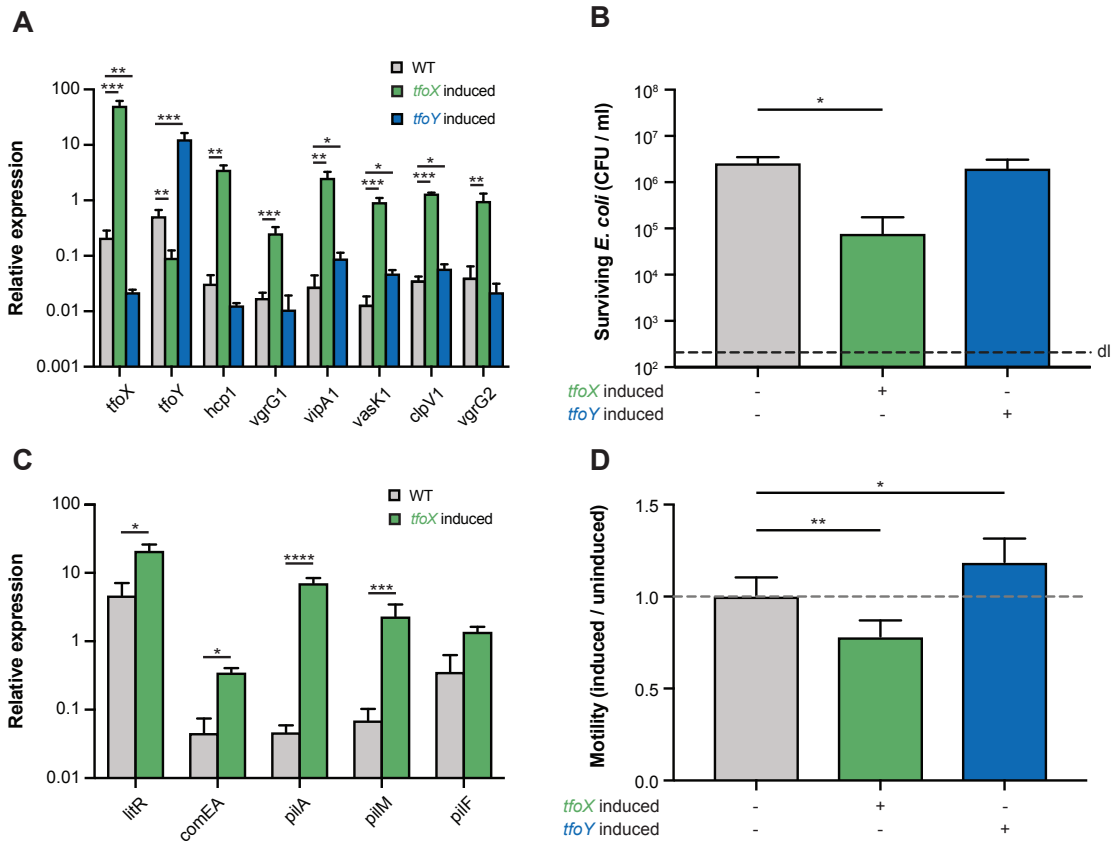

Figure 2.3: TfoX but not TfoY induce *V. fischeri*'s T6SS. The effect of TfoX (green) and TfoY (blue) production in *V. fischeri* ES114 was scored by qRT-PCR, and the relative expression values comparing WT versus TfoX- or TfoY-induced conditions are indicated for representative (A) T6SS or (C) competence genes. (B) TfoX induction in *V. fischeri* leads to interbacterial killing of *E. coli* prey cells. *V. fischeri* strains were co-cultured with *E. coli* for 4 hours at 28°C on plain LBS agar plates supplemented with arabinose to induce the arabinose-inducible copy of *tfoX* or *tfoY* (as indicated below the graph). The values for the recovered prey are indicated on the Y-axis. (D) TfoY fosters motility in *V. fischeri.* Quantification of the motility phenotype of TfoX- or TfoY-induced bacteria normalized by the uninduced conditions. The WT strain without any inducible gene served as a control. (A-D) Bar plots represent the average of at least three independent biological replicates (± SD). Statistical significance is indicated (*$p < 0.05$; **p < 0.01; ***p <0.001; ****p <0.0001).

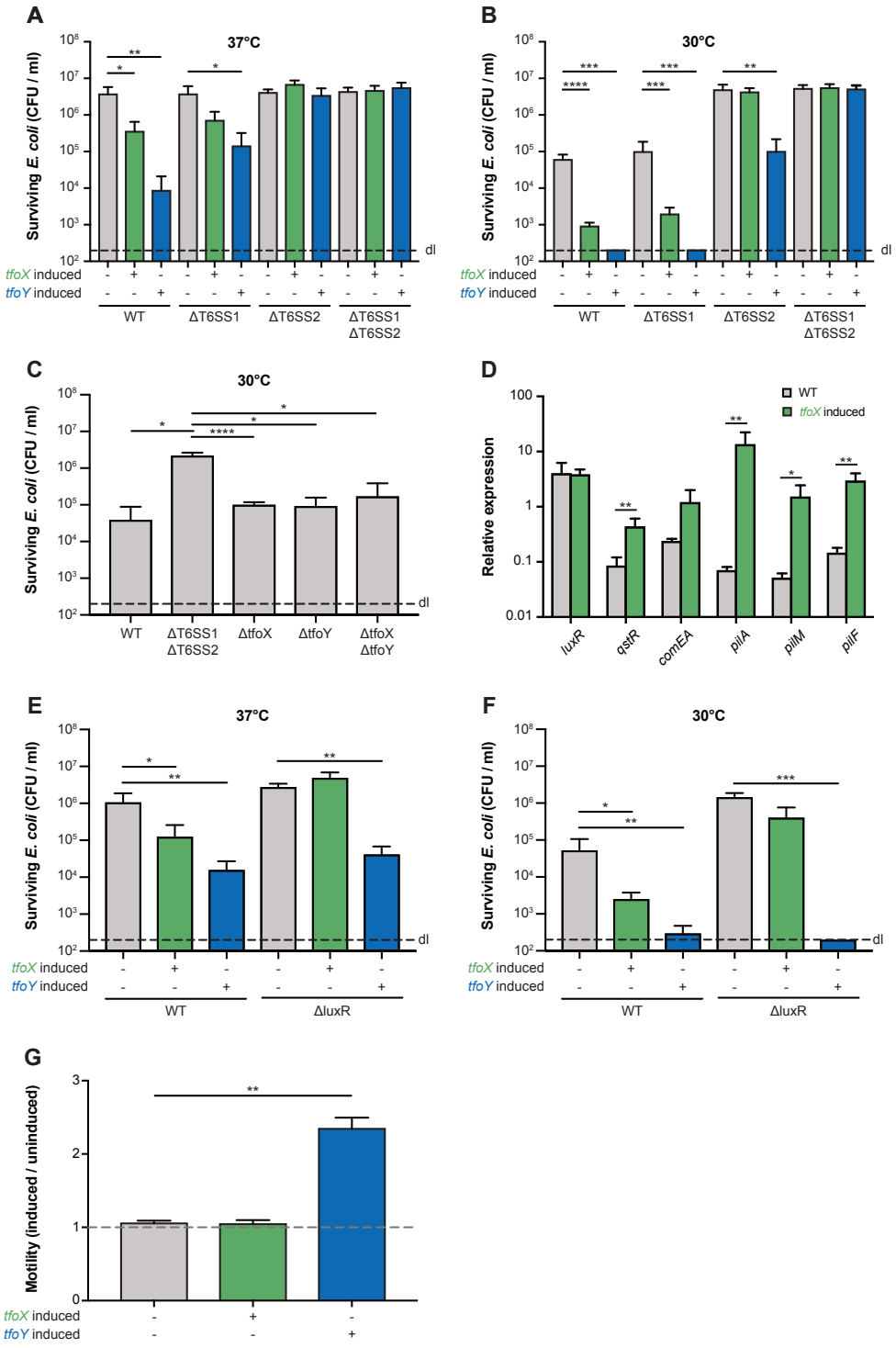

Figure 2.4: TfoY is a universal T6SS inducer in *V. alginolyticus*, while TfoX is specific for T6SS2. (A, B, C, E, F) Interspecies killing assay of *V. alginolyticus* with *E. coli* as prey. *V. alginolyticus* strains were co-cultured with *E. coli* prey for 4 hours at (A, E) 37°C or (B, C, F) 30°C on plain LB agar plates (C) or plates supplemented with arabinose (A, B, E, F; to induce *tfoX* or *tfoY,* as indicated below the graph). The recovery of the prey is indicated as CFU/ml on the Y-axis. (D) TfoX-induces competence genes in *V. alginolyticus.* The relative expression of representative competence genes was scored in WT and *tfoX*-induced strains as indicated on the Y-axis. (G) Motility ratio between uninduced and induced *V. alginolyticus* strains is indicated. Details as in Fig. 2.3D. Abbreviations: WT, *V. alginolyticus* strain 12G01; ΔT6SS1, 12G01Δhcp1; ΔT6SS2, 12G01Δhcp2; ΔT6SS1ΔT6SS2, 12G01Δhcp1Δhcp2; ΔtfoX, 12G01ΔtfoX; ΔtfoY, 12G01ΔtfoY; ΔtfoXΔtfoY, 12G01ΔtfoXΔtfoY; ΔluxR, 12G01ΔluxR. Bar plots represent the average of at least three independent biological replicates (± SD). Statistical significance is indicated (*$p < 0.05$; **$p < 0.01$; ***$p < 0.001$; ****$p < 0.0001$).

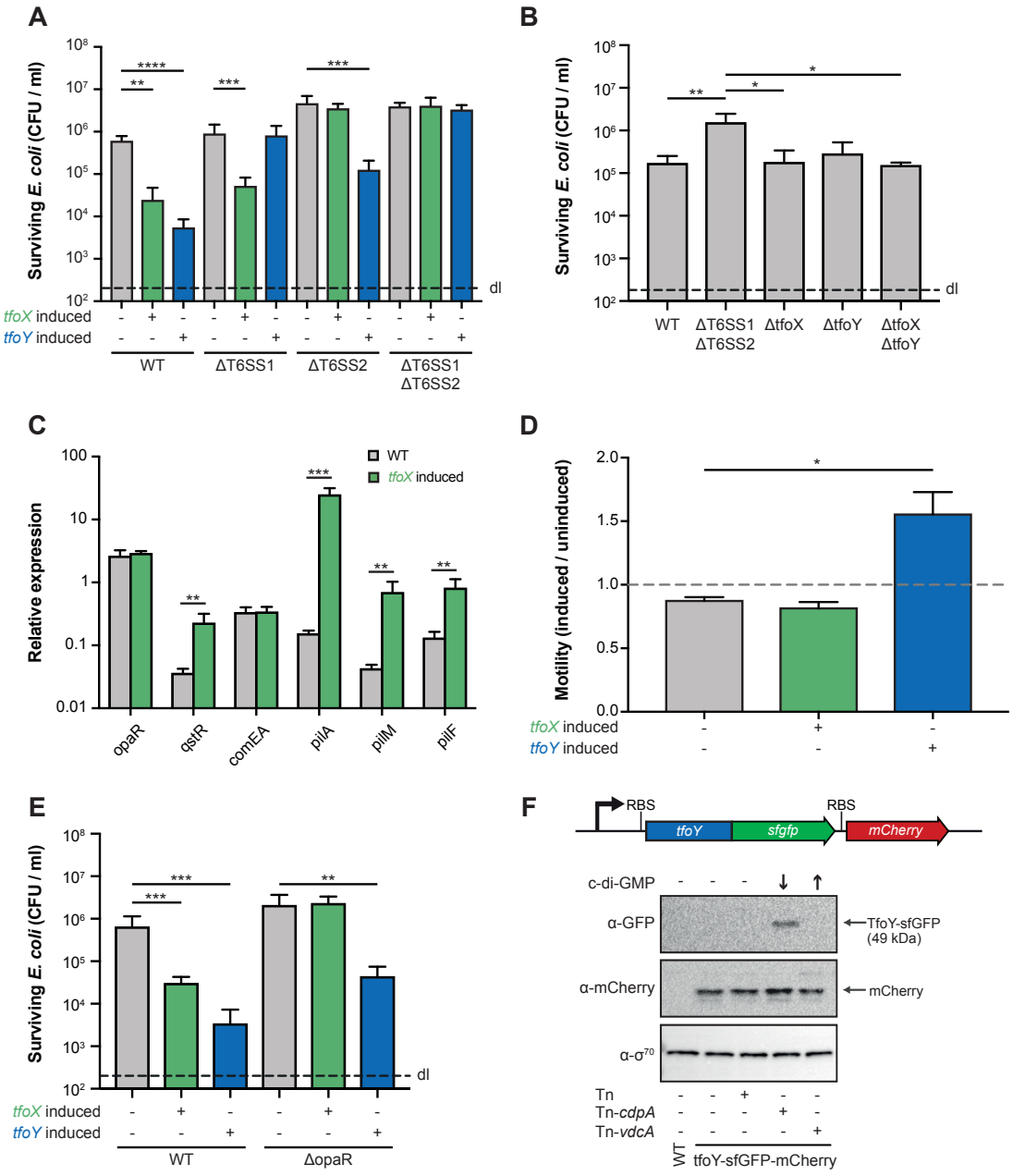

Figure 2.5: TfoX and TfoY each induce a dedicated T6SS in *V. parahaemolyticus*. (A, E) Interspecies killing of *E. coli* by *V. parahaemolyticus*. *V. parahaemolyticus* strains (WT, T6SS1-, T6SS2-, T6SS1/T6SS2-minus or *opaR*-minus) were co-cultured with *E. coli* prey for 4 hours at 30°C on LB agar plates supplemented with arabinose to induce *tfoX* or *tfoY* (as indicated below the graph). The recovery of the prey is indicated on the Y-axis. (B) Basal T6SS activity is independent of TfoX and TfoY. WT *V. parahaemolyticus* or its *tfoX*-, *tfoY*-, or *tfoX/tfoY*-minus variants were tested for their ability to reduce the number of *E. coli* prey cells. The T6SS double mutant (ΔT6SS1ΔT6SS2) served as a control. (C) Relative expression of representative competence genes in WT or *tfoX*-induced bacteria. (D) Quantification of TfoX- or TfoY-induced motility phenotypes. Details as in Fig. 2.3D. (F) TfoY is produced under low c-di-GMP conditions in *V. parahaemolyticus*. Detection of TfoY-sfGFP and mCherry by western blotting in *cdpA*- or *vdcA*-inducible reporter strains that contain increased or decreased intracellular c-di-GMP levels, as indicated by the arrows. The transposon-less or empty transposon-carrying reporter strain as well as the parental WT strain served as controls. Detection of σ^{70} served as a loading control. RBS, ribosome-binding site. Abbreviations: WT, *V. parahaemolyticus* POR1 (RIMD2210633 derivative); ΔT6SS1, POR1Δhcp1; ΔT6SS2, POR1Δhcp2; ΔT6SS1ΔT6SS2, POR1Δhcp1Δhcp2. Bar plots represent the average of at least three independent biological replicates (± SD). Statistical significance is indicated (*$p < 0.05$; **$p < 0.01$; ***$p < 0.001$; ****$p < 0.0001$).

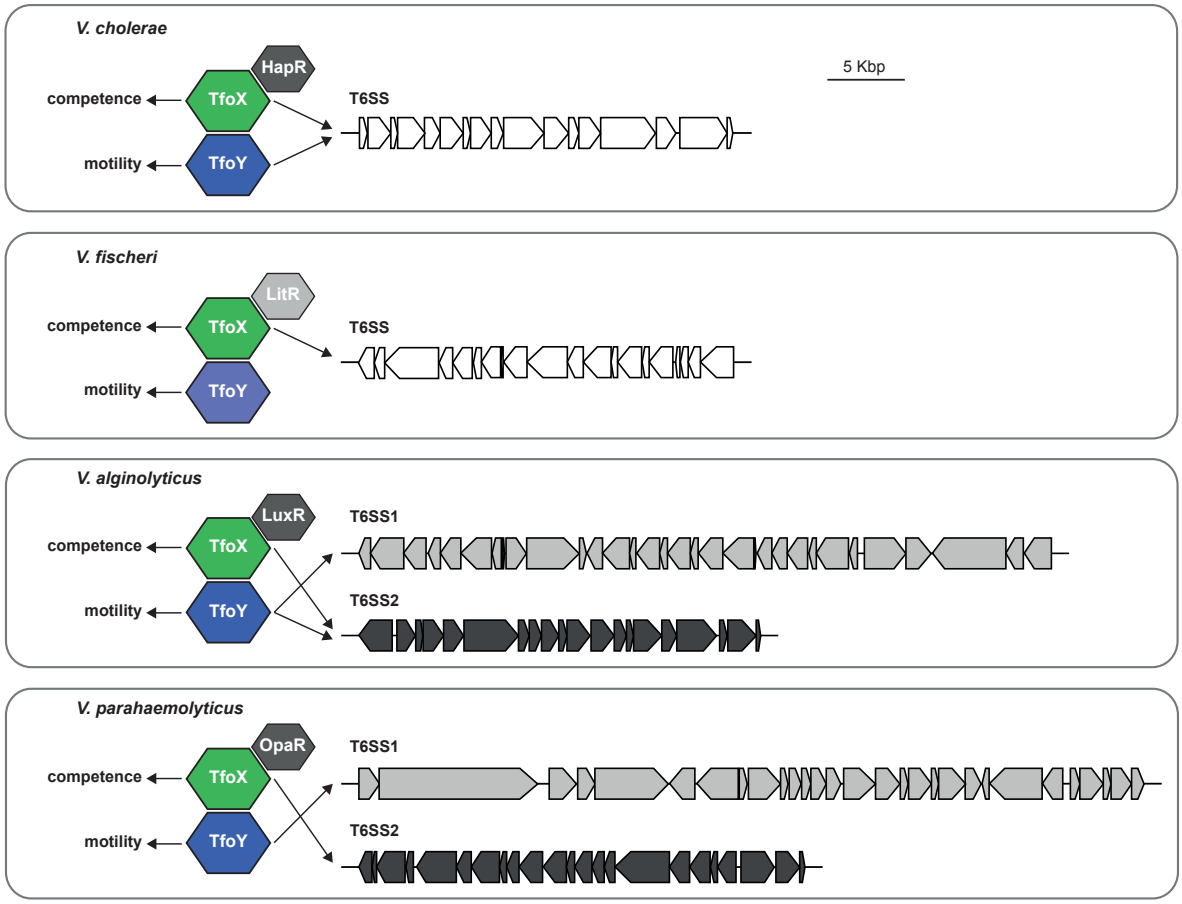

Figure 2.6: Summary scheme of TfoX- and TfoY-induced phenotypes in *V. cholerae* and non-cholera *Vibrio* species. TfoX- and TfoY-mediated regulation of natural competence, motility, and type VI secretion is depicted. The T6SS clusters of *V. cholerae* (only the major cluster is shown), *V. fischeri* (only the conserved T6SS cluster is shown), *V. alginolyticus,* and *V. parahaemolyticus* are indicated (scale corresponds to 5 kbp as indicated). Arrows indicate positive regulation by the respective regulator TfoX or TfoY. The scheme also shows the co-regulating QS master regulators of TfoX-mediated phenotypes (experimentally demonstrated for HapR, LuxR, and OpaR and predicted for LitR).

2.10 SUPPORTING INFORMATION

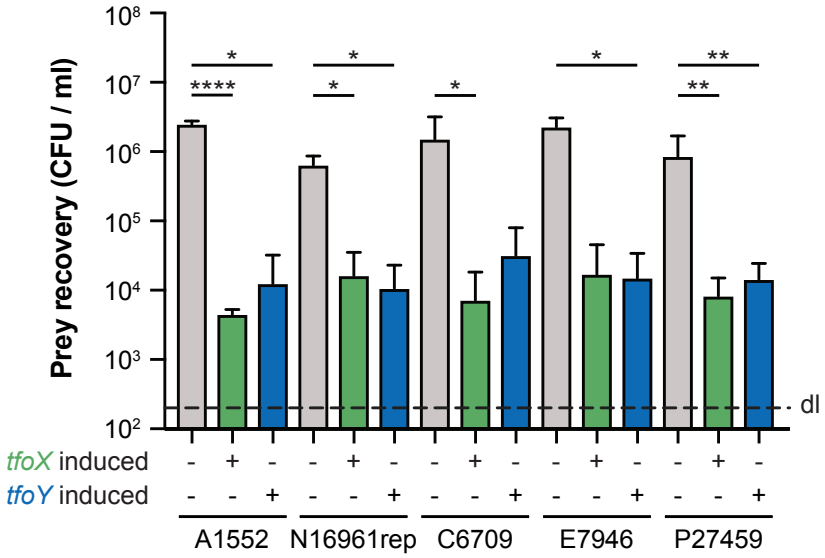

Figure S2.1: TfoX- and TfoY-induced T6SS production is conserved in pandemic *V. cholerae* strains. Interspecies killing assay between diverse *V. cholerae* strains and *E. coli* as prey. The *V. cholerae* O1 El Tor strains tested are as follows: A1552, N16961rep (with repaired frameshift mutation in *hapR*), C6709, E7946, and P27459 as indicated below the graph. Co-culturing with *E. coli* occurred on LB agar plates supplemented with arabinose to induce *tfoX* or *tfoY* where indicated. The parental strains without inducible copies of the regulatory genes served as a control. Prey recovery is indicated as CFU/ml on the Y-axis. Bar plots represent the average of three independent biological replicates (± SD). Statistical significance is indicated (*$p < 0.05$; **$p < 0.01$; ***$p < 0.001$; ****$p < 0.0001$).

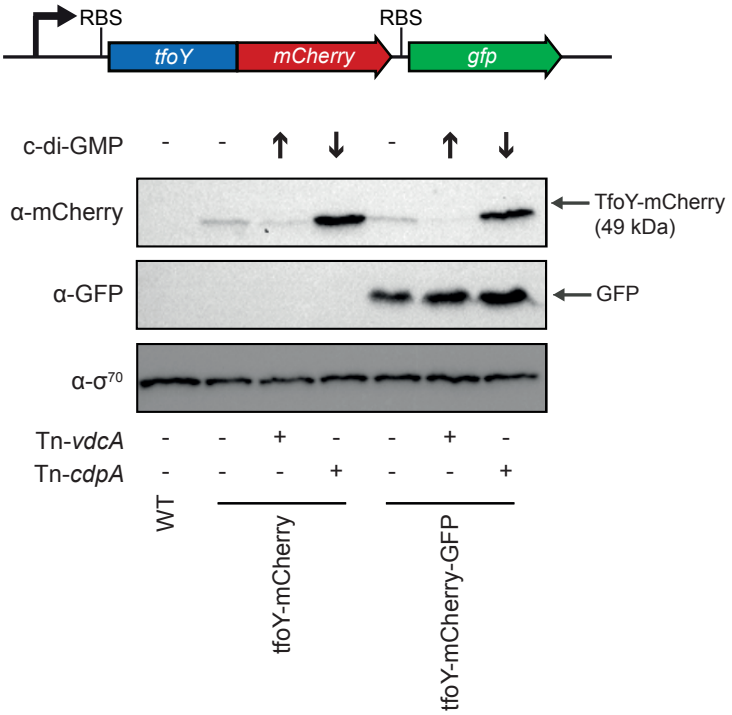

Figure S2.2: TfoY production is translationally but not transcriptionally controlled by c-di-GMP in *V. cholerae*. *V. cholerae* reporter strains carrying a gene encoding for a translational fusion between TfoY and mCherry (*tfoY-mCherry*) with or without a downstream transcriptional reporter gene (*gfp*) at the gene's native chromosomal locus were genetically manipulated to insert inducible copies *vdcA* or *cdpA* into their genome (inside a mini-Tn7 transposon). Cells were then grown under inducible conditions to increase or decrease intracellular c-di-GMP concentrations, as shown by the arrows above the images. Detection of TfoY-mCherry and GFP occurred through western blotting. The reporter strain lacking the transposon as well as the parental WT served as controls. Detection of σ^{70} served as a loading control.

Table S2.1: Bacterial strains and plasmids used in this study

Strains or plasmids	Genotype*/description	Internal strain #	Reference
Strains			
V. cholerae			
A1552 (WT)	Wild-type, O1 El Tor Inaba; Rif^R	MB_1	([56])
A1552-lacZ-Kan	A1552 strain with aph cassette in lacZ gene; Rif^R, Kan^R	MB_135	([93])
A1552-Tn*tfoX-strep*	A1552 containing mini-Tn7-*araC*-P_{BAD}-*tfoX-strep*; Rif^R, $Gent^R$	MB_3420	([3])
A1552-Tn*tfoY-strep*	A1552 containing mini-Tn7-*araC*-P_{BAD}-*tfoY-strep*; Rif^R, $Gent^R$	MB_2978	([3])
A1552-Tn-Cm^R-$tfoX_{VC}$-*strep*	A1552 containing mini-Tn7-*araC*-P_{BAD}-$tfoX_{VC}$-*strep*; Rif^R, Cm^R	MB_6753	This study
A1552-Tn-Cm^R-$tfoY_{VC}$-*strep*	A1552 containing mini-Tn7-*araC*-P_{BAD}-$tfoY_{VC}$-*strep*; Rif^R, Cm^R	MB_6754	This study
A1552-Tn-Cm^R-$tfoX_{VA}$-*strep*	A1552 containing mini-Tn7-*araC*-P_{BAD}-$tfoX_{VA}$-*strep*; Rif^R, Cm^R	MB_6755	This study
A1552-Tn-Cm^R-$tfoY_{VA}$-*strep*	A1552 containing mini-Tn7-*araC*-P_{BAD}-$tfoY_{VA}$-*strep*; Rif^R, Cm^R	MB_6756	This study
A1552-Tn-Cm^R-$tfoX_{VP}$-*strep*	A1552 containing mini-Tn7-*araC*-P_{BAD}-$tfoX_{VP}$-*strep*; Rif^R, Cm^R	MB_6757	This study
A1552-Tn-Cm^R-$tfoY_{VP}$-*strep*	A1552 containing mini-Tn7-*araC*-P_{BAD}-$tfoY_{VP}$-*strep*; Rif^R, Cm^R	MB_6758	This study
A1552-Tn-Cm^R-$tfoX_{VF}$-*strep*	A1552 containing mini-Tn7-*araC*-P_{BAD}-$tfoX_{VF}$-*strep*; Rif^R, Cm^R	MB_6759	This study
A1552-Tn-Cm^R-$tfoY_{VF}$-*strep*	A1552 containing mini-Tn7-*araC*-P_{BAD}-$tfoY_{VF}$-*strep*; Rif^R, Cm^R	MB_6760	This study
A1552-tfoY-mCherry	A1552 carrying *tfoY-mCherry* translational fusion (TransFLP); Rif^R	MB_4262	([3])
A1552-tfoY-mCherry-Tn-*vdcA*	A1552-tfoY-mCherry (TransFLP) containing mini-Tn7-*araC*-P_{BAD}-*vdcA*; Rif^R, $Gent^R$	MB_4324	([3])
A1552-tfoY-mCherry-Tn-*cdpA*	A1552-tfoY-mCherry (TransFLP) containing mini-Tn7-*araC*-P_{BAD}-*cdpA*; Rif^R, $Gent^R$	MB_4325	([3])
A1552-tfoY-mCherry::GFP	A1552 carrying *tfoY-mCherry* translational fusion, transcriptionally fused to *gfp* (TransFLP); Rif^R	MB_5055	This study
A1552-tfoY-mCherry::GFP-Tn-*vdcA*	A1552-tfoY-mCherry::GFP (TransFLP) containing mini-Tn7-*araC*-P_{BAD}-*vdcA*; Rif^R, $Gent^R$	MB_6761	This study
A1552-tfoY-mCherry::GFP-Tn-*cdpA*	A1552-tfoY-mCherry:: GFP (TransFLP) containing mini-Tn7-*araC*-P_{BAD}-*cdpA*; Rif^R, $Gent^R$	MB_6762	This study
N16961rep	N16961 repaired for *hapR* (*hapR*+); Str^R	MB_2254	([59])
N16961rep-Tn*tfoX-strep*	N16961rep containing mini-Tn7- *araC*-P_{BAD}-*tfoX-strep*; Str^R, $Gent^R$	MB_4142	This study

Strains or plasmids	Genotype*/description	Internal strain #	Reference
N16961rep-Tn*tfoY-strep*	N16961rep containing mini-Tn7- *araC*-P_{BAD}-*tfoY-strep*; Str^R, $Gent^R$	MB_4143	This study
C6709	*V. cholerae* O1 El Tor Inaba; isolated in 1991, Peru; Str^R	MB_1503	([95])
C6709-Tn*tfoX-strep*	C6709 containing mini-Tn7-*araC*-P_{BAD}-*tfoX-strep*; Str^R, $Gent^R$	MB_4156	This study
C6709-Tn*tfoY-strep*	C6709 containing mini-Tn7-*araC*-P_{BAD}-*tfoY-strep*; Str^R, $Gent^R$	MB_4157	This study
E7946	*V. cholerae* strain El Tor Ogawa; isolated in 1978, Bahrain; Str^R	MB_2600	([96])
E7946-Tn*tfoX-strep*	E7946 containing mini-Tn7-*araC*-P_{BAD}-*tfoX-strep*; Str^R, $Gent^R$	MB_4162	This study
E7946-Tn*tfoY-strep*	E7946 containing mini-Tn7-*araC*-P_{BAD}-*tfoY-strep* Str^R, $Gent^R$	MB_4163	This study
P27459	*V. cholerae* O1 El Tor Inaba; isolated in 1976, Bangladesh; Str^R	MB_1504	([97])
P27459-Tn*tfoX-strep*	P27459 containing mini-Tn7-*araC*-P_{BAD}-*tfoX-strep*; Str^R, $Gent^R$	MB_4158	This study
P27459-Tn*tfoY-strep*	P27459 containing mini-Tn7-*araC*-P_{BAD}-*tfoY-strep* Str^R, $Gent^R$	MB_4159	This study
V. parahaemolyticus			
POR1 (WT)	RIMD 2210633 Δ*tdhAS*	MB_5862	([18])
POR1-Tn-Cm^R-$tfoX_{VP}$-*strep*	POR1 containing mini-Tn7-*araC*-P_{BAD}-$tfoX_{VP}$-*strep*; Cm^R	MB_6763	This study
POR1-Tn-Cm^R-$tfoY_{VP}$-*strep*	POR1 containing mini-Tn7-*araC*-P_{BAD}-$tfoY_{VP}$-*strep*; Cm^R	MB_6764	This study
POR1Δhcp1	POR1ΔVP1393	MB_5863	([18])
POR1Δhcp1-Tn-Cm^R-$tfoX_{VP}$-*strep*	POR1Δhcp1 containing mini-Tn7-*araC*-P_{BAD}-$tfoX_{VP}$-*strep*; Cm^R	MB_6765	This study
POR1Δhcp1-Tn-Cm^R-$tfoY_{VP}$-*strep*	POR1Δhcp1containing mini-Tn7-*araC*-P_{BAD}-$tfoY_{VP}$-*strep*; Cm^R	MB_6766	This study
POR1Δhcp2	POR1ΔVPA1027	MB_5864	Gift from D. Salomon
POR1Δhcp2-Tn-Cm^R-$tfoX_{VP}$-*strep*	POR1Δhcp2 containing mini-Tn7-*araC*-P_{BAD}-$tfoX_{VP}$-*strep*; Cm^R	MB_6767	This study
POR1Δhcp2-Tn-Cm^R-$tfoY_{VP}$-*strep*	POR1Δhcp2 containing mini-Tn7-*araC*-P_{BAD}-$tfoY_{VP}$-*strep*; Cm^R	MB_6768	This study
POR1Δhcp1Δhcp2	POR1ΔVP1393ΔVPA1027	MB_5865	Gift from D. Salomon
POR1Δhcp1Δhcp2-Tn-Cm^R-$tfoX_{VP}$-*strep*	POR1Δhcp1Δhcp2 containing mini-Tn7-*araC*-P_{BAD}-$tfoX_{VP}$-*strep*; Cm^R	MB_6769	This study
POR1Δhcp1Δhcp2-Tn-Cm^R-$tfoY_{VP}$-*strep*	POR1Δhcp1Δhcp2 containing mini-Tn7-*araC*-P_{BAD}-$tfoY_{VP}$-*strep*; Cm^R	MB_6770	This study
POR1ΔtfoX	POR1ΔVP1241 (deleted using suicide plasmid pGP704-Sac-Kan-tfoX_{VP})	MB_6771	This study
POR1ΔtfoY	POR1ΔVP1028 (deleted using suicide plasmid pGP704-Sac-Kan-tfoY_{VP})	MB_6774	This study

Strains or plasmids	Genotype*/description	Internal strain #	Reference
POR1ΔtfoXΔtfoY	POR1ΔtfoX ΔVP1028 (deleted using suicide plasmid pGP704-Sac-Kan-tfoY$_{VP}$)	MB_6777	This study
POR1ΔopaR	POR1ΔVP2516 (deleted using suicide plasmid pGP704-Sac-Kan-opaR$_{VP}$)	MB_6780	This study
POR1ΔopaR-Tn-Cm^R-*tfoX$_{VP}$-strep*	POR1ΔopaR containing mini-Tn7-*araC*-P$_{BAD}$-*tfoX$_{VP}$-strep*; Cm^R	MB_6781	This study
POR1ΔopaR-Tn-Cm^R-*tfoY$_{VP}$-strep*	POR1ΔopaR containing mini-Tn7-*araC*-P$_{BAD}$-*tfoY$_{VP}$-strep*; Cm^R	MB_6782	This study
POR1-tfoY-sfGFP::mCherry	POR1 carrying a *tfoY-sfgfp* translational fusion, transcriptionally fused to *mCherry* (inserted using suicide plasmid pGP704-Sac-Kan-*tfoY$_{VP}$-sfGFP-mCherry*)	MB_6787	This study
POR1-tfoY-sfGFP::mCherry-Tn-Cm^R-*cdpA*	POR1-tfoY-sfGFP::mCherry containing mini-Tn7-*araC*-P$_{BAD}$-*cdpA*; Cm^R	MB_6788	This study
POR1-tfoY-sfGFP::mCherry-Tn-Cm^R-*vdcA*	POR1-tfoY-sfGFP::mCherry containing mini-Tn7-*araC*-P$_{BAD}$-*vdcA*; Cm^R	MB_6789	This study
POR1-tfoY-sfGFP::mCherry-Tn-Cm^R	POR1-tfoY-sfGFP::mCherry containing mini-Tn7; Cm^R	MB_6790	This study
V. alginolyticus			
12G01 (WT)	Wild-type	MB_5857	([21])
12G01-Tn-Cm^R-*tfoX$_{VA}$-strep*	12G01 containing mini-Tn7-*araC*-P$_{BAD}$-*tfoX$_{VA}$-strep*; Cm^R	MB_6791	This study
12G01-Tn-Cm^R-*tfoY$_{VA}$-strep*	12G01 containing mini-Tn7-*araC*-P$_{BAD}$-*tfoY$_{VA}$-strep*; Cm^R	MB_6792	This study
12G01Δhcp1	12G01ΔV12G01_01540	MB_5858	([21])
12G01Δhcp1-Tn-Cm^R-*tfoX$_{VA}$-strep*	12G01Δhcp1 containing mini-Tn7-*araC*-P$_{BAD}$-*tfoX$_{VA}$-strep*; Cm^R	MB_6793	This study
12G01Δhcp1-Tn-Cm^R-*tfoY$_{VA}$-strep*	12G01Δhcp1containing mini-Tn7-*araC*-P$_{BAD}$-*tfoY$_{VA}$-strep*; Cm^R	MB_6794	This study
12G01Δhcp2	12G01ΔV12G01_07583	MB_5859	([21])
12G01Δhcp2-Tn-Cm^R-*tfoX$_{VA}$-strep*	12G01Δhcp2 containing mini-Tn7-*araC*-P$_{BAD}$-*tfoX$_{VA}$-strep*; Cm^R	MB_6795	This study
12G01Δhcp2-Tn-Cm^R-*tfoY$_{VA}$-strep*	12G01Δhcp2 containing mini-Tn7-*araC*-P$_{BAD}$-*tfoY$_{VA}$-strep*; Cm^R	MB_6796	This study
12G01Δhcp1Δhcp2	12G01ΔV12G01_01540ΔV12G01_07583	MB_5860	([21])
12G01Δhcp1Δhcp2-Tn-Cm^R-*tfoX$_{VA}$-strep*	12G01Δhcp1Δhcp2 containing mini-Tn7-*araC*-P$_{BAD}$-*tfoX$_{VA}$-strep*; Cm^R	MB_6797	This study
12G01Δhcp1Δhcp2-Tn-Cm^R-*tfoY$_{VA}$-strep*	12G01Δhcp1Δhcp2 containing mini-Tn7-*araC*-P$_{BAD}$-*tfoY$_{VA}$-strep*; Cm^R	MB_6798	This study

Strains or plasmids	Genotype*/description	Internal strain #	Reference
12G01ΔtfoX	12G01ΔtfoX (12G01ΔV12G01_19736)	MB_6994	This study
12G01ΔtfoY	12G01ΔtfoY (12G01ΔV12G01_20658)	MB_6995	This study
12G01ΔtfoXΔtfoY	12G01ΔtfoXΔtfoY (12G01ΔV12G01_19736 ΔV12G01_20658)	MB_6996	This study
12G01ΔluxR	12G01ΔluxR (12G01ΔV12G01_21538)	MB_6997	This study
12G01ΔluxR-Tn-Cm^R-*tfoX$_{VA}$-strep*	12G01ΔluxR containing mini-Tn7-*araC*-P$_{BAD}$-*tfoX$_{VA}$-strep*; Cm^R	MB_6998	This study
12G01ΔluxR-Tn-Cm^R-*tfoY$_{VA}$-strep*	12G01ΔluxR containing mini-Tn7-*araC*-P$_{BAD}$-*tfoY$_{VA}$-strep*; Cm^R	MB_6999	This study
V. fischeri			
ES114 (WT)	Wild-type	MB_5869	ATCC-700601; via LGC standards
ES114-Tn-Cm^R-*tfoX$_{VF}$-strep*	ES114 containing mini-Tn7-*araC*-P$_{BAD}$-*tfoX$_{VF}$-strep*; Cm^R	MB_6799	This study
ES114-Tn-Cm^R-*tfoY$_{VF}$-strep*	ES114 containing mini-Tn7-*araC*-P$_{BAD}$-*tfoY$_{VF}$-strep*; Cm^R	MB_6800	This study
E. coli			
SM10λpir	thi-1 thr leu tonA lacY supE recA::RP4-2-Tc::Mu, Kmr (λpir); Kan^R	MB_647	([84])
TOP10	F- mcrA Δ(mrr-hsdRMS-mcrBC) φ80lacZΔM15 ΔlacX74 nupG recA1 araΔ139 Δ(ara-leu)7697 galE15 galK16 rpsL(Str^R) endA1λ$^-$	MB_741	Invitrogen
TOP10-TnKan	TOP10 containing mini-Tn7-*aph*(Kan^R); Str^R, Kan^R, Gent^R	MB_4119	([3])
DH5α	F$^-$ endA1 glnV44 thi-1 recA1 relA1 gyrA96 deoR nupG φ80lacZΔM15 Δ(lacZYA-argF) U169 hsdR17 (r_K^- m_K^+) phoA, λ-	MB_736	([83])
S17-1λpir	Tpr Smr recA thi pro hsdR2M1 RP4:2-Tc:Mu:Kmr Tn7 (λpir); Str^R	MB_648	([84])
MFDpir	MG1655 RP4-2-Tc::[ΔMu1::aac(3)IV-ΔaphA-Δnic35-ΔMu2::zeo] ΔdapA::(erm-pir) ΔrecA	MB_4662	([85])

Strains or plasmids	Genotype*/description	Internal strain #	Reference
Plasmids			
pBAD/myc-HisA	pBR322-derived expression vector; *araBAD* promoter (P_{BAD}); Amp^R	MB_24	Invitrogen
pBAD-*tfoX-strep*	*tfoX*$_{VC}$ in pBAD/Myc-HisA with C-terminal Strep-tagII®, arabinose inducible; Amp^R	MB_3616	([3])
pBAD-*tfoY-strep*	*tfoY*$_{VC}$ in pBAD/Myc-HisA with C-terminal Strep-tagII®, arabinose inducible; Amp^R	MB_2945	([3])
pBAD -*tfoX*$_{VP}$-*strep*	*tfoX*$_{VP}$ in pBAD/Myc-HisA with C-terminal Strep-tagII®, arabinose inducible; Amp^R	MB_6801	This study
pBAD-*tfoY*$_{VP}$-*strep*	*tfoY*$_{VP}$ in pBAD/Myc-HisA with C-terminal Strep-tagII®, arabinose inducible; Amp^R	MB_6802	This study
pBAD -*tfoX*$_{VA}$-*strep*	*tfoX*$_{VA}$ in pBAD/Myc-HisA with C-terminal Strep-tagII®, arabinose inducible; Amp^R	MB_6803	This study
pBAD-*tfoY*$_{VA}$-*strep*	*tfoY*$_{VA}$ in pBAD/Myc-HisA with C-terminal Strep-tagII®, arabinose inducible; Amp^R	MB_6804	This study
pBAD-*tfoX*$_{VF}$-*strep*	*tfoX*$_{VF}$ in pBAD/Myc-HisA with C-terminal Strep-tagII®,, arabinose inducible; Amp^R	MB_6805	This study
pBAD-*tfoY*$_{VF}$-*strep*	*tfoY*$_{VF}$ in pBAD/Myc-HisA with C-terminal Strep-tagII®,, arabinose inducible; Amp^R	MB_6806	This study
pGP704-mTn7-minus SacI	pGP704 with mini-*Tn*7 harboring *aacC1* gene; Amp^R, $Gent^R$	MB_645	([91])
pGP704-mTn*tfoX-strep*	pGP704 with mini-Tn7 carrying *araC* and P_{BAD}-driven *tfoX-strep*; Amp^R, $Gent^R$	MB_3664	([3])
pGP704-mTn*tfoY-strep*	pGP704 with mini-Tn7 carrying *araC* and P_{BAD}-driven *tfoY-strep*; Amp^R, $Gent^R$	MB_2941	([3])
pGP704-mTn-*vdcA*	pGP704 with mini-Tn7 carrying *araC* and P_{BAD}-driven *vdcA*; Amp^R, $Gent^R$	MB_2943	([3])
pGP704-mTn-*cdpA*	pGP704 with mini-Tn7 carrying *araC* and P_{BAD}-driven *cdpA*; Amp^R, $Gent^R$	MB_2944	([3])
pGP704-mTn-Cm^R	pGP704 with mini-*Tn*7 harboring *cat* gene; Amp^R, Cm^R	MB_5427	This study
pGP704-mTn-Cm^R-*tfoX*$_{VC}$-*strep*	pGP704 with mini-Tn7 carrying *araC* and P_{BAD}-driven *tfoX*$_{VC}$-*strep*; Amp^R, Cm^R	MB_6807	This study
pGP704-mTn-Cm^R-*tfoY*$_{VC}$-*strep*	pGP704 with mini-Tn7 carrying *araC* and P_{BAD}-driven *tfoY*$_{VC}$-*strep*; Amp^R, Cm^R	MB_6808	This study

Strains or plasmids	Genotype*/description	Internal strain #	Reference
pGP704-mTn-Cm^R-*tfoX$_{VP}$-strep*	pGP704 with mini-Tn7 carrying *araC* and P$_{BAD}$-driven *tfoX$_{VP}$-strep*; Amp^R, Cm^R	MB_6809	This study
pGP704-mTn-Cm^R-*tfoY$_{VP}$-strep*	pGP704 with mini-Tn7 carrying *araC* and P$_{BAD}$-driven *tfoY$_{VP}$-strep*; Amp^R, Cm^R	MB_6810	This study
pGP704-mTn-Cm^R-*tfoX$_{VA}$-strep*	pGP704 with mini-Tn7 carrying *araC* and P$_{BAD}$-driven *tfoX$_{VA}$-strep*; Amp^R, Cm^R	MB_6811	This study
pGP704-mTn-Cm^R-*tfoY$_{VA}$-strep*	pGP704 with mini-Tn7 carrying *araC* and P$_{BAD}$-driven *tfoY$_{VA}$-strep*; Amp^R, Cm^R	MB_6812	This study
pGP704-mTn-Cm^R-*tfoX$_{VF}$-strep*	pGP704 with mini-Tn7 carrying *araC* and P$_{BAD}$-driven *tfoX$_{VF}$-strep*; Amp^R, Cm^R	MB_6813	This study
pGP704-mTn-Cm^R-*tfoY$_{VF}$-strep*	pGP704 with mini-Tn7 carrying *araC* and P$_{BAD}$-driven *tfoY$_{VF}$-strep*; Amp^R, Cm^R	MB_6814	This study
pUX-BF-13	*ori*R6K, helper plasmid with Tn7 transposition function; Amp^R	MB_457	([92])
pGP704-TnKan	pGP704 with mini-Tn7 carrying *aph* (Kan^R) gene; Amp^R, Gent^R, Kan^R	MB_4117	([3])
pGP704-Sac28	Suicide vector, *ori*R6K, *sacB*; Amp^R	MB_649	([78])
pGP704-Sac-Kan	Suicide vector, *ori*R6K, *sacB*; Kan^R	MB_6038	This study
pGP704-Sac-Kan-*tfoX$_{VP}$*	pGP704-Sac-Kan with gene fragment resulting in a 390-bp deletion within *VP1241*; Kan^R	MB_6815	This study
pGP704-Sac-Kan-*tfoY$_{VP}$*	pGP704-Sac-Kan with gene fragment resulting in a 393-bp deletion within *VP1028*; Kan^R	MB_6816	This study
pGP704-Sac-Kan-*opaR$_{VP}$*	pGP704-Sac-Kan with gene fragment resulting in a 417-bp deletion within *VP2516*; Kan^R	MB_6817	This study
pGP704-Sac-Kan-*tfoY$_{VP}$-sfGFP::mCherry*	pGP704-Sac-Kan with gene fragment resulting in a transcriptional fusion of *mCherry* to fusion of *VP1028-sfgfp*; Kan^R	MB_6819	This study
pGP704-Sac-Kan-*tfoX$_{VA}$*	pGP704-Sac-Kan with gene fragment resulting in a 402-bp deletion within *V12G01_19736*; Kan^R	MB_6991	This study
pGP704-Sac-Kan-*tfoY$_{VA}$*	pGP704-Sac-Kan with gene fragment resulting in a 444-bp deletion within *V12G01_20658;* Kan^R	MB_6992	This study
pGP704-Sac-Kan-*luxR$_{VA}$*	pGP704-Sac-Kan with gene fragment resulting in a 456-bp deletion within *V12G01_21538*; Kan^R	MB_6993	This study

*VC numbers according to ([58])

2.11 ADDITIONAL DISCUSSION

The present study highlights the importance of TfoX and TfoY, which are present in all *Vibrionaceae* ([8]). We demonstrated that TfoX and TfoY regulate the T6SS in all four *Vibrio* species tested and, in addition, that TfoX induces competence genes, while TfoY enhances bacterial motility, emphasizing the conservation of these regulators.

Interestingly, our results showed that TfoX positively regulates the competence genes together with the T6SS. This co-regulation was previously demonstrated in *V. cholerae* and, as a result, fosters the acquisition of novel genes by HGT ([2]). It is tempting to speculate that this biological function is conserved among vibrios and that the TfoX-dependent regulation of these nanomachines might have an effect on bacterial evolution. As the chitin utilization and sensing pathways inducing *tfoX* in *V. cholerae* are highly conserved in the majority of *Vibrio* species ([9–12]), we suggest that the environmental cues leading to TfoX production might be similar among vibrios. Along those lines, previous studies have demonstrated that chitin induces natural competence in other non-cholera *Vibrio* including *V. fischeri* ([8]), *V. parahaemolyticus* ([15]) and *V. vulnificus* ([98]). In *V. cholerae*, the production of the DNA-uptake machinery, as well as the T6SS, is dependent on TfoX and on the QS regulator HapR, which together regulate QstR ([65,66]). It is important to remind that *V. fischeri* lacks a QstR-homolog ([13,14]) and, the exact regulatory cascade will therefore not be identical among all *Vibrio* species. In addition, among the competence genes regulated by TfoX, we detected that the transcript levels of *comEA,* which encodes the DNA-binding protein required for DNA uptake and successful transformation ([61,63]), was low in the non-cholera *Vibrio* species investigated in this study. Intriguingly, in *V. fischeri* and *V. alginolyticus* we observed a small increase of *comEA* expression upon TfoX production as compared to the transcript level detected in *V. cholerae*, while TfoX did not induce *comEA* in *V. parahaemolyticus.* These observations open novel questions on the regulation of natural competence in the latter *Vibrio* species, starting with: Are these strains of vibrios naturally transformable? And are homologous proteins of HapR and QstR also required to regulate competence genes? Interestingly, a recent preprint article by Simpson and colleagues showed that, while TfoX and QstR are essential, the HapR-homolog is not required for successful transformation in *V. campbellii* and in *V. parahaemolyticus*, highlighting some variability in the competence regulatory cascade among vibrios ([99]). Although the *V. parahaemolyticus* strain used in this study was not transformable (potentially due to the absence of *comEA's* induction), previous

studies have shown that *V. parahaemolyticus* knockout could be engineered either by natural transformation on chitin surfaces ([15]) or by chitin-independent transformation via the overproduction of TfoX from a plasmid ([17]). Among these studies, three different isolates of *V. parahaemolyticus* were used, which, according to the literature, are highly clonal and are considered as derivative of the clinical isolate RIMD2210633 ([15,17,18,100]). However, we cannot ensure that they all produce the same variant of TfoX or that they required the same environmental cues and have a conserved regulatory pathway for natural competence induction. Along those lines, Simpson and colleagues identified variation of transformation capability among different isolates of *Vibrio campbellii* ([99]). While some isolates become competent upon overexpression of *V. cholerae's tfoX* homolog, other strains were non-transformable. The defect of transformability recorded in some isolates correlated with low induction of competence genes, however the reason why the regulation differed among these *V. campbellii* isolates remains unknown ([99]). Further studies are therefore required to uncover the complexity of competence regulation in *V. cholerae* and among diverse *Vibrio* species.

Remarkably, in this chapter we demonstrated that, as for *V. cholerae* ([2,3]), TfoX and TfoY are major regulators of the T6SS in *V. parahaemolyticus* and *V. alginolyticus*. Interestingly, a study by Ben-Yaakov and Salomon, which was co-submitted with our work, identified TfoY as the major regulator of the T6SS1 in *V. parahaemolyticus* ([101]). Even though some environmental cues inducing the T6SS in *V. parahaemolyticus* were previously identified ([18]), the authors emphasized that "it remains largely unknown how this bacterium senses and translates surface, salinity and temperature conditions into a T6SS1-activating signal" ([101]). To identify the regulator of the T6SS1, Ben-Yaakov and Salomon developed a screening method, which consisted of: mixing the strains of a mutant transposon library with a fluorescent bacterial prey and, after incubation, evaluating the fluorescence of the spotted mixtures. The absence or presence of fluorescence correlates with the killing or survival of the fluorescent prey, respectively. In the latter case, the transposon inserted resulted in the absence of T6SS activity and was considered as a potential hit. In their study, Ben-Yaakov and Salomon screened 12'000 mutants and ultimately obtained 10 hits that were further investigated, as the transposon of these mutants was not directly inserted into the T6SS cluster. Remarkably, among these hits, only two genes (*vp2049* and *vp1028*) were abolishing the secretion of the T6SS. While the influence of *vp2049* on T6SS activity remains unclear, *vp1028* encodes the TfoY homolog in this organism and therefore confirmed our study as TfoY being a major regulator of T6SSs in *Vibrio* species ([101]). In addition, Ben-Yaakov and

Salomon demonstrated that TfoY positively regulates the two regulators encoded within the T6SS cluster, which are required for its expression. Moreover, the authors showed that upon TfoY overexpression, the T6SS1 is activated without a need of surface sensing and salinity, suggesting that these environmental cues activate TfoY, which in turn induces T6SS1 in *V. parahaemolyticus* ([18,101]). Along those lines, we showed that low intracellular level of c-di-GMP, which have been linked to surface sensing ([23]), led to the production of TfoY at the translational level in *V. parahaemolyticus* and *V. cholerae*. We therefore proposed that surface sensing leads to low c-di-GMP level, which results in the translation of the *tfoY* mRNA and subsequently the induction of the T6SS. Further studies are required to directly demonstrate that low level of c-di-GMP leads to the TfoY-dependent induction of the T6SS and that surface sensing fosters TfoY production.

2.12 REFERENCES

1. Meibom, K. L., Blokesch, M., Dolganov, N. A., Wu, C.-Y. and Schoolnik, G. K. Chitin induces natural competence in *Vibrio cholerae*. *Science* **310**, 1824–1827 (2005).
2. Borgeaud, S., Metzger, L. C., Scrignari, T. and Blokesch, M. The type VI secretion system of *Vibrio cholerae* fosters horizontal gene transfer. *Science* **347**, 63–67 (2015).
3. Metzger, L. C., Stutzmann, S., Scrignari, T., Van der Henst, C., Matthey, N., and Blokesch, M. Independent Regulation of Type VI Secretion in *Vibrio cholerae* by TfoX and TfoY. *Cell Rep* **15**, 951–958 (2016).
4. Le Roux, F. and Blokesch, M. Eco-evolutionary dynamics linked to horizontal gene transfer in vibrios. *Annu Rev Microbiol* **72**, 89–110 (2018).
5. Lukjancenko, O. and Ussery, D. W. Vibrio chromosome-specific families. *Front. Microbiol.* **5**, 1–8 (2014).
6. Ghenem, L., Elhadi, N., Alzahrani, F., and Nishibuchi, M. *Vibrio parahaemolyticus*: a review on distribution, pathogenesis, virulence determinants and epidemiology. *Saudi Journal of medicine and Medical Science* 93–103 (2017).
7. Ravikumar, V. and Vijayakumar, R. *Vibrio alginolyticus* emerging food born pathogen. *Asian J Sci Technol* **08**, 4887–4891 (2017).
8. Pollack-Berti, A., Wollenberg, M. S. and Ruby, E. G. Natural transformation of *Vibrio fischeri* requires *tfoX* and *tfoY*. *Environ Microbiol* **12**, 2302–2311 (2010).
9. Hunt, D. E., Gevers, D., Vahora, N. M. and Polz, M. F. Conservation of the chitin utilization pathway in the *Vibrionaceae*. *Appl Environ Microbiol* **74**, 44–51 (2008).
10. Li, X. and Roseman, S. The chitinolytic cascade in vibrios is regulated by chitin oligosaccharides and a two-component chitin catabolic sensor/kinase. *Proc Natl Acad Sci USA* **101**, 627–631 (2004).
11. Yamamoto, S., Izumiya, H., Mitobe, J., Morita, M., Arakawa, E., Ohnishi, M., and Watanabe, H. Identification of a chitin-induced small RNA that regulates translation of the *tfoX* gene, encoding a positive regulator of natural competence in vibrio cholerae. *J. Bacteriol.* **193**, 1953–1965 (2011).
12. Yamamoto, S., Mitobe, J., Ishikawa, T., Wai, S.N., Ohnishi, M., Watanabe, H., and Izumiya, H. Regulation of natural competence by the orphan two-component system sensor kinase ChiS involves a non-canonical transmembrane regulator in *Vibrio cholerae*. *Mol Microbiol* **91**, 326–347 (2014).
13. Antonova, E. S. and Hammer, B. K. Genetics of natural competence in *Vibrio cholerae* and other vibrios. *Microbiol Spectr* **3**, 1–18 (2015).
14. Ball, A. S., Chaparian, R. R. and van Kessel, J. C. Quorum sensing gene regulation by LuxR/HapR master regulators in vibrios. *J Bacteriol* **199**, (2017).
15. Chen, Y., Dai, J., Morris, J. G. and Johnson, J. A. Genetic analysis of the capsule polysaccharide (K antigen) and exopolysaccharide genes in pandemic *Vibrio parahaemolyticus* O3:K6. *BMC Microbiol.* **10**, 274 (2010).
16. Frischer, M. E., Thurmond, J. M. and Paul, J. H. Natural plasmid transformation in a high-frequency-of-transformation marine *Vibrio* strain. *Appl Environ Microbiol* **56**, 3439–3444 (1990).
17. Chimalapati, S., de Souza Santos, M., Servage, K., De Nisco, N. J., Dalia, A. B. and Orth, K. Natural transformation in *Vibrio parahaemolyticus*: a rapid method to create genetic deletions. **200**, 1–8 (2018).
18. Salomon, D., Gonzalez, H., Updegraff, B. L. and Orth, K. *Vibrio parahaemolyticus* type VI

secretion system 1 is activated in marine conditions to target bacteria, and is differentially regulated from system 2. *PLoS One* **8**, e61086 (2013).

19. Salomon, D., Klimko, J. A. and Orth, K. H-NS regulates the *Vibrio parahaemolyticus* type VI secretion system 1. *Microbiology* **160**, 1867–1873 (2014).
20. Salomon, D., Kinch, N.D., Trudgian, D.C., Guo. X., Klimko, J.A., Grishin, N. V., Mirzaei, H., and Orth, K. Marker for type VI secretion system effectors. *Proc. Natl. Acad. Sci.USA* **111**, 9271–9276 (2014).
21. Salomon, D., Klimko, J.A., Trudgian, D.C., Kinch, L.N., Grishin, N.V., Mirzaei, H., and Orth, K. Type VI secretion system toxins horizontally shared between marine bacteria. PLoS Pathog. 11, e1005128 (2015).
22. Speare, L., Cecere, A., K., Guckes, K. R., Smith, S., Wollenberg, M., Mandel, M., Miyashiro, T., and Septer, A. N. Bacterial symbionts use a type VI secretion system to eliminate competitors in their natural host. Proc Natl Acad Sci USA 115, E8528–E8537 (2018).
23. Gode-Potratz, C. J., Kustusch, R.J., Breheny, P.J., Weiss, D.S., and McCarter, L.L. Surface sensing in *Vibrio parahaemolyticus* triggers a programme of gene expression that promotes colonization and virulence. *Mol Microbiol* **79**: 240-263 (2011).
24. Yu, Y., Yang, H., Li, J., Zhang, P., Wu, B., Zhu, B., Zhang, Y. and Fang, W. Putative type VI secretion systems of *Vibrio parahaemolyticus* contribute to adhesion to cultured cell monolayers. *Arch Microbiol* **194**, 827–835 (2012).
25. Yu, Y., Fang, L., Zhang, Y., Sheng, H. and Fang, W. VgrG2 of type VI secretion system 2 of *Vibrio parahaemolyticus* induces autophagy in macrophages. *Front. Microbiol.* **6**, 168 (2015).
26. Izutsu, K., Kurokawa, K., Tashiro, K., Kuhara, S., Hayashi, T., Honda, T. and Iida, T. Comparative genomic analysis using microarray demonstrates a strong correlation between the presence of the 80-kilobase pathogenicity island and pathogenicity in kanagawa phenomenon-positive *Vibrio parahemolyticus* strains. *Infect Immun* **76**, 1016–1023 (2008).
27. Sheng, L., Gu, D., Wang, Q., Liu, Q. and Zhang, Y. Quorum sensing and alternative sigma factor RpoN regulate type VI secretion system I (T6SSVA1) in fish pathogen *Vibrio alginolyticus*. *Arch Microbiol* **194**, 379–390 (2012).
28. Matthey, N., Drebes Dörr, N. C. and Blokesch, M. Long-read-based genome sequences of pandemic and environmental *Vibrio cholerae* strains. *Microbiol Resour Annoucements* **7**, (2018).
29. Blokesch, M. A quorum sensing-mediated switch contributes to natural transformation of *Vibrio cholerae*. *Mob Genet Elements* **2**, 224–227 (2012).
30. Lo Scrudato, M. and Blokesch, M. The regulatory network of natural competence and transformation of *Vibrio cholerae*. *PLoS Genet* **8**,e1002778 (2012).
31. Jerry Reen, F., Almagro-Moreno, S., Ussery, D. and Fidelma Boyd, E. The genomic code: inferring Vibrionaceae niche specialization. *Nat Rev Microbiol* **4**, 697–704 (2006).
32. Costa, T. R. D. Felisberto-Rodrigues, C., Meir, A., Prevost, M.S., Redzej, A., Trokter, M., and Waksman, G. Secretion systems in Gram-negative bacteria: structural and mechanistic insights. *Nature Reviews Microbiology* **13**, 343-359 (2015).
33. Green, E.R., and Mecsas, J. Bacterial secretion systems – an overview. *Microbiol. Spectr.* **4**, (2016).
34. Pukatzki, S., Ma, A.T., Sturtevant, D., Krastins, B., Sarracino, D., Nelson, W.C., Heidelberg, J.F. and Mekalanos, J.J. Identification of a conserved bacterial protein secretion system in *Vibrio cholerae* using the *Dictyostelium* host model system. *Proc. Natl. Acad. Sci.USA* **103**, 1528–1533 (2006).
35. Ho, B. T., Dong, T. G. and Mekalanos, J. J. A view to a kill: the bacterial type VI secretion system. *Cell Host Microbe* **15**, 9–21 (2014).

36. Russell, A. B., Peterson, S. B. and Mougous, J. D. Type VI secretion system effectors: poisons with a purpose. *Nat Rev Microbiol* **12**, 137–148 (2014).
37. Das, S. and Chaudhuri, K. Identification of a unique IAHP (IcmF associated homologous proteins) cluster in *Vibrio cholerae* and other proteobacteria through *in silico* analysis. *In Silico Biol.* **3**, 287–300 (2003).
38. Bingle, L. E., Bailey, C. M. and Pallen, M. J. Type VI secretion: a beginner's guide. *Curr Opin Microbiol* **11**, 3–8 (2008).
39. Boyer, F., Fichant, G., Berthod, J., Vandenbrouck, Y. and Attree, I. Dissecting the bacterial type VI secretion system by a genome wide *in silico* analysis: What can be learned from available microbial genomic resources? *BMC Genomics* **10**, 104 (2009).
40. Leiman, P. G., Basler, M., Ramagopal, U.A., Bonanno, J.B., Sauder, J.M., Pukatzki, S., Burley, S. K., Almo, S. C. and Mekalanos, J. J. Type VI secretion apparatus and phage tail-associated protein complexes share a common evolutionary origin. *Proc Natl Acad Sci USA.* **106**, 4154–9 (2009).
41. Basler, M. Type VI secretion system: secretion by a contractile nanomachine. *Philosophical Transactions of the Royal Society B: Biological Sciences* **370**, 20150021 (2015).
42. Taylor, N. M. I., van Raaij, M. J. and Leiman, P. G. Contractile injection systems of bacteriophages and related systems. *Mol Microbiol* **108**, 6–15 (2018).
43. Zoued, A. Brunet, Y.R., Durand, E., Aschtgen, M.S., Logger, L., Douzi, B., Journet, L., Cambillaud, C. and Cascales, E. Architecture and assembly of the type VI secretion system. *Biochim Biophys Acta* **1843**, 1664–1673 (2014).
44. Cianfanelli, F. R., Monlezun, L. and Coulthurst, S. J. Aim, load, fire: the type VI secretion system, a bacterial nanoweapon. *Trends in Microbiology* **24**, 51-62 (2016).
45. Durand, E., Cambillau, C., Cascales, E. and Journet, L. VgrG, Tae, Tle, and beyond: the versatile arsenal of type VI secretion effectors. *Trends Microbiol* **22**, 498–507 (2014).
46. Alcoforado Diniz, J., Liu, Y. C. and Coulthurst, S. J. Molecular weaponry: diverse effectors delivered by the type VI secretion system. *Cell Microbiol* **17**, 1742–1751 (2015).
47. Miyata, S. T., Bachmann, V. and Pukatzki, S. Type VI secretion system regulation as a consequence of evolutionary pressure. *J Med Microbiol* **62**, 663–676 (2013).
48. Church, S. R., Lux, T., Baker-Austin, C., Buddington, S. P. and Michell, S. L. *Vibrio vulnificus* type 6 secretion system 1 contains anti-bacterial properties. *PLoS One* **11**, e0165500 (2016).
49. Unterweger, D., Kitaoka, M., Miyata, S.T., Bachmann, V., Brooks, T.M., Moloney, J. *et al.* Constitutive type VI secretion system expression gives *Vibrio cholerae* intra- and interspecific competitive advantages. *PLoS One* **7**, e48320 (2012).
50. Bernardy, E. E., Turnsek, M. A., Wilson, S. K., Tarr, C. L. and Hammer, B. K. Diversity of Clinical and Environmental Isolates of *Vibrio cholerae* in Natural Transformation and Contact-Dependent Bacterial Killing Indicative of Type VI Secretion System Activity. *Appl. Environ. Microbiol.* **82**, 2833–2842 (2016).
51. Van der Henst, C. C., Vanhove, A.S., Drebes Dörr, N.C., Stutzmann, S., Stoudmann, C., Clerc, S. *et al.* Molecular insights into *Vibrio cholerae's* intra-amoebal host-pathogen interactions. *Nature Commun.* **9**, 3460 (2018).
52. Joshi, A. Kostiuk, B., Rogers, A., Teschler, J., Pukatzki, S., and Yildiz, F.H. Rules of Engagement: The Type VI Secretion System in *Vibrio cholerae*. *Trends in Microbiology* **25**, 267-279 (2017).
53. Redfield, R. J. *sxy-1*, a Haemophilus influenzae mutation causing greatly enhanced spontaneous competence. *J. Bacteriol.* **173**, 5612–5618 (1991).
54. Veening, J. W. and Blokesch, M. Interbacterial predation as a strategy for DNA acquisition in

naturally competent bacteria. *Nat. Rev. Microbiol.* **15**, 621–629 (2017).
55. Inuzuka, S., Nishimura, K., Kakizawa, H., Fujita, Y., Furuta, H., Matsumura, S., and Ikawa, Y. Mutational analysis of structural elements in a class-I cyclic di-GMP riboswitch to elucidate its regulatory mechanism. *J Biochem* **160**: 153-162 (2016).
56. Yildiz, F. H. and Schoolnik, G. K. Role of *rpoS* in stress survival and virulence of *Vibrio cholerae*. *J. Bacteriol.* **180**, 773–784 (1998).
57. Domman, D. Quilici, M.L., Dorman, M.J., Njamkepo, E., Mutreja, A., Mather, A.E. *et al.* Integrated view of *Vibrio cholerae* in the Americas. *Science* **358**, 789–793 (2017).
58. Heidelberg, J. F. Eisen, J.A., Nelson, W.C., Clayton, R.A., Gwinn, M.L., Dodson, R.J. *et al.* DNA sequence of both chromosomes of the cholera pathogen *Vibrio cholerae*. *Nature* **406**, 477–483 (2000).
59. Kühn, J. Finger, F., Bertuzzo, E., Borgeaud, S., Gatto, M., Rinaldo, A., and Blokesch, M. Glucose- but Not Rice-Based Oral Rehydration Therapy Enhances the Production of Virulence Determinants in the Human Pathogen *Vibrio cholerae*. *PLoS Negl. Trop. Dis.* **8**, e3347 (2014).
60. Metzger, L. C. and Blokesch, M. Regulation of competence-mediated horizontal gene transfer in the natural habitat of *Vibrio cholerae*. *Curr. Opin. Microbiol.* **30**, 1–7 (2016).
61. Seitz, P. and Blokesch, M. DNA-uptake machinery of naturally competent *Vibrio cholerae*. *Proc. Natl. Acad. Sci.USA* **110**, 17987–17992 (2013).
62. Seitz, P. and Blokesch, M. DNA Transport across the Outer and Inner Membranes of Naturally Transformable *Vibrio cholerae* Is Spatially but Not Temporally Coupled. *MBio* **5**, e01409-14 (2014).
63. Seitz, P. Pezeshgi Modarres, H., Borgeaud, S., Bulushev, R.D., Steinbock, L.J., Radenovic, A. *et al*. ComEA Is Essential for the Transfer of External DNA into the Periplasm in Naturally Transformable *Vibrio cholerae* Cells. *PLoS Genet.* **10**, e1004066 (2014).
64. Matthey, N. and Blokesch, M. The DNA-Uptake Process of Naturally Competent *Vibrio cholerae*. *Trends Microbiol.* **24**, 98–110 (2016).
65. Lo Scrudato, M. and Blokesch, M. A transcriptional regulator linking quorum sensing and chitin induction to render *Vibrio cholerae* naturally transformable. *Nucleic Acids Res.* **41**, 3644–3658 (2013).
66. Jaskólska, M., Stutzmann, S., Stoudmann, C. and Blokesch, M. QstR-dependent regulation of natural competence and type VI secretion in *Vibrio cholerae*. *Nucleic Acids Res.* **46**, 10619–10634 (2018).
67. Milton, D. L. Quorum sensing in vibrios: Complexity for diversification. *Int. J. Med. Microbiol.* **296**, 61–71 (2006).
68. Verma, S. C. and Miyashiro, T. Quorum sensing in the squid-*Vibrio* symbiosis. *Int. J. Mol. Sci.* **14**, 16386–16401 (2013).
69. Blokesch, M. and Schoolnik, G. K. The extracellular nuclease Dns and its role in natural transformation of *Vibrio cholerae*. *J. Bacteriol.* **190**, 7232–7240 (2008).
70. Suckow, G., Seitz, P. and Blokesch, M. Quorum sensing contributes to natural transformation of *Vibrio cholerae* in a species-specific manner. *J. Bacteriol.* **193**, 4914–4924 (2011).
71. Yang, Z., Zhou, X., Ma, Y., Zhou, M., Waldor, M.K., Zhang, Y., and Wang, Q. Serine/threonine kinase PpkA coordinates the interplay between T6SS2 activation and quorum sensing in the marine pathogen *Vibrio alginolyticus*. *Environ. Microbiol.* **20**, 903–919 (2018).
72. McCarter, L. L. Polar Flagellar Motility of the Vibrionaceae. *Microbiol. Mol. Biol. Rev.* **65**, 445–462 (2001).
73. Ishikawa, T., Rompikuntal, P. K., Lindmark, B., Milton, D. L. and Wai, S. N. Quorum sensing regulation of the two *hcp* alleles in *Vibrio cholerae* O1 strains. *PLoS One* **4**,e6734 (2009).
74. Jiang, N., Tang, L., Xie, R., Li, Z., Burkinshaw, B., Liang, X. *et al..Vibrio parahaemolyticus*

RhsP represents a widespread group of pro-effectors for type VI secretion systems. *Nat. Commun.* **9**, (2018).

75. Kimbrough, J. H. and Stabb, E. V. Antisocial *luxO* Mutants Provide a Stationary-Phase Survival Advantage in *Vibrio fischeri* ES114 . *J. Bacteriol.* **198**, 673–687 (2016).
76. Stutzmann, S. and Blokesch, M. Circulation of a quorum-sensing-impaired variant of *Vibrio cholerae* strain C6706 masks important phenotypes. *mSphere* **1**, e00098-16 (2016).
77. Kernell Burke, A. A., Guthrie, L.T., Modise, T., Cormier, G., Jensen, R.V., McCarter, L.L., and Stevens, A.M. OpaR controls a network of downstream transcription factors in *Vibrio parahaemolyticus* BB22OP. *PLoS One* **10**, e0121863 (2015).
78. Meibom, K. L., Li, X.B., Nielsen, A.T., Wu, C.Y., Roseman, S., and Schoolnik, G.K. The *Vibrio cholerae* chitin utilization program. *Proc. Natl. Acad. Sci. USA*. **101**, 2524–9 (2004).
79. Pursley, B. R., Maiden, M.M., Hsieh, M.L., Fernandez, N.L., Severin, G.B., and Waters, C.M. Cyclic di-GMP Regulates TfoY in *Vibrio cholerae* To Control Motility by both Transcriptional and Posttranscriptional Mechanisms . *J. Bacteriol.* **200**, e00578-17 (2018).
80. Yildiz, F. H., Dolganov, N. A. and Schoolnik, G. K. VpsR, a member of the response regulators of the two-component regulatory systems, is required for expression of *vps* biosynthesis genes and EPS(ETr)-associated phenotypes in *Vibrio cholerae* O1 El tor. *J. Bacteriol.* **183**, 1716–1726 (2001).
81. Livny, J., Zhou, X., Mandlik, A., Hubbard, T., Davis, B.M., and Waldor, M.K. Comparative RNA-Seq based dissection of the regulatory networks and environmental stimuli underlying *Vibrio parahaemolyticus* gene expression during infection. *Nucleic Acids Res.* **42**, 12212–12223 (2014).
82. Keyhani, N. O. and Roseman, S. Physiological aspects of chitin catabolism in marine bacteria. *Biochim. Biophys. Acta* **1473**, 108–122 (1999).
83. Yanisch-Perron, C., Vieira, J. and Messing, J. Improved M13 phage cloning vectors and host strains: nucleotide sequences of the M13mp18 and pUC19 vectors. *Gene* **33**, 103–119 (1993).
84. Simon, R., Priefer, U. and Pühler, A. A broad host range mobilization system for *in vivo* genetic engineering: Transposon mutagenesis in gram negative bacteria. *Biotechnology* 784–790 (1983).
85. Ferrières, L., Hemery, G., Nham, T., Guerout, A.M., Mazel, D., Beloin, C., and Ghigo, J.M. Silent mischief: Bacteriophage Mu insertions contaminate products of *Escherichia coli* random mutagenesis performed using suicidal transposon delivery plasmids mobilized by broad-host-range RP4 conjugative machinery. *J. Bacteriol.* **192**, 6418–6427 (2010).
86. Dunlap, P. V. Regulation of luminescence by cyclic AMP in cya-like and crp-like mutants of *Vibrio fischeri*. *J. Bacteriol.* **171**, 1199–1202 (1989).
87. Sambrook, J., Fritsch, E. F. and Maniatis, T. Molecular Cloning: A laboratory Manual. *Cold Spring Harb. NY. Cold Spring Harb. Lab. Press* (1982).
88. De Souza Silva, O. and Blokesch, M. Genetic manipulation of *Vibrio cholerae* by combining natural transformation with FLP recombination. *Plasmid* **64**, 186–195 (2010).
89. Blokesch, M. TransFLP - A Method to Genetically Modify *Vibrio cholerae* Based on Natural Transformation and FLP-recombination. *J. Vis. Exp.* e3761 doi:10.3791/3761 (2012).
90. Borgeaud, S. and Blokesch, M. Overexpression of the *tcp* Gene Cluster Using the T7 RNA Polymerase/Promoter System and Natural Transformation-Mediated Genetic Engineering of *Vibrio cholerae*. *PLoS One* **8**, 1–10 (2013).
91. Nielsen, A. T., Dolganov, N.A., Otto, G., Miller, M.C., Wu, C.Y., and Schoolnik, G.K. RpoS controls the *Vibrio cholerae* mucosal escape response. *PLoS Pathog.* **2**, 0933–0948 (2006).
92. Bao, Y., Lies, D. P., Fu, H. and Roberts, G. P. An improved Tn7-based system for the single-copy insertion of cloned genes into chromosomes of Gram-negative bacteria. *Gene* **109**, 167–

168 (1991).
93. Marvig, R. L. and Blokesch, M. Natural transformation of *Vibrio cholerae* as a tool - Optimizing the procedure. *BMC Microbiol.* **10**, 155 (2010).
94. Keene, O. N. The log transformation is special. *Stat. Med.* **14**, 811–819 (1995).
95. Wachsmuth, I. K., Evins, G.M., Fields, P.I., Olsvik, O., Popovic, T., Bopp, C.A. *et al*. The molecular epidemiology of cholera in Latin America. *J. Infect. Dis.* **167**, 621–626 (1993).
96. Miller, V. L., DiRita, V. J. and Mekalanos, J. J. Identification of *toxS*, a regulatory gene whose product enhances ToxR-mediated activation of the cholera toxin promoter. *J. Bacteriol.* **171**, 1288–1293 (1989).
97. Pearson, G. D., Woods, A., Chiang, S. L. and Mekalanos, J. J. CTX genetic element encodes a site-specific recombination system and an intestinal colonization factor. *Proc. Natl. Acad. Sci. USA*. **90**, 3750–4 (1993).
98. Gulig, P. A., Tucker, M. S., Thiaville, P. C., Joseph, J. L. and Brown, R. N. USER Friendly Cloning Coupled with Chitin-Based Natural Transformation Enables Rapid Mutagenesis of *Vibrio vulnificus*. *Appl. Environ. Microbiol.* **75**, 4936–4949 (2009).
99. Simpson, C. A., Podicheti, R., Rusch, D. B., Dalia, A. B. and van Kessel, J. C. Diversity in natural transformation frequencies and regulation across *Vibrio* species. *bioRxiv* (2019).
100. Chen, Y, Stine, O. C, Badger, J. H, Gil, A. I., Nair, G. B, Nishibuchi, M. and Fouts, D., E.. Comparative genomic analysis of *Vibrio parahaemolyticus* : serotype conversion and virulence. *BMC Genomics* **12**, 294 (2011).
101. Ben-Yaakov, R. and Salomon, D. The regulatory network of *Vibrio parahaemolyticus* type VI secretion system 1. *Environ. Microbiol.* doi:10.1111/1462–2920.14594 (2019).
102. Graf, J., Dunlap, P.V., and Ruby, E.G. Effect of transposon-induced motility mutations on colonization of the host light organ by *Vibrio fischeri*. *J Bacteriol* **176**: 6986-6991 (1994).
103 Frischer, M. E., Williams, H. G., Bennison, B., Drake, G. R., Balkwill, D. L. and Paul, J. H. The naturally transformable marine bacterium WJT-1C formally identified as "*Vibrio*" is a Pseudomonad. *Current Microbiology* **33** 287-291(1996)

3. NEIGHBOR PREDATION LINKED TO NATURAL COMPETENCE FOSTERS THE TRANSFER OF LARGE GENOMIC REGIONS IN *VIBRIO CHOLERAE*

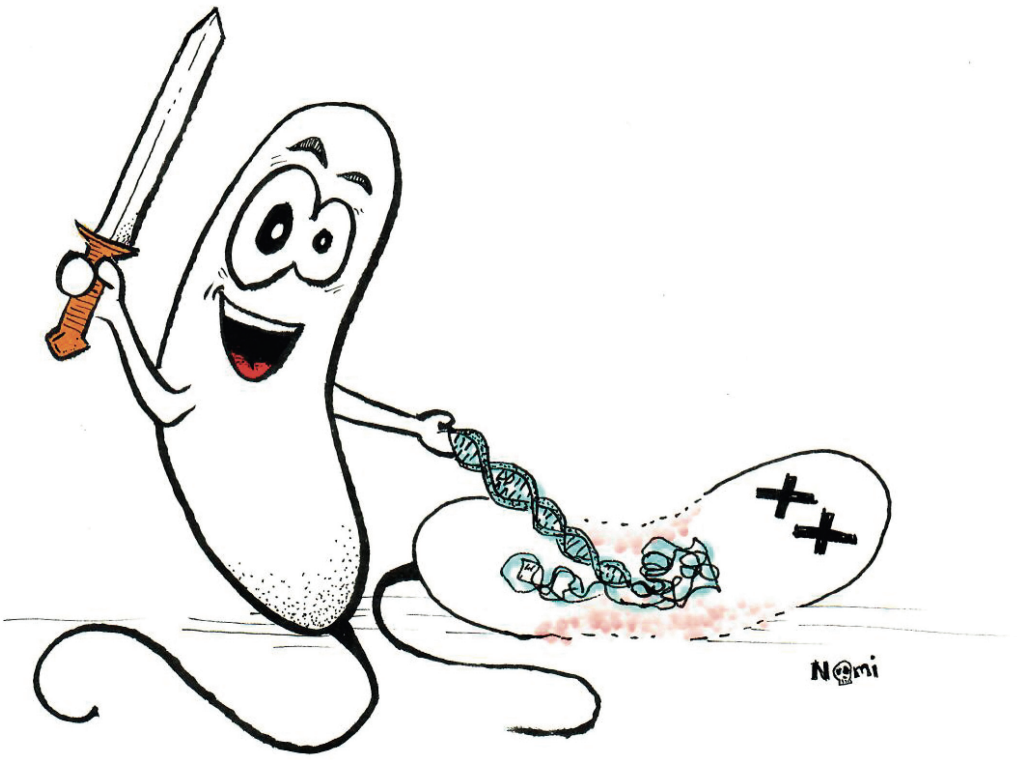

3.1 OVERVIEW: AIM AND SIGNIFICANCE

In this chapter, we provide novel insights into the benefit of the co-regulation of the T6SS and the DNA-uptake machinery using *V. cholerae* as a model organism. In the previous chapter, we highlighted that the TfoX-dependent induction of competence genes and the T6SS is conserved among diverse *Vibrio* species investigated. As the co-regulation of these two nanomachines fosters HGT in *V. cholerae* ([1]), we suggested that the TfoX-driven phenotypes might have an important impact on bacterial evolution in vibrios. In their study, Borgeaud and colleagues showed that, upon competence induction (e.g., on chitin surfaces or via *tfoX* induction), *V. cholerae* uses its T6SS to kill neighboring competitors and subsequently acquire their DNA. Consequently, *V. cholerae* acquires "fresh" and potentially intact DNA and does not rely on the acquisition of DNA present in the environment, which is often highly damaged and fragmented ([2,3]). Moreover, we suggested that the T6SS might lead to the release of large fragments of DNA or even intact chromosomes from targeted prey cells, which could be subsequently acquired by the competent attacker and, thus, could impact bacterial evolution. Therefore, in the study presented below, we aimed at gaining insight into the biological function of the TfoX regulon (e.g., DNA uptake and T6SS) by investigating whether the coordination of neighbor predation and DNA uptake can foster the transfer of large genomic regions.

Previous study from our group had determined that the transfer of a single selective marker is enhanced by interbacterial predation mediated by the T6SS ([1]). Our first aim of this study was therefore to gain insights on the potential impact of this killing device into the acquisition of large DNA fragments. For this purpose, we investigated the transfer of multiple genes in T6SS-positive and T6SS-negative *V. cholerae* strains (referred as acceptor). Briefly, we co-cultured on chitin the acceptor strains with non-kin prey strains (referred as donor) that carried two different antibiotic-resistance genes in their genome, and further scored the transfer of these markers into the acceptor strains. The prey strains carried the antibiotic resistance genes at variable distances from each other (from 50 kbp to >500 kbp) on the same chromosome (located *in cis*), or on two separate chromosomes (located *in trans*). The rationale for these different constructions were that the acquisition of the two selective markers located *in trans* required two events of DNA uptake, whereas in the former case, the resistance genes could be integrated through the recombination of a single long DNA fragment. Our results demonstrated that the T6SS-positive acceptor strain could efficiently

acquire both selective markers, while the transformation frequencies of the T6SS-negative strain, which acquired DNA from randomly lysed prey, were mostly below the detection limit. Moreover, we observed that the transformation frequencies scored for the acquisitions of the resistance genes located *in cis* were increased as compared with the location *in trans*, for which two homologous recombination events were required. This suggested that the markers located *in cis* could be acquired from a single uptake and integration event of a large DNA fragment, which exceeded 50 kbp.

At this point, it was still unclear what the extent of DNA integrated in the competent acceptor strain was after the T6SS-mediated bacterial predation. To properly address this question, we used a whole genome sequencing (WGS) approach in order to identify and quantify the horizontally acquired DNA regions. In a first step, we compared the sequenced genomes of the acceptor and donor strains ([4]) and we confirmed, due to the frequency of SNPs among conserved genes, that we will be able to properly identify the donor DNA that was horizontally transferred into the competent acceptor strain. Then, in order to select acceptor strains that had at least one gene integrated from the donor bacteria, we screened for the transfer of an antibiotic resistance gene carried on the genome of the donor strain. Based on a previous study, which suggested that the entire chromosome 2 could be mobilized between strains of *Vibrio cyclitrophicus* ([5]), we initially used donor strains that encoded the selective marker on the chromosome 2 in order to investigate the maximum size of DNA exchanges on this chromosome. However, we were intrigued to know whether large fragments could also be exchanged on chromosome 1, and, thus we also determined the extent of HGT events using donor strain that carried the selective marker on this chromosome. Our results demonstrated that, for both chromosomes, large DNA regions were exchanged in *V. cholerae* through T6SS-dependent bacterial predation. On average, acceptor strains had horizontally acquired 50-70 kbp, which represent approximately 50-70 genes. The maximum length of horizontally acquired DNA was also determined and was above 160 kbp. Moreover, our data suggested that the total length of transferred DNA could represent a single HGT event or could be the result of multiple HGT events, which occurred on both chromosomes. These results therefore support the notion that natural transformation could serve for DNA repair or bacterial evolution as large fragments of DNA were recombined into the genome.

We also demonstrated that, when competence was induced, large transfer of DNA occurred using purified genomic DNA (gDNA) as transforming material. However, the

generation of acceptor transformants with purified gDNA was strongly dependent on the timing (e.g., when gDNA was added). Notably, the acceptor strain was first cultured on chitin to induce competence before adding gDNA to ensure that the extracellular nuclease *dns* was repressed and thus, that the gDNA was not degraded ([6–8]). Indeed, we observed that no transformants were recovered when gDNA was added on chitin simultaneously with the acceptor strain at the beginning of the experiment. This result highlighted the importance of low nuclease activity to ensure successful uptake and integration of DNA. We concluded that the induction of the T6SS and the DNA-uptake machinery concomitantly with *dns* repression was required to allow efficient uptake of prey-released DNA.

The next question we addressed was whether the T6SS-dependent counter attacks of the donor strain could influence the pattern of transferred DNA. In the conditions initially investigated, the donor strains were T6SS-negative, which indicates that only the acceptor strain could kill the donor strain. In a condition with T6SS-positive acceptor and T6SS-positive donor strains, we expected to have lysis of both strains, as they would efficiently kill each other due to their non-compatible effector and immunity proteins. This suggests that DNA of kin and non-kin origin would be present in the environment, and hypothetically that the integration of kin DNA could remove or "repair" a DNA fragment from non-kin origin that was previously acquired. To test this hypothesis, we compared the extent of HGT events in conditions with T6SS-positive acceptor and either T6SS-positive or T6SS-negative donor strains. However we did not observe a significant difference between these conditions and potential experimental biases are discussed in the manuscript below.

We also investigated whether the large transfer of DNA observed were dependent on the T6SS-mediated DNA release. For this purpose we determined and compared the extent of HGT events in condition with or without any T6SS-dependent bacterial predation. Therefore, we used acceptor strains that were either T6SS-positive or T6SS-negative with a donor strain that was T6SS-negative. Our results demonstrated that rare transfer events occurred without predation and that these rare transfers led to shorter DNA exchanges. Overall, this study showed that the co-regulation of the T6SS and the DNA-uptake machinery during competence do not solely increase the transformability ([1]), but also leads to the transfer of large genomic regions. We therefore suggest that these two nanomachines drive bacterial evolution in *V. cholerae*.

NEIGHBOR PREDATION LINKED TO NATURAL COMPETENCE FOSTERS THE TRANSFER OF LARGE GENOMIC REGIONS IN *VIBRIO CHOLERAE*

This chapter is a pre-printed version of a submitted article as:

Noémie Matthey[1], Sandrine Stutzmann[1], Candice Stoudmann[1], Nicolas Guex[2], Christian Iseli[2] and Melanie Blokesch[1]*

[1]Laboratory of Molecular Microbiology, Global Health Institute, School of Life Sciences, Ecole Polytechnique Fédérale de Lausanne (Swiss Federal Institute of Technology Lausanne; EPFL), Lausanne, Switzerland; [2]Swiss Institute of Bioinformatics, Lausanne, Switzerland

* *Corresponding author:*
Melanie Blokesch, Station 19, EPFL-SV-UPBLO, Ecole Polytechnique Fédérale de Lausanne (EPFL), CH-1015 Lausanne, Switzerland; Phone: +41 21 693 0653; Email: melanie.blokesch@epfl.ch

Abbreviations: horizontal gene transfer – HGT; genomic DNA – gDNA; transforming DNA – tDNA; quorum-sensing – QS

Short title: DNA transfer among co-cultured *V. cholerae*

Keywords: DNA uptake, natural competence, transformation, type VI secretion

Contributions: Design of the experiment, wetlab data generation (including: strain constructions, natural transformation assay, and purification of genomic DNA), data analysis, and figure preparation.

3.2 ABSTRACT

Natural competence for transformation is a primary mode of horizontal gene transfer. Competent bacteria are able to absorb free DNA from their surroundings and exchange this DNA against pieces of their own genome when sufficiently homologous. However, the prevalence of non-degraded DNA with sufficient coding capacity is not well understood. In this context, we previously showed that naturally competent *Vibrio cholerae* use their type VI secretion system (T6SS) to actively acquire DNA from non-kin neighbors. Here, we explored the conditions of the DNA released through T6SS-mediated killing versus passive cell lysis and the extent of the transfers that occur due to these conditions. We show that competent *V. cholerae* acquire DNA fragments with a length exceeding 150 kbp in a T6SS-dependent manner. Collectively, our data support the notion that the environmental lifestyle of *V. cholerae* fosters the exchange of genetic material with sufficient coding capacity to significantly accelerate bacterial evolution.

3.3 IMPACT STATEMENT

Whole-genome sequencing reveals the remarkable extent of horizontally moving genetic material in naturally competent *Vibrio cholerae* after a prey-killing DNA acquisition process.

3.4 INTRODUCTION

The causative agent of the diarrheal disease cholera, *Vibrio cholerae*, is responsible for seven major pandemics since 1817, one of which is still ongoing. Due to its ability to rapidly spread in contaminated water, cholera poses a serious world health risk, affecting between 1 and 4 million people and causing 21,000–143,000 deaths per year, especially in poor or underdeveloped countries ([9]). Many disease-causing bacteria have developed mechanisms for rapidly evolving in response to environmental pressures, and these rapid changes are often responsible for the formation of new serogroups with pandemic potential. One way in which *V. cholerae* acquire new phenotypes is through horizontal gene transfer (HGT), which is the direct movement of DNA from one organism to another. A major mode of HGT is natural competence for transformation in which bacteria are able to absorb free DNA from their surroundings using their competence-induced DNA-uptake complex ([10–12]). When sufficient homology is present between the incoming DNA and the bacterial genome, the absorbed genetic material can be integrated into the genome via double homologous recombination at the expense of the initial DNA region. As an example of the significant power of this natural competence for gene uptake, we previously witnessed the gain of an ~40 kbp O139-antigen cluster at the expense of the original ~30 kbp O1-antigen cluster through natural transformation (followed by strong selective pressure exerted by antibiotics or phages; ([13])), which significantly changed the phenotypes of these bacteria. And while Griffith's experiment in 1928 unambiguously proved that transformation contributes to evolution and pathogen emergence, the general prevalence of non-degraded DNA with sufficient coding capacity has been questioned ([14]), drawing inquiries as to whether this mode of HGT could be responsible for the major changes causing pandemic strains to emerge.

The induction of competence in *V. cholerae* is tightly regulated (recently reviewed by ([15])). Briefly, upon growth on the (molted) chitin-rich exoskeletons of zooplankton ([16]), the most abundant polysaccharide in the aquatic environment and therefore an important carbon source for chitinolytic bacteria ([17]), the expression pattern of *V. cholerae* is altered ([18]) to render it naturally competent for genetic transformation ([19]). Initially, when chitin degradation products are sensed by *V. cholerae*, it produces the regulatory protein TfoX ([18–23]). This competence activator positively regulates the expression of the major DNA-uptake machinery in the cell ([12]), providing a direct connection between growth on chitin and competence activation. Apart from TfoX, natural competence and transformation also depend

on the master regulator of quorum sensing, HapR, in two ways: i) HapR acts as repressor of *dns*, which encodes an extracellular nuclease that inhibits transformation ([6]); and ii) HapR together with TfoX co-activates the transcription factor QstR, which further represses *dns* as well as activates several DNA-uptake genes ([7,8]).

While the chitin-induced DNA-uptake complex of *V. cholerae* is able to absorb DNA from the surrounding ([24–28]), environmental DNA is often heavily degraded and therefore short in size ([2,3]). In addition, free DNA is thought to originate from dead and therefore less fit bacteria, which renders the coding part of such genetic material non-favorable for naturally competent bacteria ([29]). In line with these arguments, we recently showed that *V. cholerae* does not solely rely on randomly released environmental DNA. Instead, it actively acquires "fresh" DNA from healthy, living bacteria through kin-discriminatory neighbor predation ([1]), which, conceptually, also occurs in other naturally competent bacteria ([30]). Neighbor predation in *V. cholerae* is accomplished by a contractile injection system known as the type VI secretion system (T6SS) that transports toxic effector proteins into prey ([31–34]). Intriguingly, the T6SS of pandemic *V. cholerae* is exquisitely co-regulated with its DNA-uptake machinery in a TfoX-, HapR-, and QstR-dependent manner when the bacterium grows on chitin ([1,8,35]), which increases the chances of the competent bacterium to take up freshly released DNA compared to free-floating "unfit" DNA. Notably, this coupling of competence and type VI secretion is also conserved in several non-cholera vibrios ([36]).

In the current study, we determined the extent of the absorbed and chromosomally-integrated prey-derived DNA. Previous studies had scored transformation events in other naturally competent Gram-negative bacteria such as *Haemophilus influenzae*, *Helicobacter pylori,* and *Neisseria meningitides* ([37–39]). These former studies, however, relied on the supplementation of large quantities of purified DNA (with up to 50 donor genome equivalents per cell ([38])) at the peak of the organism's competence program ([37]). Such an approach, however, neither recapitulates the natural onset of competence nor discloses the fate of the DNA that is released from dying cells. Thus, to address these points and to mimic natural settings, we determined the frequency and extent of DNA exchanges under chitin-dependent co-culture conditions of two non-clonal *V. cholerae* strains. We show that the DNA transfer frequency is significantly enhanced in T6SS-positive compared to T6SS-negative strains and that large genomic regions are transferred from the killed prey to the competent acceptor bacterium.

3.5 RESULTS AND DISCUSSION

The T6SS fosters horizontal co-transfer events encompassing two selective markers

To compare the absorption of T6SS-mediated prey-derived DNA as opposed to environmental DNA (released through, for example, random lysis), we first scored the transformability of T6SS-positive (wild-type [WT] predator) and T6SS-negative (acceptor) *V. cholerae* strains, which would allow us to directly measure the contribution of the T6SS on gene uptake. These two strains were co-cultured with non-kin prey (donor) bacteria that were all derived from the environmental isolate Sa5Y ([1,4,40,41]) and contained two antibiotic resistance genes in their genomes: 1) An *aph* cassette (Kan^R), which was integrated in the *vipA* gene on the small chromosome (chr 2); and 2) a *cat* cassette (Cm^R), which was inserted at variable distances from the *aph* cassette on the same chromosome or, alternatively, on the large chromosome (chr 1). As shown in Figure 3.1, the WT predator strain efficiently absorbed and integrated the prey-released resistance cassettes (*aph* or *cat*), while the transformation efficiency for the T6SS-defective acceptor strain was significantly reduced (by 97.8% and 99.2% for *aph* and *cat*, respectively) (Fig. 3.1A). Moreover, comparable frequencies were observed for both selective markers, suggesting that their acquisition does not significantly affect the strains' fitness under non-selective conditions. We tested whether these transfer events were indeed competence-mediated and not based on other modes of HGT using a strain with a competence-related DNA import deficiency in that it lacked the competence protein ComEA that reels external DNA into the periplasm ([26]). This *comEA*-minus strain was never transformed under these predator-prey co-culture conditions, confirming that the gene transfer did depend entirely on natural competence.

Next, we scored the frequencies of transformants that had adopted resistance against both antibiotics, which would show the possibility of two transformation events or the transfer of a large piece of DNA (indicated by the distance between the two genes on the same chromosome). These transformations occurred, as expected, at lower rates compared to single-resistant clones and were mostly below the limit of detection for the T6SS-minus acceptor strain (Fig. 3.1B). Interestingly, we observed a gradual decrease in the frequencies the further the two resistance genes were apart from each other on the same chromosome, while a sharp drop occurred in the number of recovered transformants when the two resistance genes were carried on the two separate prey chromosomes (Fig. 3.1B). While the latter scenario unambiguously requires at least two separate DNA-uptake events, the former,

in which the resistance markers are carried *in cis,* could reflect a mix between single and multiple DNA absorption and integration events. When purified genomic DNA was instead provided as the transforming material to simplify the experiment and provide measurable results for all conditions, the *in cis* double-resistance acquisition efficiencies reached a comparable range to the *in trans* efficiencies when the two resistance genes were separated by at least 100 kbp. This suggested that the more efficient transformations of less than 100 kbp likely often occurred through a single acquisition (Fig. 3.1C). Furthermore, the WT predator and T6SS-minus acceptor behaved similarly when purified DNA was provided, which makes sense as the need for active DNA release through neighbor predation was eliminated. Based on these data and the fact that the double-acquisition rates for the T6SS-minus acceptor strain were mostly below the detection limit in the prey scenario, we hypothesized that neighbor predation might foster the transfer of long DNA stretches, which frequently exceeded 50 kbp and therefore carry significant coding capacity.

Comparative genomics of pandemic strain A1552 and environmental isolate Sa5Y

To test our hypothesis that the T6SS contributes to the horizontal transfer of large DNA fragments, we used a whole-genome sequencing (WGS) approach to properly outline the transferred DNA regions. To do this using WGS, we first needed to characterize the genomes of both the predator/acceptor (A1552) and the prey/donor (Sa5Y) strains for which long-read PacBio sequencing data and *de novo* assemblies without further analysis were recently announced ([4]). A1552 is a pandemic O1 El Tor strain ([42]) belonging to the LAT-1 sublineage of the West-African South American (WASA) lineage of seventh pandemic *V. cholerae* strains ([43]) while strain Sa5Y was isolated from the Californian Coast ([40,41]). To understand their genomic arrangements, we also compared these strains to the reference sequence of *V. cholerae* (O1 El Tor strain N16961; ([44])) and a re-sequenced laboratory stock of the latter. Details on the comparative genomics between the three pandemic strains (N16961 ([44]), the newly sequenced and *de novo*-assembled genome sequence of the laboratory stock of N16961, and A1552) are provided in Material and Methods section and as supplementary figures 3.1 and 3.2. We expected to see significant differences in the pandemic A1552 strain compared to the environmental isolate Sa5Y in terms of the absence/presence of genomic features and single nucleotide polymorphisms (SNPs) in core genes that would allow us to measure HGT events occurring between the strains, and several of these major differences are highlighted here. Indeed, as expected from its non-clinical origin, the environmental

isolate lacked several genomic regions, including those that encode major virulence features, namely *Vibrio* pathogenicity islands 1 and 2 (VPI-1, VPI-2), *Vibrio* seventh pandemic islands I and II (VSP-I, VSP-II; ([45])), the cholera toxin prophage CTX ([46]), and the WASA-1 element. In addition, the strain's O-antigen cluster differed significantly from the O1-encoding genes of pandemic strain A1552 (Fig. 3.2). The region that differed the most between both strains was the integron island, which is consistent with the role of this assembly platform in fostering the incorporation of exogenous open reading frames ([47]). Given these major differences between strain A1552 and Sa5Y and, in addition, an overall SNP frequency of approximately 1 in 55 nucleotides for conserved genes, we concluded that HGT events occurring between these two strains on chitinous surfaces could be precisely scored using short-read sequencing. Apart from this important genomic information, we also noted that the pandemic strains as well as Sa5Y contained previously unrecognized rRNA operons, with nine or ten rRNA clusters in total compared to the initially reported eight ([44]).

Released DNA from T6SS-killed prey leads to the transfer of large genomic regions

As our previous study witnessed gene transfers between *V. cholerae* bacteria ([13]) though neither scored the full extent of the transferred DNA region nor took T6SS-mediated neighbor predation into consideration, we sought to next determine how much genetic material would be absorbed and integrated by competent *V. cholerae* upon neighbor predation. To do this, we co-cultured the predator (A1552) and prey (Sa5Y) strains on chitinous surfaces for 30 h without any deliberate selection pressure. To be able to afterwards screen for the transfer of at least one gene, we first integrated an *aph* cassette within the *vipA* of strain Sa5Y, which concomitantly deactivated the prey's T6SS, to select kanamycin-resistant transformants of strain A1552. Using this system, resistant transformants of A1552 were selected at an average frequency of 1.8×10^{-4} after the 30 h co-culturing on chitin (supplementary figure 3.3), and 20 of those transformants were randomly picked for further analysis. After three independent experiments, the whole genome of each of the 60 transformants was sequenced, and the reads were mapped to either the predator's or the prey's genome sequence (see material and method section for detailed bioinformatic analysis). As shown in Figure 3.3, apart from the common acquisition of the *aph* resistance cassette, the location and the size of the prey-donated genomic region differed significantly between most transformants. Previous estimates of the average length of total acquired DNA were made in experiments using purified donor gDNA and were considered to be ~23 kbp

([41]). Importantly, we observed in these new experiments that the average length of the total acquired DNA, meaning the DNA surrounding the *aph* cassette plus any transferred regions elsewhere on either of the two chromosomes (supplementary figure 3.4), was almost 70 kbp and therefore significantly larger than the previous estimates. Around 15% of all transformants acquired and integrated more than 100 kbp (Fig. 3.3B), which was previously considered unlikely due to absence of such long DNA fragments in the environment. Consistent with the principle of natural transformation, it should be noted that the new DNA was acquired through double homologous recombination such that it replaced the initial DNA region and the overall genome size did not significantly change. Further analysis indicated that about 50% of the strains experienced a single HGT event around the *aph* cassette, while the others exchanged regions in up to eight different locations on the two chromosomes (Fig. 3.3C). Finally, we analyzed the length of continuous DNA stretches that were acquired from the prey and observed that those ranged from a few kbp up to 168 kbp (Fig. 3.3D). Collectively, these data indicate that *V. cholerae* can acquire large genomic regions from killed neighbors with an average exchange of more than 50 kbp or ~50 genes. This finding contradicts the notion that natural transformation cannot serve for DNA repair or acquisition of new genetic information due to the insufficient length and coding capacity of the acquired genetic material.

Transformation by purified DNA only occurs if correctly timed

To better understand the DNA acquisition and integration potential of naturally competent *V. cholerae*, we next compared the data described above, which we refer to from now on as condition ① using experiments varying the aspects of neighbor predation and DNA supplementation (Fig. 3.4A). First, the acceptor strain was grown in a monoculture immediately supplemented with purified genomic DNA (gDNA) derived from the same donor (prey) strain as described above. Notably, when the gDNA was added at the start of the chitin-dependent culture, no transformants were reproducibly detected from three independent biological experiments, suggesting that free DNA is rapidly degraded under such conditions. This finding is consistent with our previous work in which we demonstrated that *V. cholerae* produces an extracellular and periplasmic nuclease Dns ([6,25]) that degrades transforming material. At high cell density (HCD), where competence is induced, *dns* is partially repressed through direct binding of HapR ([6,7]), and this repression is reinforced by the transcription factor QstR ([7,8]). We therefore concluded that the simultaneous expression

of both machineries, concomitantly with a strong repression of *dns*, is a prerequisite for successful DNA transfer. Indeed, such coordinated expression would ensure that T6SS-mediated attacks are exquisitely timed with low nuclease activity so that the prey-released DNA can be efficiently absorbed.

As we previously showed that the addition of purified gDNA after ~20–24 h of growth on chitin wasn't prone to degradation by Dns ([48]), we next choose this time point to probe the DNA acquisition capability using purified DNA (condition ②; Fig. 3.4A). Doing so led to similar transformation frequencies as those observed for the prey-released DNA caused by T6SS attacks (condition ①; supplementary figure 3.3A). WGS of 20 transformants from two biologically independent experiments likewise resulted in similar DNA acquisition patterns with average and maximum DNA acquisitions of 70 kbp and 188 kbp, respectively, and the presence of multiple exchanged regions of varying sizes (Fig. 3.4 and supplementary figure 3.5). While we cannot entirely exclude that the maximum length of individual DNA stretches was biased by the purification step, despite the fact that we chose a method that was designed for chromosomal DNA isolation of 20–150 kbp sized fragments (see methods), our results suggest that the maximum DNA acquisition length of single fragments is probably reached between 100–110 kbp (supplementary figure 3.5). Moreover, the comparable acquisition patterns between conditions ① and ② (Fig. 3.4) imply that the prey-released DNA in condition ① is neither heavily fragmented nor is its accessibility or absorption by the competent acceptor bacterium significantly hindered due to, for example, DNA-binding proteins.

Prey-exerted T6SS counter attacks do not change the DNA transfer pattern

Since the *aph* cassette was located within the T6SS sheath protein gene *vipA* in the above experiments, we wondered if this T6SS inactivation biased the DNA transfer efficiency. We therefore repeated the above-described experiments using prey strains that carried the *aph* cassette on the opposite site of chr 2 (within gene VCA0747; condition ③). As shown in supplementary figure 3.3, similar transformation frequencies were observed independent of the position of the *aph* cassette. Moreover, WGS of 2 x 20 transformants showed similar average and maximum DNA acquisition values (55.7 kbp and 227.4 kbp, respectively; Fig. 3.4) as well as similar distribution patterns around the resistance marker (supplementary figure 3.6). However, while not statistically supported, it appeared as if these conditions were prone to the acquisition of multiple non-connected regions, as transformants with only

single/connected exchanges dropped from ~50% (supplementary figure 3.4 for condition ①) to around 20% (supplementary figure 3.6 for condition ③). Based on this observation, we hypothesized that the now-restored T6SS-mediated killing capacity of the prey led to the additional release of genomic DNA from the predator, which interfered with the uptake of prey-released DNA. To test this idea, we repeated condition ③ (e.g., *aph* within VCA0747) though again inactivated the T6SS of the prey using a non-selected marker (*cat*; condition ④), expecting the results to be similar to those of condition ① if this hypothesis was correct. No statistically significant differences were observed between both conditions (③ and ④) for all tested characteristics including transformation frequency (supplementary figure 3.3B), number of exchanges, and separate and collective length (Fig. 3.4 and supplementary figures 3.6 and 3.7), suggesting that predator-released DNA does not interfere with the predator's overall transformability by the prey-released DNA. However, we acknowledge that the technical limitations of the experimental setup did not allow the identification of complete revertants that first acquired and then again lost the *aph* cassette.

T6SS-independent prey lysis rarely triggers DNA transfer and results in shorter DNA exchanges

We next tested whether T6SS-mediated DNA release impacted the length of the exchanged region, which would support the above speculation that the intimate co-regulation of type VI secretion, nuclease repression, and DNA uptake ensures that freshly released DNA is rapidly absorbed by the predator and is therefore less prone to fragmentation. Such co-regulation would not hold true for T6SS-independent DNA release as a result of random cell lysis, so we tested the transfer efficiency of the *aph* cassette under conditions in which both donor and acceptor strains were T6SS-defective (condition ⑤; Fig. 3.4 and supplementary figure 3.8). Under such conditions, the transformation frequency dropped by 99.7% (supplementary figure 3.3B), and WGS of 2 x 20 of these rare transformants showed significant differences. Indeed, the average and maximal length of acquired DNA (Fig. 3.4A) and the number of exchanged regions (Fig. 3.4B) were significantly different when T6SS+ versus T6SS- acceptor strains were compared, with the latter exchanges never exceeding four events compared to up to 13 events for T6SS-mediated DNA release (supplementary figures 3.7 and 3.8). Based on these data, we conclude that T6SS-mediated DNA acquisition not only increases the transfer efficiency by ~100-fold but also fosters the exchange of multiple DNA stretches of extended lengths.

T6SS-mediated DNA exchanges are not limited to the small chromosome

The experiments described above were designed to primarily score the transfer efficiency of DNA fragments localized on chr 2. The rationale behind this approach was a recent population genomic study on *Vibrio cyclitrophicus* that suggested the mobilization of the entire chr 2 and caused the authors to speculate: "how often and by what mechanism are entire chromosomes mobilized?" ([49]). In the current study, we were unable to experimentally show such large transfer events. We considered four potential reasons for the absence of such large transfers: 1) mild fragmentation of prey-released DNA that excluded fragments above ~200 kb; 2) limited DNA uptake and periplasmic storage capacity of the acceptor strain ([25,26]); 3) limited protection of the incoming single-stranded DNA by dedicated proteins (such as Ssb and DprA; ([50,51])); or 4) lethality of larger exchanges due to the presence of multiple toxin/antitoxin modules within the integron island on chr 2 of *V. cholerae* ([52]). While technical limitations did not allow us to address the first three points, we followed up on the last idea by repeating the above-described experiments using prey strains in which the *aph* cassette was integrated on the large chromosome 1 (inside *lacZ*). We used these to test three (co-)culture conditions in which the prey strain was either T6SS-positive (condition ⑥), T6SS-negative (condition ⑦), or replaced by purified gDNA (condition ⑧; Fig. 3.4A). As shown in supplementary figure 3.3, the *aph* cassette was again transferred with high efficiency from the killed prey strain to the acceptor strain. However, comparing conditions ⑥ (co-culture conditions) and ⑧ (prey-derived purified gDNA as transforming material) revealed a small but significant transformation increase (~ 4-fold; supplementary figure 3.3A). Based on these data, we speculate that the larger size of chr 1 (~3 Mb) compared to chr 2 (~1 Mb) slightly lowers the probability of acquiring the *aph* cassette when released from killed prey. This effect becomes negligible when purified gDNA is provided, most likely due to the size constraints of the purification procedure (max. 150 kb). Consistent with this idea was the finding that purified gDNA from all those prey strains described in this study resulted in the same level of transformation no matter where the selective marker was located (supplementary figure 3.3D).

Next, we randomly picked 20 transformants from two biologically independent experiments for each of these three experimental conditions (⑥ to ⑧) and sequenced their genomes (supplementary figures 3.9 to 3.11). The analysis of these transformants showed that the average and maximum DNA acquisition values were highly comparable to those described above for DNA exchanges on chr 2 (Fig. 3.4A) and that multiple exchanged

regions were likewise observed (Fig. 3.4B). We therefore conclude that prey-derived transforming DNA can equally modify both chromosomes. Moreover, our data suggest that consecutive stretches of exchanged DNA above ~200 kbp either do not occur or occur at levels below the detection limit of this study, and that this size limitation is not caused by the toxin/antitoxin–module-containing integron island on chr 2.

3.6 CONCLUSION

Based on the data presented above, we conclude that T6SS-mediated predation followed by DNA uptake leads to the exchange of large DNA regions that can bring about bacterial evolution. This finding is consistent with the heterogeneous environmental *V. cholerae* populations that were observed in cholera-endemic areas ([53]). Still, an open question that remains is why pandemic cholera isolates are seemingly clonal in nature ([43,54–56]), and we propose two explanations for this. First, sampling strategies might be biased for the selection of the most pathogenic strains and, concomitantly, exclude less virulent variants that have undergone HGT events. Secondly, transformation-inhibiting nucleases similar to Dns ([6]) have recently spread throughout pandemic *V. cholerae* isolates as part of mobile genetic elements (experimentally shown for VchInd5 ([57]) and predicted for SXT ([58])), which makes these pandemic strains less likely to undergo HGT events. One could also argue that pandemic *V. cholerae* are rarely exposed to competence-inducing chitinous surfaces due to the prevalence of inter-household transmission throughout cholera outbreaks ([59]). Yet *in vivo*-induced antigen technology (IVIAT) assays showed strong human immune responses against proteins of the DNA-uptake pilus that fosters natural transformation, kin recognition, and chitin colonization ([18,19,24,28]), which contradicts this idea. Indeed, the major pilin PilA was most frequently identified by IVIAT together with the outer-membrane secretin PilQ ([60]), which suggests that the bacteria encounter competence-inducing conditions either before entering the human host or after its colonization. The latter option is not, however, supported by *in vivo* expression data from human volunteers ([61]). Notably, our work shows the incredible DNA exchange potential that chitin-induced *V. cholerae* strains exert under co-culture conditions and future studies are therefore required to better understand strain diversity in clinical and environmental settings in the absence of sampling biases.

3.7 MATERIALS AND METHODS

Bacterial strains, plasmids, and growth conditions

The bacterial strains and plasmids used in this study are described in supplementary file 3.1. Bacteria were routinely grown aerobically in lysogeny broth (LB) or on LB agar plates (1.5% agar) at 30°C or 37°C. Half-concentrated defined artificial seawater medium (0.5x DASW) containing HEPES and vitamins ([19]) was used for growth on chitinous surfaces for chitin-induced T6SS killing and natural transformation experiments (as previously described; ([1,48])). Agar plates containing M9 minimal medium (Sigma-Aldrich) supplemented with vitamins (MEM vitamin solution; Gibco), 0.001% casamino acids (Merck), and 0.2% mannose were used to select *V. cholerae* strain A1552 and to exclude strain Sa5Y (to check the direction of transformation for *comEC*-positive prey). Thiosulfate-citrate-bile salts-sucrose (TCBS; Sigma-Aldrich) agar plates were used to counterselect *E. coli* strains after mating with *V. cholerae*. Antibiotics were used at the following concentrations whenever required: chloramphenicol (Cm), 2.5 μg/ml; kanamycin (Kan), 75 μg/ml; streptomycin (Strep), 100 μg/ml; ampicillin (Amp), 100 μg/ml; and rifampicin (Rif), 100 μg/ml.

DNA manipulation techniques

Recombinant DNA techniques were performed following standard molecular–biology-based protocols ([62]). DNA-modifying enzymes such as Pwo DNA polymerase (Roche), Taq DNA polymerase (GoTaq; Promega), and restriction modification enzymes (New England Biolabs) were used according to the manufacturer's recommendations. Genetically modified strains were verified by colony PCR and, if required, also by Sanger sequencing (Microsynth, Switzerland) for their correctness.

Genetic engineering of bacterial strains

To delete gene(s) from the parental WT strains (A1552 or Sa5Y), a gene-disruption method based on either a counter-selectable suicide plasmid pGP704-Sac28 ([18]) or on natural transformation and FLP recombination was used (TransFLP method; ([63–65])). Natural transformation was also used to insert the antibiotic resistance cassettes *aph* (Kan^R), *cat* (Cm^R), and/or *bla* (Amp^R) into target gene(s) of *V. cholerae*.

Preparation of genomic DNA

Genomic DNA (gDNA) was purified from a 2 ml culture of the respective strain. DNA extraction was performed using 100/G Genomic-tips together with a Genomic DNA buffer set as described in the manufacturer's instructions (Qiagen). After precipitation, the DNA samples were transferred into Tris buffer (10 mM Tris-HCl, pH 8.0). This was preferred over rapid gDNA isolation kits such as the DNeasy Blood & Tissue kit (Qiagen), as the latter isolation kit is strongly biased towards shorter DNA fragments (predominantly 30kb in length compared to up to 150kb for the 100/G columns, as stated by the manufacturer).

Natural transformation assay

Natural transformation assays were performed by adding purified gDNA to the chitin-grown bacteria or by co-culturing the two non-clonal *V. cholerae* strains. To set up the experiments, the bacterial strains were grown as an overnight culture in LB medium at 30°C. After back dilution, the cells were incubated in the presence of chitin flakes (~80 mg; Sigma-Aldrich) submerged in half-concentrated (0.5x) defined artificial seawater medium ([19]). When purified DNA served as the transforming material, 2 μg of the indicated gDNA was added after 24 h of growth on chitin, and the cells were incubated for another 6 hours. At that point, the bacteria were detached from the chitin surfaces by vigorous vortexing and then were serially diluted. Colony-forming units (CFUs) were enumerated on selective (antibiotic-containing) or non-selective (plain LB) agar plates, and the transformation frequency was calculated by dividing the number of transformants by the total number of CFUs. For mixed community assays, the two strains were inoculated simultaneously at a ratio of 1:1. These mixtures were incubated for 30 h before the bacteria were harvested, diluted, and plated, as described above. All transformation frequency values are averages of three biologically independent experiments except for WGS conditions ② and ④–⑧, wherein the averages of two independent experiments are depicted.

Genome comparisons

Each chromosome was segmented in contiguous fragments of 10 kb, which were locally aligned against the corresponding chromosome of a reference genome. Each fragment was aligned in the forward and reverse orientation, and the best alignment was retained. The number of differences per 10 kb was evaluated by counting the number of events necessary to mutate the reference to obtain the 10 kb fragment (e.g. an insertion or deletion of an arbitrary

number of nucleotides would count as one event). To visualize the overall architecture and differences, circular plots in which each 10 kb fragment was linked to its reference genome counterpart and colored according to the number of differences were made in R using the circlize package ([66]). Black and blue linkers indicated whether the 10 kb fragment had the same or reverse orientation relative to the reference.

As a recent study identified a large inversion close to the origin of replication of chr 1 in the original genome sequence of N16961 ([67]), which most likely resulted from an imperfect assembly or a lab domestication event, we sequenced and *de novo* assembled the genome of our laboratory stock of strain N16961 ([4]). This stock is resistant to streptomycin, which is consistent with most literature reports on strain N16961, while the original reference strain N16961 remained sensitive to streptomycin according to its genome sequence. This difference suggests that mutagenesis event(s), including the characteristic streptomycin-resistance mutation within *rpsL* (encoding for RpsL[K43R]) must have occurred while the strain was domesticated. Comparative genomics between our laboratory stock of N16961 and the reference genome ([44]) showed a high level of sequence identity, though also confirmed the previously reported inversion around the origin of chromosome 1 ([67]) (supplementary figure 3.1). Additionally, significant differences were observed between the two N16961 genome sequences with respect to the number and arrangement of the ribosomal RNA clusters, which could have resulted from assembly artifacts. Indeed, while Heidelberg and colleagues described the presence of eight rRNA operons (16S-23S-5S) ([44]), we found ten rRNA operons (plus an additional 5S copy close to the tRNA-Thr). The only other major differences observed between the strains were in genes VC1620 and *vasX* (VCA0020) on chromosome 1 and 2, respectively, as also mentioned in the main text (supplementary figure 3.1; marked with * and #). VC1620, or *frhA,* on chr 1 encodes a large protein with several cadherin tandem repeat domains, the number of which vary among different *V. cholerae* strains ([68]). Due to the repetitive nature of this DNA region, an assembly mistake in either of the two genome assemblies can therefore not be excluded. The sequence of the newly sequenced stock of N16961 was identical to the region in pandemic strain A1552 (supplementary figure 3.2). For the discrepancy within *vasX* on chr 2, we observed a significant number of single nucleotide polymorphisms (SNPs; n = 11) or nucleotide insertions (n = 14) within this 3,272-bp-long gene. One of these nucleotide insertions caused a frameshift that therefore resulted in a premature stop codon. As BLAST analyses suggested that this change was strain specific and not previously observed, we Sanger sequenced the

corresponding DNA region using the same genomic DNA preparation that was used for the long-read PacBio sequencing, which allowed us to elucidate whether the mutations reflected a lab domestication event or whether the PacBio sequence was of low quality in this specific area of the genome. The latter turned out to be the case, as the mutations described above were absent from the Sanger sequencing reads. We therefore conclude that the two genomes are highly identical and that the major differences involve imperfect rRNA cluster assembly in the reference genome, which resulted in the underestimation of the number of rRNA clusters and the inverted assembly around the origin of replication of chr 1.

V. cholerae O1 El Tor (Inaba) strain A1552 (formerly known as 92A1552-Rif^r) is a rifampicin-resistant derivative of strain 92A1552 ([42]), which was isolated in California from a traveller returning from South America. Epidemiological investigations concluded that the transmission of this strain occurred via a contaminated seafood salad that was served on an airplane between Lima, Peru and Los Angeles, California ([69,70]), which links this strain to the Peruvian cholera outbreak in the 1990s.

Comparing the *de novo* assembled genome sequence of A1552 ([4]) to the genome of our laboratory stock of N16961 showed a large degree of genomic conservation between both isolates despite the fact that strain A1552 contained only nine rRNA operons (16S-23S-5S) instead of the ten operons in strain N16961. The genome architecture, however, was not maintained, as strain A1552 had undergone a large inversion of approximately 2.7 Mbp between two rRNA clusters on chr 1 (supplementary figure 3.2; genome sequence inverted to simplify visualization), a finding that is consistent with a previous report ([71]). Apart from this inversion, the major differences between both strains were the presence of the WASA-1 island (a 44-gene-carrying element of unknown function; ([54])) and a modified *Vibrio* seventh pandemic island II (VSP-II) in strain A1552 (supplementary figure 3.2). These features allowed us to classify strain A1552 as belonging to the LAT-1 sublineage of the West-African South American (WASA) lineage of the seventh pandemic *V. cholerae* strains ([43,54]).

Whole-genome sequencing of transformants

For WGS, transformation assays were performed as described above using eight different experimental conditions (Fig. 3.4 and listed in supplementary file 3.2). To focus on the acquisition potential of strain A1552, conditions ⑤–⑧ used transformation-deficient prey strains (e.g., Sa5Y derivatives in which a *bla* cassette interrupted the DNA translocation channel protein encoding gene *comEC* ([24])). The 360 recovered transformants (3 x 20 for

experimental conditions ① and ③, which showed high levels of reproducibly, followed by 2 x 20 for all other conditions; see supplementary file 3.2) were grown overnight in LB medium. Genomic DNA extraction was performed as described above. Further processing of the samples was conducted by Microsynth (Balgach, Switzerland). The quality of the DNA samples was verified before DNA libraries were prepared using a Nextera XT Library Prep kit (Illumina). Paired-end sequencing was performed using a NextSeq 500 sequencer (Illumina) with read lengths of 75 nt resulting in mean fragment lengths of around 200 nucleotides.

Scoring of horizontal gene transfer events through bioinformatics analyses

HGT events were scored for the 360 transformants that were derived from the eight different experimental conditions (Fig. 3.4 and listed in supplementary file 3.2). For each condition, a predator/acceptor strain (A1552 or its derivative) and a prey/donor strain (derivatives of Sa5Y; used in mixed cultures or as purified gDNA) were defined, and their genomic sequences were generated *in silico*. These *in silico* templates were based on the recently announced genome sequences of the parental strains ([4]) to which the integrated genomic features were added (e.g., integration of *aph*, *cat*, and/or *bla* cassettes proceeded by constitutive promoters). Each DNA template contained two parts reflecting the large ~3.0 Mbp chr 1 and the small ~1.1 Mbp chr 2. Preliminary analyses identified the presence of systematic differences in each sample, which can be attributed to errors in the reference templates. Thus, before starting the final analysis process, the following patches were applied to the chr 2 of the predator/acceptor reference genomes:

- Coordinate (in reference genome CP028895): 445515–445520 => TTTTTT replaced by TTTTT.
- Coordinate (in reference genome CP028895): 447288–447289 => GC replaced by G.
- Coordinate (in reference genome CP028895): 467939–467940 => AT replaced by A (resulting in a replacement of TTTTTTT [467940–467946] by TTTTTT).

The correctness of these *in silico* changes was confirmed by Sanger sequencing.

The FASTA sequences of the corrected reference templates used for this work are available in the Reference directory on GitHub: https://github.com/sib-swiss/VibrioCholerae_HGT.

Each read pair was aligned against both genomes of the donor and acceptor strains, and the position with the least number of mismatches was kept. If multiple possibilities with the

same number of mismatches were possible, the possibilities were kept for later processing. The alignments were performed with an in-house code derived from the fetchGWI tool [https://sourceforge.net/projects/tagger/files/fetchGWI-tagger/], but other tools such as BWA or bowtie2 would equally qualify for the same purpose. The results of this first analysis phase were obtained as tab-delimited lists of read pairs with their alignment positions, number of mismatches for each of the reads of the pair, and number of matching positions with the same number of mismatches.

The second step of the analysis consisted of a C program that parsed the tab-delimited file of the previous step and recorded the accumulated coverage and the observed nucleotide for each position of each of the donors' and acceptors' chromosomes. For each analysis, two separate recordings were kept: the first recording took only those read pairs into account that showed zero mismatches together with a unique unambiguous matching position, while the second recording took all other matches into account (e.g., a coverage of 1 was counted in each matched position regardless of whether the match was unique or not). At the end of this process, regions with continuous coverage were created by looking for positions in the first recording (unique and exact matches) for which the observed coverage was at least 3. The start and end positions of such continuous stretches were determined by extending as far as possible from this seed position, taking into account the total coverage from both recordings. If the length of the so-defined fragment was at least 500 nucleotides it was kept for output. The output consisted of a FASTA file containing all the defined fragments and the FASTA header of each fragment. This header recorded which reference was covered (e.g., which strain [acceptor or donor] and which chromosome [large chr 1 or small chr 2]). For each position, the nucleotide that composed more than half of the coverage of that position was generated in the output. If no single nucleotide represented more than half of the coverage, an N was used.

The expectation was that the fragments obtained in the previous step constituted a full coverage of the transformant, which had inherited its genomic material mostly from the parental acceptor strain with some DNA regions originating from the donor strain by HGT; this referred particularly to those regions containing the antibiotic resistance cassette, which was used as selective marker. A global DNA alignment for each output fragment was therefore performed by mapping the fragments onto the corresponding chromosomes of the donor and acceptor strains. Since we determined that the donor and acceptor genomes differed on average by 1 nucleotide every 55 nucleotides, it was expected that several

mismatches would be found when a fragment originating from the donor strain was aligned to the genome of the acceptor strain. The first and last mismatches of those fragments were defined as outer bounds of the transferred fragments, as they arguably represented the minimal length of the transferred DNA region. The summary data of these alignments and boundary information were determined using Perl scripts as were those regions of the acceptor genomes that were not covered by reads derived from the analyzed transformant (e.g., transformed acceptor strain). The output of those scripts (available on GitHub: https://github.com/sib-swiss/VibrioCholerae_HGT) was then used to generate a final table of transferred segments as well as summary plots by applying the R package circlize ([66]). Finally, the data were transferred to Excel to calculate the total length of horizontally acquired DNA per transformant as well as the number of HGT events per transformant. The GraphPad Prism software was used for graphic visualization. To validate the bioinformatic approach, the mapped reads obtained for >50 samples were also visually inspected for transferred regions using the software Geneious®.

Statistics

Statistically significant differences were determined by the two-tailed Student's *t*-test where indicated. For natural transformation assays, data were log-transformed ([72]) before statistical testing. When the number of transformants was below the detection limit, the value was set to the detection limit to allow for statistical analysis.

Data availability

WGS reads of the 360 transformants have been deposited in NCBI's Sequence Read Archive (SRA) under SRA accession numbers SRR6934824 to SRR6935183 according to Supplementary File 3.3. The Bioproject accession number is PRJNA447902.

ACKNOWLEDGEMENT

The authors thank members of the Blokesch laboratory and F. Le Roux for discussions and A. Boehm for strain Sa5Y. We also acknowledge preliminary bioinformatic analyses by S. Strempel (Microsynth), A.-C. Portmann, and I. Mateus, who also uploaded the sequencing reads to NCBI. This work was supported by EPFL intramural funding, the Swiss National Science Foundation grant 31003A_162551, and a Starting (309064-VIR4ENV) and Consolidator (724630-CholeraIndex) grant from the European Research Council to MB. M.B. is a Howard Hughes Medical Institute (HHMI) International Research Scholar (grant #55008726).

AUTHOR CONTRIBUTIONS

N.M. and M.B. designed research; N.M., S.S, C.S, and M.B. performed wetlab experiments; N.G. and C.I. performed bioinformatic analyses; N.M., N.G., C.I., and M.B. discussed the bioinformatic data; M.B. wrote the manuscript with input from N.M., N.G., and C.I. All authors approved the final version.

The authors declare no conflict of interest.

3.8 FIGURES

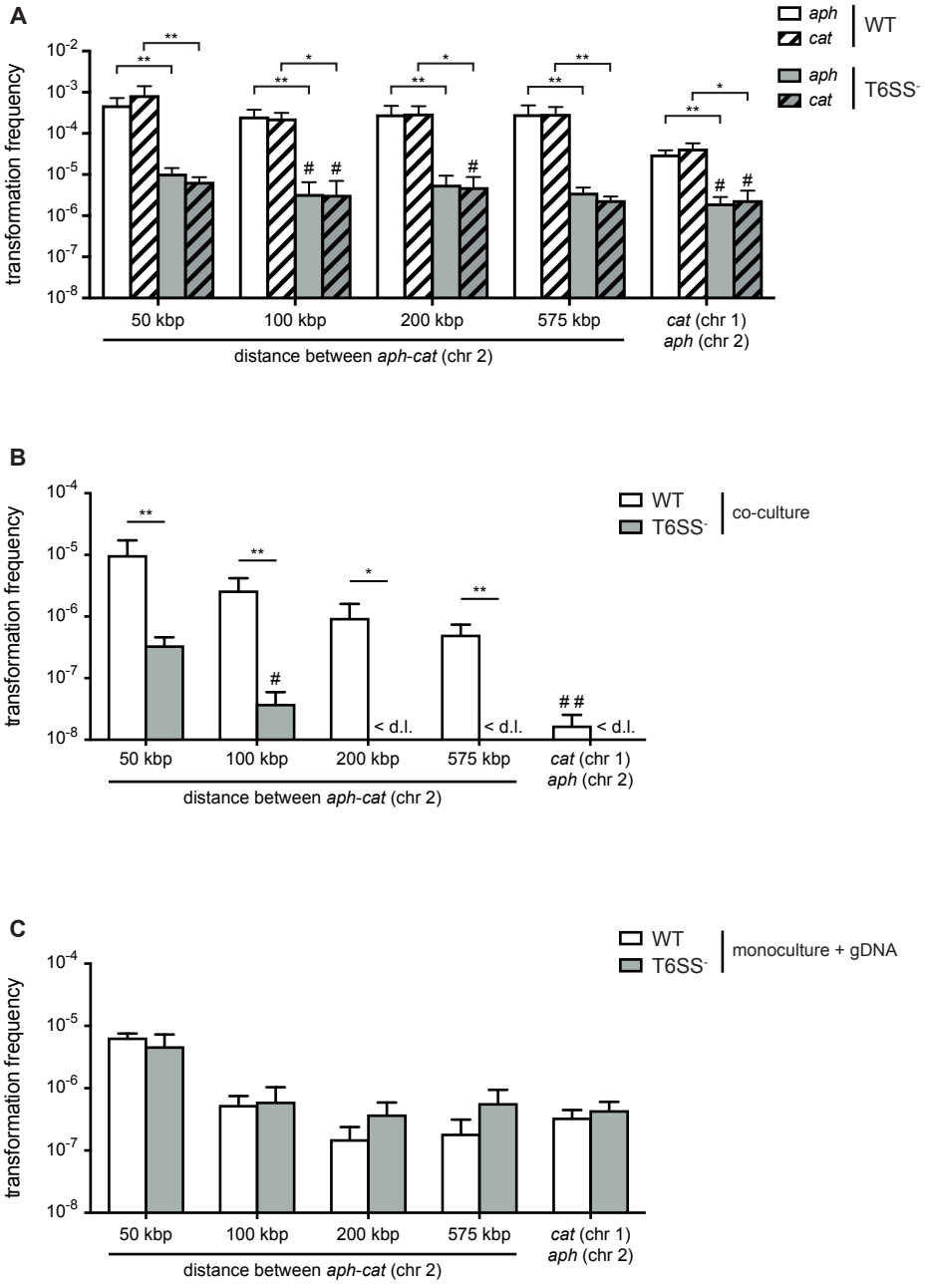

Figure 3.1: Type VI secretion system (T6SS) enhances horizontal gene transfer (HGT) of single- and double-resistance cassettes if carried *in cis*. (A-B) Transformation occurs in predator/prey co-cultures. To induce natural competence, the WT or a T6SS-negative derivative (A1552Δ*vasK*; T6SS $^-$) was co-cultured on chitin with different prey strains (Sa5Y-derived) that carried two antibiotic resistance cassettes: *aph* in *vipA* (chr 2) and *cat* at variable distances from *aph* on the same chromosome or on chr 1, as indicated on the X-axis. Transformation frequencies (Y-axis) indicate the number of transformants that acquired (A) a single resistance cassette or (*B*) both resistance cassettes divided by the total number of predator colony forming units (CFUs). (C) Natural transformation is not impaired in the T6SS$^-$ acceptor strain. Purified genomic DNA (gDNA) was added to competent WT or T6SS$^-$ strains. (A-C) Data represent the average of three independent biological experiments (± SD, as depicted by the error bars). For values in which one (#) or two (##) experiments resulted in the absence of transformants, the detection limit was used to calculate the average. <d.l., below detection limit. Statistical significance is indicated (*$p < 0.05$; **$p < 0.01$).

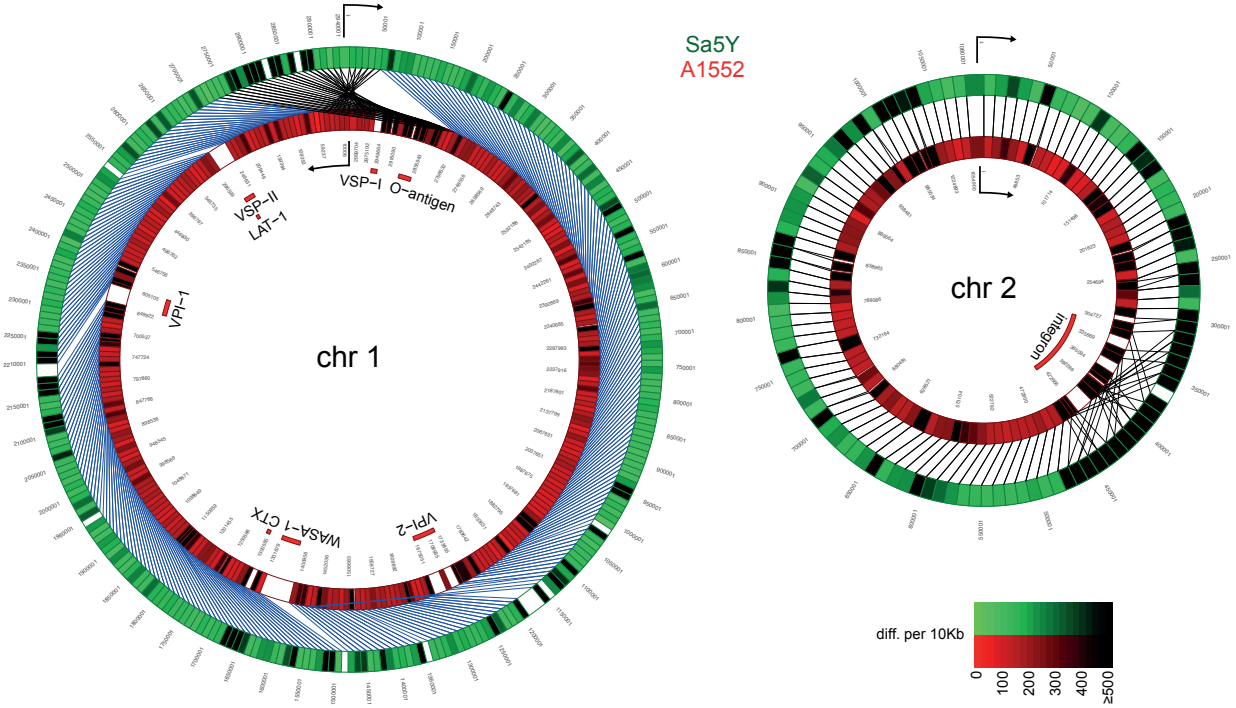

Figure 3.2: Comparative genomics of pandemic strain A1552 and the environmental isolate Sa5Y. The genomic sequences of chr 1 and 2 of Sa5Y (green) were segmented in 10-kbp-long fragments and aligned against the respective chromosome of the reference A1552 (red). To simplify visualization, chr 1 of strain A1552 was inverted and plotted counter-clockwise relative to Sa5Y (due to the large inversion in this strain; see Material and Methods sections), as indicated by the arrow. To represent the differences between the two genomes, a color intensity scale was used that corresponded to the number of differences (SNP or indel), from 0 to ≥500 as measured per 10 kbp fragment. White regions show no homology. Important genomic features of pandemic *V. cholerae* are highlighted inside the rings.

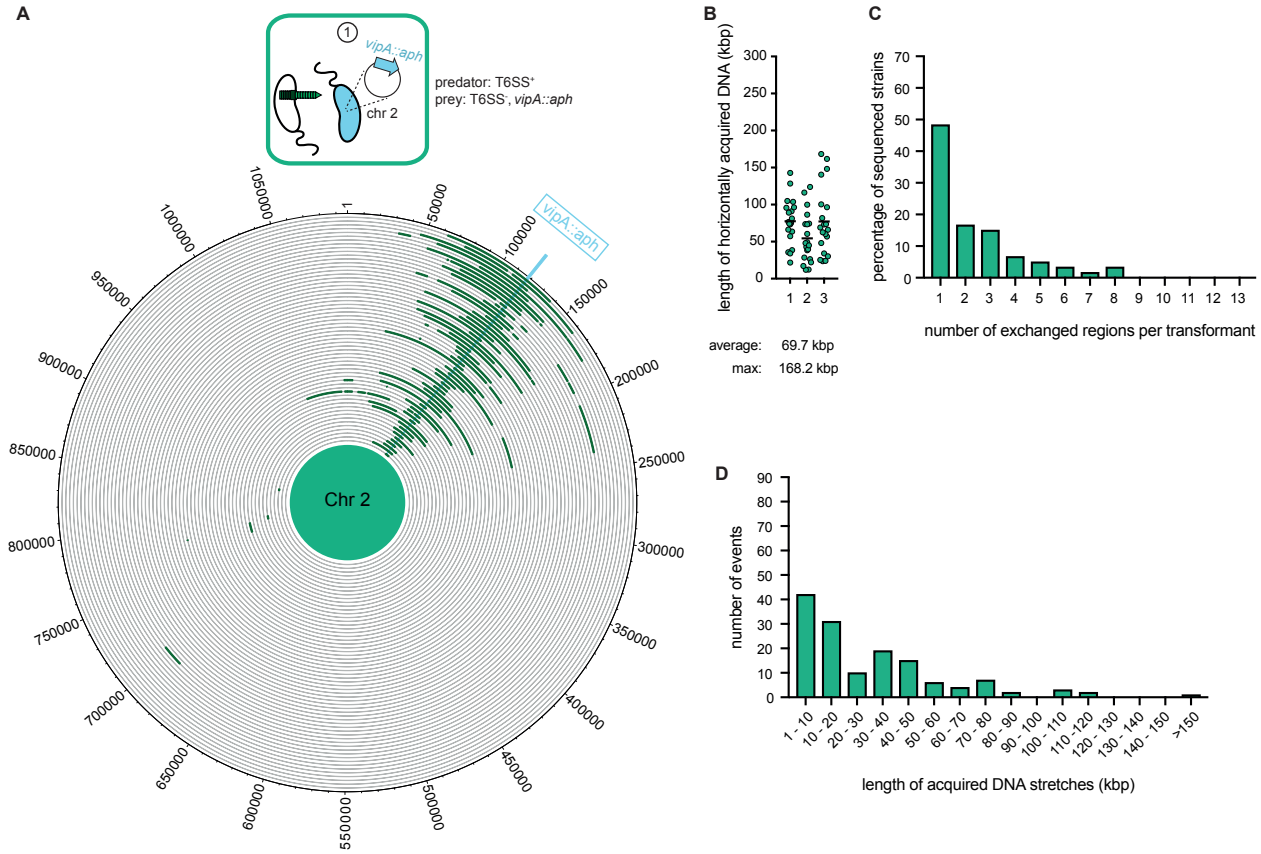

Figure 3.3: Whole-genome sequencing (WGS)-based quantification of horizontally acquired DNA. WGS analysis of transformants after prey killing and DNA transfer. Twenty kanamycin-resistant transformants were selected per independent biological experiment (n = 3). (A) The scheme represents the experimental setup of the co-culture experiment (condition ①). Sequencing reads for each transformant were mapped onto the prey genomes to visualize the transferred DNA regions (in dark green; see supplementary figure 3.4 for both chromosomes). The position of the resistance cassette (*aph*) is indicated by the light blue line. (B) Total DNA acquisition frequently exceeds 100 kb. The total length of horizontally acquired DNA is indicated on the Y-axis for each transformant. Data are from three biologically independent experiments as indicated on the X-axis. Average and maximum lengths are indicated below the graph. (C) Multiple transferred DNA regions were identified in the transformants. Percentage of transformants (n = 60) that exchanged one or more DNA regions, as indicated on the X-axis. (D) Large DNA stretches are transferrable by transformation. The length of individual consecutive DNA stretches was determined as indicated on the X-axis.

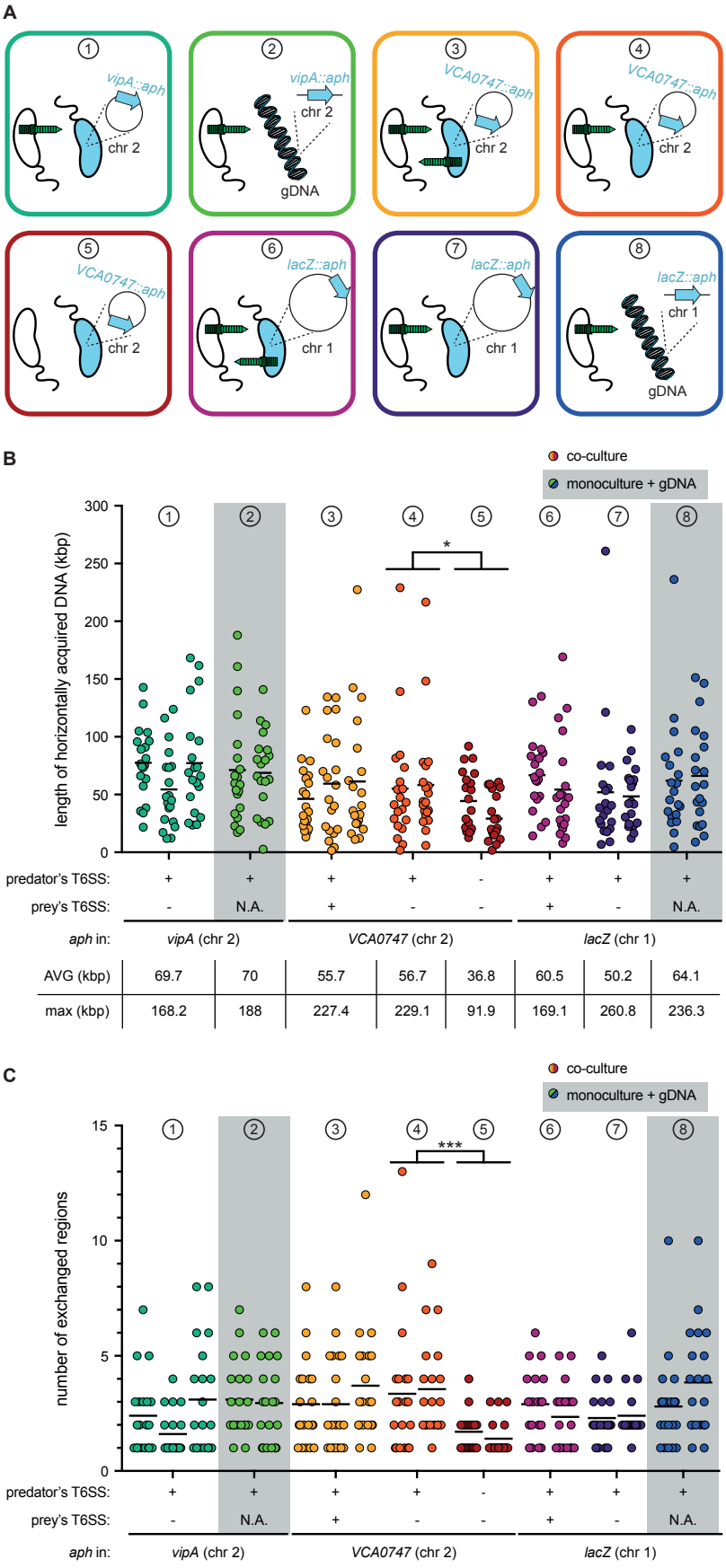

Figure 3.4: T6SS-mediated neighbor predation followed by DNA uptake enhances the frequency and length of transferred DNA stretches. (A) Scheme representing the eight experimental conditions tested in this study. Each scheme indicates whether the transformants acquired the *aph* resistance gene from a prey bacterium (blue) (position of *aph* indicated on the zoomed-in circles of chr 1 or chr 2) or from purified genomic DNA (gDNA). In the former case, the killing capacity of the predator (white) and prey (blue) is shown by the presence or absence of the dark green T6SS structure. The same color code is maintained throughout all figures. (B-C) Transformants from independent biological experiments ($n \geq 2$) were analyzed by WGS for each of the conditions ①-⑧, as indicated at the top of each graph. The main features of predator and prey/gDNA are summarized below the X-axis. Panels (B) and (C) depict the total length of acquired DNA and the number of exchanged DNA stretches, respectively, for each transformant. N.A., not applicable. Statistical analysis is based on a pairwise comparison between different conditions. *$p < 0.05$, ***$p < 0.001$.

3.9 SUPPLEMENTARY FILES

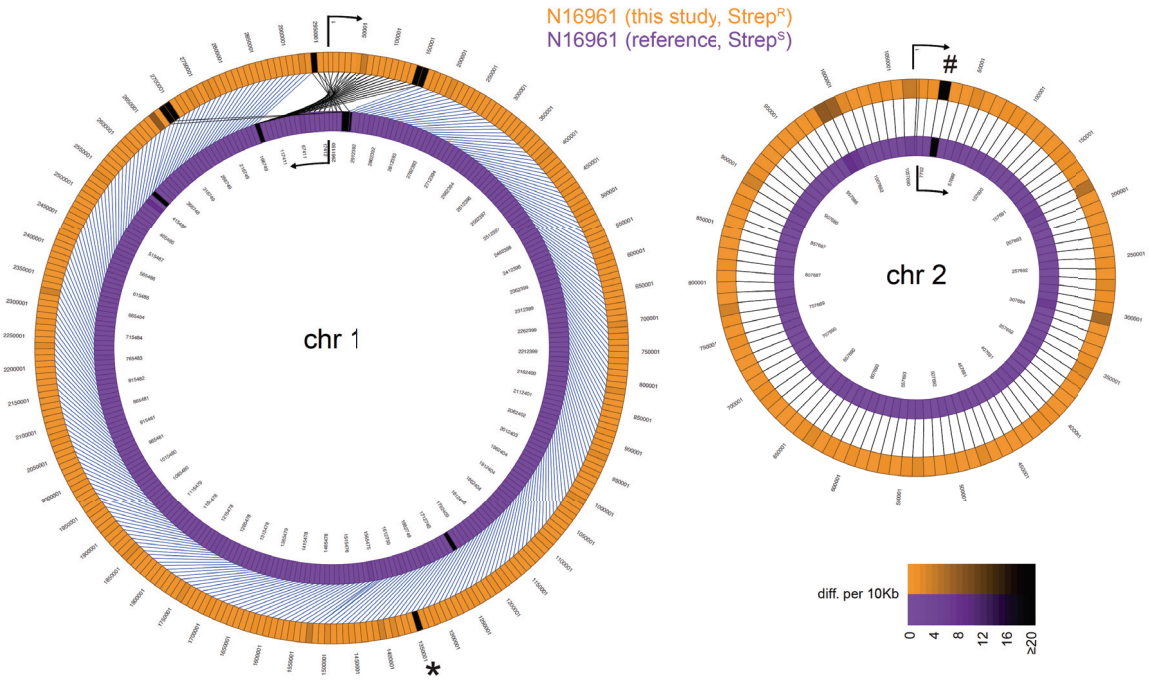

Supplementary figure 3.1: Comparative genomics of *V. cholerae* reference strain N16961 and a newly sequenced laboratory stock of the same strain. The newly sequenced genome of the streptomycin-resistant laboratory stock of strain N16961 (long-read PacBio sequencing technology; ([4])) was compared to the genome sequence of the reference genome ([44]). Detailed explanations on the comparison are as described for Figure 3.2. Marked discrepancies are based on repetitive sequences (*) or a sequencing error (#) as discussed in the Material and Methods section.

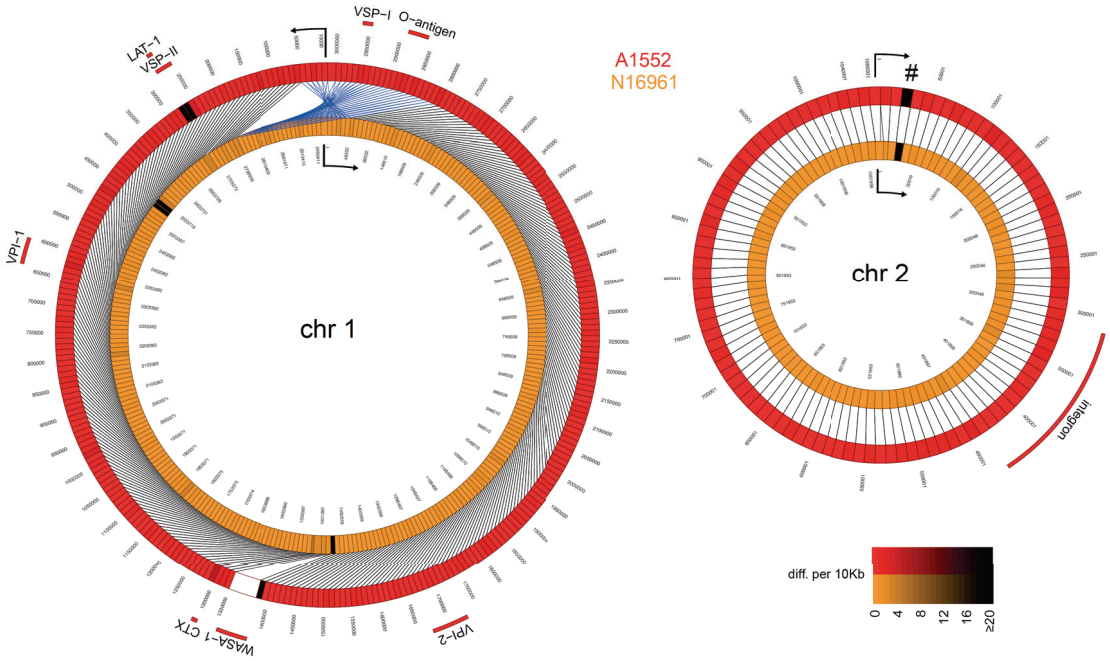

Supplementary figure 3.2: Comparative genomics of pandemic *V. cholerae* strains N16961 and A1552. The genome sequences of our laboratory stock of pandemic strains N16961 and A1552 were compared. Details are as described in Figure 3.2. The marked discrepancy (#) resulted from a sequencing error, as discussed in the Material and Methods section.

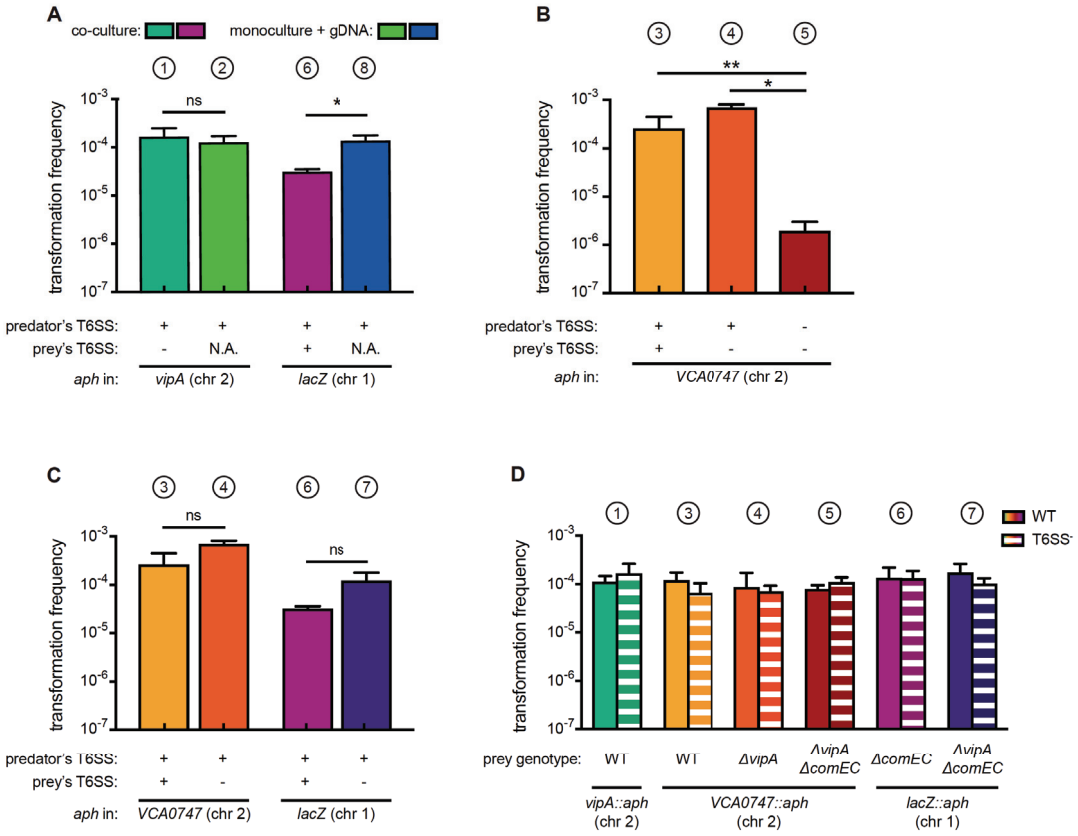

Supplementary figure 3.3: Natural transformation is enhanced by T6SS-mediated killing of prey bacteria. (A-C) Transformation is enhanced in T6SS-positive predator cells. To induce natural competence, cultures were grown on chitin flakes. Bacteria were grown as co-cultures (predator + prey) or as monocultures (predator only). In the latter case, purified gDNA served as the transforming material. Transformants were selected based on their acquisition of the *aph* resistance cassette located in *vipA*, *VCA0747,* or *lacZ* on chr1 or chr2, as indicated below the graphs. The killing capability of each strain is indicated below the graph (e.g., T6SS + or -). Transformation frequencies are shown on the Y-axis (± SD, as depicted by the error bars) and depict averages of at least two biologically independent experiments (corresponding to the experiments described in Figure 3.4 and maintaining the same color code). N.A., not applicable. (D) The location of the resistance genes does not influence the transformation efficiency. Natural transformability of the WT (plain bars) or its T6SS-minus derivative (T6SS$^-$; Δ*vipA;* hashed bars) was scored using gDNA as the transforming material. The gDNA samples were derived from the prey strains of conditions ① and ③–⑦ and the respective genotype is shown below the graph. Transformation frequencies were scored based on the acquisition of the *aph* resistance cassette, which was integrated into different genes on chromosome 1 or 2 (chr 1/chr 2). Data represent the average of three independent experiments (±SD). (A-D) Statistical significance is indicated (*p < 0.05; **p < 0.01).

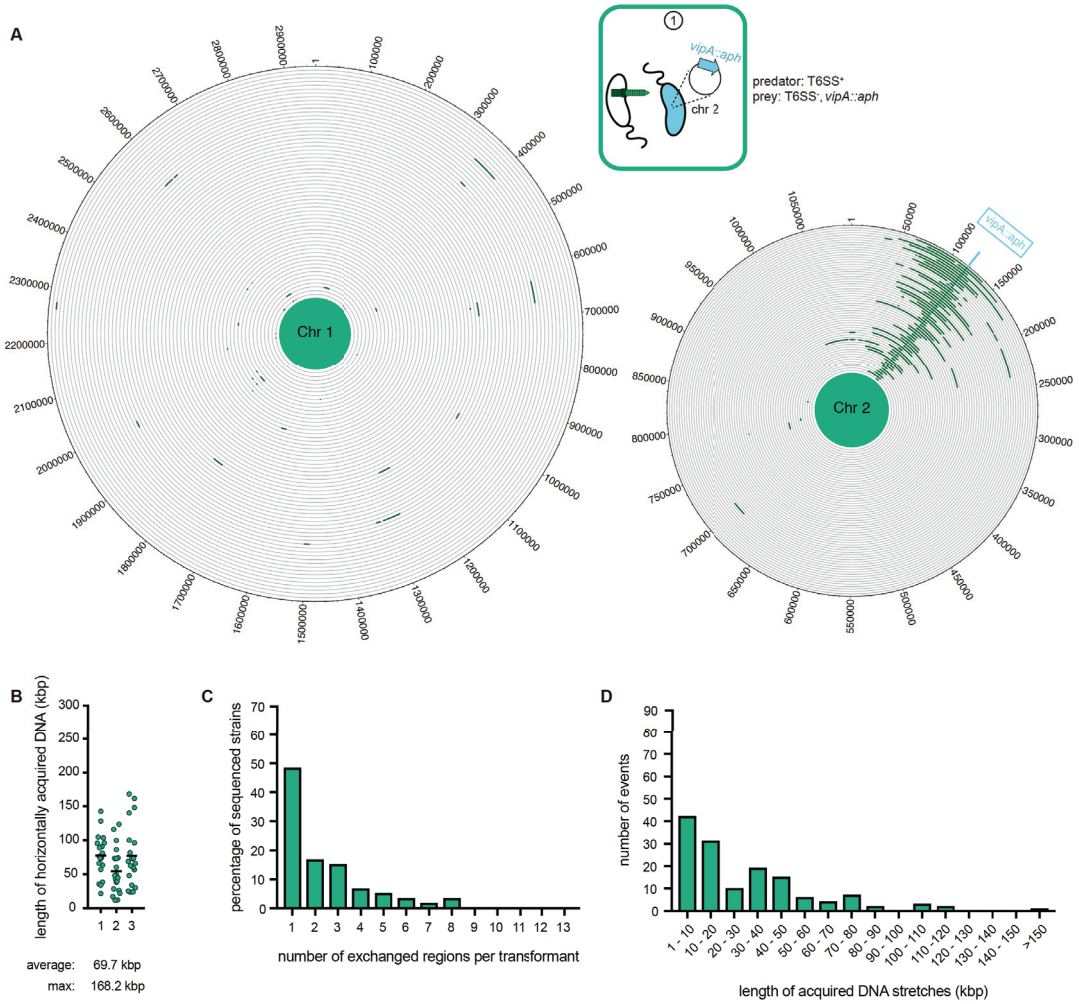

Supplementary figure 3.4: WGS-based quantification of horizontally acquired DNA under condition ①. Data as in Figure 3.3 with the addition of the map of both chromosomes in panel A.

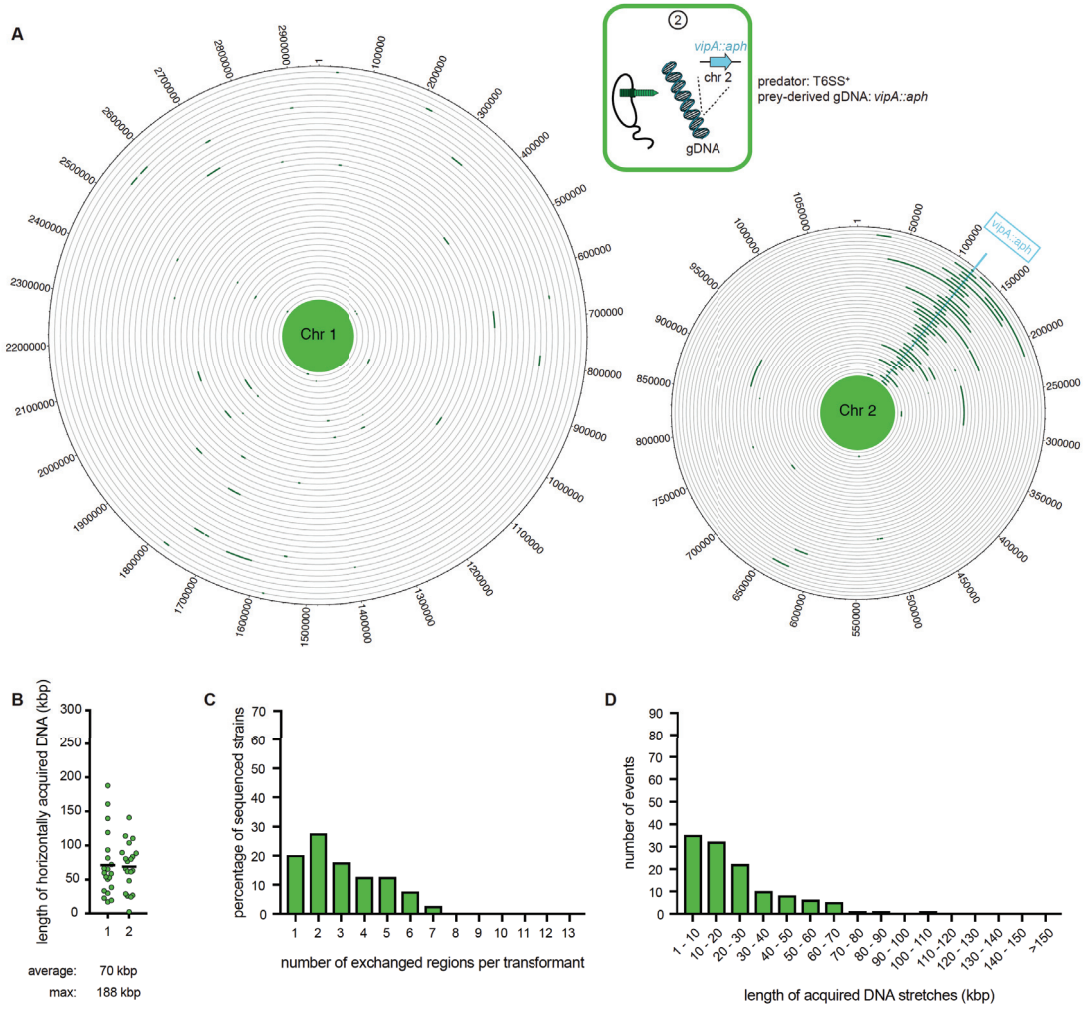

Supplementary figure 3.5: WGS-based quantification of horizontally acquired DNA under condition ②. Details as described for Figure 3.3 with the addition of the map of both chromosomes in panel A.

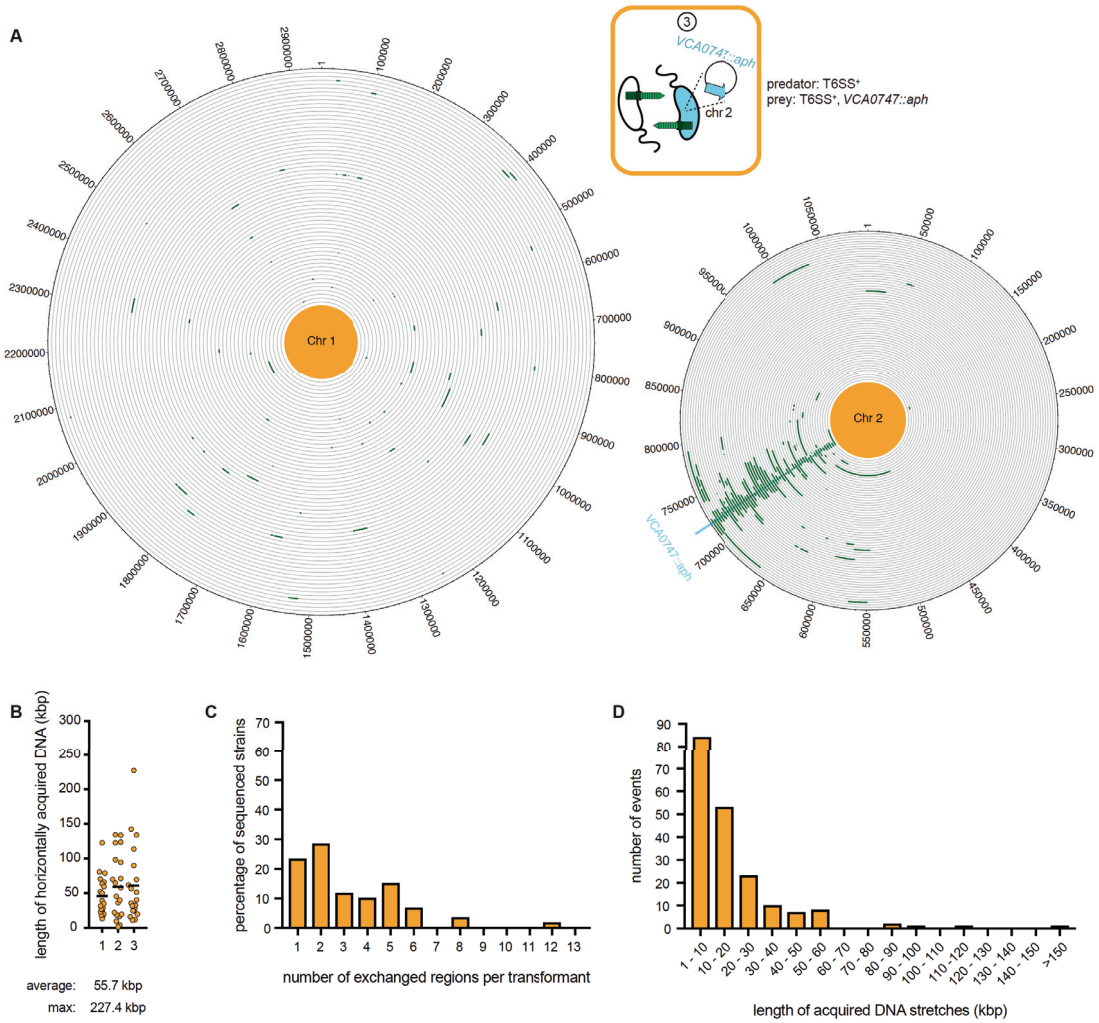

Supplementary figure 3.6: WGS-based quantification of horizontally acquired DNA under condition ③. Details as described for Figure 3.3 with the addition of the map of both chromosomes in panel A.

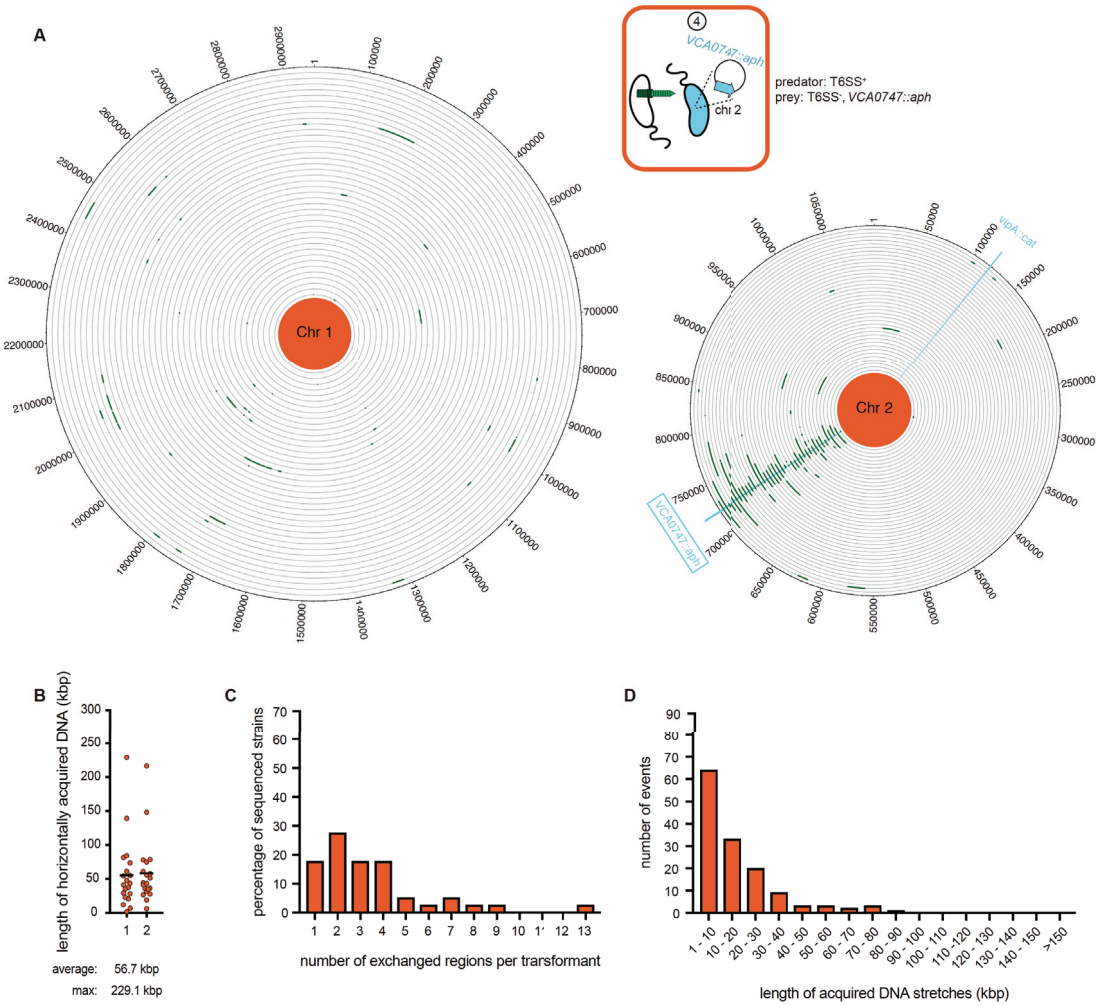

Supplementary figure 3.7: WGS-based quantification of horizontally acquired DNA under condition ④. Details as described for Figure 3.3 with the addition of the map of both chromosomes in panel A.

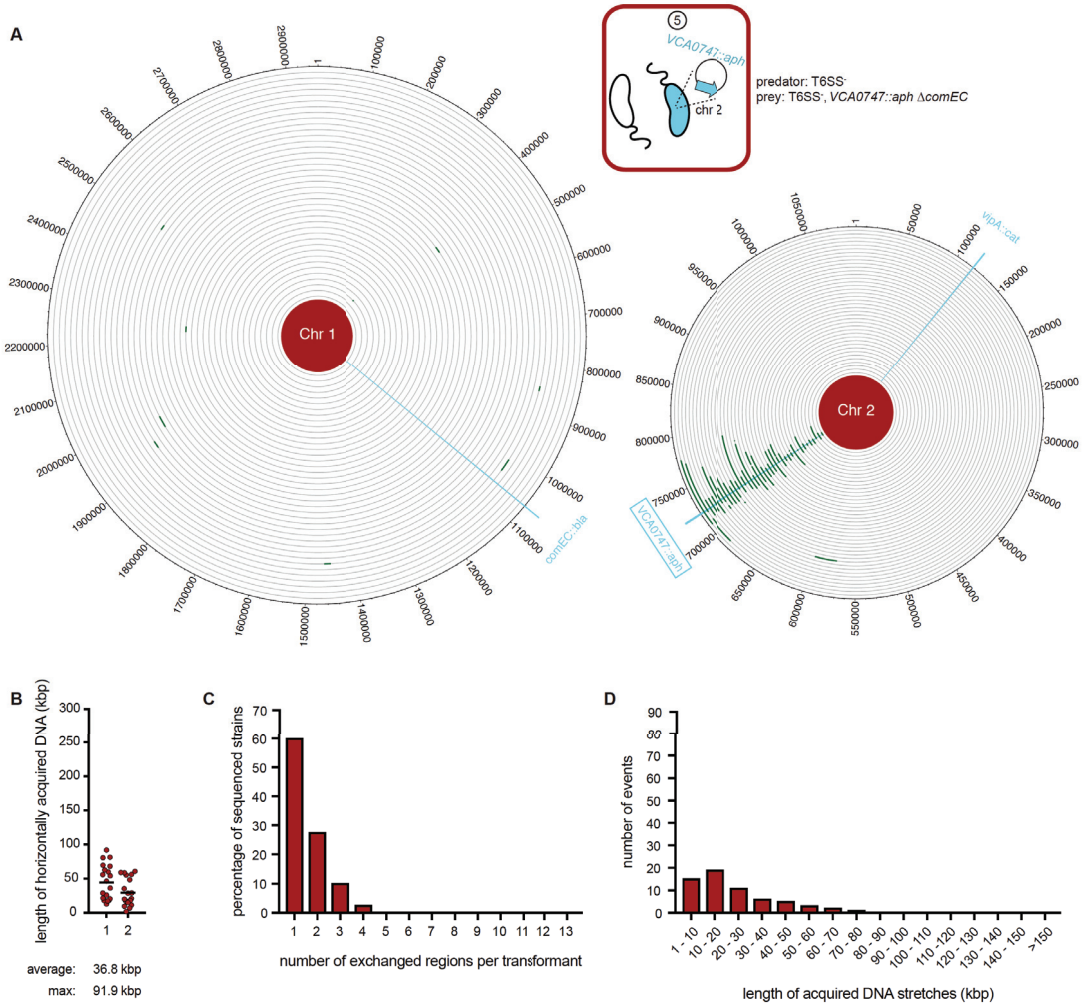

Supplementary figure 3.8: WGS-based quantification of horizontally acquired DNA under condition ⑤. Details as described for Figure 3.3 with the addition of the map of both chromosomes in panel A.

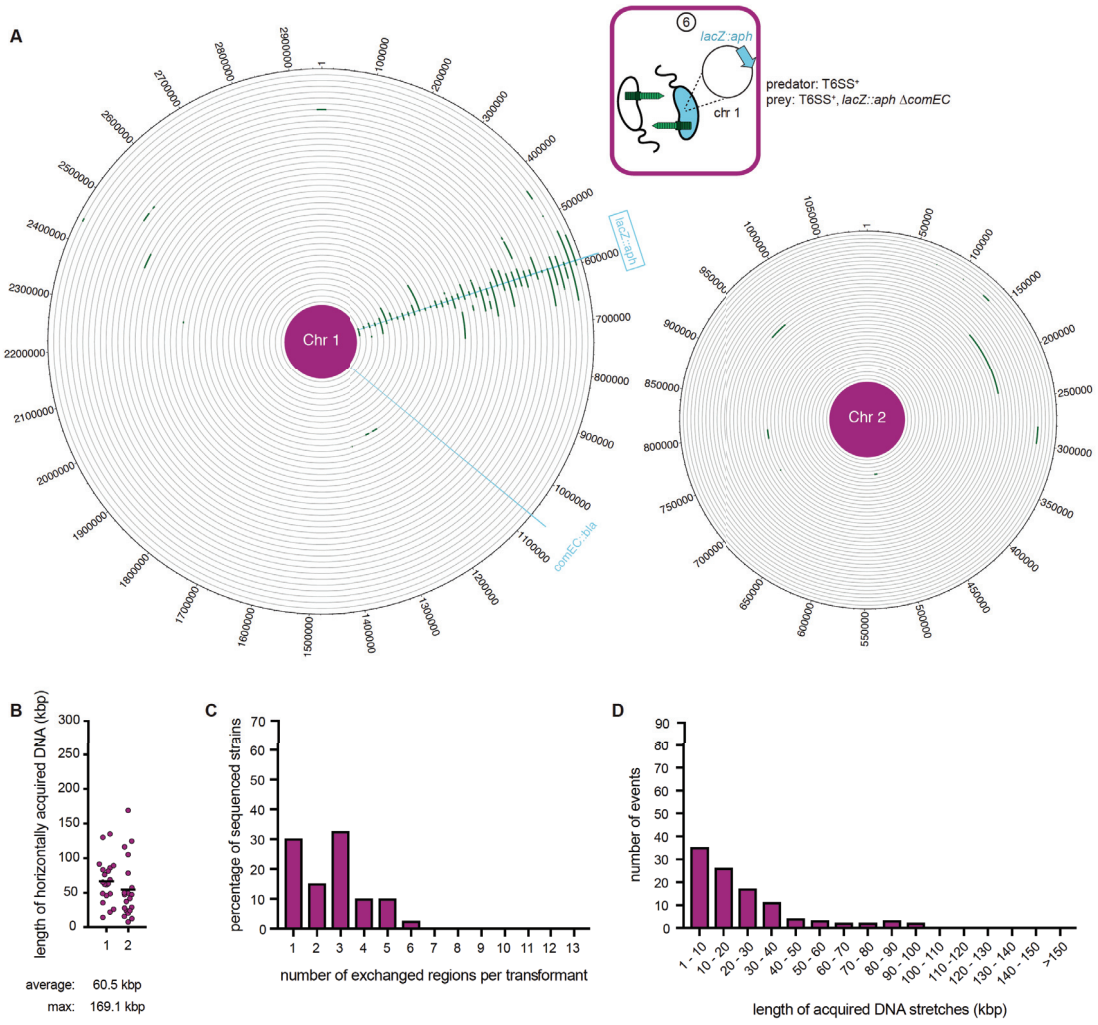

Supplementary figure 3.9: WGS-based quantification of horizontally acquired DNA under condition ⑥. Details as described for Figure 3.3 with the addition of the map of both chromosomes in panel A.

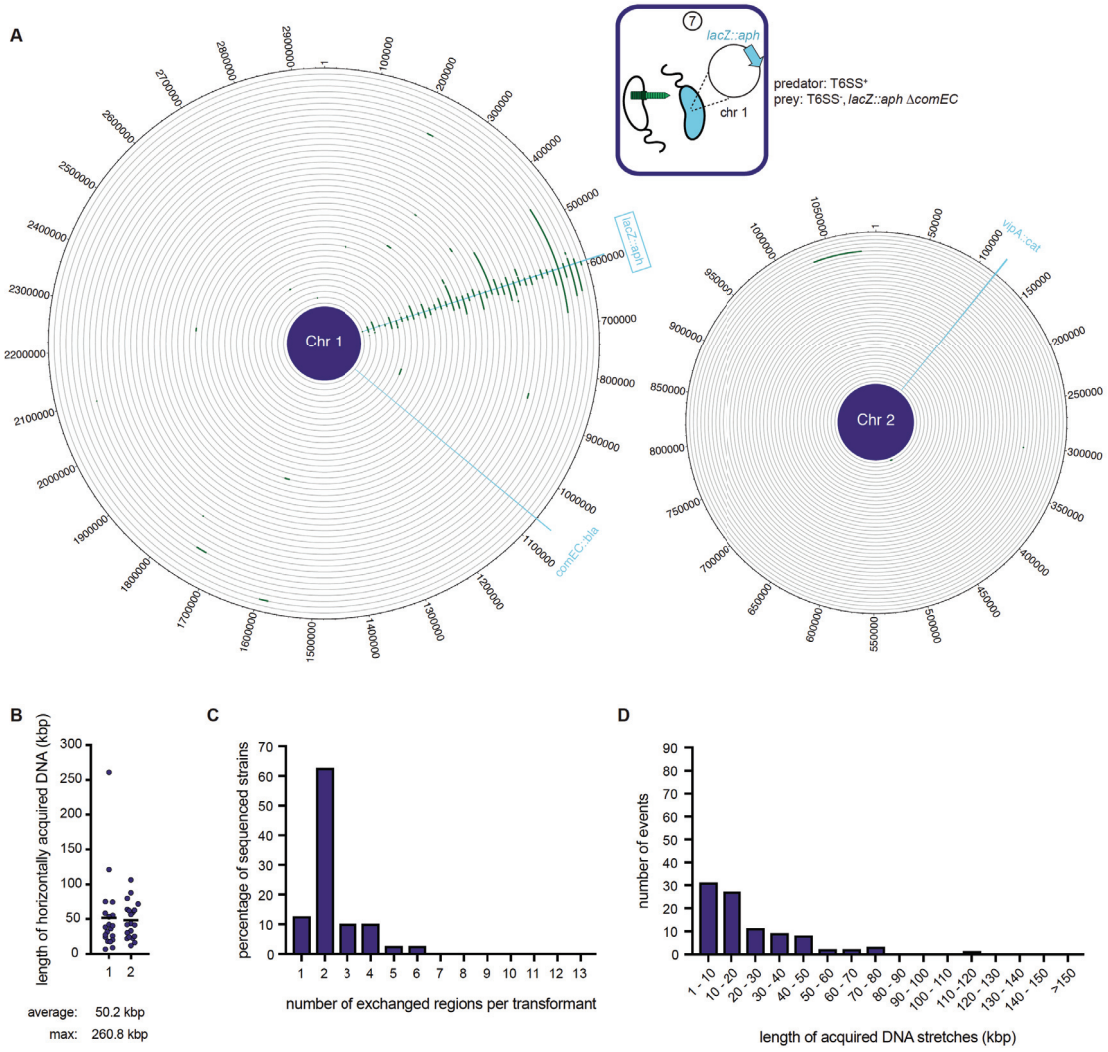

Supplementary figure 3.10: WGS-based quantification of horizontally acquired DNA under condition ⑦. Details as described for Figure 3.3 with the addition of the map of both chromosomes in panel A.

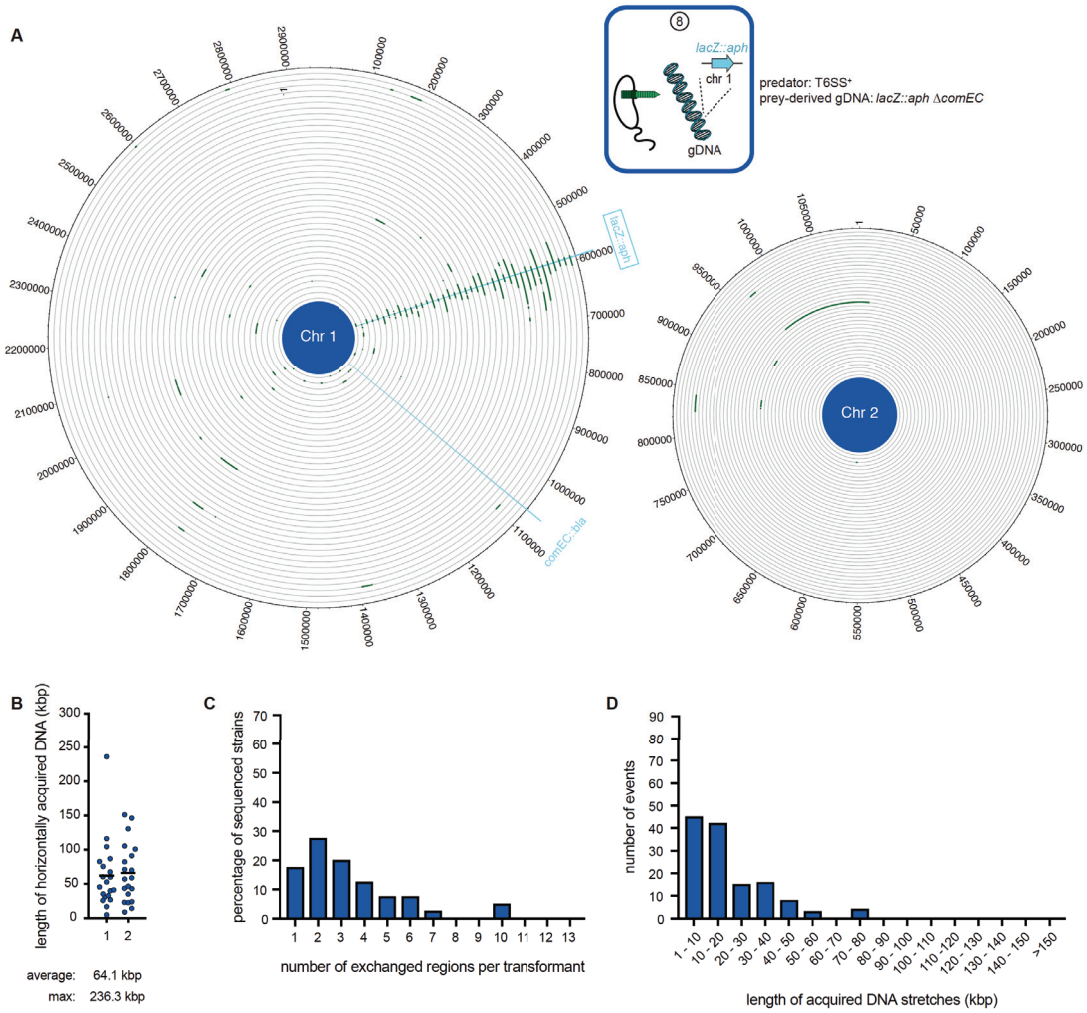

Supplementary figure 3.11: WGS-based quantification of horizontally acquired DNA under condition ⑧. Details as described for Figure 3.3 with the addition of the map of both chromosomes in panel A.

Supplementary file 3.1. Strains and plasmids used in this study.

Strains	Genotype/description*	Internal strain number	Reference
V. cholerae			
A1552 (WT)	Wild-type, O1 El Tor Inaba; Rif^R	MB_1	([42])
A1552ΔvasK	A1552 deleted for *vasK* (VCA0120), Rif^R	MB_585	([1])
A1552ΔvipA::FRT-cat-FRT	A1552 deleted for *vipA* (VCA0107; *cat* insertion); Rif^R, Cm^R	MB_5215	This study
A1552 HGT chr 2 ΔvipA::FRT-aph-FRT (T6SS- prey)	A1552 naturally transformed with prey strain Sa5YΔvipA::FRT-*aph*-FRT; Rif^R, Kan^R; 20 transformants selected, biological replicate 1	MB_4663 to MB_4682	This study
A1552 HGT chr 2 ΔvipA::FRT-aph-FRT (T6SS- prey)	A1552 naturally transformed with prey strain Sa5YΔvipA::FRT-*aph*-FRT; Rif^R, Kan^R; 20 transformants selected, biological replicate 2	MB_4683 to MB_4702	This study
A1552 HGT chr 2 ΔvipA::FRT-aph-FRT (T6SS- prey)	A1552 naturally transformed with prey strain Sa5YΔvipA::FRT-*aph*-FRT; Rif^R, Kan^R; 20 transformants selected, biological replicate 3	MB_4703 to MB_4722	This study
A1552 HGT chr 2 ΔVCA0747::FRT-aph-FRT_A (T6SS+ prey)	A1552 naturally transformed with prey strain Sa5YΔVCA0747::FRT-*aph*-FRT; Rif^R, Kan^R; 20 transformants selected, biological replicate 1	MB_4723 to MB_4742	This study
A1552 HGT chr 2 ΔVCA0747::FRT-aph-FRT_A (T6SS+ prey)	A1552 naturally transformed with prey strain Sa5YΔVCA0747::FRT-*aph*-FRT; Rif^R, Kan^R; 20 transformants selected, biological replicate 2	MB_4743 to MB_4762	This study
A1552 HGT chr 2 ΔVCA0747::FRT-aph-FRT_A (T6SS+ prey)	A1552 naturally transformed with prey strain Sa5YΔVCA0747::FRT-*aph*-FRT; Rif^R, Kan^R; 20 transformants selected, biological replicate 3	MB_4763 to MB_4782	This study
A1552 HGT chr 2 ΔVCA0747::FRT-aph-FRT_B (T6SS- prey)	A1552 naturally transformed with prey strain Sa5YΔvipA::FRT-*cat*-FRTΔVCA0747::FRT-*aph*-FRT; Rif^R, Kan^R; 20 transformants selected, biological replicate 1	MB_5175 to MB_5194	This study

A1552 HGT chr 2 ΔVCA0747::FRT-aph-FRT_B (T6SS- prey)	A1552 naturally transformed with prey strain Sa5YΔvipA::FRT-*cat*-FRTΔVCA0747::FRT-*aph*-FRT; Rif^R, Kan^R; 20 transformants selected, biological replicate 2	MB_5195 to MB_5214	This study
A1552ΔvipA::FRT-cat-FRT HGT chr 2 ΔVCA0747::FRT-aph-FRT_B (T6SS- prey)	A1552 ΔvipA::FRT-*cat*-FRT naturally transformed with prey strain Sa5YΔvipA::FRT-*cat*-FRTΔVCA0747::FRT-*aph*-FRTΔcomEC::*bla*; Rif^R, Kan^R, Cm^R; 20 transformants selected, biological replicate 1	MB_5217 to MB_5236	This study
A1552ΔvipA::FRT-cat-FRT HGT chr 2 ΔVCA0747::FRT-aph-FRT_B (T6SS- prey)	A1552 ΔvipA::FRT-*cat*-FRT naturally transformed with prey strain Sa5YΔvipA::FRT-*cat*-FRTΔVCA0747::FRT-*aph*-FRTΔcomEC::*bla*; Rif^R, Kan^R, Cm^R; 20 transformants selected, biological replicate 2	MB_5237 to MB_5256	This study
A1552 HGT chr 1 ΔlacZ::FRT-aph-FRT_A (T6SS+ prey)	A1552 naturally transformed with prey strain Sa5YΔlacZ::FRT-*aph*-FRTΔcomEC::*bla*; Rif^R, Kan^R; 20 transformants selected, biological replicate 1	MB_5257 to MB_5276	This study
A1552 HGT chr 1 ΔlacZ::FRT-aph-FRT_A (T6SS+ prey)	A1552 naturally transformed with prey strain Sa5YΔlacZ::FRT-*aph*-FRTΔcomEC::*bla*; Rif^R, Kan^R; 20 transformants selected, biological replicate 2	MB_5277 to MB_5296	This study
A1552 HGT chr 1 ΔlacZ::FRT-aph-FRT_B (T6SS- prey)	A1552 naturally transformed with prey strain Sa5YΔvipA::FRT-*cat*-FR ΔlacZ::FRT-*aph*-FRTΔcomEC::*bla*; Rif^R, Kan^R; 20 transformants selected, biological replicate 1	MB_5301 to MB_5320	This study
A1552 HGT chr 1 ΔlacZ::FRT-aph-FRT_B (T6SS- prey)	A1552 naturally transformed with prey strain Sa5YΔvipA::FRT-*cat*-FR ΔlacZ::FRT-*aph*-FRTΔcomEC::*bla*; Rif^R, Kan^R; 20 transformants selected, biological replicate 2	MB_5321 to MB_5340	This study
A1552 HGT chr 2 ΔvipA::FRT-aph-FRT	A1552 naturally transformed with gDNA of Sa5YΔvipA::FRT-*aph*-FRT; Rif^R, Kan^R; 20 transformants selected, biological replicate 1	MB_5343 to MB_5362	This study
A1552 HGT chr 2 ΔvipA::FRT-aph-FRT	A1552 naturally transformed with gDNA of Sa5YΔvipA::FRT-*aph*-FRT; Rif^R, Kan^R; 20 transformants selected, biological replicate 2	MB_5363 to MB_5382	This study

A1552 HGT chr 1 ΔlacZ::FRT-aph-FRT	A1552 naturally transformed with gDNA of strain Sa5YΔlacZ::FRT-*aph*-FRTΔcomEC::*bla*; Rif^R, Kan^R; 20 transformants selected, biological replicate 1	MB_5385 to MB_5404	This study
A1552 HGT chr 1 ΔlacZ::FRT-aph-FRT	A1552 naturally transformed with gDNA of strain Sa5YΔlacZ::FRT-*aph*-FRTΔcomEC::*bla*; Rif^R, Kan^R; 20 transformants selected, biological replicate 2	MB_5405 to MB_5424	This study
Sa5Y (WT)	non-O1/O139 environmental *V. cholerae* strains; isolated from the central California coast	MB_353	([40])
Sa5YΔvipA::FRT-aph-FRT	Sa5Y deleted for *vipA* (VCA0107) (*aph* insertion); Kan^R	MB_4614	This study
Sa5YΔvipA::FRT-aph-FRT ΔVCA0059::FRT-cat-FRT ΔcomEC::bla	Sa5Y deleted for *vipA* (*aph* insertion), for VCA0059 (*cat* insertion) and for *comEC* (*bla* insertion); Kan^R, Cm^R, Amp^R	MB_6066	This study
Sa5YΔvipA::FRT-aph-FRT ΔVCA0014::FRT-cat-FRT ΔcomEC::bla	Sa5Y deleted for *vipA* (*aph* insertion), for VCA0014 (*cat* insertion) and for *comEC* (*bla* insertion); Kan^R, Cm^R, Amp^R	MB_5776	This study
Sa5YΔvipA::FRT-aph-FRT ΔVCA1034::FRT-cat-FRT ΔcomEC::bla	Sa5Y deleted for *vipA* (*aph* insertion), for VCA1034 (*cat* insertion) and for *comEC* (*bla* insertion); Kan^R, Cm^R, Amp^R	MB_6067	This study
Sa5YΔvipA::FRT-aph-FRT ΔVCA0665::FRT-cat-FRT ΔcomEC::bla	Sa5Y deleted for *vipA* (*aph* insertion), for VCA0665 (*cat* insertion) and for *comEC* (*bla* insertion); Kan^R, Cm^R, Amp^R	MB_6069	This study
Sa5YΔvipA::FRT-aph-FRT ΔlacZ::FRT-cat-FRT ΔcomEC::bla	Sa5Y deleted for *vipA* (*aph* insertion), for *lacZ* (VC2338) (*cat* insertion) and for *comEC* (*bla* insertion); Kan^R, Cm^R, Amp^R	MB_6070	This study
Sa5YΔVCA0747::FRT-aph-FRT	Sa5Y deleted for VCA0747 (*aph* insertion); Kan^R	MB_5076	This study
Sa5YΔvipA::FRT-cat-FRTΔVCA0747::FRT-aph-FRT	Sa5Y deleted for *vipA* (*cat* insertion) and for VCA0747 (*aph* insertion); Kan^R, Cm^R	MB_5174	This study
Sa5YΔvipA::FRT-cat-FRTΔVCA0747::FRT-aph-FRTΔcomEC::bla	Sa5Y deleted for *vipA* (*cat* insertion), for VCA0747 (*aph* insertion) and for *comEC* (*bla* insertion); Kan^R, Cm^R, Amp^R	MB_5216	This study
Sa5YΔlacZ::FRT-aph-FRTΔcomEC::bla	Sa5Y deleted for *lacZ* (*aph* insertion), and for *comEC* (*bla* insertion); Kan^R, Amp^R	MB_5298	This study

Sa5YΔvipA::FRT-cat-FRTΔlacZ::FRT-aph-FRTΔcomEC::bla	Sa5Y deleted for *vipA* (*cat* insertion), for *lacZ* (*aph* insertion), and for *comEC* (*bla* insertion); Kan^R, Cm^R, Amp^R	MB_5300	This study
N16961	Wild-type; Isolate from Bangladesh (1971), O1 El Tor Inaba; $Strep^R$	MB_2	([4,44])
E. coli			
TOP10	F- mcrA Δ(mrr-hsdRMS-mcrBC) φ80lacZΔM15 ΔlacX74 nupG recA1 araΔ139 Δ(ara-leu)7697 galE15 galK16 rpsL(StrR) endA1λ-; $Strep^R$	MB_741	Invitrogen
Plasmids			
pBR-FRT-aph-FRT2	pBR322 derivative containing improved FRT-*aph*-FRT cassette, used as template for gene deletion; Amp^R, Kan^R	MB_3782	([35])
pBR-FRT-cat-FRT2	pBR322 derivative containing improved FRT-*cat*-FRT cassette, used as template for gene deletion; Amp^R, Kan^R	MB_3783	([35])

*VC/VCA locus tag numbers according to ([44])

Supplementary file 3.2. Details of eight experimental conditions and corresponding strain numbers.

Comment	Strains	Genotype*/description	internal strain number	Reference (template used for mapping)	Acceptor strain 1 (T6SS +/-)	Donor strain 2 (T6SS +/-)	Donor gDNA
Acceptor strain 1	A1552 (WT)	Wild-type, O1 El Tor Inaba; Rif^R	**MB_1**				
Donor strain 1	Sa5YΔvipA::FRT-aph-FRT	Sa5Y deleted for *vipA* (*aph* insertion); Kan^R	**MB_4614**				
Transformants	A1552 HGT chr 2 ΔvipA::FRT-aph-FRT	A1552 naturally transformed with prey strain Sa5YΔvipA::FRT-aph-FRT; Rif^R, Kan^R; 20 transformants selected, biological replicate 1	**MB_4663 to MB_4682**	**Experimental condition 1**	**T6SS +**	**T6SS -**	-
Transformants	A1552 HGT chr 2 ΔvipA::FRT-aph-FRT	A1552 naturally transformed with prey strain Sa5YΔvipA::FRT-aph-FRT; Rif^R, Kan^R; 20 transformants selected, biological replicate 2	**MB_4683 to MB_4702**	**Experimental condition 1**	**T6SS +**	**T6SS -**	-
Transformants	A1552 HGT chr 2 ΔvipA::FRT-aph-FRT	A1552 naturally transformed with prey strain Sa5YΔvipA::FRT-aph-FRT; Rif^R, Kan^R; 20 transformants selected, biological replicate 3	**MB_4703 to MB_4722**	**Experimental condition 1**	**T6SS +**	**T6SS -**	-
Acceptor strain 2	A1552 (WT)	Wild-type, O1 El Tor Inaba; Rif^R	**MB_5341 (=MB_1)**				
Donor strain 2	Sa5YΔvipA::FRT-aph-FRT	Sa5Y deleted for *vipA* (*aph* insertion); Kan^R	**MB_5342 (=MB_4614)**				
Transformants	A1552 HGT chr 2 ΔvipA::FRT-aph-FRT	A1552 naturally transformed with gDNA of Sa5YΔvipA::FRT-aph-FRT; Rif^R, Kan^R; 20 transformants selected, biological replicate 1	**MB_5343 to MB_5362**	**Experimental condition 2**	**T6SS +**	-	**gDNA**
Transformants	A1552 HGT chr 2 ΔvipA::FRT-aph-FRT	A1552 naturally transformed with gDNA of Sa5YΔvipA::FRT-aph-FRT; Rif^R, Kan^R; 20 transformants selected, biological replicate 2	**MB_5363 to MB_5382**	**Experimental condition 2**	**T6SS +**	-	**gDNA**
Acceptor strain 3	A1552 (WT)	Wild-type, O1 El Tor Inaba; Rif^R	**MB_1**				
Donor strain 3	Sa5Y ΔVCA0747::FRT-aph-FRT	Sa5Y deleted for VCA0747 (*aph* insertion); Kan^R	**MB_5076**				
Transformants	A1552 HGT chr 2 ΔVCA0747::FRT-aph-FRT_A (T6SS+	A1552 naturally transformed with prey strain Sa5YΔVCA0747::FRT-aph-FRT; Rif^R, Kan^R; 20 transformants selected, biological replicate 1	**MB_4723 to MB_4742**	**Experimental condition 3**	**T6SS +**	**T6SS +**	-
Transformants	A1552 HGT chr 2 ΔVCA0747::FRT-aph-FRT_A (T6SS+	A1552 naturally transformed with prey strain Sa5YΔVCA0747::FRT-aph-FRT; Rif^R, Kan^R; 20 transformants selected, biological replicate 2	**MB_4743 to MB_4762**	**Experimental condition 3**	**T6SS +**	**T6SS +**	-
Transformants	A1552 HGT chr 2 ΔVCA0747::FRT-aph-FRT_A (T6SS+	A1552 naturally transformed with prey strain Sa5YΔVCA0747::FRT-aph-FRT; Rif^R, Kan^R; 20 transformants selected, biological replicate 3	**MB_4763 to MB_4782**	**Experimental condition 3**	**T6SS +**	**T6SS +**	-
Acceptor strain 4	A1552 (WT)	Wild-type, O1 El Tor Inaba; Rif^R	**MB_5173 (=MB_1)**				
Donor strain 4	Sa5YΔvipA::FRT-cat-FRT ΔVCA0747::FRT-aph-FRT	Sa5Y deleted for *vipA* (*cat* insertion) and for VCA0747 (*aph* insertion); Kan^R, Cm^R	**MB_5174**				
Transformants	A1552 HGT chr 2 ΔVCA0747::FRT-aph-FRT_B (T6SS- prey)	A1552 naturally transformed with prey strain Sa5YΔvipA::FRT-cat-FRT ΔVCA0747::FRT-aph-FRT; Rif^R, Kan^R; 20 transformants selected, biological replicate 1	**MB_5175 to MB_5194**	**Experimental condition 4**	**T6SS +**	**T6SS -**	-
Transformants	A1552 HGT chr 2 ΔVCA0747::FRT-aph-FRT_B (T6SS- prey)	A1552 naturally transformed with prey strain Sa5YΔvipA::FRT-cat-FRT ΔVCA0747::FRT-aph-FRT; Rif^R, Kan^R; 20 transformants selected, biological replicate 2	**MB_5195 to MB_5214**	**Experimental condition 4**	**T6SS +**	**T6SS -**	-
Acceptor strain 5	A1552 ΔvipA::FRT-cat-FRT	A1552 deleted for *vipA* (*cat* insertion); Rif^R, Cm^R	**MB_5215**				
Donor strain 5	Sa5Y ΔvipA::FRT-cat-FRT ΔVCA0747::FRT-aph-FRT ΔcomEC::bla	Sa5Y deleted for *vipA* (TransFLP; *cat* insertion), for VCA0747 (TransFLP; *aph* insertion) and for *comEC* (TransFLP; *bla* insertion); Kan^R, Cm^R, Amp^R	**MB_5216**				
Transformants	A1552 ΔvipA::FRT-cat-FRT HGT chr 2 ΔVCA0747::FRT-aph-FRT_B (T6SS- prey)	A1552 ΔvipA::FRT-cat-FRT naturally transformed with prey strain Sa5Y ΔvipA::FRT-cat-FRT ΔVCA0747::FRT-aph-FRT ΔcomEC::bla; Rif^R, Kan^R, Cm^R; 20 transformants selected, biological replicate 1	**MB_5217 to MB_5236**	**Experimental condition 5**	**T6SS -**	**T6SS -**	-
Transformants	A1552 ΔvipA::FRT-cat-FRT HGT chr 2 ΔVCA0747::FRT-aph-FRT_B (T6SS- prey)	A1552 ΔvipA::FRT-cat-FRT naturally transformed with prey strain Sa5Y ΔvipA::FRT-cat-FRT ΔVCA0747::FRT-aph-FRT ΔcomEC::bla; Rif^R, Kan^R, Cm^R; 20 transformants selected, biological replicate 2	**MB_5237 to MB_5256**	**Experimental condition 5**	**T6SS -**	**T6SS -**	-
Acceptor strain 6	A1552 (WT)	Wild-type, O1 El Tor Inaba; Rif^R	**MB_5297 (=MB_1)**				
Donor strain 6	Sa5Y ΔlacZ::FRT-aph-FRT comEC::bla	Sa5Y deleted for *lacZ* (*aph* insertion), and for *comEC* (*bla* insertion); Kan^R, Amp^R	**MB_5298**				
Transformants	A1552 HGT chr 1 ΔlacZ::FRT-aph-FRT_A (T6SS+ prey)	A1552 naturally transformed with prey strain Sa5Y ΔlacZ::FRT-aph-FRT ΔcomEC::bla; Rif^R, Kan^R; 20 transformants selected, biological replicate 1	**MB_5257 to MB_5276**	**Experimental condition 6**	**T6SS +**	**T6SS +**	-
Transformants	A1552 HGT chr 1 ΔlacZ::FRT-aph-FRT_A (T6SS+ prey)	A1552 naturally transformed with prey strain Sa5Y ΔlacZ::FRT-aph-FRT ΔcomEC::bla; Rif^R, Kan^R; 20 transformants selected, biological replicate 2	**MB_5277 to MB_5296**	**Experimental condition 6**	**T6SS +**	**T6SS +**	-
Acceptor strain 7	A1552 (WT)	Wild-type, O1 El Tor Inaba; Rif^R	**MB_299 (=MB_1)**				
Donor strain 7	Sa5Y ΔvipA::FRT-cat-FRT ΔlacZ::FRT-aph-FRT comEC::bla	Sa5Y deleted *vipA* (*cat* insertion), for *lacZ* (*aph* insertion), and for *comEC* (*bla* insertion); Kan^R, Cm^R, Amp^R	**MB_5300**				
Transformants	A1552 HGT chr 1 ΔlacZ::FRT-aph-FRT_B (T6SS- prey)	A1552 naturally transformed with prey strain Sa5Y ΔvipA::FRT-cat-FRT ΔlacZ::FRT-aph-FRT ΔcomEC::bla; Rif^R, Kan^R; 20 transformants selected, biological replicate 1	**MB_5301 to MB_5320**	**Experimental condition 7**	**T6SS +**	**T6SS -**	-
Transformants	A1552 HGT chr 1 ΔlacZ::FRT-aph-FRT_B (T6SS- prey)	A1552 naturally transformed with prey strain Sa5Y ΔvipA::FRT-cat-FRT ΔlacZ::FRT-aph-FRT ΔcomEC::bla; Rif^R, Kan^R; 20 transformants selected, biological replicate 2	**MB_5321 to MB_5340**	**Experimental condition 7**	**T6SS +**	**T6SS -**	-
Acceptor strain 8	A1552 (WT)	Wild-type, O1 El Tor Inaba; Rif^R	**MB_5383 (=MB_1)**				
Donor strain 8	Sa5Y ΔlacZ::FRT-aph-FRT comEC::bla	Sa5Y deleted for *lacZ* (*aph* insertion), and for *comEC* (*bla* insertion); Kan^R, Amp^R	**MB_5384 (=MB_5298)**				
Transformants	A1552 HGT chr 1 ΔlacZ::FRT-aph-FRT	A1552 naturally transformed with gDNA of strain Sa5Y ΔlacZ::FRT-aph-FRT ΔcomEC::bla; Rif^R, Kan^R; 20 transformants selected, biological replicate 1	**MB_5385 to MB_5404**	**Experimental condition 8**	**T6SS +**	-	**gDNA**
Transformants	A1552 HGT chr 1 ΔlacZ::FRT-aph-FRT	A1552 naturally transformed with gDNA of strain Sa5Y ΔlacZ::FRT-aph-FRT ΔcomEC::bla; Rif^R, Kan^R; 20 transformants selected, biological replicate 2	**MB_5405 to MB_5424**	**Experimental condition 8**	**T6SS +**	-	**gDNA**

Supplementary file 3.3. Sequence Read Archive (SRA) submission details.

Access-ion	Internal strain No	Library_ID	filename	filename2	strain number within set	library_ strategy	library_ source	library_ layout	plat-form	instrument _model	file type
SRR6935178	4663	4663	4663_R1.fastq.gz	4663_R2.fastq.gz	1	WGS	GENOMIC	paired	ILLUMINA	NextSeq 500	fastq
SRR6935179	4664	4664	4664_R1.fastq.gz	4664_R2.fastq.gz	2	WGS	GENOMIC	paired	ILLUMINA	NextSeq 500	fastq
SRR6935180	4665	4665	4665_R1.fastq.gz	4665_R2.fastq.gz	3	WGS	GENOMIC	paired	ILLUMINA	NextSeq 500	fastq
SRR6935181	4666	4666	4666_R1.fastq.gz	4666_R2.fastq.gz	4	WGS	GENOMIC	paired	ILLUMINA	NextSeq 500	fastq
SRR6935174	4667	4667	4667_R1.fastq.gz	4667_R2.fastq.gz	5	WGS	GENOMIC	paired	ILLUMINA	NextSeq 500	fastq
SRR6935175	4668	4668	4668_R1.fastq.gz	4668_R2.fastq.gz	6	WGS	GENOMIC	paired	ILLUMINA	NextSeq 500	fastq
SRR6935176	4669	4669	4669_R1.fastq.gz	4669_R2.fastq.gz	7	WGS	GENOMIC	paired	ILLUMINA	NextSeq 500	fastq
SRR6935177	4670	4670	4670_R1.fastq.gz	4670_R2.fastq.gz	8	WGS	GENOMIC	paired	ILLUMINA	NextSeq 500	fastq
SRR6935172	4671	4671	4671_R1.fastq.gz	4671_R2.fastq.gz	9	WGS	GENOMIC	paired	ILLUMINA	NextSeq 500	fastq
SRR6935173	4672	4672	4672_R1.fastq.gz	4672_R2.fastq.gz	10	WGS	GENOMIC	paired	ILLUMINA	NextSeq 500	fastq
SRR6934940	4673	4673	4673_R1.fastq.gz	4673_R2.fastq.gz	11	WGS	GENOMIC	paired	ILLUMINA	NextSeq 500	fastq
SRR6934941	4674	4674	4674_R1.fastq.gz	4674_R2.fastq.gz	12	WGS	GENOMIC	paired	ILLUMINA	NextSeq 500	fastq
SRR6934942	4675	4675	4675_R1.fastq.gz	4675_R2.fastq.gz	13	WGS	GENOMIC	paired	ILLUMINA	NextSeq 500	fastq
SRR6934943	4676	4676	4676_R1.fastq.gz	4676_R2.fastq.gz	14	WGS	GENOMIC	paired	ILLUMINA	NextSeq 500	fastq
SRR6934944	4677	4677	4677_R1.fastq.gz	4677_R2.fastq.gz	15	WGS	GENOMIC	paired	ILLUMINA	NextSeq 500	fastq
SRR6934945	4678	4678	4678_R1.fastq.gz	4678_R2.fastq.gz	16	WGS	GENOMIC	paired	ILLUMINA	NextSeq 500	fastq
SRR6934946	4679	4679	4679_R1.fastq.gz	4679_R2.fastq.gz	17	WGS	GENOMIC	paired	ILLUMINA	NextSeq 500	fastq
SRR6934947	4680	4680	4680_R1.fastq.gz	4680_R2.fastq.gz	18	WGS	GENOMIC	paired	ILLUMINA	NextSeq 500	fastq
SRR6934938	4681	4681	4681_R1.fastq.gz	4681_R2.fastq.gz	19	WGS	GENOMIC	paired	ILLUMINA	NextSeq 500	fastq
SRR6934939	4682	4682	4682_R1.fastq.gz	4682_R2.fastq.gz	20	WGS	GENOMIC	paired	ILLUMINA	NextSeq 500	fastq
SRR6935044	4683	4683	4683_R1.fastq.gz	4683_R2.fastq.gz	21	WGS	GENOMIC	paired	ILLUMINA	NextSeq 500	fastq
SRR6935043	4684	4684	4684_R1.fastq.gz	4684_R2.fastq.gz	22	WGS	GENOMIC	paired	ILLUMINA	NextSeq 500	fastq
SRR6935046	4685	4685	4685_R1.fastq.gz	4685_R2.fastq.gz	23	WGS	GENOMIC	paired	ILLUMINA	NextSeq 500	fastq
SRR6935045	4686	4686	4686_R1.fastq.gz	4686_R2.fastq.gz	24	WGS	GENOMIC	paired	ILLUMINA	NextSeq 500	fastq
SRR6935040	4687	4687	4687_R1.fastq.gz	4687_R2.fastq.gz	25	WGS	GENOMIC	paired	ILLUMINA	NextSeq 500	fastq
SRR6935039	4688	4688	4688_R1.fastq.gz	4688_R2.fastq.gz	26	WGS	GENOMIC	paired	ILLUMINA	NextSeq 500	fastq
SRR6935042	4689	4689	4689_R1.fastq.gz	4689_R2.fastq.gz	27	WGS	GENOMIC	paired	ILLUMINA	NextSeq 500	fastq
SRR6935041	4690	4690	4690_R1.fastq.gz	4690_R2.fastq.gz	28	WGS	GENOMIC	paired	ILLUMINA	NextSeq 500	fastq
SRR6935048	4691	4691	4691_R1.fastq.gz	4691_R2.fastq.gz	29	WGS	GENOMIC	paired	ILLUMINA	NextSeq 500	fastq
SRR6935047	4692	4692	4692_R1.fastq.gz	4692_R2.fastq.gz	30	WGS	GENOMIC	paired	ILLUMINA	NextSeq 500	fastq
SRR6935168	4693	4693	4693_R1.fastq.gz	4693_R2.fastq.gz	31	WGS	GENOMIC	paired	ILLUMINA	NextSeq 500	fastq

SRR6935169	4694	4694	4694_R1.fastq.gz	4694_R2.fastq.gz	32	WGS	GENOMIC	paired	ILLUMINA	NextSeq 500	fastq
SRR6935166	4695	4695	4695_R1.fastq.gz	4695_R2.fastq.gz	33	WGS	GENOMIC	paired	ILLUMINA	NextSeq 500	fastq
SRR6935167	4696	4696	4696_R1.fastq.gz	4696_R2.fastq.gz	34	WGS	GENOMIC	paired	ILLUMINA	NextSeq 500	fastq
SRR6935164	4697	4697	4697_R1.fastq.gz	4697_R2.fastq.gz	35	WGS	GENOMIC	paired	ILLUMINA	NextSeq 500	fastq
SRR6935165	4698	4698	4698_R1.fastq.gz	4698_R2.fastq.gz	36	WGS	GENOMIC	paired	ILLUMINA	NextSeq 500	fastq
SRR6935162	4699	4699	4699_R1.fastq.gz	4699_R2.fastq.gz	37	WGS	GENOMIC	paired	ILLUMINA	NextSeq 500	fastq
SRR6935163	4700	4700	4700_R1.fastq.gz	4700_R2.fastq.gz	38	WGS	GENOMIC	paired	ILLUMINA	NextSeq 500	fastq
SRR6935170	4701	4701	4701_R1.fastq.gz	4701_R2.fastq.gz	39	WGS	GENOMIC	paired	ILLUMINA	NextSeq 500	fastq
SRR6935171	4702	4702	4702_R1.fastq.gz	4702_R2.fastq.gz	40	WGS	GENOMIC	paired	ILLUMINA	NextSeq 500	fastq
SRR6934901	4703	4703	4703_R1.fastq.gz	4703_R2.fastq.gz	41	WGS	GENOMIC	paired	ILLUMINA	NextSeq 500	fastq
SRR6934900	4704	4704	4704_R1.fastq.gz	4704_R2.fastq.gz	42	WGS	GENOMIC	paired	ILLUMINA	NextSeq 500	fastq
SRR6934899	4705	4705	4705_R1.fastq.gz	4705_R2.fastq.gz	43	WGS	GENOMIC	paired	ILLUMINA	NextSeq 500	fastq
SRR6934898	4706	4706	4706_R1.fastq.gz	4706_R2.fastq.gz	44	WGS	GENOMIC	paired	ILLUMINA	NextSeq 500	fastq
SRR6934905	4707	4707	4707_R1.fastq.gz	4707_R2.fastq.gz	45	WGS	GENOMIC	paired	ILLUMINA	NextSeq 500	fastq
SRR6934904	4708	4708	4708_R1.fastq.gz	4708_R2.fastq.gz	46	WGS	GENOMIC	paired	ILLUMINA	NextSeq 500	fastq
SRR6934903	4709	4709	4709_R1.fastq.gz	4709_R2.fastq.gz	47	WGS	GENOMIC	paired	ILLUMINA	NextSeq 500	fastq
SRR6934902	4710	4710	4710_R1.fastq.gz	4710_R2.fastq.gz	48	WGS	GENOMIC	paired	ILLUMINA	NextSeq 500	fastq
SRR6934907	4711	4711	4711_R1.fastq.gz	4711_R2.fastq.gz	49	WGS	GENOMIC	paired	ILLUMINA	NextSeq 500	fastq
SRR6934906	4712	4712	4712_R1.fastq.gz	4712_R2.fastq.gz	50	WGS	GENOMIC	paired	ILLUMINA	NextSeq 500	fastq
SRR6935005	4713	4713	4713_R1.fastq.gz	4713_R2.fastq.gz	51	WGS	GENOMIC	paired	ILLUMINA	NextSeq 500	fastq
SRR6935006	4714	4714	4714_R1.fastq.gz	4714_R2.fastq.gz	52	WGS	GENOMIC	paired	ILLUMINA	NextSeq 500	fastq
SRR6935007	4715	4715	4715_R1.fastq.gz	4715_R2.fastq.gz	53	WGS	GENOMIC	paired	ILLUMINA	NextSeq 500	fastq
SRR6935008	4716	4716	4716_R1.fastq.gz	4716_R2.fastq.gz	54	WGS	GENOMIC	paired	ILLUMINA	NextSeq 500	fastq
SRR6935001	4717	4717	4717_R1.fastq.gz	4717_R2.fastq.gz	55	WGS	GENOMIC	paired	ILLUMINA	NextSeq 500	fastq
SRR6935002	4718	4718	4718_R1.fastq.gz	4718_R2.fastq.gz	56	WGS	GENOMIC	paired	ILLUMINA	NextSeq 500	fastq
SRR6935003	4719	4719	4719_R1.fastq.gz	4719_R2.fastq.gz	57	WGS	GENOMIC	paired	ILLUMINA	NextSeq 500	fastq
SRR6935004	4720	4720	4720_R1.fastq.gz	4720_R2.fastq.gz	58	WGS	GENOMIC	paired	ILLUMINA	NextSeq 500	fastq
SRR6934999	4721	4721	4721_R1.fastq.gz	4721_R2.fastq.gz	59	WGS	GENOMIC	paired	ILLUMINA	NextSeq 500	fastq
SRR6935000	4722	4722	4722_R1.fastq.gz	4722_R2.fastq.gz	60	WGS	GENOMIC	paired	ILLUMINA	NextSeq 500	fastq
SRR6935110	5343	5343	5343_R1.fastq.gz	5343_R2.fastq.gz	1	WGS	GENOMIC	paired	ILLUMINA	NextSeq 500	fastq
SRR6935109	5344	5344	5344_R1.fastq.gz	5344_R2.fastq.gz	2	WGS	GENOMIC	paired	ILLUMINA	NextSeq 500	fastq
SRR6935112	5345	5345	5345_R1.fastq.gz	5345_R2.fastq.gz	3	WGS	GENOMIC	paired	ILLUMINA	NextSeq 500	fastq
SRR6935111	5346	5346	5346_R1.fastq.gz	5346_R2.fastq.gz	4	WGS	GENOMIC	paired	ILLUMINA	NextSeq 500	fastq
SRR6935114	5347	5347	5347_R1.fastq.gz	5347_R2.fastq.gz	5	WGS	GENOMIC	paired	ILLUMINA	NextSeq 500	fastq
SRR6935113	5348	5348	5348_R1.fastq.gz	5348_R2.fastq.gz	6	WGS	GENOMIC	paired	ILLUMINA	NextSeq 500	fastq

SRR6935116	5349	5349	5349_R1.fastq.gz	5349_R2.fastq.gz	7	WGS	GENOMIC	paired	ILLUMINA	NextSeq 500	fastq
SRR6935115	5350	5350	5350_R1.fastq.gz	5350_R2.fastq.gz	8	WGS	GENOMIC	paired	ILLUMINA	NextSeq 500	fastq
SRR6935108	5351	5351	5351_R1.fastq.gz	5351_R2.fastq.gz	9	WGS	GENOMIC	paired	ILLUMINA	NextSeq 500	fastq
SRR6935107	5352	5352	5352_R1.fastq.gz	5352_R2.fastq.gz	10	WGS	GENOMIC	paired	ILLUMINA	NextSeq 500	fastq
SRR6934862	5353	5353	5353_R1.fastq.gz	5353_R2.fastq.gz	11	WGS	GENOMIC	paired	ILLUMINA	NextSeq 500	fastq
SRR6934863	5354	5354	5354_R1.fastq.gz	5354_R2.fastq.gz	12	WGS	GENOMIC	paired	ILLUMINA	NextSeq 500	fastq
SRR6934860	5355	5355	5355_R1.fastq.gz	5355_R2.fastq.gz	13	WGS	GENOMIC	paired	ILLUMINA	NextSeq 500	fastq
SRR6934861	5356	5356	5356_R1.fastq.gz	5356_R2.fastq.gz	14	WGS	GENOMIC	paired	ILLUMINA	NextSeq 500	fastq
SRR6934866	5357	5357	5357_R1.fastq.gz	5357_R2.fastq.gz	15	WGS	GENOMIC	paired	ILLUMINA	NextSeq 500	fastq
SRR6934867	5358	5358	5358_R1.fastq.gz	5358_R2.fastq.gz	16	WGS	GENOMIC	paired	ILLUMINA	NextSeq 500	fastq
SRR6934864	5359	5359	5359_R1.fastq.gz	5359_R2.fastq.gz	17	WGS	GENOMIC	paired	ILLUMINA	NextSeq 500	fastq
SRR6934865	5360	5360	5360_R1.fastq.gz	5360_R2.fastq.gz	18	WGS	GENOMIC	paired	ILLUMINA	NextSeq 500	fastq
SRR6934858	5361	5361	5361_R1.fastq.gz	5361_R2.fastq.gz	19	WGS	GENOMIC	paired	ILLUMINA	NextSeq 500	fastq
SRR6934859	5362	5362	5362_R1.fastq.gz	5362_R2.fastq.gz	20	WGS	GENOMIC	paired	ILLUMINA	NextSeq 500	fastq
SRR6934955	5363	5363	5363_R1.fastq.gz	5363_R2.fastq.gz	21	WGS	GENOMIC	paired	ILLUMINA	NextSeq 500	fastq
SRR6934954	5364	5364	5364_R1.fastq.gz	5364_R2.fastq.gz	22	WGS	GENOMIC	paired	ILLUMINA	NextSeq 500	fastq
SRR6934953	5365	5365	5365_R1.fastq.gz	5365_R2.fastq.gz	23	WGS	GENOMIC	paired	ILLUMINA	NextSeq 500	fastq
SRR6934952	5366	5366	5366_R1.fastq.gz	5366_R2.fastq.gz	24	WGS	GENOMIC	paired	ILLUMINA	NextSeq 500	fastq
SRR6934951	5367	5367	5367_R1.fastq.gz	5367_R2.fastq.gz	25	WGS	GENOMIC	paired	ILLUMINA	NextSeq 500	fastq
SRR6934950	5368	5368	5368_R1.fastq.gz	5368_R2.fastq.gz	26	WGS	GENOMIC	paired	ILLUMINA	NextSeq 500	fastq
SRR6934949	5369	5369	5369_R1.fastq.gz	5369_R2.fastq.gz	27	WGS	GENOMIC	paired	ILLUMINA	NextSeq 500	fastq
SRR6934948	5370	5370	5370_R1.fastq.gz	5370_R2.fastq.gz	28	WGS	GENOMIC	paired	ILLUMINA	NextSeq 500	fastq
SRR6934957	5371	5371	5371_R1.fastq.gz	5371_R2.fastq.gz	29	WGS	GENOMIC	paired	ILLUMINA	NextSeq 500	fastq
SRR6934956	5372	5372	5372_R1.fastq.gz	5372_R2.fastq.gz	30	WGS	GENOMIC	paired	ILLUMINA	NextSeq 500	fastq
SRR6935049	5373	5373	5373_R1.fastq.gz	5373_R2.fastq.gz	31	WGS	GENOMIC	paired	ILLUMINA	NextSeq 500	fastq
SRR6935050	5374	5374	5374_R1.fastq.gz	5374_R2.fastq.gz	32	WGS	GENOMIC	paired	ILLUMINA	NextSeq 500	fastq
SRR6935051	5375	5375	5375_R1.fastq.gz	5375_R2.fastq.gz	33	WGS	GENOMIC	paired	ILLUMINA	NextSeq 500	fastq
SRR6935052	5376	5376	5376_R1.fastq.gz	5376_R2.fastq.gz	34	WGS	GENOMIC	paired	ILLUMINA	NextSeq 500	fastq
SRR6935053	5377	5377	5377_R1.fastq.gz	5377_R2.fastq.gz	35	WGS	GENOMIC	paired	ILLUMINA	NextSeq 500	fastq
SRR6935054	5378	5378	5378_R1.fastq.gz	5378_R2.fastq.gz	36	WGS	GENOMIC	paired	ILLUMINA	NextSeq 500	fastq
SRR6935055	5379	5379	5379_R1.fastq.gz	5379_R2.fastq.gz	37	WGS	GENOMIC	paired	ILLUMINA	NextSeq 500	fastq
SRR6935056	5380	5380	5380_R1.fastq.gz	5380_R2.fastq.gz	38	WGS	GENOMIC	paired	ILLUMINA	NextSeq 500	fastq
SRR6935057	5381	5381	5381_R1.fastq.gz	5381_R2.fastq.gz	39	WGS	GENOMIC	paired	ILLUMINA	NextSeq 500	fastq
SRR6935058	5382	5382	5382_R1.fastq.gz	5382_R2.fastq.gz	40	WGS	GENOMIC	paired	ILLUMINA	NextSeq 500	fastq
SRR6934937	4723	4723	4723_R1.fastq.gz	4723_R2.fastq.gz	1	WGS	GENOMIC	paired	ILLUMINA	NextSeq 500	fastq

SRR6934936	4724	4724	4724_R1.fastq.gz	4724_R2.fastq.gz	2	WGS	GENOMIC	paired	ILLUMINA	NextSeq 500	fastq
SRR6934935	4725	4725	4725_R1.fastq.gz	4725_R2.fastq.gz	3	WGS	GENOMIC	paired	ILLUMINA	NextSeq 500	fastq
SRR6934934	4726	4726	4726_R1.fastq.gz	4726_R2.fastq.gz	4	WGS	GENOMIC	paired	ILLUMINA	NextSeq 500	fastq
SRR6934933	4727	4727	4727_R1.fastq.gz	4727_R2.fastq.gz	5	WGS	GENOMIC	paired	ILLUMINA	NextSeq 500	fastq
SRR6934932	4728	4728	4728_R1.fastq.gz	4728_R2.fastq.gz	6	WGS	GENOMIC	paired	ILLUMINA	NextSeq 500	fastq
SRR6934931	4729	4729	4729_R1.fastq.gz	4729_R2.fastq.gz	7	WGS	GENOMIC	paired	ILLUMINA	NextSeq 500	fastq
SRR6934930	4730	4730	4730_R1.fastq.gz	4730_R2.fastq.gz	8	WGS	GENOMIC	paired	ILLUMINA	NextSeq 500	fastq
SRR6934929	4731	4731	4731_R1.fastq.gz	4731_R2.fastq.gz	9	WGS	GENOMIC	paired	ILLUMINA	NextSeq 500	fastq
SRR6934928	4732	4732	4732_R1.fastq.gz	4732_R2.fastq.gz	10	WGS	GENOMIC	paired	ILLUMINA	NextSeq 500	fastq
SRR6934842	4733	4733	4733_R1.fastq.gz	4733_R2.fastq.gz	11	WGS	GENOMIC	paired	ILLUMINA	NextSeq 500	fastq
SRR6934843	4734	4734	4734_R1.fastq.gz	4734_R2.fastq.gz	12	WGS	GENOMIC	paired	ILLUMINA	NextSeq 500	fastq
SRR6935025	4735	4735	4735_R1.fastq.gz	4735_R2.fastq.gz	13	WGS	GENOMIC	paired	ILLUMINA	NextSeq 500	fastq
SRR6935026	4736	4736	4736_R1.fastq.gz	4736_R2.fastq.gz	14	WGS	GENOMIC	paired	ILLUMINA	NextSeq 500	fastq
SRR6934846	4737	4737	4737_R1.fastq.gz	4737_R2.fastq.gz	15	WGS	GENOMIC	paired	ILLUMINA	NextSeq 500	fastq
SRR6934847	4738	4738	4738_R1.fastq.gz	4738_R2.fastq.gz	16	WGS	GENOMIC	paired	ILLUMINA	NextSeq 500	fastq
SRR6934848	4739	4739	4739_R1.fastq.gz	4739_R2.fastq.gz	17	WGS	GENOMIC	paired	ILLUMINA	NextSeq 500	fastq
SRR6934849	4740	4740	4740_R1.fastq.gz	4740_R2.fastq.gz	18	WGS	GENOMIC	paired	ILLUMINA	NextSeq 500	fastq
SRR6935027	4741	4741	4741_R1.fastq.gz	4741_R2.fastq.gz	19	WGS	GENOMIC	paired	ILLUMINA	NextSeq 500	fastq
SRR6935028	4742	4742	4742_R1.fastq.gz	4742_R2.fastq.gz	20	WGS	GENOMIC	paired	ILLUMINA	NextSeq 500	fastq
SRR6935140	4743	4743	4743_R1.fastq.gz	4743_R2.fastq.gz	21	WGS	GENOMIC	paired	ILLUMINA	NextSeq 500	fastq
SRR6935139	4744	4744	4744_R1.fastq.gz	4744_R2.fastq.gz	22	WGS	GENOMIC	paired	ILLUMINA	NextSeq 500	fastq
SRR6935142	4745	4745	4745_R1.fastq.gz	4745_R2.fastq.gz	23	WGS	GENOMIC	paired	ILLUMINA	NextSeq 500	fastq
SRR6935141	4746	4746	4746_R1.fastq.gz	4746_R2.fastq.gz	24	WGS	GENOMIC	paired	ILLUMINA	NextSeq 500	fastq
SRR6935144	4747	4747	4747_R1.fastq.gz	4747_R2.fastq.gz	25	WGS	GENOMIC	paired	ILLUMINA	NextSeq 500	fastq
SRR6935143	4748	4748	4748_R1.fastq.gz	4748_R2.fastq.gz	26	WGS	GENOMIC	paired	ILLUMINA	NextSeq 500	fastq
SRR6935146	4749	4749	4749_R1.fastq.gz	4749_R2.fastq.gz	27	WGS	GENOMIC	paired	ILLUMINA	NextSeq 500	fastq
SRR6935145	4750	4750	4750_R1.fastq.gz	4750_R2.fastq.gz	28	WGS	GENOMIC	paired	ILLUMINA	NextSeq 500	fastq
SRR6935138	4751	4751	4751_R1.fastq.gz	4751_R2.fastq.gz	29	WGS	GENOMIC	paired	ILLUMINA	NextSeq 500	fastq
SRR6935137	4752	4752	4752_R1.fastq.gz	4752_R2.fastq.gz	30	WGS	GENOMIC	paired	ILLUMINA	NextSeq 500	fastq
SRR6935033	4753	4753	4753_R1.fastq.gz	4753_R2.fastq.gz	31	WGS	GENOMIC	paired	ILLUMINA	NextSeq 500	fastq
SRR6935034	4754	4754	4754_R1.fastq.gz	4754_R2.fastq.gz	32	WGS	GENOMIC	paired	ILLUMINA	NextSeq 500	fastq
SRR6935031	4755	4755	4755_R1.fastq.gz	4755_R2.fastq.gz	33	WGS	GENOMIC	paired	ILLUMINA	NextSeq 500	fastq
SRR6935032	4756	4756	4756_R1.fastq.gz	4756_R2.fastq.gz	34	WGS	GENOMIC	paired	ILLUMINA	NextSeq 500	fastq
SRR6935037	4757	4757	4757_R1.fastq.gz	4757_R2.fastq.gz	35	WGS	GENOMIC	paired	ILLUMINA	NextSeq 500	fastq
SRR6935038	4758	4758	4758_R1.fastq.gz	4758_R2.fastq.gz	36	WGS	GENOMIC	paired	ILLUMINA	NextSeq 500	fastq

SRR6935035	4759	4759	4759_R1.fastq.gz	4759_R2.fastq.gz	37	WGS	GENOMIC	paired	ILLUMINA	NextSeq 500	fastq
SRR6935036	4760	4760	4760_R1.fastq.gz	4760_R2.fastq.gz	38	WGS	GENOMIC	paired	ILLUMINA	NextSeq 500	fastq
SRR6935029	4761	4761	4761_R1.fastq.gz	4761_R2.fastq.gz	39	WGS	GENOMIC	paired	ILLUMINA	NextSeq 500	fastq
SRR6935030	4762	4762	4762_R1.fastq.gz	4762_R2.fastq.gz	40	WGS	GENOMIC	paired	ILLUMINA	NextSeq 500	fastq
SRR6934893	4763	4763	4763_R1.fastq.gz	4763_R2.fastq.gz	41	WGS	GENOMIC	paired	ILLUMINA	NextSeq 500	fastq
SRR6934892	4764	4764	4764_R1.fastq.gz	4764_R2.fastq.gz	42	WGS	GENOMIC	paired	ILLUMINA	NextSeq 500	fastq
SRR6934891	4765	4765	4765_R1.fastq.gz	4765_R2.fastq.gz	43	WGS	GENOMIC	paired	ILLUMINA	NextSeq 500	fastq
SRR6934890	4766	4766	4766_R1.fastq.gz	4766_R2.fastq.gz	44	WGS	GENOMIC	paired	ILLUMINA	NextSeq 500	fastq
SRR6934897	4767	4767	4767_R1.fastq.gz	4767_R2.fastq.gz	45	WGS	GENOMIC	paired	ILLUMINA	NextSeq 500	fastq
SRR6934896	4768	4768	4768_R1.fastq.gz	4768_R2.fastq.gz	46	WGS	GENOMIC	paired	ILLUMINA	NextSeq 500	fastq
SRR6934895	4769	4769	4769_R1.fastq.gz	4769_R2.fastq.gz	47	WGS	GENOMIC	paired	ILLUMINA	NextSeq 500	fastq
SRR6934894	4770	4770	4770_R1.fastq.gz	4770_R2.fastq.gz	48	WGS	GENOMIC	paired	ILLUMINA	NextSeq 500	fastq
SRR6934889	4771	4771	4771_R1.fastq.gz	4771_R2.fastq.gz	49	WGS	GENOMIC	paired	ILLUMINA	NextSeq 500	fastq
SRR6934888	4772	4772	4772_R1.fastq.gz	4772_R2.fastq.gz	50	WGS	GENOMIC	paired	ILLUMINA	NextSeq 500	fastq
SRR6935158	4773	4773	4773_R1.fastq.gz	4773_R2.fastq.gz	51	WGS	GENOMIC	paired	ILLUMINA	NextSeq 500	fastq
SRR6935159	4774	4774	4774_R1.fastq.gz	4774_R2.fastq.gz	52	WGS	GENOMIC	paired	ILLUMINA	NextSeq 500	fastq
SRR6935160	4775	4775	4775_R1.fastq.gz	4775_R2.fastq.gz	53	WGS	GENOMIC	paired	ILLUMINA	NextSeq 500	fastq
SRR6935161	4776	4776	4776_R1.fastq.gz	4776_R2.fastq.gz	54	WGS	GENOMIC	paired	ILLUMINA	NextSeq 500	fastq
SRR6935154	4777	4777	4777_R1.fastq.gz	4777_R2.fastq.gz	55	WGS	GENOMIC	paired	ILLUMINA	NextSeq 500	fastq
SRR6935155	4778	4778	4778_R1.fastq.gz	4778_R2.fastq.gz	56	WGS	GENOMIC	paired	ILLUMINA	NextSeq 500	fastq
SRR6935156	4779	4779	4779_R1.fastq.gz	4779_R2.fastq.gz	57	WGS	GENOMIC	paired	ILLUMINA	NextSeq 500	fastq
SRR6935157	4780	4780	4780_R1.fastq.gz	4780_R2.fastq.gz	58	WGS	GENOMIC	paired	ILLUMINA	NextSeq 500	fastq
SRR6935152	4781	4781	4781_R1.fastq.gz	4781_R2.fastq.gz	59	WGS	GENOMIC	paired	ILLUMINA	NextSeq 500	fastq
SRR6935153	4782	4782	4782_R1.fastq.gz	4782_R2.fastq.gz	60	WGS	GENOMIC	paired	ILLUMINA	NextSeq 500	fastq
SRR6935148	5175	5175	5175_R1.fastq.gz	5175_R2.fastq.gz	1	WGS	GENOMIC	paired	ILLUMINA	NextSeq 500	fastq
SRR6935147	5176	5176	5176_R1.fastq.gz	5176_R2.fastq.gz	2	WGS	GENOMIC	paired	ILLUMINA	NextSeq 500	fastq
SRR6935088	5177	5177	5177_R1.fastq.gz	5177_R2.fastq.gz	3	WGS	GENOMIC	paired	ILLUMINA	NextSeq 500	fastq
SRR6935087	5178	5178	5178_R1.fastq.gz	5178_R2.fastq.gz	4	WGS	GENOMIC	paired	ILLUMINA	NextSeq 500	fastq
SRR6935082	5179	5179	5179_R1.fastq.gz	5179_R2.fastq.gz	5	WGS	GENOMIC	paired	ILLUMINA	NextSeq 500	fastq
SRR6935081	5180	5180	5180_R1.fastq.gz	5180_R2.fastq.gz	6	WGS	GENOMIC	paired	ILLUMINA	NextSeq 500	fastq
SRR6935084	5181	5181	5181_R1.fastq.gz	5181_R2.fastq.gz	7	WGS	GENOMIC	paired	ILLUMINA	NextSeq 500	fastq
SRR6935083	5182	5182	5182_R1.fastq.gz	5182_R2.fastq.gz	8	WGS	GENOMIC	paired	ILLUMINA	NextSeq 500	fastq
SRR6935151	5183	5183	5183_R1.fastq.gz	5183_R2.fastq.gz	9	WGS	GENOMIC	paired	ILLUMINA	NextSeq 500	fastq
SRR6935150	5184	5184	5184_R1.fastq.gz	5184_R2.fastq.gz	10	WGS	GENOMIC	paired	ILLUMINA	NextSeq 500	fastq
SRR6934985	5185	5185	5185_R1.fastq.gz	5185_R2.fastq.gz	11	WGS	GENOMIC	paired	ILLUMINA	NextSeq 500	fastq

SRR6934986	5186	5186	5186_R1.fastq.gz	5186_R2.fastq.gz	12	WGS	GENOMIC	paired	ILLUMINA	NextSeq 500	fastq
SRR6934983	5187	5187	5187_R1.fastq.gz	5187_R2.fastq.gz	13	WGS	GENOMIC	paired	ILLUMINA	NextSeq 500	fastq
SRR6934984	5188	5188	5188_R1.fastq.gz	5188_R2.fastq.gz	14	WGS	GENOMIC	paired	ILLUMINA	NextSeq 500	fastq
SRR6934981	5189	5189	5189_R1.fastq.gz	5189_R2.fastq.gz	15	WGS	GENOMIC	paired	ILLUMINA	NextSeq 500	fastq
SRR6934982	5190	5190	5190_R1.fastq.gz	5190_R2.fastq.gz	16	WGS	GENOMIC	paired	ILLUMINA	NextSeq 500	fastq
SRR6934979	5191	5191	5191_R1.fastq.gz	5191_R2.fastq.gz	17	WGS	GENOMIC	paired	ILLUMINA	NextSeq 500	fastq
SRR6934980	5192	5192	5192_R1.fastq.gz	5192_R2.fastq.gz	18	WGS	GENOMIC	paired	ILLUMINA	NextSeq 500	fastq
SRR6934987	5193	5193	5193_R1.fastq.gz	5193_R2.fastq.gz	19	WGS	GENOMIC	paired	ILLUMINA	NextSeq 500	fastq
SRR6934988	5194	5194	5194_R1.fastq.gz	5194_R2.fastq.gz	20	WGS	GENOMIC	paired	ILLUMINA	NextSeq 500	fastq
SRR6935060	5195	5195	5195_R1.fastq.gz	5195_R2.fastq.gz	21	WGS	GENOMIC	paired	ILLUMINA	NextSeq 500	fastq
SRR6935059	5196	5196	5196_R1.fastq.gz	5196_R2.fastq.gz	22	WGS	GENOMIC	paired	ILLUMINA	NextSeq 500	fastq
SRR6935014	5197	5197	5197_R1.fastq.gz	5197_R2.fastq.gz	23	WGS	GENOMIC	paired	ILLUMINA	NextSeq 500	fastq
SRR6935013	5198	5198	5198_R1.fastq.gz	5198_R2.fastq.gz	24	WGS	GENOMIC	paired	ILLUMINA	NextSeq 500	fastq
SRR6935012	5199	5199	5199_R1.fastq.gz	5199_R2.fastq.gz	25	WGS	GENOMIC	paired	ILLUMINA	NextSeq 500	fastq
SRR6935011	5200	5200	5200_R1.fastq.gz	5200_R2.fastq.gz	26	WGS	GENOMIC	paired	ILLUMINA	NextSeq 500	fastq
SRR6935010	5201	5201	5201_R1.fastq.gz	5201_R2.fastq.gz	27	WGS	GENOMIC	paired	ILLUMINA	NextSeq 500	fastq
SRR6935009	5202	5202	5202_R1.fastq.gz	5202_R2.fastq.gz	28	WGS	GENOMIC	paired	ILLUMINA	NextSeq 500	fastq
SRR6935078	5203	5203	5203_R1.fastq.gz	5203_R2.fastq.gz	29	WGS	GENOMIC	paired	ILLUMINA	NextSeq 500	fastq
SRR6935077	5204	5204	5204_R1.fastq.gz	5204_R2.fastq.gz	30	WGS	GENOMIC	paired	ILLUMINA	NextSeq 500	fastq
SRR6934910	5205	5205	5205_R1.fastq.gz	5205_R2.fastq.gz	31	WGS	GENOMIC	paired	ILLUMINA	NextSeq 500	fastq
SRR6934911	5206	5206	5206_R1.fastq.gz	5206_R2.fastq.gz	32	WGS	GENOMIC	paired	ILLUMINA	NextSeq 500	fastq
SRR6934912	5207	5207	5207_R1.fastq.gz	5207_R2.fastq.gz	33	WGS	GENOMIC	paired	ILLUMINA	NextSeq 500	fastq
SRR6934913	5208	5208	5208_R1.fastq.gz	5208_R2.fastq.gz	34	WGS	GENOMIC	paired	ILLUMINA	NextSeq 500	fastq
SRR6934914	5209	5209	5209_R1.fastq.gz	5209_R2.fastq.gz	35	WGS	GENOMIC	paired	ILLUMINA	NextSeq 500	fastq
SRR6934915	5210	5210	5210_R1.fastq.gz	5210_R2.fastq.gz	36	WGS	GENOMIC	paired	ILLUMINA	NextSeq 500	fastq
SRR6934916	5211	5211	5211_R1.fastq.gz	5211_R2.fastq.gz	37	WGS	GENOMIC	paired	ILLUMINA	NextSeq 500	fastq
SRR6934917	5212	5212	5212_R1.fastq.gz	5212_R2.fastq.gz	38	WGS	GENOMIC	paired	ILLUMINA	NextSeq 500	fastq
SRR6934908	5213	5213	5213_R1.fastq.gz	5213_R2.fastq.gz	39	WGS	GENOMIC	paired	ILLUMINA	NextSeq 500	fastq
SRR6934909	5214	5214	5214_R1.fastq.gz	5214_R2.fastq.gz	40	WGS	GENOMIC	paired	ILLUMINA	NextSeq 500	fastq
SRR6934836	5217	5217	5217_R1.fastq.gz	5217_R2.fastq.gz	1	WGS	GENOMIC	paired	ILLUMINA	NextSeq 500	fastq
SRR6934837	5218	5218	5218_R1.fastq.gz	5218_R2.fastq.gz	2	WGS	GENOMIC	paired	ILLUMINA	NextSeq 500	fastq
SRR6934838	5219	5219	5219_R1.fastq.gz	5219_R2.fastq.gz	3	WGS	GENOMIC	paired	ILLUMINA	NextSeq 500	fastq
SRR6934839	5220	5220	5220_R1.fastq.gz	5220_R2.fastq.gz	4	WGS	GENOMIC	paired	ILLUMINA	NextSeq 500	fastq
SRR6934832	5221	5221	5221_R1.fastq.gz	5221_R2.fastq.gz	5	WGS	GENOMIC	paired	ILLUMINA	NextSeq 500	fastq
SRR6934833	5222	5222	5222_R1.fastq.gz	5222_R2.fastq.gz	6	WGS	GENOMIC	paired	ILLUMINA	NextSeq 500	fastq

SRR6934834	5223	5223	5223_R1.fastq.gz	5223_R2.fastq.gz	7	WGS	GENOMIC	paired	ILLUMINA	NextSeq 500	fastq
SRR6934835	5224	5224	5224_R1.fastq.gz	5224_R2.fastq.gz	8	WGS	GENOMIC	paired	ILLUMINA	NextSeq 500	fastq
SRR6934840	5225	5225	5225_R1.fastq.gz	5225_R2.fastq.gz	9	WGS	GENOMIC	paired	ILLUMINA	NextSeq 500	fastq
SRR6934841	5226	5226	5226_R1.fastq.gz	5226_R2.fastq.gz	10	WGS	GENOMIC	paired	ILLUMINA	NextSeq 500	fastq
SRR6934921	5227	5227	5227_R1.fastq.gz	5227_R2.fastq.gz	11	WGS	GENOMIC	paired	ILLUMINA	NextSeq 500	fastq
SRR6934920	5228	5228	5228_R1.fastq.gz	5228_R2.fastq.gz	12	WGS	GENOMIC	paired	ILLUMINA	NextSeq 500	fastq
SRR6934919	5229	5229	5229_R1.fastq.gz	5229_R2.fastq.gz	13	WGS	GENOMIC	paired	ILLUMINA	NextSeq 500	fastq
SRR6934918	5230	5230	5230_R1.fastq.gz	5230_R2.fastq.gz	14	WGS	GENOMIC	paired	ILLUMINA	NextSeq 500	fastq
SRR6934925	5231	5231	5231_R1.fastq.gz	5231_R2.fastq.gz	15	WGS	GENOMIC	paired	ILLUMINA	NextSeq 500	fastq
SRR6934924	5232	5232	5232_R1.fastq.gz	5232_R2.fastq.gz	16	WGS	GENOMIC	paired	ILLUMINA	NextSeq 500	fastq
SRR6934923	5233	5233	5233_R1.fastq.gz	5233_R2.fastq.gz	17	WGS	GENOMIC	paired	ILLUMINA	NextSeq 500	fastq
SRR6934922	5234	5234	5234_R1.fastq.gz	5234_R2.fastq.gz	18	WGS	GENOMIC	paired	ILLUMINA	NextSeq 500	fastq
SRR6934927	5235	5235	5235_R1.fastq.gz	5235_R2.fastq.gz	19	WGS	GENOMIC	paired	ILLUMINA	NextSeq 500	fastq
SRR6934926	5236	5236	5236_R1.fastq.gz	5236_R2.fastq.gz	20	WGS	GENOMIC	paired	ILLUMINA	NextSeq 500	fastq
SRR6935023	5237	5237	5237_R1.fastq.gz	5237_R2.fastq.gz	21	WGS	GENOMIC	paired	ILLUMINA	NextSeq 500	fastq
SRR6935024	5238	5238	5238_R1.fastq.gz	5238_R2.fastq.gz	22	WGS	GENOMIC	paired	ILLUMINA	NextSeq 500	fastq
SRR6935021	5239	5239	5239_R1.fastq.gz	5239_R2.fastq.gz	23	WGS	GENOMIC	paired	ILLUMINA	NextSeq 500	fastq
SRR6935022	5240	5240	5240_R1.fastq.gz	5240_R2.fastq.gz	24	WGS	GENOMIC	paired	ILLUMINA	NextSeq 500	fastq
SRR6935019	5241	5241	5241_R1.fastq.gz	5241_R2.fastq.gz	25	WGS	GENOMIC	paired	ILLUMINA	NextSeq 500	fastq
SRR6935020	5242	5242	5242_R1.fastq.gz	5242_R2.fastq.gz	26	WGS	GENOMIC	paired	ILLUMINA	NextSeq 500	fastq
SRR6935017	5243	5243	5243_R1.fastq.gz	5243_R2.fastq.gz	27	WGS	GENOMIC	paired	ILLUMINA	NextSeq 500	fastq
SRR6935018	5244	5244	5244_R1.fastq.gz	5244_R2.fastq.gz	28	WGS	GENOMIC	paired	ILLUMINA	NextSeq 500	fastq
SRR6935015	5245	5245	5245_R1.fastq.gz	5245_R2.fastq.gz	29	WGS	GENOMIC	paired	ILLUMINA	NextSeq 500	fastq
SRR6935016	5246	5246	5246_R1.fastq.gz	5246_R2.fastq.gz	30	WGS	GENOMIC	paired	ILLUMINA	NextSeq 500	fastq
SRR6935124	5247	5247	5247_R1.fastq.gz	5247_R2.fastq.gz	31	WGS	GENOMIC	paired	ILLUMINA	NextSeq 500	fastq
SRR6935123	5248	5248	5248_R1.fastq.gz	5248_R2.fastq.gz	32	WGS	GENOMIC	paired	ILLUMINA	NextSeq 500	fastq
SRR6935126	5249	5249	5249_R1.fastq.gz	5249_R2.fastq.gz	33	WGS	GENOMIC	paired	ILLUMINA	NextSeq 500	fastq
SRR6935125	5250	5250	5250_R1.fastq.gz	5250_R2.fastq.gz	34	WGS	GENOMIC	paired	ILLUMINA	NextSeq 500	fastq
SRR6935120	5251	5251	5251_R1.fastq.gz	5251_R2.fastq.gz	35	WGS	GENOMIC	paired	ILLUMINA	NextSeq 500	fastq
SRR6935119	5252	5252	5252_R1.fastq.gz	5252_R2.fastq.gz	36	WGS	GENOMIC	paired	ILLUMINA	NextSeq 500	fastq
SRR6935122	5253	5253	5253_R1.fastq.gz	5253_R2.fastq.gz	37	WGS	GENOMIC	paired	ILLUMINA	NextSeq 500	fastq
SRR6935121	5254	5254	5254_R1.fastq.gz	5254_R2.fastq.gz	38	WGS	GENOMIC	paired	ILLUMINA	NextSeq 500	fastq
SRR6935118	5255	5255	5255_R1.fastq.gz	5255_R2.fastq.gz	39	WGS	GENOMIC	paired	ILLUMINA	NextSeq 500	fastq
SRR6935117	5256	5256	5256_R1.fastq.gz	5256_R2.fastq.gz	40	WGS	GENOMIC	paired	ILLUMINA	NextSeq 500	fastq
SRR6934870	5257	5257	5257_R1.fastq.gz	5257_R2.fastq.gz	1	WGS	GENOMIC	paired	ILLUMINA	NextSeq 500	fastq

SRR6934871	5258	5258	5258_R1.fastq.gz	5258_R2.fastq.gz	2	WGS	GENOMIC	paired	ILLUMINA	NextSeq 500	fastq
SRR6934872	5259	5259	5259_R1.fastq.gz	5259_R2.fastq.gz	3	WGS	GENOMIC	paired	ILLUMINA	NextSeq 500	fastq
SRR6934873	5260	5260	5260_R1.fastq.gz	5260_R2.fastq.gz	4	WGS	GENOMIC	paired	ILLUMINA	NextSeq 500	fastq
SRR6934874	5261	5261	5261_R1.fastq.gz	5261_R2.fastq.gz	5	WGS	GENOMIC	paired	ILLUMINA	NextSeq 500	fastq
SRR6934875	5262	5262	5262_R1.fastq.gz	5262_R2.fastq.gz	6	WGS	GENOMIC	paired	ILLUMINA	NextSeq 500	fastq
SRR6934876	5263	5263	5263_R1.fastq.gz	5263_R2.fastq.gz	7	WGS	GENOMIC	paired	ILLUMINA	NextSeq 500	fastq
SRR6934877	5264	5264	5264_R1.fastq.gz	5264_R2.fastq.gz	8	WGS	GENOMIC	paired	ILLUMINA	NextSeq 500	fastq
SRR6934868	5265	5265	5265_R1.fastq.gz	5265_R2.fastq.gz	9	WGS	GENOMIC	paired	ILLUMINA	NextSeq 500	fastq
SRR6934869	5266	5266	5266_R1.fastq.gz	5266_R2.fastq.gz	10	WGS	GENOMIC	paired	ILLUMINA	NextSeq 500	fastq
SRR6934965	5267	5267	5267_R1.fastq.gz	5267_R2.fastq.gz	11	WGS	GENOMIC	paired	ILLUMINA	NextSeq 500	fastq
SRR6934964	5268	5268	5268_R1.fastq.gz	5268_R2.fastq.gz	12	WGS	GENOMIC	paired	ILLUMINA	NextSeq 500	fastq
SRR6934963	5269	5269	5269_R1.fastq.gz	5269_R2.fastq.gz	13	WGS	GENOMIC	paired	ILLUMINA	NextSeq 500	fastq
SRR6934962	5270	5270	5270_R1.fastq.gz	5270_R2.fastq.gz	14	WGS	GENOMIC	paired	ILLUMINA	NextSeq 500	fastq
SRR6934961	5271	5271	5271_R1.fastq.gz	5271_R2.fastq.gz	15	WGS	GENOMIC	paired	ILLUMINA	NextSeq 500	fastq
SRR6934960	5272	5272	5272_R1.fastq.gz	5272_R2.fastq.gz	16	WGS	GENOMIC	paired	ILLUMINA	NextSeq 500	fastq
SRR6934959	5273	5273	5273_R1.fastq.gz	5273_R2.fastq.gz	17	WGS	GENOMIC	paired	ILLUMINA	NextSeq 500	fastq
SRR6934958	5274	5274	5274_R1.fastq.gz	5274_R2.fastq.gz	18	WGS	GENOMIC	paired	ILLUMINA	NextSeq 500	fastq
SRR6934973	5275	5275	5275_R1.fastq.gz	5275_R2.fastq.gz	19	WGS	GENOMIC	paired	ILLUMINA	NextSeq 500	fastq
SRR6934972	5276	5276	5276_R1.fastq.gz	5276_R2.fastq.gz	20	WGS	GENOMIC	paired	ILLUMINA	NextSeq 500	fastq
SRR6935063	5277	5277	5277_R1.fastq.gz	5277_R2.fastq.gz	21	WGS	GENOMIC	paired	ILLUMINA	NextSeq 500	fastq
SRR6935064	5278	5278	5278_R1.fastq.gz	5278_R2.fastq.gz	22	WGS	GENOMIC	paired	ILLUMINA	NextSeq 500	fastq
SRR6935061	5279	5279	5279_R1.fastq.gz	5279_R2.fastq.gz	23	WGS	GENOMIC	paired	ILLUMINA	NextSeq 500	fastq
SRR6935062	5280	5280	5280_R1.fastq.gz	5280_R2.fastq.gz	24	WGS	GENOMIC	paired	ILLUMINA	NextSeq 500	fastq
SRR6935067	5281	5281	5281_R1.fastq.gz	5281_R2.fastq.gz	25	WGS	GENOMIC	paired	ILLUMINA	NextSeq 500	fastq
SRR6935068	5282	5282	5282_R1.fastq.gz	5282_R2.fastq.gz	26	WGS	GENOMIC	paired	ILLUMINA	NextSeq 500	fastq
SRR6935065	5283	5283	5283_R1.fastq.gz	5283_R2.fastq.gz	27	WGS	GENOMIC	paired	ILLUMINA	NextSeq 500	fastq
SRR6935066	5284	5284	5284_R1.fastq.gz	5284_R2.fastq.gz	28	WGS	GENOMIC	paired	ILLUMINA	NextSeq 500	fastq
SRR6934976	5285	5285	5285_R1.fastq.gz	5285_R2.fastq.gz	29	WGS	GENOMIC	paired	ILLUMINA	NextSeq 500	fastq
SRR6934977	5286	5286	5286_R1.fastq.gz	5286_R2.fastq.gz	30	WGS	GENOMIC	paired	ILLUMINA	NextSeq 500	fastq
SRR6935183	5287	5287	5287_R1.fastq.gz	5287_R2.fastq.gz	31	WGS	GENOMIC	paired	ILLUMINA	NextSeq 500	fastq
SRR6935182	5288	5288	5288_R1.fastq.gz	5288_R2.fastq.gz	32	WGS	GENOMIC	paired	ILLUMINA	NextSeq 500	fastq
SRR6934825	5289	5289	5289_R1.fastq.gz	5289_R2.fastq.gz	33	WGS	GENOMIC	paired	ILLUMINA	NextSeq 500	fastq
SRR6934824	5290	5290	5290_R1.fastq.gz	5290_R2.fastq.gz	34	WGS	GENOMIC	paired	ILLUMINA	NextSeq 500	fastq
SRR6934827	5291	5291	5291_R1.fastq.gz	5291_R2.fastq.gz	35	WGS	GENOMIC	paired	ILLUMINA	NextSeq 500	fastq
SRR6934826	5292	5292	5292_R1.fastq.gz	5292_R2.fastq.gz	36	WGS	GENOMIC	paired	ILLUMINA	NextSeq 500	fastq

SRR6934829	5293	5293	5293_R1.fastq.gz	5293_R2.fastq.gz	37	WGS	GENOMIC	paired	ILLUMINA	NextSeq 500	fastq
SRR6934828	5294	5294	5294_R1.fastq.gz	5294_R2.fastq.gz	38	WGS	GENOMIC	paired	ILLUMINA	NextSeq 500	fastq
SRR6934831	5295	5295	5295_R1.fastq.gz	5295_R2.fastq.gz	39	WGS	GENOMIC	paired	ILLUMINA	NextSeq 500	fastq
SRR6934830	5296	5296	5296_R1.fastq.gz	5296_R2.fastq.gz	40	WGS	GENOMIC	paired	ILLUMINA	NextSeq 500	fastq
SRR6935093	5301	5301	5301_R1.fastq.gz	5301_R2.fastq.gz	1	WGS	GENOMIC	paired	ILLUMINA	NextSeq 500	fastq
SRR6935094	5302	5302	5302_R1.fastq.gz	5302_R2.fastq.gz	2	WGS	GENOMIC	paired	ILLUMINA	NextSeq 500	fastq
SRR6934978	5303	5303	5303_R1.fastq.gz	5303_R2.fastq.gz	3	WGS	GENOMIC	paired	ILLUMINA	NextSeq 500	fastq
SRR6935096	5304	5304	5304_R1.fastq.gz	5304_R2.fastq.gz	4	WGS	GENOMIC	paired	ILLUMINA	NextSeq 500	fastq
SRR6935149	5305	5305	5305_R1.fastq.gz	5305_R2.fastq.gz	5	WGS	GENOMIC	paired	ILLUMINA	NextSeq 500	fastq
SRR6935090	5306	5306	5306_R1.fastq.gz	5306_R2.fastq.gz	6	WGS	GENOMIC	paired	ILLUMINA	NextSeq 500	fastq
SRR6935091	5307	5307	5307_R1.fastq.gz	5307_R2.fastq.gz	7	WGS	GENOMIC	paired	ILLUMINA	NextSeq 500	fastq
SRR6935092	5308	5308	5308_R1.fastq.gz	5308_R2.fastq.gz	8	WGS	GENOMIC	paired	ILLUMINA	NextSeq 500	fastq
SRR6935085	5309	5309	5309_R1.fastq.gz	5309_R2.fastq.gz	9	WGS	GENOMIC	paired	ILLUMINA	NextSeq 500	fastq
SRR6935086	5310	5310	5310_R1.fastq.gz	5310_R2.fastq.gz	10	WGS	GENOMIC	paired	ILLUMINA	NextSeq 500	fastq
SRR6934853	5311	5311	5311_R1.fastq.gz	5311_R2.fastq.gz	11	WGS	GENOMIC	paired	ILLUMINA	NextSeq 500	fastq
SRR6934852	5312	5312	5312_R1.fastq.gz	5312_R2.fastq.gz	12	WGS	GENOMIC	paired	ILLUMINA	NextSeq 500	fastq
SRR6934851	5313	5313	5313_R1.fastq.gz	5313_R2.fastq.gz	13	WGS	GENOMIC	paired	ILLUMINA	NextSeq 500	fastq
SRR6934850	5314	5314	5314_R1.fastq.gz	5314_R2.fastq.gz	14	WGS	GENOMIC	paired	ILLUMINA	NextSeq 500	fastq
SRR6934857	5315	5315	5315_R1.fastq.gz	5315_R2.fastq.gz	15	WGS	GENOMIC	paired	ILLUMINA	NextSeq 500	fastq
SRR6934856	5316	5316	5316_R1.fastq.gz	5316_R2.fastq.gz	16	WGS	GENOMIC	paired	ILLUMINA	NextSeq 500	fastq
SRR6934855	5317	5317	5317_R1.fastq.gz	5317_R2.fastq.gz	17	WGS	GENOMIC	paired	ILLUMINA	NextSeq 500	fastq
SRR6934854	5318	5318	5318_R1.fastq.gz	5318_R2.fastq.gz	18	WGS	GENOMIC	paired	ILLUMINA	NextSeq 500	fastq
SRR6934845	5319	5319	5319_R1.fastq.gz	5319_R2.fastq.gz	19	WGS	GENOMIC	paired	ILLUMINA	NextSeq 500	fastq
SRR6934844	5320	5320	5320_R1.fastq.gz	5320_R2.fastq.gz	20	WGS	GENOMIC	paired	ILLUMINA	NextSeq 500	fastq
SRR6935074	5321	5321	5321_R1.fastq.gz	5321_R2.fastq.gz	21	WGS	GENOMIC	paired	ILLUMINA	NextSeq 500	fastq
SRR6935073	5322	5322	5322_R1.fastq.gz	5322_R2.fastq.gz	22	WGS	GENOMIC	paired	ILLUMINA	NextSeq 500	fastq
SRR6935076	5323	5323	5323_R1.fastq.gz	5323_R2.fastq.gz	23	WGS	GENOMIC	paired	ILLUMINA	NextSeq 500	fastq
SRR6935075	5324	5324	5324_R1.fastq.gz	5324_R2.fastq.gz	24	WGS	GENOMIC	paired	ILLUMINA	NextSeq 500	fastq
SRR6935070	5325	5325	5325_R1.fastq.gz	5325_R2.fastq.gz	25	WGS	GENOMIC	paired	ILLUMINA	NextSeq 500	fastq
SRR6935069	5326	5326	5326_R1.fastq.gz	5326_R2.fastq.gz	26	WGS	GENOMIC	paired	ILLUMINA	NextSeq 500	fastq
SRR6935072	5327	5327	5327_R1.fastq.gz	5327_R2.fastq.gz	27	WGS	GENOMIC	paired	ILLUMINA	NextSeq 500	fastq
SRR6935071	5328	5328	5328_R1.fastq.gz	5328_R2.fastq.gz	28	WGS	GENOMIC	paired	ILLUMINA	NextSeq 500	fastq
SRR6934975	5329	5329	5329_R1.fastq.gz	5329_R2.fastq.gz	29	WGS	GENOMIC	paired	ILLUMINA	NextSeq 500	fastq
SRR6934974	5330	5330	5330_R1.fastq.gz	5330_R2.fastq.gz	30	WGS	GENOMIC	paired	ILLUMINA	NextSeq 500	fastq
SRR6935089	5331	5331	5331_R1.fastq.gz	5331_R2.fastq.gz	31	WGS	GENOMIC	paired	ILLUMINA	NextSeq 500	fastq

SRR6935095	5332	5332	5332_R1.fastq.gz	5332_R2.fastq.gz	32	WGS	GENOMIC	paired	ILLUMINA	NextSeq 500	fastq
SRR6934970	5333	5333	5333_R1.fastq.gz	5333_R2.fastq.gz	33	WGS	GENOMIC	paired	ILLUMINA	NextSeq 500	fastq
SRR6934971	5334	5334	5334_R1.fastq.gz	5334_R2.fastq.gz	34	WGS	GENOMIC	paired	ILLUMINA	NextSeq 500	fastq
SRR6934968	5335	5335	5335_R1.fastq.gz	5335_R2.fastq.gz	35	WGS	GENOMIC	paired	ILLUMINA	NextSeq 500	fastq
SRR6934969	5336	5336	5336_R1.fastq.gz	5336_R2.fastq.gz	36	WGS	GENOMIC	paired	ILLUMINA	NextSeq 500	fastq
SRR6934966	5337	5337	5337_R1.fastq.gz	5337_R2.fastq.gz	37	WGS	GENOMIC	paired	ILLUMINA	NextSeq 500	fastq
SRR6934967	5338	5338	5338_R1.fastq.gz	5338_R2.fastq.gz	38	WGS	GENOMIC	paired	ILLUMINA	NextSeq 500	fastq
SRR6935079	5339	5339	5339_R1.fastq.gz	5339_R2.fastq.gz	39	WGS	GENOMIC	paired	ILLUMINA	NextSeq 500	fastq
SRR6935080	5340	5340	5340_R1.fastq.gz	5340_R2.fastq.gz	40	WGS	GENOMIC	paired	ILLUMINA	NextSeq 500	fastq
SRR6934881	5385	5385	5385_R1.fastq.gz	5385_R2.fastq.gz	1	WGS	GENOMIC	paired	ILLUMINA	NextSeq 500	fastq
SRR6934880	5386	5386	5386_R1.fastq.gz	5386_R2.fastq.gz	2	WGS	GENOMIC	paired	ILLUMINA	NextSeq 500	fastq
SRR6934879	5387	5387	5387_R1.fastq.gz	5387_R2.fastq.gz	3	WGS	GENOMIC	paired	ILLUMINA	NextSeq 500	fastq
SRR6934878	5388	5388	5388_R1.fastq.gz	5388_R2.fastq.gz	4	WGS	GENOMIC	paired	ILLUMINA	NextSeq 500	fastq
SRR6934885	5389	5389	5389_R1.fastq.gz	5389_R2.fastq.gz	5	WGS	GENOMIC	paired	ILLUMINA	NextSeq 500	fastq
SRR6934884	5390	5390	5390_R1.fastq.gz	5390_R2.fastq.gz	6	WGS	GENOMIC	paired	ILLUMINA	NextSeq 500	fastq
SRR6934883	5391	5391	5391_R1.fastq.gz	5391_R2.fastq.gz	7	WGS	GENOMIC	paired	ILLUMINA	NextSeq 500	fastq
SRR6934882	5392	5392	5392_R1.fastq.gz	5392_R2.fastq.gz	8	WGS	GENOMIC	paired	ILLUMINA	NextSeq 500	fastq
SRR6934887	5393	5393	5393_R1.fastq.gz	5393_R2.fastq.gz	9	WGS	GENOMIC	paired	ILLUMINA	NextSeq 500	fastq
SRR6934886	5394	5394	5394_R1.fastq.gz	5394_R2.fastq.gz	10	WGS	GENOMIC	paired	ILLUMINA	NextSeq 500	fastq
SRR6935131	5395	5395	5395_R1.fastq.gz	5395_R2.fastq.gz	11	WGS	GENOMIC	paired	ILLUMINA	NextSeq 500	fastq
SRR6935132	5396	5396	5396_R1.fastq.gz	5396_R2.fastq.gz	12	WGS	GENOMIC	paired	ILLUMINA	NextSeq 500	fastq
SRR6935133	5397	5397	5397_R1.fastq.gz	5397_R2.fastq.gz	13	WGS	GENOMIC	paired	ILLUMINA	NextSeq 500	fastq
SRR6935134	5398	5398	5398_R1.fastq.gz	5398_R2.fastq.gz	14	WGS	GENOMIC	paired	ILLUMINA	NextSeq 500	fastq
SRR6935127	5399	5399	5399_R1.fastq.gz	5399_R2.fastq.gz	15	WGS	GENOMIC	paired	ILLUMINA	NextSeq 500	fastq
SRR6935128	5400	5400	5400_R1.fastq.gz	5400_R2.fastq.gz	16	WGS	GENOMIC	paired	ILLUMINA	NextSeq 500	fastq
SRR6935129	5401	5401	5401_R1.fastq.gz	5401_R2.fastq.gz	17	WGS	GENOMIC	paired	ILLUMINA	NextSeq 500	fastq
SRR6935130	5402	5402	5402_R1.fastq.gz	5402_R2.fastq.gz	18	WGS	GENOMIC	paired	ILLUMINA	NextSeq 500	fastq
SRR6935135	5403	5403	5403_R1.fastq.gz	5403_R2.fastq.gz	19	WGS	GENOMIC	paired	ILLUMINA	NextSeq 500	fastq
SRR6935136	5404	5404	5404_R1.fastq.gz	5404_R2.fastq.gz	20	WGS	GENOMIC	paired	ILLUMINA	NextSeq 500	fastq
SRR6935098	5405	5405	5405_R1.fastq.gz	5405_R2.fastq.gz	21	WGS	GENOMIC	paired	ILLUMINA	NextSeq 500	fastq
SRR6935097	5406	5406	5406_R1.fastq.gz	5406_R2.fastq.gz	22	WGS	GENOMIC	paired	ILLUMINA	NextSeq 500	fastq
SRR6935100	5407	5407	5407_R1.fastq.gz	5407_R2.fastq.gz	23	WGS	GENOMIC	paired	ILLUMINA	NextSeq 500	fastq
SRR6935099	5408	5408	5408_R1.fastq.gz	5408_R2.fastq.gz	24	WGS	GENOMIC	paired	ILLUMINA	NextSeq 500	fastq
SRR6935102	5409	5409	5409_R1.fastq.gz	5409_R2.fastq.gz	25	WGS	GENOMIC	paired	ILLUMINA	NextSeq 500	fastq
SRR6935101	5410	5410	5410_R1.fastq.gz	5410_R2.fastq.gz	26	WGS	GENOMIC	paired	ILLUMINA	NextSeq 500	fastq

SRR6935104	5411	5411	5411_R1.fastq.gz	5411_R2.fastq.gz	27	WGS	GENOMIC	paired	ILLUMINA	NextSeq 500	fastq
SRR6935103	5412	5412	5412_R1.fastq.gz	5412_R2.fastq.gz	28	WGS	GENOMIC	paired	ILLUMINA	NextSeq 500	fastq
SRR6935106	5413	5413	5413_R1.fastq.gz	5413_R2.fastq.gz	29	WGS	GENOMIC	paired	ILLUMINA	NextSeq 500	fastq
SRR6935105	5414	5414	5414_R1.fastq.gz	5414_R2.fastq.gz	30	WGS	GENOMIC	paired	ILLUMINA	NextSeq 500	fastq
SRR6934991	5415	5415	5415_R1.fastq.gz	5415_R2.fastq.gz	31	WGS	GENOMIC	paired	ILLUMINA	NextSeq 500	fastq
SRR6934992	5416	5416	5416_R1.fastq.gz	5416_R2.fastq.gz	32	WGS	GENOMIC	paired	ILLUMINA	NextSeq 500	fastq
SRR6934989	5417	5417	5417_R1.fastq.gz	5417_R2.fastq.gz	33	WGS	GENOMIC	paired	ILLUMINA	NextSeq 500	fastq
SRR6934990	5418	5418	5418_R1.fastq.gz	5418_R2.fastq.gz	34	WGS	GENOMIC	paired	ILLUMINA	NextSeq 500	fastq
SRR6934995	5419	5419	5419_R1.fastq.gz	5419_R2.fastq.gz	35	WGS	GENOMIC	paired	ILLUMINA	NextSeq 500	fastq
SRR6934996	5420	5420	5420_R1.fastq.gz	5420_R2.fastq.gz	36	WGS	GENOMIC	paired	ILLUMINA	NextSeq 500	fastq
SRR6934993	5421	5421	5421_R1.fastq.gz	5421_R2.fastq.gz	37	WGS	GENOMIC	paired	ILLUMINA	NextSeq 500	fastq
SRR6934994	5422	5422	5422_R1.fastq.gz	5422_R2.fastq.gz	38	WGS	GENOMIC	paired	ILLUMINA	NextSeq 500	fastq
SRR6934997	5423	5423	5423_R1.fastq.gz	5423_R2.fastq.gz	39	WGS	GENOMIC	paired	ILLUMINA	NextSeq 500	fastq
SRR6934998	5424	5424	5424_R1.fastq.gz	5424_R2.fastq.gz	40	WGS	GENOMIC	paired	ILLUMINA	NextSeq 500	fastq

3.10 ADDITIONAL RESULTS AND DISCUSSION

The present study highlighted that neighbor predation and DNA uptake foster the transfer of large genomic regions in *V. cholerae*. Importantly, we detected transfers of large DNA fragments, exceeding 100 kbp, which contradicts a common thinking that natural transformation cannot be used for DNA repair or for bacterial evolution. As we isolated and identified the HGT events of 360 transformants in this study, the next question we addressed was whether some of these transfers were associated with a potential gain or loss of function. It was previously shown that natural transformation could lead to the transfer of novel gene clusters such as a metabolic operons or O-antigen clusters ([13,41]). We demonstrated that the acceptor (pandemic strain A1552) and the donor (environmental isolate Sa5Y) used in this study have different SNPs in core genes and that they also contained some major genotypic variations (Fig. 3.2). Indeed, various genomic islands, including the VPI-1, VPI-2, VSP-I, VSP-II, the CTX prophage, and the WASA-1 element, are present in the pandemic A1552 strain but absent from the Sa5Y environmental isolate. We also showed that the O-antigen cluster varied between the two strains. We hypothesized that integration of donor DNA in these regions might lead to serogroup conversion, with the transfer of the O-antigen cluster, or to the potential loss of an entire genomic island. Therefore, among the 360 transformants sequenced, we specifically looked for DNA transfer occurring in close proximity to the O-antigen cluster or the different genomic islands mentioned above. Interestingly, we detected that one transformant (strain #5347), which was isolated from condition ②, had lost the VSP-II (VC0490-VC0516; Fig. 3.5). Indeed, this transformant had not only acquired the antibiotic resistance gene on chromosome 2 but had undergone multiple HGT events on both chromosomes, including one transfer on chromosome 1, which resulted in the loss of the 26.5 kbp VSP-II (Fig. 3.5). This island is a mobile genetic element composed of 24 genes encoding a type IV pilin of unknown function, chemotaxis proteins, a DNA repair protein, a transcriptional regulator and an integrase; however, its role in the pathogenesis of *V. cholerae* is not yet understood ([73,74]). Interestingly, in a recent study Croucher and colleagues proposed, using mathematical modeling, that natural transformation might be used to cure the genome from costly selfish mobile genetic elements ([14]). They proposed that especially the uptake of short DNA fragments present in the environment will favor the loss of mobile genetic element ([14]). Here, we propose that the acquisition and integration of large genomic region could also cure the genome from selfish genetic element.

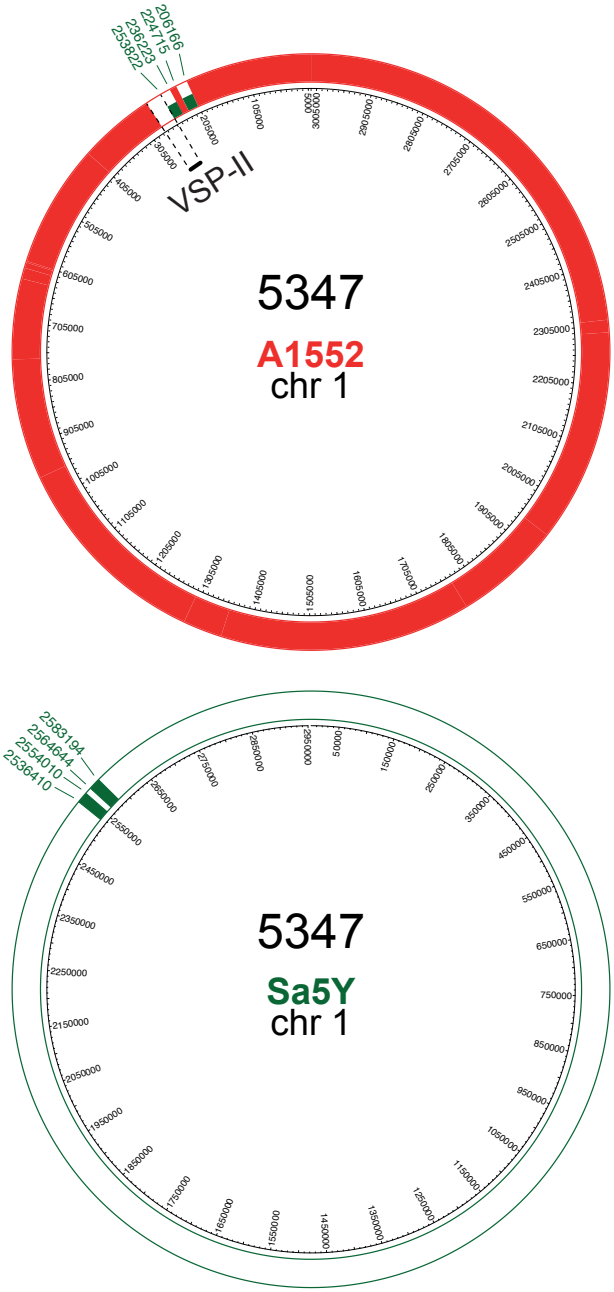

Figure 3.5: Natural transformation can lead to the loss of the VSP-II. The sequencing reads obtained for the transformant (5347) were mapped onto the chromosome 1 (chr 1) of the acceptor (A1552, red) and the donor (Sa5Y, green) strains to identify the transferred fragments. The reads mapping on the chromosomes of the acceptor or the donor are highlighted in red or green, respectively. Chromosomal regions where reads could not be mapped remained white. The location of the VSP-II is highlighted. Abbreviation: VSP-II, *Vibrio* Seventh Pandemic island II

Acquisition of genomic island by natural transformation

As we investigated the transfer of DNA fragments in A1552 that harbored diverse genomic island absent from Sa5Y, the experimental conditions designed allowed us to look for the potential loss of a genomic island but not for the novel acquisition of such cluster. Therefore,

in a preliminary study, we next investigated the potential transfer of the genomic islands carried in the pandemic strain A1552 to the environmental isolate Sa5Y. We hypothesized that, in a mixed population of *V. cholerae*, an environmental isolate might be able to integrate a pathogenicity island by natural transformation via the acquisition of large DNA fragments released by T6SS-killing of pandemic isolates. If this were the case, natural transformation could lead to the emergence of novel pathogenic *V. cholerae*.

To test our hypothesis, we used pandemic A1552 strains (donor) that harbored an antibiotic resistance gene within a genomic island of interest, in order to screen for its transfer. As these strains were already existing in our laboratory, we focused on the transfer of the O-antigen cluster as well as the following genomic islands: VSP-I, VSP-II and VPI-1. First, we determined the transfer of these clusters in A1552 and Sa5Y (acceptor) using purified gDNA as transforming material. It is important to mention that in A1552 we do not necessarily measure the transfer of the entire operon but potentially only the transfer of one or few genes close to the selective marker. However, to also investigate the transfer of an entire cluster in A1552, we measured the transfer of the O139-antigen using gDNA derived from an A1552 strain that had exchanged the O1 by the O139-antigen. In addition, we also determined the transfer of VPI-1 back into an acceptor mutant strain that lacked this complete island (ΔVPI-1). As expected, we observed that the transformation frequencies were significantly lower for the transfer of an entire cluster as compared with the transfer of a single/few gene(s) in A1552 (Fig. 3.6A-B). Moreover, we determined that rare transformants of Sa5Y could acquire the 42 kbp O139-antigen cluster or the 15 kbp VSP-I (Fig. 3.6A-B). Based on these results, we further decided to investigate whether the O139-antigen cluster and the VSP-I could be acquired through neighbor predation and DNA uptake in Sa5Y. The preliminary result obtained indicated that both cluster could be transferred at a low frequency into Sa5Y (Fig. 3.6C). Altogether, we propose that large heterologous genomic regions could be acquired at low frequency by natural transformation. However, further studies are still required to demonstrate that pathogenic isolates could emerge via natural transformation in *V. cholerae*.

Transfer of T6SS effector and immunity pair(s) by HGT

Although in depth bioinformatics analysis should be used to identify all the potential gain and loss of functions in the 360 transformants isolated in this study, we next sought to investigate

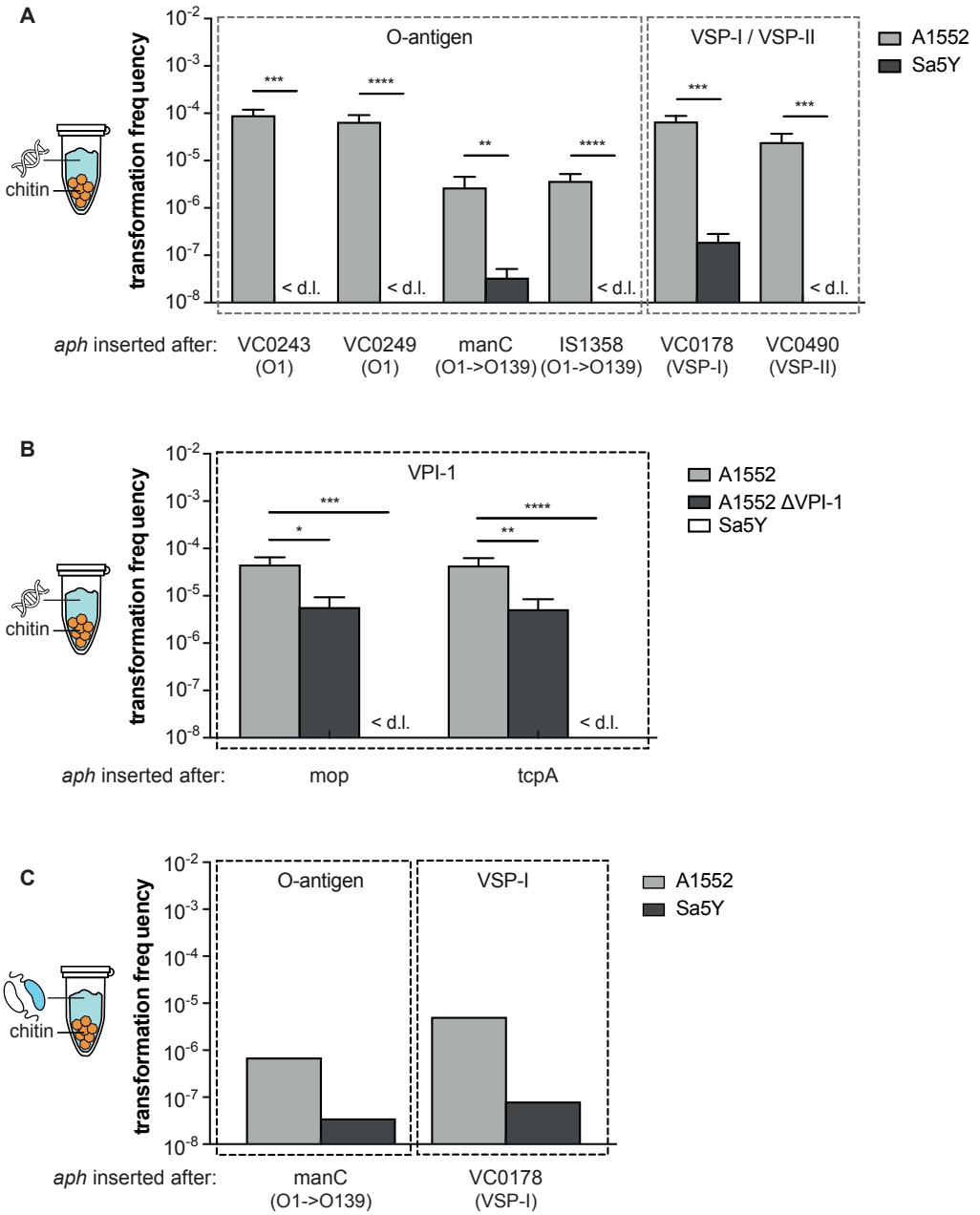

Figure 3.6: Pathogenicity islands can be acquired by natural transformation. (A-C) Transformability of large gene clusters. Cultures were grown on chitin flakes to induce natural competence. Bacteria were grown as a monoculture (acceptor only) or as co-cultures (acceptor + donor). In the former case, purified gDNA served as transforming material. The gDNA used are derived from A1552 variants. A scheme of each experimental setup is depicted on the left. Transformants were selected based on the acquisition of the *aph* resistance cassette that was integrated in large gene clusters, as indicated below the graph. The transfer of the O-antigen, the *Vibrio* Seventh Pandemic islands I and II (VSP-I, VSP-II), and the *Vibrio* Pathogenicity Island 1 (VPI-1) was scored, as shown in the title of each graph. (A). Sa5Y can horizontally acquire the O139-antigen cluster and the VSP-I. Transfer of O-antigen (O1 and O139), VSP-I and VSP-II was scored in A1552 or Sa5Y as acceptor strains. (B) The transfer of VPI-1 was scored in the strains A1552, A1552ΔVPI-1, and Sa5Y. (C) Preliminary data indicating that neighbor predation can lead to the acquisition of novel large gene cluster in Sa5Y. The transfers of O139-antigen and VSP-I were scored after co-culture of A1552 variants carrying *aph* resistance gene (in O139-antigen cluster or VSP-I; donors) with either A1552 or Sa5Y (acceptors). A1552 competent strain cannot attack the A1552 Kan^R variants and, therefore, rely on random lysis of A1552 donors to acquire DNA. By contrast, Sa5Y can mediate T6SS-dependent killing of A1552 donors and subsequently acquire their released DNA. The data represent one biological replicate. (A-B) The data represent the average of three independent biological replicates (±SD, as depicted by the error bars). Statistical significance is indicated (* $p < 0.05$; ** $p < 0.01$; *** $p < 0.001$; **** $p < 0.0001$).

whether some transformants had acquired a novel T6SS effector and immunity (E-I) pair derived from the prey. Indeed, the E-I pairs of the large cluster and the two auxiliary clusters of strain A1552 and Sa5Y do not share homology, which lead to successful T6SS-killing between these strains. In a previous study, Kirchberger and colleagues analyzed the E-I pairs of several *V. cholerae* strains and suggested that E-I pairs could be exchanged via HGT ([75]). Among the 360 transformants sequenced, we determined that 31 transformants (8.6%) exchanged the E-I pair of the large cluster (E-I_{LC}) and 2 transformants (0.55%) transferred the E-I pair of the secondary auxiliary cluster (E-I_{A2}), while no transformants did exchange the E-I pair of the auxiliary cluster 1. For the transfer of E-I_{LC}, we determined that these transformants were all recovered from condition ① and ②, in which we screened for transformant that have at least acquired an antibiotic resistance gene located within the same large T6SS cluster as the E-I genes. Therefore, as the E-I_{LC} is ~24 kbp after the selective marker, the screen in condition ① and ② most likely biased the exchange of these two genes.

At this point, we observed that E-I pair could be horizontally transferred, however we did not know whether these genes were functional in the novel strain background. For this purpose, we focused on two transformants: one isolate from condition ① that had exchanged the E-I_{LC} and became T6SS deficient (T6SS$^-$) by the acquisition of the selective marker; and one isolate from condition ④ that had transferred the E-I_{A2} and remained T6SS$^+$ (Fig. 3.7A). It is important to mention that these transformants did not only exchange the E-I pair by itself but they transferred the entire T6SS clusters by HGT. As these A1552 transformants encode a mix of E-I pairs derived from A1552 and Sa5Y, we hypothesized that i) they became non-immune against attacks of previous kin cells (A1552); and ii) the transformant that remained T6SS$^+$ might now be able to attack its initial sisters cells (A1552) due to the novel effector gene.

To test the first hypothesis, we investigated the survival of these transformants in an intraspecies killing assay using A1552 WT as a predator or a strain lacking the non-compatible E-I pair (A1552ΔE-I_{LC} or A1552ΔE-I_{A2}). To artificially express the T6SS under the conditions tested, the predator strain also carried the arabinose-inducible copy of *tfoX-strep* ([1,35]). As expected, both transformants lost their immunity to the T6SS-mediated attack of the predatory strains, as they could not block the toxic activity of these non-compatible effectors (Fig. 3.7B-C). Moreover, we observed a higher killing effect when the effector of the auxiliary cluster 2 (E_{A2}) was replaced in A1552 by the corresponding region of strain Sa5Y compared to the same situation in which the effector of the large cluster was exchanged

(E_{LC}). Notably, the E_{A2} of the predatory strain A1552 disrupts the membranes through its pore-forming activity, whereas E_{LC} targets the peptidoglycan ([76,77]). Based on their toxic activities, we hypothesized that each of these effectors should efficiently lyse the bacteria. However, several reasons could explain the different killing rates that we observed including, but not limited to, variations in T6SS loading or secretion. Indeed, a common question in the field remains whether all effectors are secreted at once by the T6SS (that is, each VgrG of the trimeric tip loads a different effector protein) or whether some effectors are more efficiently secreted than others. Along those lines, it remains unclear whether one contraction of the T6SS is sufficient to kill the neighboring cell or whether multiple attacks are required. Interestingly, Zheng and colleagues proposed that the spike of the T6SS in *V. cholerae* is formed of heterotrimeric complexes composed of VgrG-2 interacting with either VgrG1 or VgrG3, which both are specialized effectors containing a C-terminal effector extension ([78]). In fact, as E_{LC} is VgrG3, we hypothesized that E_{LC} might not be secreted at each attack of the T6SS and consequently, that it increased the survival of the transformant that exchanged E-I_{LC} (Fig. 3.7B). Similarly, we hypothesized that VgrG-2 with its cargo associated effector protein, namely E_{A2}, will potentially be secreted at each attack of the T6SS. This might suggest that E_{A2} is secreted twice as often than E_{LC}, which could explain the higher killing effect observed with the transformant that replaced E-I_{A2} in A1552 by the corresponding region of strain Sa5Y (Fig. 3.7B-C). Further studies are required to better understand the differences observed with respect to the toxicity of these effectors.

As mentioned above, the next question we wanted to address was whether the novel effector acquired could be secreted and was functional. If the novel Sa5Y-derived E-I pair of the A1552 transformant is functional, its secretion should lead to successful killing of A1552 strain. This hypothesis could only be investigated with the T6SS-positive transformant isolated from condition ④. However, as the killing assay is performed under conditions that do not lead to natural induction of the T6SS, we artificially expressed the T6SS with an arabinose-inducible copy of *tfoX-strep* ([1,35]). Upon TfoX production, we observed significant killing of A1552 (Fig. 3.7D), indicating that the novel E_{A2} was indeed secreted by the T6SS. Based on these data, we conclude that the novel pair of E-I acquired is fully functional in the acceptor strain. In addition, we hypothesize that the exchange of a novel E-I pair might bring an ecological advantage to the transformant, which can now target both the acceptor and

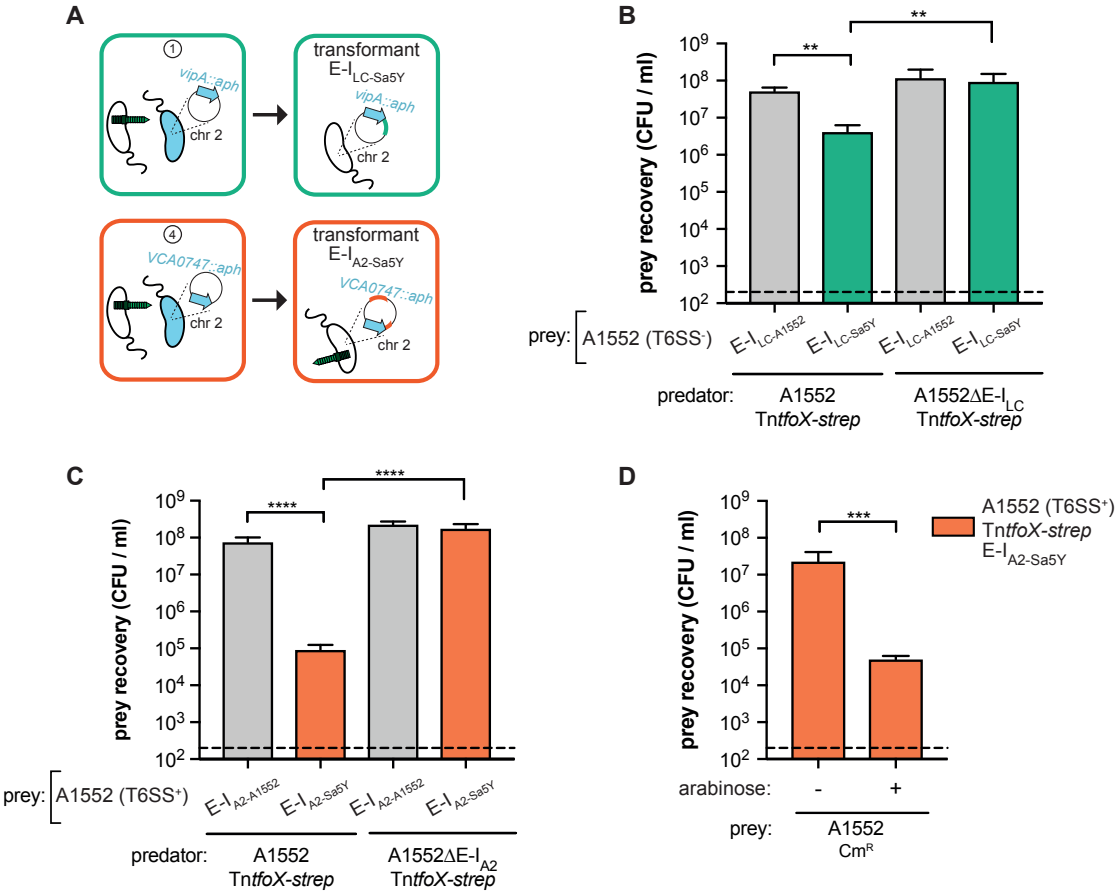

Figure 3.7: The horizontally acquired T6SS effector and immunity genes are functional. (A) Scheme representing the transformants that have exchanged and acquired a novel T6SS effector and immunity (E-I) pair. The transformants were isolated from condition ① and ④, as described in figure 3.4A. The predator transformants (white) have integrated DNA from the killed prey (Sa5Y-derived strains). The depicted transformants have acquired the E-I pair from the large cluster (E-$I_{LC\text{-}Sa5Y}$; condition ①) or from the auxiliary cluster 2 (E-$I_{A2\text{-}Sa5Y}$; condition ④) of the T6SS. The presence or absence of the T6SS green structure indicates whether the bacteria harbor a functional or deficient T6SS ($T6SS^+$ or $T6SS^-$). (B-D) *V. cholerae* killing assay. Predator strains contained the arabinose-inducible copy of *tfoX-strep* for competence/T6SS induction. Genotypes of predator and prey strains used are indicated below the graph. Predator and prey strains were co-cultured, mixed in a 1:1 ratio and spotted on agar plates in the presence of arabinose (B-C) or in absence (-) and presence (+) of arabinose (D). After 4 hours of incubations, the cells were recovered from the agar plates, serially diluted, and spotted on selective plates. Recovery of *V. cholerae* prey strains is shown on the Y-axis (in CFU/ml). (B-C) Transformants that exchanged an E-I pair lost their immunity against A1552 predatory attacks. (D) The acquired E-I pair efficiently kills A1552-derived prey strain. (B-D) The data represent the average of three independent biological replicates (±SD, as depicted by the error bars). Statistical significance is indicated (** $p < 0.01$; *** $p < 0.001$; **** $p < 0.0001$).

donor strains that are present in the community. Interestingly, our results supported a previous study by Thomas and colleagues, which demonstrated that E-I pairs exchanged by HGT were functional in *V. cholerae* ([79]). However, in their study, the authors directly selected for the transfer of the E-I pair by integrating a selection marker adjacent to these genes. Moreover, Thomas and colleagues not only showed that the novel effectors transferred

led to efficient killing of neighboring cells, but pointed out that the transformant strains could outcompete the parental strains (acceptor and donor). Indeed, even though the transformant is non-immune anymore to the attack of its former kin-cells, the acquisition of a novel "superior" toxic effector could lead to a selective fitness advantage. Moreover, we hypothesize that the transformant with a novel E-I pair might have an immediate fitness advantage after the integration of DNA, as: i) the transformant might still be immune against previous kin cells as it should contain, for a certain period of time, the previously produced immunity proteins, and ii) the transformant express in parallel a novel E-I proteins that were acquired from a non-kin cell, which might partially give immunity against the attack of these non-kin cells. We conclude that, in the natural habitats, exchanges of E-I pair can occur among *V. cholerae* strains and that this could potentially result in a fitness advantage when facing competition. This, on the other hand, could enhance the survival of a subpopulation of the community.

3.11 REFERENCES

1. Borgeaud, S., Metzger, L. C., Scrignari, T. and Blokesch, M. The type VI secretion system of *Vibrio cholerae* fosters horizontal gene transfer. *Science* **347**, 63–67 (2015).
2. Nielsen, K. M., Johnsen, P. J., Bensasson, D. and Daffonchio, D. Release and persistence of extracellular DNA in the environment. *Environ. Biosafety Res.* **6**, 37–53 (2007).
3. Overballe-Petersen, S., Harms. K., Orlando, L. A. A., Mayar, J. V. M., Rasmussen, S., *et al.* Bacterial natural transformation by highly fragmented and damaged DNA. *Proc. Natl. Acad. Sci.USA* **110**, 19860–19865 (2013).
4. Matthey, N., Drebes Dörr, N. C. and Blokesch, M. Long-read-based genome sequences of pandemic and environmental *Vibrio cholerae* strains. *Microbiol Resour Annoucements* **7**, (2018).
5. Shapiro, B. J., Friedman, J., Cordero, O. X., Preheim, S. P., Timberlake, S. C., *et al.* Population genomics of early events in the ecological differentiation of bacteria. *Science.* **336**,(6077): 48–51 (2012).
6. Blokesch, M. and Schoolnik, G. K. The extracellular nuclease Dns and its role in natural transformation of *Vibrio cholerae*. *J. Bacteriol.* **190**, 7232–7240 (2008).
7. Lo Scrudato, M. and Blokesch, M. A transcriptional regulator linking quorum sensing and chitin induction to render *Vibrio cholerae* naturally transformable. *Nucleic Acids Res.* **41**, 3644–3658 (2013).
8. Jaskólska, M., Stutzmann, S., Stoudmann, C. and Blokesch, M. QstR-dependent regulation of natural competence and type VI secretion in *Vibrio cholerae*. *Nucleic Acids Res.* **46**, 10619–10634 (2018).
9. WHO (January 2019) Cholera-Key facts.
10. Chen, I. and Dubnau, D. DNA uptake during bacterial transformation. *Nat. Rev. Microbiol.* **2**, 241–249 (2004).
11. Johnston, C., Martin, B., Fichant, G., Polard, P. and Claverys, J. P. Bacterial transformation: distribution, shared mechanisms and divergent control. *Nat. Rev. Microbiol.* **12**, 181–196 (2014).
12. Matthey, N. and Blokesch, M. The DNA-Uptake Process of Naturally Competent *Vibrio cholerae*. *Trends Microbiol.* **24**, 98–110 (2016).
13. Blokesch, M. and Schoolnik, G. K. Serogroup conversion of *Vibrio cholerae* in aquatic reservoirs. *PLoS Pathog.* **3**:e81 (2007).
14. Croucher, N. J., Mostowy, R., Wymant, C., Turner, P., Bentley, S. D., and Fraser, C. Horizontal DNA transfer mechanisms of bacteria as weapons of intragenomic conflict. *PLoS Biol.* **14**:e1002394 (2016).
15. Metzger, L. C. and Blokesch, M. Regulation of competence-mediated horizontal gene transfer in the natural habitat of *Vibrio cholerae*. *Curr. Opin. Microbiol.* **30**, 1–7 (2016).
16. Pruzzo, C., Vezzulli, L. and Colwell, R. R. Global impact of *Vibrio cholerae* interactions with chitin. *Environ. Microbiol.* **10**, 1400–1410 (2008).
17. Gooday, G. W. Physiology of microbial degradation of chitin and chitosan. *Biodegradation* **1**, 177–190 (1990).
18. Meibom, K. L., Li, X.B., Nielsen, A.T., Wu, C.Y., Roseman, S., and Schoolnik, G.K. The *Vibrio cholerae* chitin utilization program. *Proc. Natl. Acad. Sci. USA.* **101**, 2524–9 (2004).
19. Meibom, K. L., Blokesch, M., Dolganov, N. A., Wu, C.-Y. and Schoolnik, G. K. Chitin induces natural competence in *Vibrio cholerae*. *Science* **310**, 1824–1827 (2005).

20. Li, X. and Roseman, S. The chitinolytic cascade in vibrios is regulated by chitin oligosaccharides and a two-component chitin catabolic sensor/kinase. *Proc Natl Acad Sci USA* **101**, 627–631 (2004).
21. Yamamoto, S., Mitobe, J., Ishikawa, T., Wai, S.N., Ohnishi, M., Watanabe, H., and Izumiya, H. Regulation of natural competence by the orphan two-component system sensor kinase ChiS involves a non-canonical transmembrane regulator in *Vibrio cholerae*. *Mol Microbiol* **91**, 326–347 (2014).
22. Dalia, A. B., Lazinski, D. W. and Camilli, A. Identification of a membrane-bound transcriptional regulator that links chitin and natural competence in *Vibrio cholerae*. *mBio* **5** e01028-13 (2014).
23. Yamamoto, S., Izumiya, H., Mitobe, J., Morita, M., Arakawa, E., Ohnishi, M., and Watanabe, H. Identification of a chitin-induced small RNA that regulates translation of the *tfoX* gene, encoding a positive regulator of natural competence in vibrio cholerae. *J. Bacteriol.* **193**, 1953–1965 (2011).
24. Seitz, P. and Blokesch, M. DNA-uptake machinery of naturally competent *Vibrio cholerae*. *Proc. Natl. Acad. Sci.USA* **110**, 17987–17992 (2013).
25. Seitz, P. and Blokesch, M. DNA Transport across the Outer and Inner Membranes of Naturally Transformable *Vibrio cholerae* Is Spatially but Not Temporally Coupled. *MBio* **5**, e01409-14 (2014).
26. Seitz, P. Pezeshgi Modarres, H., Borgeaud, S., Bulushev, R.D., Steinbock, L.J., Radenovic, A. *et al*. ComEA Is Essential for the Transfer of External DNA into the Periplasm in Naturally Transformable *Vibrio cholerae* Cells. *PLoS Genet.* **10**, e1004066 (2014).
27. Ellison, C. K., Dalia, T. N., Ceballos, A. V., Wang, J. C-Y., Biais, N., *et al.* Retraction of DNA-bound type IV competence pili initiates DNA uptake during natural transformation in *Vibrio cholerae*. *Nat. Microbiol.* **3**, 773–780 (2018).
28. Adams, D. W., Stutzmann, S., Stoudmann, C. and Blokesch, M. DNA-uptake pili of *Vibrio cholerae* are required for chitin colonization and capable of kin recognition via sequence-specific self-interaction. *Nat. Microbiol.* (2019). doi:10.1038/s41564-019-0479-5
29. Redfield, R. J. Evolution of bacterial transformation: is sex with dead cells ever better than no sex at all? *Genetics* **119**, 213–221 (1988).
30. Veening, J. W. and Blokesch, M. Interbacterial predation as a strategy for DNA acquisition in naturally competent bacteria. *Nat. Rev. Microbiol.* **15**, 621–629 (2017).
31. Ho, B. T., Dong, T. G. and Mekalanos, J. J. A view to a kill: The bacterial type VI secretion system. *Cell Host Microbe* **15**, 9–21 (2014).
32. Galan, J. E. and Waksman, G. Protein-injection machines in bacteria. *Cell* **172**, 1306–1318 (2019).
33. Taylor, N. M. I., van Raaij, M. J. and Leiman, P. G. Contractile injection systems of bacteriophages and related systems. *Mol Microbiol* **108**, 6–15 (2018).
34. Cianfanelli, F. R., Monlezun, L. and Coulthurst, S. J. Aim, load, fire: the type VI secretion system, a bacterial nanoweapon. *Trends in Microbiology* **24**, 51-62 (2016).
35. Metzger, L. C., Stutzmann, S., Scrignari, T., Van der Henst, C., Matthey, N., and Blokesch, M. Independent Regulation of Type VI Secretion in *Vibrio cholerae* by TfoX and TfoY. *Cell Rep* **15**, 951–958 (2016).
36. Metzger, L. C., Matthey, N., Stoudmann, C., Collas, E. J. and Blokesch, M. Ecological implications of gene regulation by TfoX and TfoY among diverse *Vibrio* species . *Environ. Microbiol.* **21**, 2231-2247 (2019).
37. Mell, J. C., Lee, J. Y., Firme, M., Sinha, S. and Redfield, R. J. Extensive Cotransformation of

Natural Variation into Chromosomes of Naturally Competent *Haemophilus influenzae*. *G3 genes genomes Genet.* **4**, 717–731 (2014).

38. Bubendorfer, S., Krebes, J., Yang, I., Hage, E., Schulz, T. F., Bahlawane, C., Didelot, X. and Suerbaum, S. Genome-wide analysis of chromosomal import patterns after natural transformation of *Helicobacter pylori*. *Nat. Commun.* **7**:11995 (2016).
39. Alfsnes, K., Frye, S. A., Eriksson, J., Eldholm, V., *et al.* A genomic view of experimental intraspecies and interspecies transformation of a rifampicin-resistance allele into *Neisseria meningitidis*. *Microb. Genomics* **4** DOI 10.1099, (2018).
40. Keymer DP, Miller MC, Schoolnik GK, and Boehm AB Genomic and phenotypic diversity of coastal *Vibrio cholerae* strains is linked to environmental factors. *Appl. Environ. Microbiol.* 73:3705-3714 (2007)
41. Miller, M. C., Keymer, D. P., Avelar, A., Boehm, A. B. and Schoolnik, G. K. Detection and transformation of genome segments that differ within a coastal population of *Vibrio cholerae* strains. *Appl. Environ. Microbiol.* **73**, 3695–3704 (2007).
42. Yildiz, F. H. and Schoolnik, G. K. Role of *rpoS* in stress survival and virulence of *Vibrio cholerae*. *J. Bacteriol.* **180**, 773–784 (1998).
43. Domman, D. Quilici, M.L., Dorman, M.J., Njamkepo, E., Mutreja, A., Mather, A.E. *et al* Integrated view of *Vibrio cholerae* in the Americas. *Science* **358**, 789–793 (2017).
44. Heidelberg, J. F. Eisen, J.A., Nelson, W.C., Clayton, R.A., Gwinn, M.L., Dodson, R.J. *et al.* DNA sequence of both chromosomes of the cholera pathogen *Vibrio cholerae*. *Nature* **406**, 477–483 (2000).
45. Dziejman, M., Serruto, D., Tam, V. C., Sturtevant, D., Diraphat, P., Faruque, S. M., *et al.* Genomic characterization of non-O1, non-O139 *Vibrio cholerae* reveals genes for a type III secretion system. *Proc. Natl. Acad. Sci. USA*. **102**, 3465–3470 (2005).
46. Waldor, M. K. and Mekalanos, J. J. Lysogenic conversion by a filamentous phage encoding cholera toxin. *Science* **272**, 1910–1914 (1996).
47. Mazel, D. Integrons : agents of bacterial evolution. *Nat. Rev. Microbiol.* **4**, 608–620 (2006).
48. Marvig, R. L. and Blokesch, M. Natural transformation of *Vibrio cholerae* as a tool - Optimizing the procedure. *BMC Microbiol.* **10**, 155 (2010).
49. Shapiro, B. J., Friedman, J., Cordero, O. X., Preheim, S. P., Timberlake, S. C., *et al.* Population genomics of early events in the ecological differentiation of bacteria. *Science.* **336**,(6077): 48–51 (2012).
50. Mortier-Barrière, I., Velten, M., Dupaigne, P., Mirouze, N., Piétrement, O., *et al.* A key presynaptic role in transformation for a widespread bacterial protein: DprA conveys incoming ssDNA to RecA. *Cell* **130**, 824–836 (2007).
51. Suckow, G., Seitz, P. and Blokesch, M. Quorum sensing contributes to natural transformation of *Vibrio cholerae* in a species-specific manner. *J. Bacteriol.* **193**, 4914–4924 (2011).
52. Iqbal, N., Guérout, A-M., Krin, E., Le Roux, F. and Mazel, D. Comprehensive functional analysis of the 18 *Vibrio cholerae* N16961 toxin-antitoxin systems substantiates their role in stabilizing the superintegron. *J. Bacteriol.* **197**, 2150–2159 (2015).
53. Faruque, S. M., Chowdhury, N., Kamruzzaman, M., Dziejman, M., Rahman, M. H., *et al.* Genetic diversity and virulence potential of environmental *Vibrio cholerae* population in a cholera-endemic area . *Proc. Natl. Acad. Sci. USA* **101**, 2123–2128 (2004).
54. Mutreja, A., Kim, D. W., Thomson, N. R., Connor, T. R., Lee, J. H., *et al.* Evidence for several waves of global transmission in the seventh cholera pandemic. *Nature* **477**, 462–465 (2011).
55. Weill, F., Domman, D., Njamkepo, E., Almesbahi, A. A., Naji, M., *et al.* Genomic insights

into the 2016-2017 cholera epidemic in Yemen. *Nature* **565**, 230–234 (2019).
56. Weill, F., Domman, D., Njamkepo, E., Tarr, C., Rauzier, J., Fawal, N., *et al.* Genomic history of the seventh pandemic of cholera in Africa. *Science* **358**, 785–789 (2017).
57. Dalia, A. B., Seed, K. D., Calderwood, S. B. and Camilli, A. A globally distributed mobile genetic element inhibits natural transformation of *Vibrio cholerae*. *Proc. Natl. Acad. Sci. USA.* **112**, 10485–10490 (2015).
58. Blokesch, M. In and out—contribution of natural transformation to the shuffling of large genomic regions. *Curr. Opin. Microbiol.* **38**, 22–29 (2017).
59. Clemens, J. D., Nair, G. B., Ahmed, T., Qadri, F. and Holmgren, J. Cholera. *Lancet* **390**, 1539–1549 (2017).
60. Hang, L., John, M., Asaduzzman, M., Bridges, E. A., Vanderspurt, C., *et al.* Use of *in vivo*-induced antigen technology (IVIAT) to identify genes uniquely expressed during human infection with *Vibrio cholerae*. *Proc. Natl. Acad. Sci. USA.* **100**, 8508–8513 (2003).
61. Lombardo, M., Michalski, J., Martinez-Wilson, H., Morin, C., Hilton, T., *et al.* An *in vivo* expression technology screen for *Vibrio cholerae* genes expressed in human volunteers. *Proc. Natl. Acad. Sci. USA.* **104**, 18229–18234 (2007).
62. Sambrook, J., Fritsch, E. . and Maniatis, T. Molecular Cloning: A laboratory Manual. *Cold Spring Harb. NY. Cold Spring Harb. Lab. Press* (1982).
63. De Souza Silva, O. and Blokesch, M. Genetic manipulation of *Vibrio cholerae* by combining natural transformation with FLP recombination. *Plasmid* **64**, 186–195 (2010).
64. Blokesch, M. TransFLP - A Method to Genetically Modify *Vibrio cholerae* Based on Natural Transformation and FLP-recombination. *J. Vis. Exp.* e3761 doi:10.3791/3761 (2012).
65. Borgeaud, S. and Blokesch, M. Overexpression of the *tcp* Gene Cluster Using the T7 RNA Polymerase/Promoter System and Natural Transformation-Mediated Genetic Engineering of *Vibrio cholerae*. *PLoS One* **8**, 1–10 (2013).
66. Gu, Z., Gu, L., Eils, R., Schlesner, M. and Brors, B. circlize implements and enhances circular visualization in R. *Bioinformatics* **30**, 2811–2812 (2014).
67. Val, M-E., Marbouty, M., de Lemos Martins, F., Kennedy, S. P., Kemble, H., *et al.* A checkpoint control orchestrates the replication of the two chromosomes of *Vibrio cholerae*. *Sci. Adv.* **2**:e1501914, (2016).
68. Syed, K. A., Beyhan, S., Correa, N., Queen, J., Liu, J., *et al.* The *Vibrio cholerae* flagellar regulatory hierarchy controls expression of virulence factors. *J. Bacteriol.* **191**, 6555–6570 (2009).
69. Blokesch, M. A quorum sensing-mediated switch contributes to natural transformation of *Vibrio cholerae*. *Mob Genet Elements* **2**, 224–227 (2012).
70. Eberhart-Phillips, J., Besser, R. E., Tormey, M. P., Feikin, D., Araneta, M. R., *et al.* An outbreak of cholera from food served on an international aircraft. *Epidemiol. Infect.* **116**, 9–13 (1996).
71. Kemter, F. S., Messerschmidt, S. J., Schallopp, N., Sobetzko, P., Lang, E., *et al.* Synchronous termination of replication of the two chromosomes is an evolutionary selected feature in Vibrionaceae. *PLoS Genet.* **14**:e1007251, (2018).
72. Keene, O. N. The log transformation is special. *Stat. Med.* **14**, 811–819 (1995).
73. O'Shea, Y. A., Finnan, S., Reen, F. J., Morrissey, J. P., *et al.* The *Vibrio* seventh pandemic island-II is a 26·9 kb genomic island present in *Vibrio cholerae* El Tor and O139 serogroup isolates that shows homology to a 43·4 kb genomic island in *V. vulnificus*. *Microbiology* **150**, 4053–4063 (2004).
74. Imamura, D., Morita, M., Sekizuka, T., Mizuno, T., Takemura, T., *et al.* Comparative genome

analysis of VSP-II and SNPs reveals heterogenic variation in contemporary strains of *Vibrio cholerae* O1 isolated from cholera patients in Kolkata, India. *PLoS Negl. Trop. Dis.* **11**:e0005386 (2017).

75. Kirchberger, P. C., Unterweger, D., Provenzano, D., Pukatzki, S. and Boucher, Y. Sequential displacement of type VI secretion system effector genes leads to evolution of diverse immunity gene arrays in *Vibrio cholerae*. *Sci. Rep.* **7**:45133 (2017).
76. Brooks, T. M., Unterweger, D., Bachmann, V., Kostiuk, B. and Pukatzki, S. Lytic activity of the *Vibrio cholerae* type VI secretion toxin VgrG-3 is inhibited by the antitoxin TsaB. *J. Biol. Chem.* **288**, 7618–7625 (2013).
77. Dong, T. G., Ho, B. T., Yoder-Himes, D. R. and Mekalanos, J. J. Identification of T6SS-dependent effector and immunity proteins by Tn-seq in *Vibrio cholerae*. *Proc. Natl. Acad. Sci. USA* **110**, 2623–2628 (2013).
78. Zheng, J., Ho, B. and Mekalanos, J. J. Genetic analysis of anti-amoebae and anti-bacterial activities of the type VI secretion system in *Vibrio cholerae*. *PLoS One* **6**:e23876 (2011).
79. Thomas, J., Watve, S. S., Ratcliff, W. C. and Hammer, B. K. Horizontal gene transfer of functional type VI killing genes by natural transformation. *mBio* **8**:e00654-17 (2017).

4. FRESHLY PREY-RELEASED DNA CAN BE SHARED WITH NON-KILLING COMPETENT BACTERIA

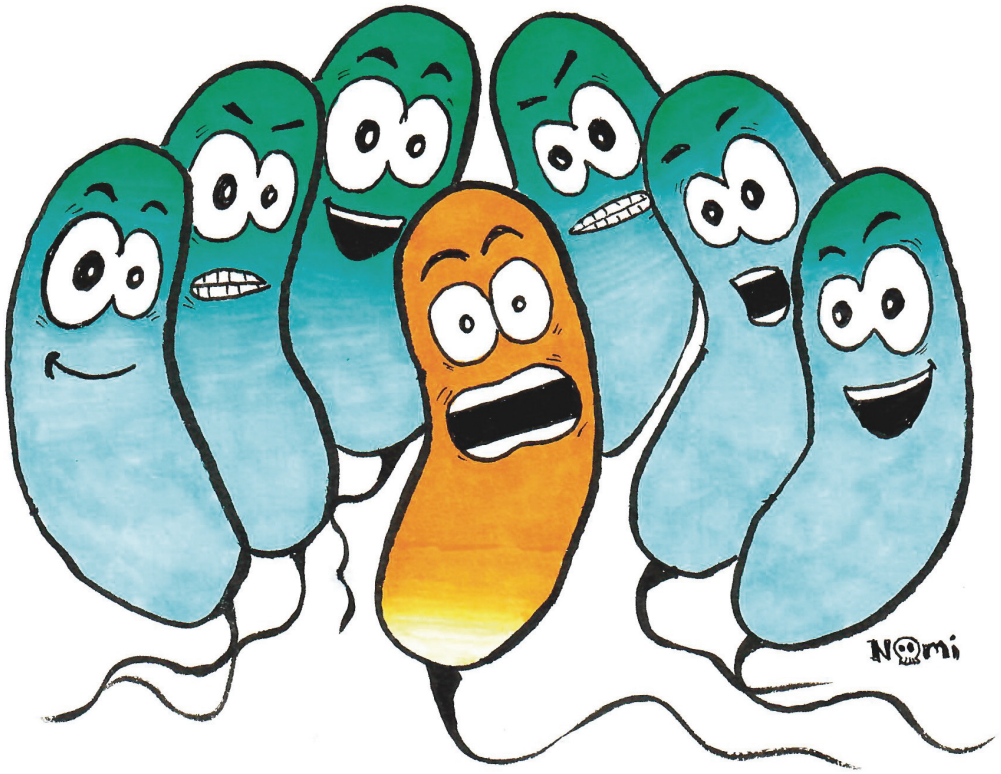

4.1 INTRODUCTION

Vibrio cholerae, the facultative human pathogen responsible of the diarrheal disease cholera, is a common inhabitant of aquatic environments. In its natural habitat, *V. cholerae* is often found in association with chitinous surfaces such as zooplankton or crustaceans ([1]). *V. cholerae* colonizes these biotic surfaces and initiates biofilm formation through the involvement of diverse structural components including the polar flagellum and type IV pili (T4P; [2,3]). T4P are cell surface appendages that play a role in diverse cellular processes including DNA uptake, motility, surface sensing and adhesion ([4]). Two distinct T4P of *V. cholerae* are implicated in adhesion to chitin surfaces: the mannose-sensitive haemagglutinin (MSHA) pilus, which binds abiotic and biotic surfaces and initiates biofilm formation ([2,3,5]), and the DNA-uptake pilus (also called chitin-regulated pilus, ChiRP), which was recently shown to be involved in chitin colonization under flow conditions ([6]). Chitin represents a colonization surface as well as a source of nutrient ([7]), but, remarkably, it also triggers the physiological state of competence for natural transformation in *V. cholerae* ([8]). Competence for natural transformation is a mode of horizontal gene transfer that is widespread among bacteria and leads to the acquisition and further integration of DNA present in the environment, therefore driving bacterial evolution ([9]). Moreover, for most bacterial species, the natural competence state is a highly regulated process, which is transient and dependent on diverse environmental signals ([9,10]).

In *V. cholerae,* the growth on chitin surfaces leads to the production of the master regulator of transformation, TfoX, which activates directly and indirectly the competence genes encoding the DNA-uptake machinery required for transformation ([8,11]). In addition, other environmental factors are necessary for competence induction such as high cell density, which is detected by quorum sensing via the regulator HapR ([11–13]). The regulators TfoX and HapR activate together an intermediate regulator QstR that induces a subset of the competence genes. Moreover, both HapR and QstR are essential for the repression of *dns,* which encodes an extracellular and periplasmic nuclease that inhibits transformation ([11,14–16]).

Remarkably, in *V. cholerae* strains that represent the currently ongoing seventh pandemic, the growth on chitin surfaces also induces the type VI secretion system (T6SS) in a TfoX-, HapR- and QstR-dependent manner ([15,17]). The T6SS, a killing device present in ~25% of all Gram-negative bacteria, resembles an inverted contractile bacteriophage tail that injects toxic effector proteins into adjacent eukaryotic or prokaryotic cells, which ultimately results in

their death ([18–20]). We previously demonstrated that the co-regulation of competence and the T6SS leads to the lysis of neighboring non-immune bacteria and the subsequent acquisition of their DNA, which enhances horizontal gene transfer in *V. cholerae* ([17]). Moreover, we determined the extent of DNA that is acquired and recombined into *V. cholerae* and we showed that T6SS-mediated DNA acquisition led to the chromosomal integration of large DNA fragments, which can exceed 100 kbp (see chapter 3). These findings highlighted how two chitin-induced nanomachines, the T6SS and the DNA-uptake machinery, could drive bacterial evolution in *V. cholerae*. However, it remained unclear how such large fragments of DNA are acquired by competent *V. cholerae*. We speculated that close proximity between the competent acceptor and the prey is not only needed for efficient T6SS killing ([21]), but might also be required to ensure the acquisition of large DNA fragments. Moreover, we hypothesized that T4P might allow such contact maintenance between the acceptor and prey cell.

Here, we investigated the possibility of a contact-maintenance mechanism for T6SS killing that could facilitate subsequent DNA acquisition. We showed that competent *V. cholerae* cells in close proximity to a T6SS-killed prey can efficiently acquire prey-released DNA. However, we also demonstrated that prey-released DNA acquisition is not restricted to the attacking cell itself as a "private good" but accessible to any surrounding competent cells. Interestingly, we also observed that *V. cholerae* exquisitely times interbacterial predation, DNA uptake and the repression of the nuclease genes, which collectively suggests that the regulatory coupling has evolved to maximize the DNA absorption process.

4.2 Results and Discussion

Interbacterial predation is not dependent on the DNA-uptake pilus, the MSHA pilus, or the flagellum

Given that the DNA-uptake machinery of *V. cholerae* contains a T4P as central part, we speculated that this T4P might also be implicated in cell contact maintenance, which would foster T6SS-mediated killing and subsequent acquisition of prey-released DNA. For this purpose, we tested different knockout strains (Δ*pilA*, Δ*pilT,* Δ*pilQ* and Δ*VC0858*), which are known to be impaired in T4P biogenesis and/or function ([22]), for their T6SS-dependent killing of *E. coli*. As shown in Fig. 4.1A, all knockout strains behaved similarly to the WT and significantly killed *E. coli* upon competence induction, which, in these experiments, was

based on an arabinose-inducible copy of *tfoX* (Tn*tfoX*; see Material and Methods). We concluded that the T4P of the DNA-uptake machinery is not required for successful T6SS-dependent killing under the tested conditions. This T4P was our first educated guess, however we also tested the adhesive pilus MSHA (Δ*mshA*) and the flagellum (Δ*flaA*) for T6SS-dependent killing of *E. coli*. Our results showed that these knockout strains also behaved similarly to the WT (Fig. 4.1B). We therefore concluded that, under the tested conditions, interbacterial predation was not dependent on the DNA-uptake pilus, the MSHA pilus, and the flagellum. It is important to mention that the condition used in the interbacterial killing assay forces the contact between the predator and the *E. coli* prey, as strains are highly concentrated before being deposited as a mixture on solid medium. This might hide the requirement for the establishment and maintenance of close contact under natural environmental conditions in which the pathogen thrives (e.g. on chitinous surfaces). Further studies are required to determine whether cell contact maintenance could ensure efficient T6SS-killing and subsequent DNA uptake. Interestingly, our laboratory recently showed that DNA-uptake pili self-interact and bind on chitin surfaces ([6]). More particularly, the major pilin subunit PilA, which is identical in most clinical isolates but varies extensively in environmental isolates, enable kin recognition by direct pilus-pilus interaction. In addition, the authors showed that in rare cases (4/45) cross-interactions between DNA-pili from two different strains were possible ([6]). It is tempting to speculate that in the latter case, cross-interactions between environmental isolates could favor T6SS-killing and DNA uptake. Further studies should address how pilus-pilus interactions influence killing of non-kin bacteria and subsequent DNA uptake.

DNA released by T6SS-mediated cell lysis is acquired by surrounding competent V. cholerae

Next, we tried another approach to better understand whether close contact was required between cells to ensure efficient DNA uptake from T6SS-killing of non-kin bacteria. Here, we used an imaging approach to investigate if the released DNA was only accessible to the predator that successfully killed the neighboring prey, or by any adjacent bacterium. Using fluorescent time-lapse microscopy we visualized the processes of prey killing and subsequent acquisition of DNA in competent predator. For this purpose, we genetically engineered the predator (referred as acceptor) to carry a translational fusion between the periplasmic DNA-binding protein ComEA and the fluorescent protein mNeonGreen. This construct enabled us to visualize the DNA uptake process into the periplasm of competent cells due to the

distinctive foci formation of the ComEA-mNeonGreen protein upon DNA binding ([23]). The competence-induced acceptor strain was mixed with unlabeled *V. cholerae* prey strain (donor). This prey strain was derived from the environmental isolate Sa5Y and was rendered T6SS-negative (T6SS$^-$) to only visualize a one-way killing action of the predator/acceptor strain towards the donor and not the other way around. In addition, propidium iodide was supplemented to the bacterial mixture in order to stain permeabilized dead bacteria as well as released DNA. Using this experimental setup, we followed the lysis of two donor cells and detected ComEA-mNeonGreen foci in five surrounding acceptor cells (Fig. 4.2A). This suggests that the T6SS-mediated prey-released DNA is accessible for several surrounding competent cells and not a "private good" of the attacking bacterium.

To confirm our hypothesis, we next assessed whether a T6SS$^-$ acceptor would be as transformable as a T6SS-positive (T6SS$^+$) acceptor in mixed communities. We established a chitin-independent transformation assay in which competence induction is arabinose-inducible (Tn*tfoX*, see Material and Methods) with three distinct strains: two acceptors, which carried different antibiotic resistance genes for selection purposes, and one T6SS$^-$ donor, which harbored the resistance gene *aph* (Kan^R) in *vipA* (Fig. 4.2B). As shown in Figure 4.2C, the T6SS$^-$ acceptor strain integrated the donor-released resistance cassette (*aph*) as efficiently as the T6SS$^+$ acceptor when they were mixed together. We therefore concluded that DNA released by T6SS-dependent cell lysis is not solely accessible to the attacking bacterium but also to other surrounding competent cells. Interestingly, a recent study performed on *Acinetobacter baylyi* also reported that, in mixed communities, T6SS-mediated DNA release is taken up by attacking and non-attacking competent cells ([24]), supporting our conclusion that prey-released DNA is not a "private good" of the attacker.

***V. cholerae* exquisitely times bacterial predation with natural transformation**

Environmental DNA is often degraded and results in short-sized fragments ([25,26]). However *V. cholerae* can acquire "fresh" and potentially intact DNA through T6SS-mediated bacterial predation ([17]). Given the close proximity observed between prey-released DNA and the competent cells that acquired DNA, we speculated that the released DNA is not too diffusible and should be more efficiently acquired compared to free-floating environmental DNA. We therefore aimed to investigate the transformability with prey-released DNA as compared with supplemented purified genomic DNA (gDNA). In our previous study (see chapter 3) we observed similar transformation frequencies on chitin with prey-released DNA or with

purified gDNA. However, in comparison to the bacterial prey strain, which was added to the acceptor strain at the start of the experiment, the supplemented DNA was added at a later time point when DNA was not prone to degradation by the extracellular and periplasmic nuclease Dns ([27]). Here, we aimed to investigate the transformability with prey-released DNA or with purified gDNA in a natural transformation assay on solid media, where each source of donor DNA (bacterial prey or gDNA) is added at comparable time to the competent acceptor. For this purpose, we first induced the *V. cholerae* acceptor strain (WT) for competence and further spotted a mixture of the acceptor supplemented with purified gDNA or with a T6SS$^-$ prey strain. The supplemented gDNA was extracted from the prey strain, which harbored the resistance gene *aph* (Kan^R) in *vipA*. We scored the acceptor cells that had integrated the antibiotic resistance gene and observed that the transformability with supplemented gDNA was 56x lower than with prey-released DNA (Fig. 4.3A). This difference could be explained by a higher quantity of DNA released by killed-prey in comparison to the 1 µg of purified gDNA initially added to the acceptor cells. We estimated that if all prey cells mixed with the acceptor would lyse, they would release in total 0.1 µg of DNA (see material and methods for details). This indicates that, at the start of the experiment, the amount of purified gDNA mixed with the acceptor was 10x higher than the quantity of DNA that could be released from all prey cells. As we observed the highest transformability with prey-released DNA (Fig. 4.3A), we speculated that the integrity and stability of the purified gDNA was reduced compared to the prey-released DNA. We hypothesized that under the tested conditions, the purified gDNA might be exposed to the nuclease Dns leading to its degradation and therefore affect the transformation rate. We knew from previous studies, which used purified gDNA as transforming material, that the repression of the nuclease gene *dns* ensures efficient transformation and that a Δ*dns* strain is more transformable and accumulates larger amount of DNA in the periplasm ([11,14,15,23]). Here, we aimed to test if the nuclease Dns is implicated in the reduced transformability observed with purified gDNA and, in addition, to investigate how the transformability obtained with prey-released DNA is affected in a *dns*-deficient strain as compared with supplemented DNA. For this purpose, we used the same transformation assay described above and we scored the transformability of the WT and Δ*dns* acceptor strains. In accordance with previous experiments ([14]), we observed that, under DNA supplementing conditions, the transformation rate of a Δ*dns* strain is >1 order of magnitude higher than the one of the WT (Fig. 4.3B). Interestingly, with prey-released DNA, we observed similar transformability for both WT and

Δ*dns* acceptor strains. Moreover, almost no difference (~2-fold even though statistically significant) between DNA supplementing versus prey-released conditions was observed for Δ*dns* strain (Fig. 4.3B). This indicates that the transformation of the WT is highly efficient under conditions of T6SS-mediated DNA acquisition and that this transformability is not further increased in a Δ*dns* strain. Altogether, we propose that the high levels of transformation linked to bacterial predation is the result of an elegant regulatory circuit, which ensures a prefect timing. Indeed, at the time of T6SS-mediated killing of prey, competent *V. cholerae* cells exert low nuclease activity while having their DNA-uptake complex ready to immediately absorb the prey-released DNA. By contrast, we propose that due to a lack of complete *dns* repression in the acceptor strain at the time of gDNA addition, this genetic material is partially degraded, which ultimately results in a decreased transformability.

4. 3 CONCLUSION

In this study, we showed that DNA released by T6SS-killed bacteria is not exclusively acquired by the attacking cell but is instead also taken up by any competent cell surrounding the lysed prey. Moreover, our results highlight that *V. cholerae* is highly transformable based on DNA acquisition through interbacterial predation and that the tight co-regulation of T6SS, competence, and nuclease repression ensures high integrity of the transforming DNA. Interestingly, a bioinformatics analysis showed that nuclease T6SS effector proteins are absent in pandemic strains and uncommon in non-pandemic *V. cholerae* isolates ([28]) when compared to other T6SS-harboring but non-transformable bacterial species (such as for instance *Agrobacterium tumefaciens* ([29]) or *Pseudomonas putida* ([30])). The absence of nuclease effectors in *V. cholerae* suggests that, during the attack of non-kin bacteria, the DNA is kept intact and can further serve as transforming material. We proposed that the repression of *dns* during competence induction together with the absence of nuclease T6SS effector ultimately favor the acquisition and integration of large prey-released DNA fragments into nearby competent *V. cholerae* (see Chapter 3). Interestingly, the co-regulation of the T6SS and the DNA-uptake machinery was also demonstrated in *Vibrio fischeri, Vibrio alginolyticus* and *Vibrio parahaemolyticus* ([31]) suggesting a conserved mechanism of bacterial evolution in these species. Moreover, kin-discriminated killing has also been observed during competence induction in the Gram-positive bacterium *Streptococcus*

pneumoniae ([32,33]). Induction of competence in *S. pneumoniae* is controlled by a tightly regulated quorum sensing system that is based on the accumulation of extracellular competence-stimulating peptides (CSP). Remarkably, CSP does not only activate competence but stimulates the production of bacteriocins via the indirect activation of the *blp* locus and the subsequent production and secretion of the bacteriocin pheromone BlpC. The accumulation of BlpC ultimately leads to the production of bacteriocins, which are secreted and cause pore formation in the membranes of non-kin bacteria ([32–34]). As the production of bacteriocin is coupled to a quorum sensing system, it was speculated that it ensures close proximity with prey and thus, that prey-released DNA is not too diffusible and can serve as transforming material ([34]). Moreover, Wholey and colleagues showed that the expression of bacteriocins enhances DNA exchange in *S. pneumoniae* ([32]), suggesting an important role in bacterial evolution through the acquisition of non-clonal DNA. We believe that interbacterial predation might be a widespread strategy used by naturally competent bacteria for the nearby release of "fresh" DNA and its subsequent acquisition. Importantly, such strategy may play a key role in the emergence of novel pathogens and multi-drug resistant bacteria. Further studies are therefore expected to identify other bacterial species that also actively acquire non-kin DNA to drive evolution.

4.4 MATERIALS AND METHODS

Bacterial strains and growth conditions

All bacterial strains and plasmids used in this study are described in Table 4.1. *E. coli* strain S17-λpir ([35]) was used for cloning purposes and served as donor in bacterial mating experiments. *V. cholerae* and *E. coli* were grown aerobically in lysogeny broth (LB from Carl Roth; 10 g/l of tryptone, 5 g/l of yeast extract, 10 g/l of sodium chloride) or on LB agar plates (Carl Roth; 1.5% agar) at 30°C or 37°C, unless otherwise stated. Bacterial cultures were grown under agitation at 40 rpm in a tube rotator or at 180 rpm in a shaking incubator. Thiosulfate Citrate Bile Salts Sucrose (TCBS; Sigma-Aldrich) agar plates, prepared according to the manufacturer's recommendation, were used to counter-select *E. coli* strains after bacterial conjugation with *V. cholerae*. Half-concentrated defined artificial seawater medium (DASW) containing HEPES and vitamins (MEM vitamin solution; Gibco) was used for experiments based on chitin flakes as previously described ([8]). When required, liquid and solidified media were supplemented with L-(+)-arabinose (ara; 0.02% or 0.2%; Sigma-

Aldrich) to induce constructs under the control of the P_{BAD} promoter (e.g., for the expression of *tfoX* or *tfoX-strep*). Whenever necessary, the following antibiotics were used at the mentioned concentrations: chloramphenicol (Cm; Carl Roth), 2.5 µg/ml; kanamycin (Kan; Carl Roth), 75 µg/ml; streptomycin (Strep; Carl Roth), 100 µg/ml; ampicillin (Amp; Carl Roth), 100 µg/ml; gentamicin (Gent; Carl Roth), 50 µg/ml; and rifampicin (Rif; AppliChem) 100 µg/ml.

Genetic engineering of bacterial strains

DNA manipulations, including polymerase chain reactions, were performed following standard molecular biology-based protocols ([36]). All DNA fragments used for genetic engineering were verified by colony PCR after integration inside the bacterium and, if required, by Sanger sequencing (Microsynth, Switzerland). To generate a deletion of gene(s) in the parental wild-type (WT) strains (A1552 or Sa5Y) of *V. cholerae*, a gene disruption method based on natural transformation and FLP recombination was used (TransFLP method; [37–39]). Natural transformation was also used to insert antibiotic resistance cassettes such as *aph* (KanR) or *cat*(CmR) into the target gene(s) of *V. cholerae* strains. The plasmids pBR-FRT-Kan-FRT2 and pBR-FRT-Cat-FRT2 served as templates for the amplification of these resistance genes.

To insert the mini-Tn7 transposon carrying *araC* and either *tfoX* or *tfoX-strep* under the control of the P_{BAD} promoter into the chromosome of *V. cholerae*, a tri-parental mating strategy involving *E. coli* S17-lλpir strains as donors was used ([40]). The donors plasmids were pUX-BF13 as a helper and derivatives of plasmid pGP704-mTn7-minus-SacI carrying the respective construct on the mTn7 ([41]).

Interbacterial killing assay using E. coli strains as prey

Interbacterial killing assay was performed according to the previously described protocol ([17]). Briefly, overnight cultures were diluted (1:100) in LB medium (± 0.2% ara to induce *tfoX* or *tfoX-strep*) and grown aerobically at 30°C under shaking condition until an OD_{600} of ~1.5 was reached for the predatory *V. cholerae.* The respective predator cells and the *E. coli* prey cells (TOP10) were harvested and concentrated to an OD_{600} of ~10 prior to be mixed at a ratio of 10:1. The mixture was spotted onto sterilized membrane filters (Supor-200, PALL) on pre-warmed LB agar plates (± 0.2% arabinose) and incubated at 37°C for 4h. At this point, bacteria were harvested from the filters and serial dilutions were spotted onto antibiotic-

containing LB agar plates to count the CFUs (shown as CFU/ml). Averages of at least three biologically independent experiments are provided.

Epifluorescence microscopy and image analysis

Wide-field microscopy images were acquired using a Zeiss Axio Imager M2 epifluorescence microscope. Details concerning the instrumentation and configurations are the following: a high-resolution AxioCamMRm camera and the Zeiss AxioVision software were used to acquire images, the objective used was a Plan-Apochromat 100X / 1.4 Oil Ph3 for fluorescence illumination, an illuminator HXP120 light source was utilized, and the filters sets employed were 63 HE mRFP shift free (Zeiss) and 38 Endow GFP shift free (Zeiss).

The bacterial overnight cultures pre-grown in LB medium were diluted (1:10) in LB medium supplemented with 0.2% arabinose and further grown aerobically for 4 hours at 30°C. To investigate intraspecies killing, the two strains of interest were mixed at a ratio of 1:1 and 0.5 μM of propidium iodide (PI) was added to stain dead cells. The mixed communities were mounted onto agarose pad (1.2% agarose 0.5x PBS) and the coverslip was sealed with heated VALAP ([42]), which is composed of vaseline (Sigma-Aldrich), lanolin (Sigma-Aldrich) and paraffin (Merck) mixed at a 1:1:1 ratio. Prepared samples were imaged shortly afterwards and images were taken at 2 minutes intervals. For comparisons, the images were acquired using the same exposure time. Image analysis and processing were performed using the Zeiss AxioVision software and Fiji/ImageJ, and Adobe Illustrator was used for image annotations.

Natural transformation assays

The purified genomic DNA (gDNA) used for natural transformation assays was isolated from *V. cholerae* strain Sa5YΔ*vipA*::FRT-*aph*-FRT using bacterial genomic DNA preparation kits (Genomic DNA buffer set, Genomic-tip 100/G; Qiagen).

Transformability of *V. cholerae* strains was assessed on solid media in chitin-independent transformation assays with expression of an arabinose-inducible chromosomal copy of *tfoX* using two different assays: 1) natural transformation assay in mixed communities based on a previously established protocol ([17]) with the co-culture of three different *V. cholerae* strains; and 2) natural transformation assay with either co-culture of *V. cholerae* strains or gDNA added to one *V. cholerae* strains. In the first case, bacterial strains were pre-grown as an overnight culture in LB medium and further harvested and concentrated 10-fold in LB

medium. Three *V. cholerae* strains were mixed at a ratio 1:1:1 and further spotted onto plain LB agar plates supplemented with the arabinose inducer (at a final concentration of 0.02%). After incubation at 37°C for 5 hours, bacteria were harvested from the agar plates and serially diluted. Serial dilutions were spotted (5 µl) on antibiotics-containing LB and plain LB agar plates to recover the number of transformants CFUs and the total number of CFUs, respectively. In the second protocol of natural transformations, overnight cultures were diluted (1:100) in LB medium supplemented with arabinose (at concentration 0.02%) and grown aerobically for 5 hours at 30°C under shaking condition. Cells were further harvested and concentrated 10x in PBS. At this point, cells were either mixed with 1 µg of gDNA as transforming material, or with another strain. The mix was spotted onto plain LB agar plates supplemented with the arabinose inducer (at concentration 0.02%) and further incubated at 37°C for 3 hours. Then, bacteria were harvested, incubated in 2YT for 2 hours at 30°C under shaking condition and then serially diluted. Serial dilutions were spotted (5 µl) on antibiotics-containing LB and plain LB agar plates to recover the number of transformants CFUs and the total number of CFUs, respectively. The transformation frequency represents the number of transformants CFUs divided by the total number of CFUs. The indicated transformation frequencies are the averages of at least three independent replicates.

Calculating amount of DNA released by lysed bacteria

To estimate the amount of DNA released by donor bacteria in our natural transformation assay (see above), we used the following formula:

$$DNA\ [g] = \frac{number\ of\ cells \times genome\ size\ [bp] \times 650\ [g/mol]}{6.022 \cdot 10^{23}\ [molecules/mol]}$$

This calculation is based on the assumption that the average molecular weight of a base pair is 650 g/mol. The Avogadro's number, which represents the number of molecules in one mole is used in the formula (6.022×10^{23}).

Statistical analysis

For interbacterial killing assays and natural transformation assays the data were log-transformed ([43]) and statistically significant differences were determined by two-tailed Student's t-test. In case the survival of *E. coli* CFUs (in interbacterial killing assays) or the number of transformants bacteria (in natural transformation assays) were below the detection limit, the value was set to the detection limit to allow statistical analysis.

4.5 FIGURES

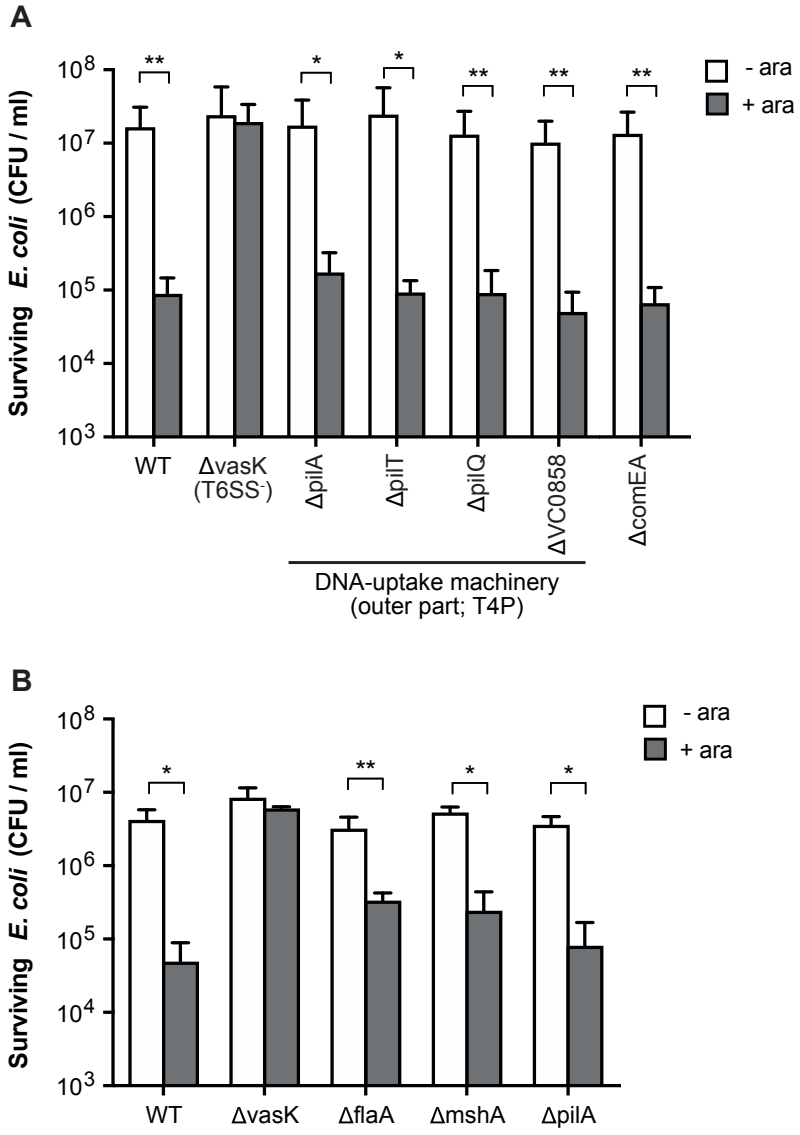

Figure 4.1: The DNA-uptake pilus, as well as the MSHA pilus and the flagellum are not required for bacterial T6SS-dependent killing. (A-B) *E. coli* killing assay using different *V. cholerae* strains as predators (derived from A1552). All *V. cholerae* strains contain the arabinose-inducible copy of *tfoX* for competence induction. *V. cholerae* and *E. coli* TOP10 were co-cultured, mixed in a 10:1 ratio, and spotted onto agar plates in the absence or presence of arabinose as indicated on the graph (-/+ ara). The survival of the prey is depicted as CFU per ml. WT and Δ*vasK* strains represent the $T6SS^+$ and $T6SS^-$ controls, respectively. Data represent the average of three independent biological replicates (±SD). Statistical significance is indicated (*p<0.05; **p<0.01).

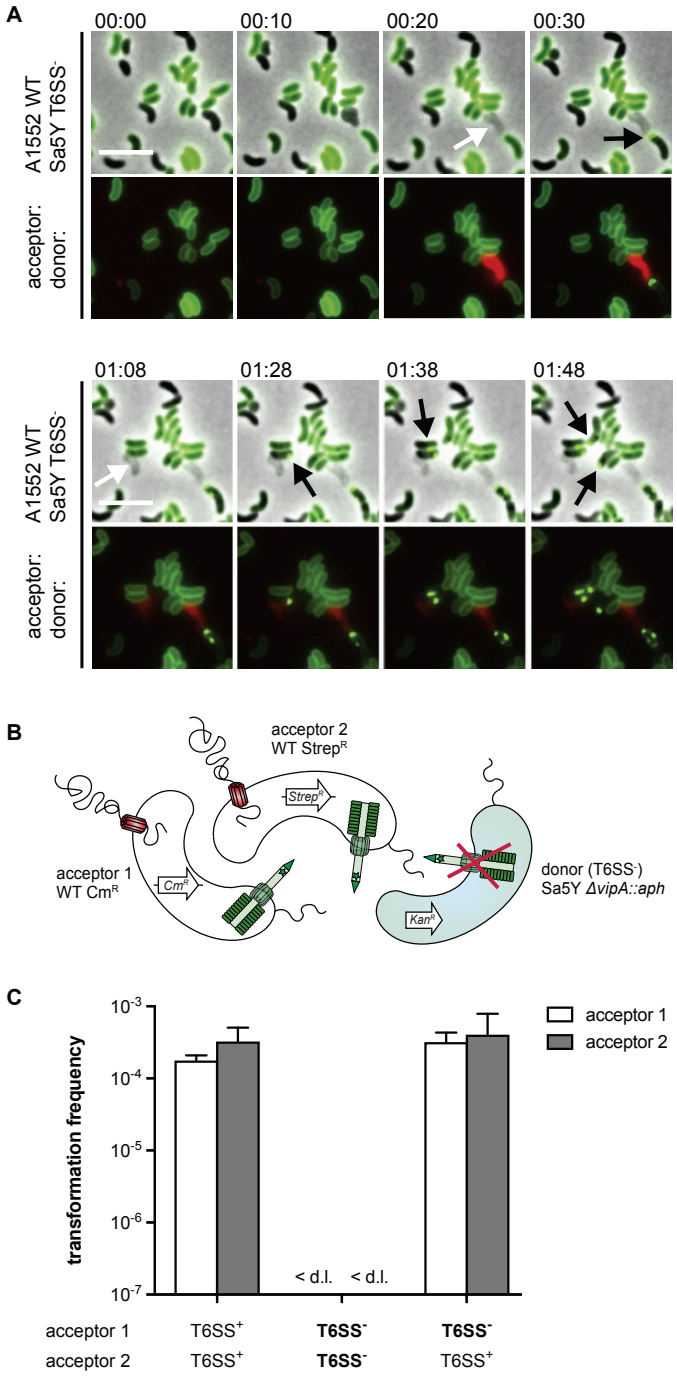

Figure 4.2: DNA released by T6SS-mediated killing is acquired by neighboring acceptors. (A) T6SS-mediated killing of a single bacterium is followed by DNA uptake in several competent *V. cholerae*. The acceptor strain (A1552 WT, T6SS$^+$) carried a ComEA-mNeonGreen translational fusion to visualize DNA uptake through relocalization and foci formation (green channel) and harbored an arabinose-inducible copy of *tfoX-strep* for competence induction. Acceptor and donor (Sa5Y T6SS$^-$) were mixed in the presence of propidium iodide to stain permeabilized dead bacteria (red channel) and the bacteria were imaged with 2 min intervals for 2 hours. Images represent snapshots of this time-lapse movie. A merge of phase contrast and green channels (top row) and a merge of red and green channels are depicted (lower row). White arrows indicate lysed donor cells and black arrows show DNA uptake events. Scale bar: 5 µm. (B) Experimental model for natural transformation assay in mixed communities. Two acceptor strains (derived from A1552; white) were mixed, in competition with a donor (Sa5Y T6SS$^-$; blue) that carried an *aph* cassette (Kan^R) in *vipA*. Due to their different resistance genes, acceptor 1 (Cm^R) and acceptor 2 (Strep^R) could be differentiated. In this scheme both acceptors harbor a functional T6SS (green structure). (C) Natural transformation assay in mixed communities. All acceptor *V. cholerae* strains carried the arabinose-inducible copy of *tfoX* for competence/T6SS induction. Two acceptor strains (T6SS$^+$ or T6SS$^-$, as indicated below the graph) were mixed with Sa5Y donor at ratio 1:1:1. Transformation frequencies (Y-axis), depicted for each acceptor strain, indicate the number of transformants that acquired the *aph* resistance cassette divided by the total number of acceptor CFUs. Data represent the average of three independent biological replicates (±SD). <d.l., below detection limit.

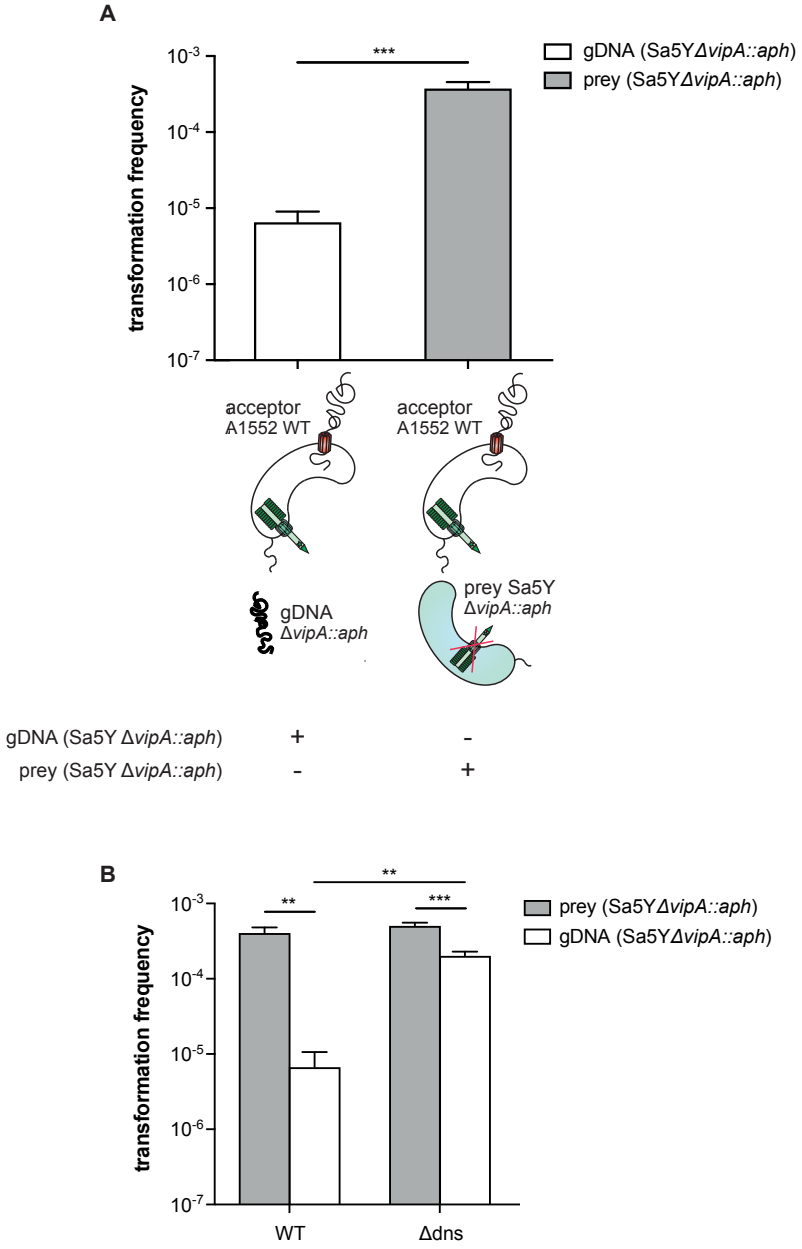

Figure 4.3: Prey-released DNA results in high transformability. Natural transformation assays of *V. cholerae* WT (A) and Δ*dns* (B) strains. (A-B) All acceptor strains (A1552-derived) harbored an arabinose-inducible copy of *tfoX* for competence induction. Acceptor strains were mixed individually with gDNA as transforming material or with the donor strain (Sa5Y T6SS^{-}; Δ*vipA::aph;* Kan^{R}). Transformation frequencies (Y-axis) indicate the number of transformants that acquired *aph* resistance cassette from prey-released DNA (gray bars) or supplemented DNA (white bars) divided by the total number of acceptor CFUs. Data represent averages of three independent biological replicates (±SD). Statistical significance is indicated (*p<0.05; ***p*<0.01; ****p*<0.001).

Table 4.1: Bacterial strains and plasmids used in this study

Strains	Genotype/description*	Internal strain No.	Reference
V. cholerae			
A1552 Tn*tfoX*	A1552 O1 El Tor Inaba; containing mini-Tn7-*araC*-P_{BAD}-*tfoX;* Rif^R ;$Gent^R$	MB_1626	([11])
A1552ΔvasK Tn*tfoX*	A1552 deleted for *vasK* (VCA0120); containing mini-Tn7-*araC*-P_{BAD}-*tfoX;* Rif^R ;$Gent^R$	MB_2985	This study
A1552ΔpilA Tn*tfoX*	A1552 deleted for *pilA* (VC1917); containing mini-Tn7-*araC*-P_{BAD}-*tfoX;* Rif^R ;$Gent^R$	MB_2345	([22])
A1552ΔpilT Tn*tfoX*	A1552 deleted for *pilT* (VC0462); containing mini-Tn7-*araC*-P_{BAD}-*tfoX;* Rif^R ;$Gent^R$	MB_2349	([22])
A1552ΔpilQ Tn*tfoX*	A1552 deleted for *pilA* (VC2630); containing mini-Tn7-*araC*-P_{BAD}-*tfoX;* Rif^R ;$Gent^R$	MB_3188	([22])
A1552ΔVC0858 Tn*tfoX*	A1552 deleted for VC0858; containing mini-Tn7-*araC*-P_{BAD}-*tfoX;* Rif^R ;$Gent^R$	MB_3150	([22])
A1552ΔcomEA Tn*tfoX*	A1552 deleted for *comEA* (VC1917); containing mini-Tn7-*araC*-P_{BAD}-*tfoX;* Rif^R ;$Gent^R$	MB_1645	([16])
A1552ΔflaA Tn*tfoX*	A1552 deleted for *flaA* (VC2188); containing mini-Tn7-*araC*-P_{BAD}-*tfoX;* Rif^R ;$Gent^R$	NM_24	This study
A1552ΔmshA Tn*tfoX*	A1552 deleted for *mshA* (VC0409); containing mini-Tn7-*araC*-P_{BAD}-*tfoX;* Rif^R ;$Gent^R$	MB_2822	([6])
A1552-comEA-mNeonGreen::FRT-Tn*tfoX-strep*	A1552 carrying *comEA::mNeonGreen* translational fusion (TransFLP) and containing mini-Tn7-*araC*-P_{BAD}-*tfoX-strep*; Rif^R, $Gent^R$	MB_3965	This study
A1552 $Strep^R$ Tn*tfoX*	A1552 $Strep^R$ containing mini-Tn7-*araC*-P_{BAD}-*tfoX-strep;* Rif^R ;$Gent^R$; $Strep^R$	NM_41	This study
A1552 ΔlacZ::FRT-Cat-FRT Tn*tfoX*	A1552 deleted for *lacZ* (TransFLP; *cat* insertion) containing mini-Tn7-*araC*-P_{BAD}-*tfoX-strep;* Rif^R ;$Gent^R$; Cm^R	NM_42	This study
A1552 ΔvasK ΔlacZ::FRT-Cat-FRT Tn*tfoX*	A1552 deleted for *vasK,* for *lacZ* (TransFLP; *cat* insertion) containing mini-Tn7-*araC*-P_{BAD}-*tfoX-strep;* Rif^R ;$Gent^R$; Cm^R	NM_43	This study
A1552 $Strep^R$ ΔvasK Tn*tfoX*	A1552 $Strep^R$ deleted for *vasK,* containing mini-Tn7-*araC*-P_{BAD}-*tfoX-strep;* Rif^R ;$Gent^R$; $Strep^R$	NM_44	This study

Strains	Genotype/description*	Internal strain No.	Reference
A1552Δdns Tn*tfoX*	A1552 deleted for *dns* (VC0470) containing mini-Tn7-*araC*-P_{BAD}-*tfoX;* Rif^R ;$Gent^R$	MB_1690	([23])
Sa5Y (WT)	non-O1/non-O139 environmental *V. cholerae* strains; isolated from the central California coast	MB_353	([44, 45])
Sa5YΔvipA::FRT-Kan-FRT	Sa5Y deleted for *vipA* (VCA0107) (TransFLP; aph insertion); Kan^R	MB_3020	([17])
Sa5Y $Strep^R$ ΔvipA::FRT-Kan-FRT	Sa5Y $Strep^R$ deleted for *vipA* (VCA0107) (TransFLP; aph insertion); Kan^R $Strep^R$	MB_3053	This study
E. coli			
S17-1λpir	Tpr Smr recA thi pro hsdR2M1 RP4:2-Tc:Mu:Kmr Tn7 (λpir); $Strep^R$	MB_648	([35])
TOP10	F- mcrA Δ(mrr-hsdRMS-mcrBC) φ80lacZΔM15 ΔlacX74 nupG recA1 araΔ139 Δ(ara-leu)7697 galE15 galK16 rpsL(StrR) endA1λ-; $Strep^R$	MB_741	Invitrogen
Plasmids			
pBR-FRT-Kan-FRT2	pBR322 derivative containing improved FRT-*aph*-FRT cassette, used as template for TransFLP; AmpR, KanR	MB_3782	([46])
pBR-FRT-Cat-FRT2	pBR322 derivative containing improved FRT-*cat*-FRT cassette, used as template for TransFLP; AmpR, KanR	MB_3783	([46])
pBR-flp	pBR322 derivative containing FLP+, λ cI857+, λ pR from pCP20 integrated into the *EcoRV* site of pBR322, used for FLP recombination; Amp^R	MB_1203	([37])
pUX-BF13	oriR6K, helper plasmid with Tn7 transposition function; Amp^R	MB_457	([40])
pGP704-Tn*tfoX*	pGP704 with mini-Tn7 carrying *araC* and P_{BAD}-driven *tfoX;* Amp^R, $Gent^R$	MB_1624	([11])

*VC number according to ([47])

4.6 REFERENCES

1. Lipp, E. K., Huq, A. and Colwell, R. R. Effects of Global Climate on Infectious Disease : the Cholera Model. *Clin. Microbiol. Rev.* **15**, 757–770 (2002).
2. Utada, A. S., Bennett, R. R., Fong, J. C. N., Gibiansky, M. L., Yildiz, F. H., Golestanian, R. and Wong, G. C. L. *Vibrio cholerae* use pili and flagella synergistically to effect motility switching and conditional surface attachment. *Nat. Commun.* **5**:4913 (2014).
3. Watnick, P. I., Fullner, K. J. and Kolter, R. A role for the mannose-sensitive hemagglutinin in biofilm formation by *Vibrio cholerae* El Tor. *J. Bacteriol.* **181**, 3606–3609 (1999).
4. Giltner, C. L., Nguyen, Y. and Burrows, L. L. Type IV Pilin Proteins: Versatile Molecular Modules. *Microbiol. Mol. Biol. Rev.* **76**:4, 740–772 (2012).
5. Watnick, P. I. and Kolter, R. Steps in the development of a *Vibrio cholerae* El Tor biofilm. *Mol. Microbiol.* **34**:3, 586–595 (1999).
6. Adams, D. W., Stutzmann, S., Stoudmann, C. and Blokesch, M. DNA-uptake pili of *Vibrio cholerae* are required for chitin colonization and capable of kin recognition via sequence-specific self-interaction. *Nat. Microbiol.* (2019). doi:10.1038/s41564-019-0479-5
7. Meibom, K. L., Li, X.B., Nielsen, A.T., Wu, C.Y., Roseman, S., and Schoolnik, G.K. The *Vibrio cholerae* chitin utilization program. *Proc. Natl. Acad. Sci. USA.* **101**, 2524–9 (2004).
8. Meibom, K. L., Blokesch, M., Dolganov, N. A., Wu, C.-Y. and Schoolnik, G. K. Chitin induces natural competence in *Vibrio cholerae*: supporting material. *Science* **310**, 1824–1827 (2005).
9. Johnston, C., Martin, B., Fichant, G., Polard, P. and Claverys, J. P. Bacterial transformation: distribution, shared mechanisms and divergent control. *Nat. Rev. Microbiol.* **12**, 181–196 (2014).
10. Seitz, P. and Blokesch, M. Cues and regulatory pathways involved in natural competence and transformation in pathogenic and environmental Gram-negative bacteria. *FEMS Microbiol. Rev.* **37**, 336–363 (2013).
11. Lo Scrudato, M. and Blokesch, M. The regulatory network of natural competence and transformation of *Vibrio cholerae*. *PLoS Genet.* **8**, e1002778 (2012).
12. Suckow, G., Seitz, P. and Blokesch, M. Quorum sensing contributes to natural transformation of *Vibrio cholerae* in a species-specific manner. *J. Bacteriol.* **193**, 4914–4924 (2011).
13. Antonova, E. S. and Hammer, B. K. Quorum-sensing autoinducer molecules produced by members of a multispecies biofilm promote horizontal gene transfer to *Vibrio cholerae*. *FEMS Microbiol. Lett.* **322**, 68–76 (2011).
14. Blokesch, M. and Schoolnik, G. K. The extracellular nuclease Dns and its role in natural transformation of *Vibrio cholerae*. *J. Bacteriol.* **190**, 7232–7240 (2008).
15. Jaskólska, M., Stutzmann, S., Stoudmann, C. and Blokesch, M. QstR-dependent regulation of natural competence and type VI secretion in *Vibrio cholerae*. *Nucleic Acids Res.* **46**, 10619–10634 (2018).
16. Lo Scrudato, M. and Blokesch, M. A transcriptional regulator linking quorum sensing and chitin induction to render *Vibrio cholerae* naturally transformable. *Nucleic Acids Res.* **41**, 3644–3658 (2013).
17. Borgeaud, S., Metzger, L. C., Scrignari, T. and Blokesch, M. The type VI secretion system of *Vibrio cholerae* fosters horizontal gene transfer. *Science.* **347**, 63–67 (2015).
18. Pukatzki, S., Ma, A. T., Sturtevant, D., Krastins, B., Sarracino, D., Nelson, W. C., Heidelberg, J. F. and Mekalanos, J. J. Identification of a conserved bacterial protein secretion system in *Vibrio cholerae* using the *Dictyostelium* host model system. *Proc. Natl. Acad. Sci. USA* **103**,

1528–1533 (2006).
19. Ho, B. T., Dong, T. G. and Mekalanos, J. J. A view to a kill: The bacterial type VI secretion system. *Cell Host Microbe* **15**, 9–21 (2014).
20. Russell, A. B., Peterson, S. B. and Mougous, J. D. Type VI secretion system effectors: Poisons with a purpose. *Nat. Rev. Microbiol.* **12**, 137–148 (2014).
21. Hood, R. D., Singh, P., Hsu, F., Güvener, T., Carl, M. A., Trinidad, R. R-S., *et al.* A Type VI Secretion System of *Pseudomonas aeruginosa* Targets a Toxin to Bacteria. *Cell Host Microbe* **7**, 25–37 (2010).
22. Seitz, P. and Blokesch, M. DNA-uptake machinery of naturally competent *Vibrio cholerae. Proc. Natl. Acad. Sci. USA* **110**, 17987–17992 (2013).
23. Seitz, P., Pezeshgi Modarres, H., Borgeaud, S., Bulushev, R.D., Steinbock, L.J., Radenovic, A. *et al*. ComEA Is Essential for the Transfer of External DNA into the Periplasm in Naturally Transformable *Vibrio cholerae* Cells. *PLoS Genet.* **10**, e1004066 (2014).
24. Cooper, R. M., Tsimring, L. and Hasty, J. Inter-species population dynamics enhance microbial horizontal gene transfer and spread of antibiotic resistance. *Elife* **6**, 1–26 (2017).
25. Nielsen, K. M., Johnsen, P. J., Bensasson, D. and Daffonchio, D. Release and persistence of extracellular DNA in the environment. *Environ. Biosafety Res.* **6**, 37–53 (2007).
26. Overballe-Petersen, S., Harms. K., Orlando, L. A. A., Mayar, J. V. M., Rasmussen, S., *et al.* Bacterial natural transformation by highly fragmented and damaged DNA. *Proc. Natl. Acad. Sci.USA* **110**, 19860–19865 (2013).
27. Marvig, R. L. and Blokesch, M. Natural transformation of *Vibrio cholerae* as a tool - Optimizing the procedure. *BMC Microbiol.* **10**, 155 (2010).
28. Unterweger, D., Miyata, S. T., Bachmann, V., Brooks, T. M., Mullins, T., *et al.* The *Vibrio cholerae* type VI secretion system employs diverse effector modules for intraspecific competition. *Nat. Commun.* **5**:3549 (2014).
29. Ma, L. S., Hachani, A., Lin, J. S., Filloux, A. and Lai, E-M. *Agrobacterium tumefaciens* deploys a superfamily of type VI secretion DNase effectors as weapons for interbacterial competition in planta. *Cell Host Microbe* **16**, 94–104 (2014).
30. Bernal, P., Allsopp, L. P., Filloux, A. and Llamas, M. A. The *Pseudomonas putida* T6SS is a plant warden against phytopathogens. *ISME J.* **11**, 972-087 (2017).
31. Metzger, L. C., Matthey, N., Stoudmann, C., Collas, E. J. and Blokesch, M. Ecological implications of gene regulation by TfoX and TfoY among diverse *Vibrio* species . *Environ. Microbiol.* **21**, 2231-2247 (2019).
32. Wholey, W., Kochan, T. J., Storck, D. N. and Dawid, S. Coordinated bacteriocin expression and competence in *Streptococcus pneumoniae* contributes to genetic adaptation through neighbor predation. *PLoS Pathog.* **12**, e1005413 (2016).
33. Kjos, M., Miller, E., Slager, J., Lake, F. B., Gericke, O., *et al.* Expression of *Streptococcus pneumoniae* bacteriocins is induced by antibiotics via regulatory interplay with the competence system. *PLoS Pathog.* **12**, e1005422 (2016).
34. Veening, J. W. and Blokesch, M. Interbacterial predation as a strategy for DNA acquisition in naturally competent bacteria. *Nat. Rev. Microbiol.* **15**, 621–629 (2017).
35. Simon, R., Priefer, U. and Pühler, A. A broad host range mobilization system for *in vivo* genetic engineering: Transposon mutagenesis in Gram negative bacteria. *Biotechnology* 784–790 (1983).
36. Sambrook, J., Fritsch, E. . and Maniatis, T. Molecular Cloning: A laboratory Manual. *Cold Spring Harb. NY. Cold Spring Harb. Lab. Press* (1982).
37. De Souza Silva, O. and Blokesch, M. Genetic manipulation of *Vibrio cholerae* by combining natural transformation with FLP recombination. *Plasmid* **64**, 186–195 (2010).

38. Blokesch, M. TransFLP - A Method to Genetically Modify *Vibrio cholerae* Based on Natural Transformation and FLP-recombination. *J. Vis. Exp.* e3761 doi:10.3791/3761 (2012).
39. Borgeaud, S. and Blokesch, M. Overexpression of the *tcp* Gene Cluster Using the T7 RNA Polymerase/Promoter System and Natural Transformation-Mediated Genetic Engineering of *Vibrio cholerae*. *PLoS One* **8**, 1–10 (2013).
40. Bao, Y., Lies, D. P., Fu, H. and Roberts, G. P. An improved Tn7-based system for the single-copy insertion of cloned genes into chromosomes of Gram-negative bacteria. *Gene* **109**, 167–168 (1991).
41. Nielsen, A. T., Dolganov, N.A., Otto, G., Miller, M.C., Wu, C.Y., and Schoolnik, G.K. RpoS controls the *Vibrio cholerae* mucosal escape response. *PLoS Pathog.* **2**, 0933–0948 (2006).
42. Valap for agar mounts. *cold spring Harb. Protoc.* doi:10.1101/pbd.rec12380, (2010).
43. Keene, O. N. The log transformation is special. *Stat. Med.* **14**, 811–819 (1995).
44. Keymer DP, Miller MC, Schoolnik GK, and Boehm AB Genomic and phenotypic diversity of coastal *Vibrio cholerae* strains is linked to environmental factors. *Appl. Environ. Microbiol.* 73:3705-3714 (2007).
45. Matthey N, Drebes Dörr NC, and Blokesch M Long-Read-Based Genome Sequences of Pandemic and Environmental *Vibrio cholerae* Strains. *Microbiol. Resour. Announc.* 7:e01574-01518 (2018).
46. Metzger, L.C., Stutzman, S., Scrignari, T., Van der Henst, C., Matthey, N. and Blokesch, M. Independent Regulation of Type VI Secretion in *Vibrio cholerae* by TfoX and TfoY. *Cell Rep.* **15**:951-958 (2016).
47. Heidelberg, J. F. Eisen, J.A., Nelson, W.C., Clayton, R.A., Gwinn, M.L., Dodson, R.J. *et al.* DNA sequence of both chromosomes of the cholera pathogen *Vibrio cholerae*. *Nature* **406**, 477–483 (2000).

5. OVERALL CONCLUSION AND PERSPECTIVES

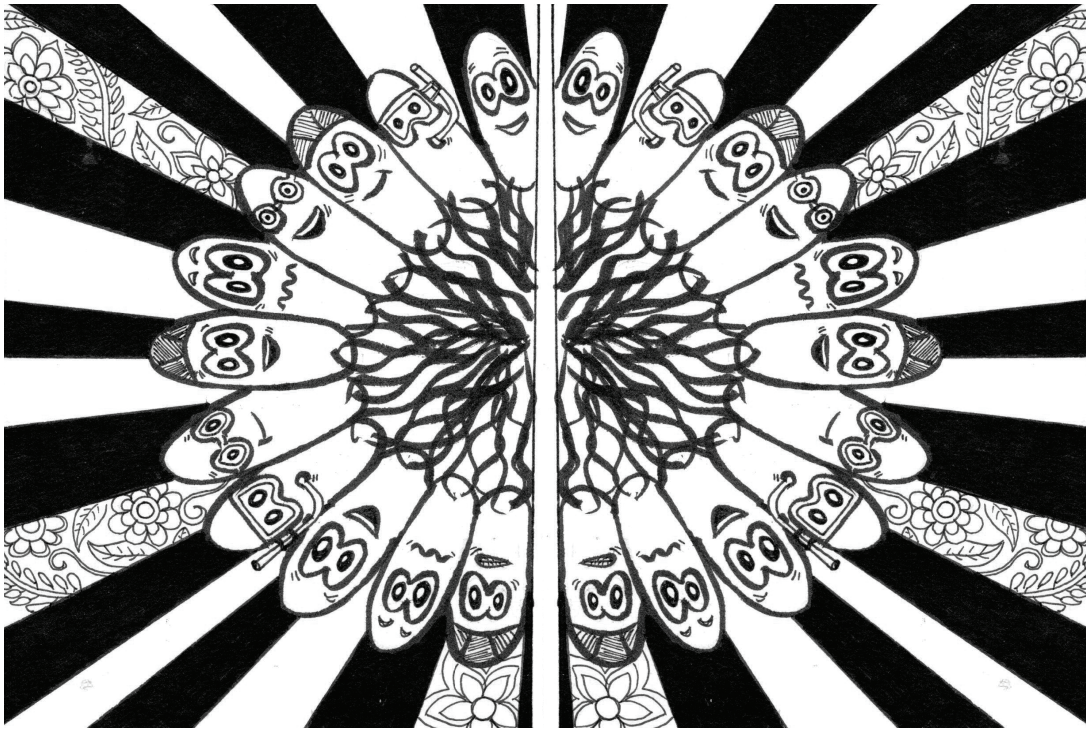

The aquatic bacterium *V. cholerae,* responsible of the disease cholera, is found in association with zooplankton. The latter organisms have a chitinous exoskeleton, which is a colonization surface, a source of nutrient and triggers the development of natural competence for transformation in *V. cholerae*. The chitin-induced regulator TfoX, together with the QS regulator HapR produced at HCD, induce the competence genes in parallel to the T6SS killing device, therefore enhancing horizontal gene transfer in pandemic *V. cholerae* ([1]). Remarkably, the homologue of TfoX, namely TfoY, which is produced at low intracellular level of c-di-GMP, also induces the T6SS and simultaneously enhances bacterial motility ([2]). While the two regulators TfoX and TfoY are present in all sequenced *Vibrionaceae*, key knowledge about their biological functions has been gained by studying *V. cholerae* as a model organism ([1–3]). Studying T6SSs and their regulation is important to get insights onto their potential implications in niche adaptation. By investigating the conservation of TfoX and TfoY regulatory pathways in diverse *Vibrio* species (*V. fischeri, V. alginolyticus* and *V. parahaemolyticus*), we contributed to the current understanding of their biological function. Based on a previously optimized approach ([2,4]), which results in low level of TfoX or TfoY production, we determined the phenotypes driven by these artificially induced regulators in different *Vibrio* species using qRT-PCR, interbacterial killing assay, and motility assay. Our results highlighted the conservation of the biological function of these regulators. We showed that TfoX activates one T6SS and the competence genes in all *Vibrio* species investigated and that TfoY is always associated with an enhance bacterial motility phenotype, whereas the TfoY-mediated T6SS regulation varied among the diverse vibrios tested. These findings are interesting, because even though the environmental cues inducing the T6SS of *V. parahaemolyticus* and *V. alginolyticus* were previously identified ([5,6]), the major regulators activating the T6SS clusters in these species and in *V. fischeri* remained unknown. Interestingly, we showed that TfoY does not regulate the T6SS of *V. fischeri,* while TfoY activates the single T6SS of *V. cholerae,* the T6SS1 but not T6SS2 of *V. parahaemolyticus* and both T6SSs of *V. alginolyticus*. The induction of a single or two T6SS clusters simultaneously might trigger different defense reactions that are adapted to the environmental niche of each species or to their interaction with a host. Currently, we know that TfoY is produced at low levels of c-di-GMP; however, the conditions in which TfoY is naturally produced are less clear compared to TfoX, which the latter being specifically induced by the growth of *V. cholerae* on chitinous surfaces in the aquatic environment. Remarkably, we noticed that TfoY does not induce the T6SS of the bacterial symbiont *V. fischeri*, but activates the T6SS(s) of the pathogenic vibrios, that can colonize the human intestine. Indeed,

V. parahaemolyticus, an emerging human pathogen, and *V. alginolyticus,* an opportunistic human pathogen, cause gastroenteritis, whereas *V. cholerae* is the causative agent of the diarrheal disease cholera. One could speculate that the T6SS might be induced by TfoY in the gut and could be used as a strategy to survive in the intestine, which is an environment limited in space and in nutrients. Along those lines, a study by Livny and colleagues identified *tfoY* (VP1028, wrongly annotated as *tfoX* in their study) among the genes expressed during *in vivo* infection of infant rabbits by *V. parahaemolyticus* ([12]), reinforcing our hypothesis that TfoY might be implicated in pathogenesis. In fact, bacterial pathogens have developed different strategies, including the use of alternative nutrient sources or the production and secretion of toxins, to face the competition from commensal bacteria that reside in the gut ([7]). For example, it was demonstrated using a *Salmonella enteria* serovar Typhimurium mouse model that *Salmonella* Typhimurim uses its T6SS to compete with other commensal bacteria in order to establish itself within the host gut ([8]). Interestingly, previous study had suggested that the T6SS of pandemic *V. cholerae* is used for colonization of the gut of infant rabbits ([9]). It is important to note that infant mammals are frequently used as cholera models due to their immature microbiota ([27]). Indeed, the natural microbiota plays a role in preventing intestinal colonization by *V. cholerae* ([28]). Nevertheless, Bachman and colleagues showed that mucin proteins, which form a thick mucosal layer protecting the intestinal epithelial cells against pathogenic and commensal bacteria, induce the T6SS of pandemic *V. cholerae in vitro*. In their study, the authors also observed that products of the bile acids metabolism generated by commensal bacteria could further enhance or inhibit the T6SS ([10]). It is also interesting to mention two studies, starting with the study by Tamayo and colleagues who investigated the role of c-di-GMP *in vivo* using the infant-mouse model and proposed that intracellular level of c-di-GMP goes down at early and late stages of infection. Upon entry in the small intestine, the low c-di-GMP allows proper expression of virulence genes, whereas the reduced c-di-GMP at later stage of infection could allow the induction of motility as part of an escape response to detach from the epithelial surface ([26]). In the second study, Koestler and Waters suggested that *V. cholerae* can modulate c-di-GMP signaling pathway in response to the local niches within the human small intestine. The authors proposed a model in which the bile present in the lumen would result in high intracellular levels of c-di-GMP, whereas the bicarbonate in the mucosal layer would lead to low levels of c-di-GMP ([11]). Based on these studies, we speculate that in the mucosal layer, the mucins proteins in addition to the low intracellular level of c-di-GMP might induce TfoY production within the intestine, followed by the induction of the T6SS. It would therefore be interesting

to investigate whether TfoY is produced in presence of mucin alone or mucin together with low intracellular level of c-di-GMP. We speculate that there is a link between mucin, low c-di-GMP levels, and the production of the TfoY-mediated T6SS, which could play a role *in vivo* in the pathogenesis of *V. cholerae* as well as in the pathogenesis of *V. parahaemolyticus* and *V. alginolyticus*.

Given the high conservation of the TfoX-mediated induction of the T6SS concomitantly with the competence genes in diverse *Vibrio* species, we sought to investigate the outcome of this co-regulation. We focused on *V. cholerae,* as it was previously demonstrated that TfoX induces the T6SS and the DNA-uptake machinery on chitinous surfaces under condition mimicking the natural marine environment ([1]). Indeed, further experiments are required to demonstrate that the production of TfoX leads to bacterial predation and subsequent DNA uptake in *V. fischeri, V. alginolyticus* and *V. parahaemolyticus*. Using *V. cholerae* as a model organism, we investigated the extent of HGTs acquired by competent acceptor strain under conditions mimicking the bacterium's natural habitat. Previous studies had already quantified the horizontally acquired DNA regions in several Gram-negative bacteria such as *Haemophilus influenzae* (6.9 kbp transferred on average ([13])), *Helicobacter pylori* (average: 2.9 kbp ([14])) and *Neisseria meningitidis* (average: 10.6 kbp ([15])). However, these studies used large amount of purified gDNA as transforming material (with up to 50 donor genome equivalents per acceptor cell ([14])), which does not reflect the natural environmental conditions. Here, under conditions that mimic the natural environment, we showed for the first time the extent of DNA acquired and integrated into *V. cholerae* after T6SS-mediated bacterial predation. Using a WGS approach, we showed that large regions of DNA, with an average of 50-70 kbp, were transferred through T6SS-dependent bacterial predation. We also quantified the maximum length of horizontally acquired DNA fragments and showed that one acceptor cell transferred up to 260.8 kbp by inserting four different DNA segments (chr 1: 64.5 kbp, 32.6 kbp, 113,7 kbp and chr 2: 50 kbp). Moreover, we compared the extent of HGT events in conditions with or without T6SS-dependent bacterial predation and demonstrated that in absence of bacterial predation the transformability was decreased and, in addition, that rare and short fragments of DNA were primarily exchanged. Our results highlighted that the co-regulation of the T6SS and the DNA-uptake machinery during competence can drive bacterial evolution in *V. cholerae.* We also emphasized how the tight regulation of competence and nuclease repression ensures DNA integrity during T6SS-mediated DNA release, which is required for the successful uptake and integration of DNA into competent

cells. Moreover, we determined that prey-released DNA is accessible to any surrounding competent cells and is not a private good of the attacking cell.

The theory of evolving competence to acquire DNA for repair or evolution is often countered by the fact that highly fragmented DNA is present in the environment, which does not permit the transfer of intact genes or larger DNA clusters ([16,17]). Our results contradict this theory and emphasize that bacterial predation is used as a strategy to acquire and integrate large fragments of DNA, which can contribute to DNA repair or bacterial evolution. Interestingly, kin-discriminated killing, by the T6SS or the secretion of bacteriocins, followed by DNA uptake has also been observed in other species (*A. baylyi* ([18]) or *S. pneumoniae* ([19,20])) and might be widespread in other naturally competent bacteria. Remarkably, the coupling of interbacterial predation and DNA uptake may play a key role in the spread of antibiotic resistances and the emergence of novel pathogenic bacteria. Along those lines, we obtained preliminary data indicating that transfer of genomic or pathogenicity islands can occur by natural transformation on chitinous surfaces. Further experiments are required to demonstrate that this strategy could lead to the emergence of novel pathogenic *V. cholerae.* Notably, a question that arises is how often pathogenicity island could be acquired by an environmental isolate in experiments with repeated transformation cycles and without any selection pressure to recover transformants. In fact, with our experimental setup we investigated the extent of transferred DNA in a short-term transformation experiment, whereas in the natural habitat multiple cycle of interbacterial predation and DNA uptake would occur, which may lead to extensive HGT events. Indeed, high genetic diversity has been observed in diverse environmental strains of *V. cholerae* isolated from cholera-endemic area ([21]).

Another exciting question that arises is how *V. cholerae* can evolve in a more complex community. The knowledge that we acquired about the extent of transferred DNA was established by co-culturing two non-clonal strains on chitinous surfaces. Therefore, it could be interesting to study the evolution of *V. cholerae* in a more complex community that include multiple strains of *V. cholerae* or even other bacterial species that can live in the same environment. In addition, the presence of bacteriophages in the aquatic environment can have an important impact on the survival of *V. cholerae* ([22]) as well as on natural transformation. Indeed, phage-mediated lysis of bacteria will lead to the release of their DNA that could be further acquired by phage-resistant competent *V. cholerae.* It is evident that the natural ecosystem of *V. cholerae* is more complex and will have an influence on its evolution

potential. Furthermore, it is also interesting to mention that we do not yet understand why pandemic isolates of *V. cholerae* are almost clonal ([23,24]). As previously discussed, this could be explained by the emergence of non-transformable pandemic strains due to the acquisition of nuclease-encoding MGE ([25]), or by a sampling bias towards the isolation of the most pathogenic strain that could hide the genetic diversity present in other potentially less virulent strains. It would therefore be interesting to perform more genomic sequencing of *V. cholerae* strains isolated from the environment in cholera-endemic area to get further insights on the genetic diversity of the pandemic strains.

In summary, our findings shed light on the importance of the two regulators, TfoX and TfoY and the conservation of their associated phenotypes in other members of the genus *Vibrio*. Moreover, we contributed to a better understanding of the consequence of the TfoX- and HapR-mediated co-regulation of a molecular weapon, the T6SS, and the DNA-uptake machinery. These two nanomachines drive bacterial evolution in *V. cholerae* and potentially in other naturally competent bacteria. With these results, we raise additional exciting questions that should be investigated to get new insights into the emergence of pathogenic bacteria by natural transformation.

5.1 REFERENCES

1. Borgeaud, S., Metzger, L. C., Scrignari, T. and Blokesch, M. The type VI secretion system of *Vibrio cholerae* fosters horizontal gene transfer. *Science* **347**, 63–67 (2015).
2. Metzger, L. C., Stutzmann, S., Scrignari, T., Van der Henst, C., Matthey, N., and Blokesch, M. Independent Regulation of Type VI Secretion in *Vibrio cholerae* by TfoX and TfoY. *Cell Rep* **15**, 951–958 (2016).
3. Meibom, K. L., Blokesch, M., Dolganov, N. A., Wu, C.-Y. and Schoolnik, G. K. Chitin induces natural competence in *Vibrio cholerae*. *Science* **310**, 1824–1827 (2005).
4. Lo Scrudato, M. and Blokesch, M. The regulatory network of natural competence and transformation of *Vibrio cholerae*. *PLoS Genet* **8**,e1002778 (2012).
5. Salomon, D., Gonzalez, H., Updegraff, B. L. and Orth, K. *Vibrio parahaemolyticus* type VI secretion system 1 is activated in marine conditions to target bacteria, and is differentially regulated from system 2. *PLoS One* **8**, e61086 (2013).
6. Salomon, D., Klimko, J.A., Trudgian, D.C., Kinch, L.N., Grishin, N.V., Mirzaei, H., and Orth, K. Type VI secretion system toxins horizontally shared between marine bacteria. PLoS Pathog. 11, e1005128 (2015).
7. Rolhion, N. and Chassaing, B. When pathogenic bacteria meet the intestinal microbiota. *Philos. Trans. R. Soc. B Biol. Sci.* **371**:201505, (2016).
8. Sana, T. G., Flaugnatti, N., Lugo, K. A., Lam, L. H., Jacobson, A., *et al. Salmonella* Typhimurium utilizes a T6SS-mediated antibacterial weapon to establish in the host gut. *Proc. Natl. Acad. Sci. U. S. A.* E5044–E505, (2016).
9. Fu, Y., Waldor, M. K. and Mekalanos, J. J. Tn-seq analysis of *Vibrio cholerae* intestinal colonization reveals a role for T6SS-mediated antibacterial activity in the host. *Cell Host Microbe* **14**, 652–663 (2013).
10. Bachmann, V., Kostiuk, B., Unterweger, D., Diaz-Satizabal, L., Ogg, S. and Pukatzki, S. Bile Salts Modulate the Mucin-Activated Type VI Secretion System of Pandemic *Vibrio cholerae*. *PLoS Negl. Trop. Dis.* **9**(8) e0004, (2015).
11. Koestler, B. J. and Waters, C. M. Bile Acids and Bicarbonate Inversely Regulate Intracellular Cyclic di-GMP in *Vibrio cholerae*. *Infect. Immun.* **82**, 3002–3014 (2014).
12. Livny, J., Zhou, X., Mandlik, A., Hubbard, T., Davis, B.M., and Waldor, M.K. Comparative RNA-Seq based dissection of the regulatory networks and environmental stimuli underlying *Vibrio parahaemolyticus* gene expression during infection. *Nucleic Acids Res.* **42**, 12212–12223 (2014).
13. Mell, J. C., Lee, J. Y., Firme, M., Sinha, S. and Redfield, R. J. Extensive Cotransformation of Natural Variation into Chromosomes of Naturally Competent *Haemophilus influenzae*. *G3 genes genomes Genet.* **4**, 717–731 (2014).
14. Bubendorfer, S., Krebes, J., Yang, I., Hage, E., Schulz, T. F., Bahlawane, C., Didelot, X. and Suerbaum, S. Genome-wide analysis of chromosomal import patterns after natural transformation of *Helicobacter pylori*. *Nat. Commun.* **7**:11995 (2016).
15. Alfsnes, K., Frye, S. A., Eriksson, J., Eldholm, V., *et al.* A genomic view of experimental intraspecies and interspecies transformation of a rifampicin-resistance allele into *Neisseria meningitidis*. *Microb. Genomics* **4** DOI 10.1099, (2018).
16. Nielsen, K. M., Johnsen, P. J., Bensasson, D. and Daffonchio, D. Release and persistence of extracellular DNA in the environment. *Environ. Biosafety Res.* **6**, 37–53 (2007).
17. Overballe-Petersen, S., Harms, K., Orlando, L. A. A., Mayar, J. V. M., Rasmussen, S., *et al.* Bacterial natural transformation by highly fragmented and damaged DNA. *Proc. Natl. Acad.*

Sci. USA **110**, 19860–19865 (2013).
18. Cooper, R. M., Tsimring, L. and Hasty, J. Inter-species population dynamics enhance microbial horizontal gene transfer and spread of antibiotic resistance. *eLife* **6**:e25950 (2017).
19. Wholey, W., Kochan, T. J., Storck, D. N. and Dawid, S. Coordinated bacteriocin expression and competence in *Streptococcus pneumoniae* contributes to genetic adaptation through neighbor predation. *PLoS Pathog.* **12**, e1005413 (2016).
20. Kjos, M., Miller, E., Slager, J., Lake, F. B., Gericke, O., *et al.* Expression of *Streptococcus pneumoniae* bacteriocins is induced by antibiotics via regulatory interplay with the competence system. *PLoS Pathog.* **12**, e1005422 (2016).
21. Faruque, S. M., Chowdhury, N., Kamruzzaman, M., Dziejman, M., Rahman, M. H., *et al.* Genetic diversity and virulence potential of environmental *Vibrio cholerae* population in a cholera-endemic area . *Proc. Natl. Acad. Sci. USA* **101**, 2123–2128 (2004).
22. Faruque, S. M. and Mekalanos, J. J. Phage-bacterial interactions in the evolution of toxigenic *Vibrio cholerae*. *Virulence* **3**:7, 556–565 (2012).
23. Weill, F., Domman, D., Njamkepo, E., Tarr, C., Rauzier, J., Fawal, N., *et al.* Genomic history of the seventh pandemic of cholera in Africa. *Science* **358**, 785–789 (2017).
24. Weill, F., Domman, D., Njamkepo, E., Almesbahi, A. A., Naji, M., *et al.* Genomic insights into the 2016-2017 cholera epidemic in Yemen. *Nature* **565**, 230–234 (2019).
25. Dalia, A. B., Seed, K. D., Calderwood, S. B. and Camilli, A. A globally distributed mobile genetic element inhibits natural transformation of *Vibrio cholerae*. *Proc. Natl. Acad. Sci. USA.* **112**, 10485–10490 (2015).
26. Tamayo, R., Schild, S, Pratt, J. T. and Camilli, A. Role of cyclic di-GMP during El Tor biotype *Vibrio cholerae* infection: characterization of the *in vivo*-induced cyclic di-GMP phosphodiesterase CdpA. *Infect. Immunity* **76** 1617-1627
27. Ritchie, JM. and Waldor, MK. *Vibrio cholerae* interactions with the gastrointestinal tract: lessons from animal studies. *Curr Top Microbiol Immunol* **337**:37-59 (2009).
28. Metchnikoff, E. Recherches sur le cholera et les vibrions. Receptivite des jeunes lapins pour le cholera intestinal. *Ann Inst Pasteur (Paris)* **8**:557 (1894)

6. ACKNOWLEDGEMENTS

I would like to express my deepest gratitude to those who gave me advice and guidance through these five years of PhD. First of all, I would like to thank my supervisor Prof. Melanie Blokesch for having offered me a position in her dynamic team and for having proposed such an exciting project. I am very grateful for her guidance, that her door remained always open for any discussion, and for her constant support during my entire PhD. I would like to thank her for not only encouraging me scientifically but also to always support my passion for art and scientific illustrations. I am also grateful for the trust she placed in me by giving me the opportunity to replace her at talks.

I feel fortunate to have been part of the amazing UPBLO team and would like to thank all present and former members of the Blokesch-lab, in particular: the former and present technicians in the lab, Tiziana Scrignari, Sandrine Stutzmann and Candice Stoudmann for helping me to get started with some of the lab' protocols and for assisting in experiments, especially for the 360 gDNA extractions; the PhD in the lab, Natália Drebes Dörr, Nina Vesel and Leonardo Rocha for many enjoyable time discussing science and for their support; the former and present post-docs in the lab, Lisa Metzger, Charles Van der Henst, Milena Jaskólska, Ivan Mateus, David Adams, Sandrine Isaac, Jorge Pereira, Audrey Vanhove, Nicolas Flaugnatti and Thibault Sana, for inspiring discussions, for their support and motivation words when needed, and for the uncountable enjoyable moments shared altogether; the former bioinformatician, Anne-Catherine Portmann for the many discussions and excitement we shared on analyzing the preliminary data on the extent of DNA transfer occurring in *Vibrio cholerae*; the lab's secretary Marisa Marciano Wynn for always gladly helping with administration (flight or train booking, conference registration and other). Huge thanks to all of you, for the great team spirit in the lab and also for all the other great moments we shared outside the laboratory. I also would like to thank the EPFL community and especially all the former and present members of the Global Health Institute for making this place a great environment for work and sharing.

I warmly thank all the jury members, Prof. Frédérique Le Roux, Prof. Jan Roelof van der Meer, Prof. Bruno Lemaitre and Prof. Elisa Oricchio for having accepted to be part of my thesis committee and for taking the time to review this work. I am also grateful to Prof. Stewart Cole for his mentoring.

Last, but not least, I would like to thank my family, especially my mom Marie-Line, and Rémy, for their love and unconditional support during my thesis. The same is true for my friends, especially Laura and Manon, who I could always count on and who encouraged me in difficult times. I would also like to thank my cat, Newton, who always loved to assist me in the data analyses done at home. Even though I think the only interest he had was the warmth of the computer, it made these moments unforgettable. Finally, thanks to my love, Quentin, for his patience, his endless support during the writing of my thesis, and for all the memorable moments we shared since we met.

Lausanne, 8th July 2019

7. CURRICULUM VITAE

curriculum vitae

PERSONAL INFORMATION

Noémie Matthey
Rue des Alpes 16
1020 Renens (VD)
Switzerland

Date of birth: 21.04.1990
Nationality: Swiss
+41 (0)76 529 77 85
noemie_m@hotmail.com

EDUCATION AND RESEARCH EXPERIENCE

Since Sept. 2014	PhD thesis in Molecular Life Sciences Ecole Polytéchnique Fédérale de Lausanne (EPFL) Supervision: Prof. Melanie Blokesch
04-08, 2014	FNS Junior Researcher, University of Lausanne (UNIL) Unit: Prof. Jan van der Meer
02-03, 2014	Research laboratory internship (6 weeks), EPFL Unit: Prof. Melanie Blokesch
2012-2014	Master of Science in Molecular Life Sciences, UNIL • Master Project (1 year) Supervison: Prof. J. van der Meer, S. Sulser "Investigating bistability and transfer regulation of the integrative and conjugative element ICE*clc* of *Pseudomonas knackmussii*" • First Step Project (3 months) Supervison: Prof. K. Lapouge, N. Wenner "Characterization of the regulatory small RNA NrsZ in *Pseudomonas protegens* Pf-5"
07-08, 2012	Research laboratory internship (3 weeks), UNIL Unit: Prof. Justine Collier
2009-2012	Bachelor of Science in Biology, University of Lausanne (UNIL)

WORK EXPERIENCE

Since Sept. 2014	PhD Student at the Global Health Institute, EPFL
04-08, 2014	FNS Junior Researcher at the Department of Fundamental Microbiology, UNIL, Unit: Prof. Jan van der Meer

LANGUAGES

native | intermediate B2/C1 | academic knowledge | academic knowledge

SKILLS

Molecular biology
Genetic engineering (diverse *Vibrio*)
Fluorescence microscopy
DNA and RNA isolation
Transcriptional analysis (qRT-PCR)
Biosafety level 2
Teaching assistant and student supervision
Communication to expert/non-expert
Microsoft Office (Word, Excel, Powerpoint)
Image editing (ImageJ, Illustrator, Photoshop)

curriculum vitae

SCIENTIFIC PUBLICATIONS

- L. C. Metzger, N. Matthey, C. Stoudmann, E. J. Collas and M. Blokesch (2019) Ecological implications of gene regulation by TfoX and TfoY among diverse *Vibrio* species. *Environmental Microbiology*. 21, p. 2231-247
- H. Jeckel, N. Matthey and K. Drescher (2019) Biophysics: common concepts for bacterial collectives. *eLife* 8:e47019
- N. Matthey, N. C. Drebes Dörr and M. Blokesch (2018) Long-read-based genome sequences of pandemic and environmental *Vibrio cholerae* strains. *Microbiology Resource Announcements* doi: 10.1128/MRA.01574-18
- L. C. Metzger, S. Stutzmann, T. Scrignari, C. Van der Henst, N. Matthey and M. Blokesch (2016) Independent regulation of type VI secretion in *Vibrio cholerae* by TfoX and TfoY. *Cell reports,* vol. 15, num.5, p.951-958
- N. Matthey and M. Blokesch (2016) The DNA-uptake process of naturally competent *Vibrio cholerae*. *Trends in Microbiology,* vol 24. num. 2, p.98-110

CONFERENCE PRESENTATIONS

- "An interbacterial killing device influences bacterial evolution in *Vibrio cholerae"*. The annual Swiss Society for Microbiology (SSM) Meeting, Lausanne, Switzerland (2018)
- "Evolution of the human pathogen *Vibrio cholerae* in aquatic habitats". Replacing Prof. M. Blokesch (invited speaker) at the 45e Congresso nazionale della società italiana di microbiologia (SIM), Genova, Italy (2017)
- "How a molecular killing device can drive bacterial evolution in *Vibrio cholerae".* The annual Swiss Society for Microbiology Meeting, Basel, Switzerland (2017)
- "How the type VI secretion system drives evolution in *Vibrio cholerae"*. EMBO conference on Bacterial Morphogenesis, Survival and Virulence: Regulation in 4D (BMSV4D), Kerala, India (2016)

AWARDS AND HONORS

- EDRC2019 logo design contest (1st position; 2018). Logo designed for the 26th European Drosophila Research Conference 2019 https://www.edrc2019.com
- Poster award (1st price) at the annual SSM Meeting, Lausanne, Switzerland (2018)
- Poster award (1st price) at the EMBO conference on Bacterial Networks (BacNet17), Sant Feliu de Guíxols, Spain (2017)
- Poster award (1st price) at the EMBO BMSV4D, Kerala, India (2016)
- LS^2 (Life Sciences Switzerland) travel grant (2017) for the EMBO BacNet17 (Spain)
- SSM (Swiss Society of Microbiology) travel grant (2016) for the EMBO BMSV4D (India)

OTHER INTERESTS

Volunteering (EPFL workshops: open days (2016), ALUMNI, JOM (2016), prospective student days (2015, 2016); mystère de l'UNIL (2013)); **Illustration** (leisure and scientific illustration: TASmania logo database, EDRC2019 conference logo, graphical abstracts); **Sport** (dance, surf, ski, running, indoor cycling); **Traveling**

**Ce document a été imprimé au Centre d'impression EPFL,
imprimerie climatiquement neutre, certifiée myClimate.**